BIOSORPTION OF URANIUM AND THORIUM

by

© Marios Tsezos

A thesis submitted to the Faculty of Graduate Studies and Research
in partial fulfilment of the requirements for the degree of
Doctor of Philosophy

Department of Chemical Engineering
McGill University
Montreal, Canada

November, 1980

ABSTRACT

The phenomenon of selective retention of cations from aqueous solutions by microbial biomass has been termed biosorption. Samples of waste microbial biomass, originating from industrial fermentations and biological waste water treatment plants, have been tested for their uranium and thorium biosorption potential. Optimum biosorption conditions have been identified. Rhizopus arrhizus was identified as the biomass presenting the highest U or Th uptake capacity, in excess of 170 mg/g. The effect of solution co-ions (namely Fe^{+2}, Zn^{+2}) on the equilibrium biosorptive uptake capacity of Rhizopus arrhizus has been examined. The study of the rapid kinetics of U and Th biosorption has been initiated. Accumulated experimental and theoretical information led to the formulation of a biosorption mechanism hypothesis for the systems U or Th - Rhizopus arrhizus. Biosorption of both U and Th by Rhizopus arrhizus occurs mainly in the cell wall of the mycelium. Complexation by the cell wall chitin, adsorption, and hydrolysis of the complex are the processes participating in the proposed mechanism hypotheses.

RESUME

La biosorption est définie comme étant la retention sélective de cations d'une solution aqueuse par une biomasse microbienne. Des échantillons de biomasse, provenant du fermentations industrielles et de traitement biologique d'eaux usées, ont été analysés pour leur potentiel de biosorption de cations d'uranium et de thorium. Des conditions optimales de biosorption ont été identifiées. Le Rhizopus arrhizus a été identifié comme étant la biomasse présentant la plus haute capacité d'adsorption d'uranium et de thorium, soit en excès de 180 mg/g. L'effet de co-ions (Fe^{+2}, Zn^{+2}) en solution sur l'équilibre biosorptif de Rhizopus arrhizus a été étudié. L'étude cinétique de biosorption d'uranium et de thorium a été initié. L'information théorique et expérimentale obtenu a conduit à la formation d'une hypothèse sur le méchanisme de biosorption pour les systèmes uranium ou thorium-Rhizopus arrhizus. La biosorption d'uranium et de thorium par Rhizopus arrhizus se produit dans l'ensemble dans le mur cellulaire de la mycelle. La formation d'un complexe avec la chitin, l'adsorption et l'hydrolyse du complexe sont les procédés participant au méchanisme proposé.

ACKNOWLEDGEMENTS

I would like to thank Dr. B. Volesky for suggesting this project and for providing encouragement and the funds to make it possible; also the members of my research committee: Dr. M.E. Weber, Dr. M.R. Kamal, Dr. J. Vera and Dr. W. Yaphe for their interest and helpful advice.

Thanks are also due to: Mrs. M. Gomershal of the Department of Microbiology and Immunology for patiently assisting the electron microscopic examination of biosorption; Dr. N. Rowlands of the Institution of Occupational Health and Therapy for his help during the X-rays Energy Dispersion Analysis studies; Mr. G. Pouskouleli of the Department of Chemistry for his help in recording IR spectra from the FTIR unit; and the staff of the departmental machine shop for their assistance in the construction of the equipment.

I would like to thank Margaret Treen for reading the manuscript and for contributing to the style of the present dissertation.

Special thanks are due to Athena Kovatsi for her graphic work on the numerous graphs that are part of the present dissertation and her assistance during the final proofreading.

Finally, I would like to express my gratitude to my parents for all they have offered me.

TABLE OF CONTENTS

LIST OF TABLES

LIST OF FIGURES

CHAPTER I

INTRODUCTION

I-1 THE PROBLEM

Industrial growth of our civilization has been fostered from its very early years by the use of fossil fuels. In the beginning coal, and in the recent decades oil, have played a dominant role in production and transportation systems around the world. The limitations in their supply have, however, been realized, and the search for alternative energy schemes has been intensified, especially during the last decade. The advent of knowledge on the structure of the basic unit of matter, the atom, led to the development of the necessary technology for the controlled atomic fission. A new energy source, atomic energy, was thus made available. Uranium, a natural element in reasonable abundance in the earth's crust, emerged as the new fuel. The nuclear fuel brought with it what many thought of as a blessing and what others thought of as a nightmare; electrical power generated from nuclear power plants on one hand, nuclear arsenals and radioactive environmental pollution on the other.

The arguments for and against nuclear power have been developed by both sides to a considerable extent and depth. What has to be realized, however, is the simple fact that there is already considerable investment in an extended industrial network based on the nuclear fuel cycle, and along with it there is a serious and difficult environmental problem for which the current solutions are inefficient. The

realization of the implications and the intensity of the environmental problems associated with nuclear power generation were at the beginning, intentionally or not, underestimated. Our recent awareness of the magnitude of the problems related to nuclear power generation suggests that until these problems have been met in a successful way - further expansion of the sector may not be beneficial.

Canada is actively involved in the area of nuclear fuel mining and processing, as well as in the area of nuclear reactor design and manufacturing (CANDU system). As a result, uranium and thorium are of special interest to Canada, since:

(1) Both elements present chemical and radiological toxicity.

(2) Both elements present interest as nuclear fuels in energy production cycles.

(3) Thorium is present in considerable amounts in Canadian uranium ores.[1]

(4) Canada is the second largest producer of uranium in the world.[1]

During the last two decades the increased demand for uranium fuel has led to the exploitation of lower quality ores as well as further exploration and location of new uranium ore bodies.

The processing of uranium ore results in the need to dispose of large quantities of solid wastes and liquid effluents, as the ore contains as little as 0.85 kg of U_3O_8 per tonne.[1] Low level quantities of uranium decay chain radionuclides are generated during uranium milling

and find their way in the tailings or the process waste waters.[2] By 1976, in the Elliot Lake area alone, there were 400 hectares of radioactive tailings. In general, approximately 15% of the total radioactivity in the ore leaves in the final product, whereas, the remaining 85% is discharged in the tailings.[1] The tailings ponds may, in some cases, constitute a public nuisance and represent a potential health hazard that may persist for more than 10^5 years.[3]

Approximately 90-95% of the uranium is recovered during the milling process. Low concentrations of uranium are, however, present in the waste streams of the uranium mining and milling industry.[1,4,5] Uranium is also present in concentrations as high as 50 mg/l in certain copper leach dumps, and can be extracted commercially from the acidic waste waters of the phosphoric acid production process whenever uranium-bearing phosphate rock is being used.[5] In general, uranium-bearing waste waters can be considered as unconventional uranium resources. Table I.1 presents some chemical and radioactive parameters of uranium mining and milling waste waters.

The low concentration of uranium in the waste waters should not lead to the conclusion that uranium removal is of no considerable environmental importance. The environmental effects of a pollutant can be best understood as the result of its accumulation in the environment. This is especially true for non-biodegradable pollutants like uranium and thorium. Consequently, one should not only examine the concentration of the pollutant in a waste stream, but also the total mass rate at which the pollutant is discharged. Given the large volumes

TABLE I.1

Chemical and Radioactive Parameters* of Uranium Mining and Milling Waste Waters

	Discharge Waste Water	Tailing Areas Waste Water
pH	2.0[4] - 2.8[4]	2.0[4] - 4.5[1]
total solids	4180[1] - 13400[4]	-
SO_4	2280[1] - 7500[5]	200[1] - 7500[5]
Na	7[1] - 200[5]	7100[5]
Ca	101[1]	50[1] - 600[1]
Fe	300[4] - 960[1]	1.0[5] - 3.200[4]
Mn	3.6[4]	0.5[1] - 5.6[4]
Zn	0.97[1] - 9.4[4]	< 0.5[1] - 11.4[4]
Cu	0.96[1] - 2.2[4]	< 0.5[1] - 3.6[4]
U	1.0[1] - 19[1]	1.0[1] - 8.0[1]
Th	7.0 pci/1[4] - 170 pci/1[4]	2[5] - 16.5[4]
Ra^{226}	-	10 pci/1[1] - 300 pci/1[1]
Gross α	-	31000 pci/1[1]
Gross β	-	13000 pci/1[1]

*All values in mg/1 except pH and wherever specified otherwise.

of industrial waste waters the mass rates can be very high. For example, one uranium mine in the U.S. alone disposes of approximately five million gallons of waste water per day, resulting in a mass rate of 10,000 to 15,000 lbs of U_3O_8 per month.[6] Generally, mine waste water and process waste water combined together result in pumping into the tailings areas one tonne of waste water per each tonne of ore mined.

Thorium is present in Canadian uranium ores in ratios usually ranging from $ThO_2/U_3O_8 = 0.15$ to 0.60.[1] In the Agnew Lake area of Ontario, the amount of thorium in the ore exceeds that of uranium. All 12 known thorium isotopes are radioactive. Thorium presently is not recovered. It is simply discharged with the tailings of uranium milling. As a result, the activity of thorium isotopes is added to that of other radioactive elements unearthed (radium, polonium, etc.) and all end up in the environment. Thorium has been identified as a potential nuclear fuel element for the nuclear breeder reactors that have been developed recently. The interest, therefore, in the removal of thorium from waste waters has extended beyond the area of environmental protection and has approached the area of new energy resources development. Recovery of thorium from the tailings may become a significant element of Canadian economy as for every tonne of uranium ore that has already been mined, 1.0 to 0.35 lbs of ThO_2 are available in the tailings with the potential of being recovered.

The current disposal practices of the uranium mining and milling industry are similar to the ones practiced by other mining and milling operations (Figure I.1). In general, following mining

FIGURE I.1 Schematic presentation of current waste water treatment scheme employed by the uranium mining and milling industry.[1]

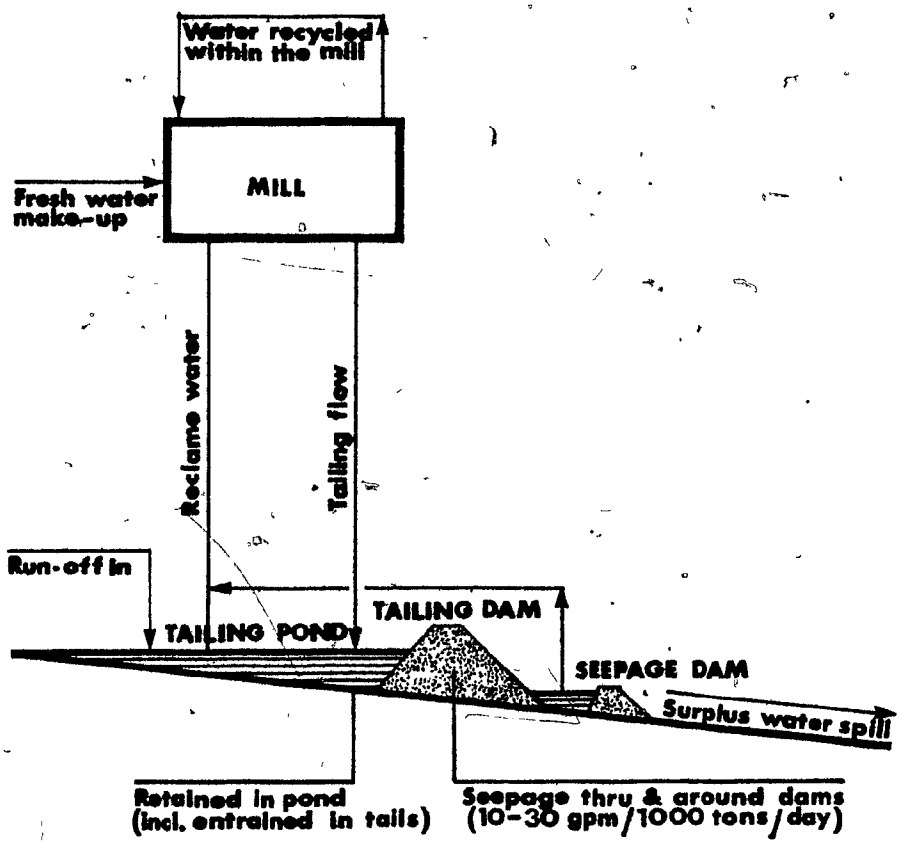
Water recycled within the mill
MILL
Fresh water make-up
Reclaim water
Tailing flow
Run-off in
TAILING POND
TAILING DAM
SEEPAGE DAM
Surplus water spill
Retained in pond (incl. entrained in tails)
Seepage thru & around dams (10-30 gpm/1000 tons/day)

and crushing the ore goes through a leaching-separation process that selectively removes uranium from the process solutions. The final slurry of the solid and liquid wastes is, following pH neutralization, disposed of in tailings disposal basins.

A controlled water outflow attempts to maintain a desired water level in the tailings pond. Seepage of waste, through the soil or the tailings dam, however, is a troublesome water loss due to the difficulties in detection and control. Water may seep into an aquifer and pollute streams and lakes or even cause the failure of the tailings dam. Seepage flows may be low in volume, compared to the outflow at the decant, but their high concentration of dissolved salts makes them significant.

The low solubility of most metallic ions at neutral pH indicates that neutralization of the waste liquor, followed by sufficient detention time in the tailings pond for sedimentation, may render the waste waters environmentally harmless. The immense abandoned tailings areas generated by the uranium industry have, however, been proven almost detrimental to the environment. Inactive tailings areas containing pyrite (FeS_2), as most Canadian ores do, generate acid regardless of the degree of neutralization at the time of disposal. Oxidation of pyrite is thermodynamically favored and is inevitable in the presence of oxygen and water. Furthermore, pyrite oxidation is accelerated by the microbial action of a group of sulfur utilizing bacteria. Produced sulfuric acid reduces the pH in the tailings pond to approximately two and resolubilizes previously precipitated radioactive and other cations. Waste waters rich in pollutants result from the tailings areas and find

their way initially into natural water bodies and finally into the food chain.

The currently practiced treatment of the uranium nuclear fuel cycle process waste waters is perceived as inefficient and there is a need for more efficient yet economical methods of treatment. The need becomes imperative if one considers treatment of nuclear reactor waste waters that contain lethal concentrations of radioactive isotopes.

I-2 THE PHENOMENON OF BIOSORPTION

Living cells have been known to concentrate cations from their aqueous environment. Microbial biomass has been documented to exhibit a selective retention of high atomic number cations.

Rothstein *et al.*[9], in 1948, presented evidence that uranium acts at the yeast cell surface "by complexing with unknown groups associated with glucose metabolism". The complex was reported to have a one-to-one ratio with certain active "groups" on the cell surface. A second complex was later postulated, with "groups not associated with glucose metabolism".

Polikarpov[10], in his study on the radioecology of aquatic organisms, pointed out that radionuclides present in aquatic (sea) environment are accumulated by marine microorganisms through "direct adsorption from the water". He pointed out that the above property appears mostly independant of the life functions of the cells. A large number of microorganisms exhibited this property, equally well, whether alive or dead.

Tezuka, in 1968[11], suggested that the reversible flocculation of activated sludge bacteria with the help of bivalent cations like Ca^{+2} or Mg^{+2}, is the result of ionic bond bridges formed among negatively charged cell surfaces and cations in solution. This indicated the ability of microbial cells to retain cations from solutions.

Cell walls of both procaryotes and eucaryotes contain different polysaccharides as basic building blocks. The ion exchange properties of certain natural polysaccharides have been studied in detail and it is a well-established fact that bivalent metal ions exchange with counter ions of the polysaccharides as shown in the following example involving alginic acid.[12,13]

$$2\ NaAlg + Me^{+2} \rightleftarrows Me(Alg)_2 + 2\ Na^+$$

With the help of an enrichment culture, Chiu[14] isolated from sewage certain fungi that could take up uranium from solution. The mycelia were not identified. In his work, Chiu noted that uranium was taken up equally well by both dead and alive mycelia, thereby suggesting a physical-chemical mechanism of uranium retention by the microbial cell.

Jilek et al.[15] investigated the capacity of "native" and "heat denatured" mycelium to uptake uranium salts from solution, following at the same time the effect of uranium on the growth of the microorganisms. They tested different Aspergilli and Penicillia and suggested that the cell acts as a "multifunctional ion-exchanger". Following a 24-hr "culture time", their "natural" Penicillum chrysogenum exhibited a

uranium uptake of approximately 175 mg/g, while dry mycelium exhibited an uptake of almost 145 mg/g. Attempting a technical application of the above property, they patented a product claiming to have a uranium uptake of approximately 100 mg/g. Samples of the supposedly marketed product, however, were not supplied when requested.

Beveridge, in 1977[16,17], working with pure cell wall preparations of Bacillus subtilis, reported that the microbial cell wall removed and retained ions of high atomic number elements. Chemical reaction among the cations and unknown active cell wall sites was hypothesized as the process responsible for the observed uptake.

Shumate et al.[18,19], in 1978 and 1979, reported rapid uptake of uranium from solution by resting Saccharomyces cereviciae, Pseudomonas aeruginosa, and a mixed culture of denitrifying bacteria. Uptake capacities of up to 140 mg/g were reported for uranium.

The above information clearly indicates that microbial cells possess the ability to bind with certain cations and remove them from solution. This potential is expressed even when the microbial cells are not alive. The phenomenon of selective retention of cations from solutions by dead microbial cells has been termed biosorption. The mechanism of biosorption is poorly understood and the information available is fragmented and rather limited.

I-3 GENERAL OBJECTIVES OF THE PRESENT WORK

It is the general objective of the present work to examine the conditions that may allow the application of biosorption for the removal/recovery of uranium and thorium from aqueous solutions.

An increasing number of microbial processes are presently being used by food and pharmaceutical industries. By-products of some of those processes are large quantities of waste microbial mass that is, in most cases, being disposed of by incineration or landfill. Waste microbial biomass may have, however, a biosorption potential and could be used as an inexpensive material for the development of a waste water scheme for the decontamination of waste streams containing elements such as uranium, thorium, radium, etc. The first stage of the work aims at the collection of different types of waste microbial biomass and their screening with the intention of identifying the biomass with the highest uptake capacity for the two selected elements of uranium and thorium. Following the selection of the biomass, the phenomenon of biosorption itself will be studied on the selected biomass type for the two elements of interest. The study will focus on the biosorption equilibrium for uranium and thorium. The preliminary examination of the kinetics of the process will be carried out and the elucidation of the mechanism of the process will be attempted.

I-4 URANIUM CHEMISTRY

Naturally occuring uranium is a mixture of three isotopes (U^{238}, U^{235} and U^{234}) in proportions 99.28%, 0.71% and 0.006%,

respectively. It has been classified as a member of the actinides.[20]

In solution, uranium can be present as ions corresponding to four states of oxidation: +3, +4, +5 and +6. Trivalent uranium reduces water to free H_2, while being oxidized to U(IV). Tetravalent uranium appears more stable, but it also can oxidize to U(VI), the reaction being appreciably accelerated by light. Pentavalent uranium solutions readily disproportionate with the formation of U(IV) and U(VI). Hexavalent uranium is the most stable oxidation state. Uranium is, in general, a fairly strong reducing agent, and has a strong complex formation ability with a variety of organic and inorganic ligands.[20,23] The uranyl ion, UO_2^{+2}, is the basic form in which U(VI) exists in solution or even in crystal lattices. It possesses a linear configuration: O-U-O.[21,22] Oxide ions cannot be displaced from the uranyl ion even by concentrated HF.[22] The stability of the O-U-O structure is remarkable. Numerous oxides and hydroxides are known and $UO_2(OH)_2.H_2O$ is the stable phase at 25°C.[22]

Hydrolysis of uranium is complicated and the available information in literature is not in complete agreement. Below pH = 2.5 uranium (VI) exists in solution exclusively in the form of the uranyl ion UO_2^{+2}.

At higher pH values a complex simultaneous equilibria system establishes.[11] Mononuclear and polynuclear ions appear as hydrolysis products. The most probable mononuclear UO_2^{+2} hydrolysis species is $UO_2(OH)^+$. In the dinuclear complex ion the uranium atoms are joined by two hydroxy bridges. In the trinuclear complex ion the uranium atoms

form an equilateral triangle. The monomer $UO_2(OH)^+$ tends to dimerize yielding $(UO_2)_2(OH)_2^{+2}$. The trinuclear $(UO_2)_3(OH)_5^+$ is another important hydrolysis product.[22] Other species like $(UO_2)_3(OH)_4^{2+}$, $(UO_2)_4(OH)_6^{+2}$ or even $U_3O_8(OH)_3^{-1}$ [20], have been proposed but their presence has not been proven.

Uranium solubility diminishes rapidly as pH increases, presenting a minimum between pH = 4 and pH = 6.[22]

I-5 THORIUM CHEMISTRY

Thorium is a fairly abundant but dispersed element in the earth's crust. Thorium has been assigned to the actinides although no definite conclusion has been reached on its electron configuration.[24]

Although the tetravalent state is the only stable oxidation state for thorium ions, it has been shown that under certain conditions thorium may exist in the bivalent and trivalent states.[24] All known thorium isotopes are radioactive, with Th^{232} being the most abundant natural isotope. Thorium ions are characterized by high charge (+4), a relatively small ionic radius (0.99 Å) and colorless aqueous solutions. Thorium shows a strong tendency for complex formation with coordination number generally of 6 or 8.[24,25]

Hydrolysis of Th(IV) becomes detectable in solutions of ordinary concentrations between pH = 2 and pH = 3.[22] The hydroxyl number of the hydrolysis products increases rapidly with increasing pH reaching a maximum near pH = 4. Hydrolysed solutions of Th(IV) are

extensively supersaturated with respect to precipitation of the hydrous oxide and, expecially, the oxide. Available thermochemical data suggest that only about 5.10^{-6}M Th^{+4} would remain in a saturated solution at pH = 3.[22] The hydrolysis of Th(IV) has been studied extensively. The complexity of the hydrolysis process, however, explains the absence, up to the present time, of unanimous consent on the mechanism of the process. A number of probable hydrolysis products have been suggested, among which are the following: Th^{+4}, $Th(OH)^{+3}$, $Th_2(OH)_2^{+6}$, $Th_4(OH)_8^{+8}$.[21,22] Hydrolysis most likely is mainly described by the formation of a solid phase of thorium hydroxide:

$$Th(OH)_4 \rightleftarrows Th^{+4} + 4\ OH^-$$

with particles below 300 Å.[21] The suggestion of the solid thorium hydroxide formation is also supported by the very low solubility of Th(IV).

Thorium hydrolysis products have been documented to exhibit increased adsorptivity.[21,26,27]

I-6 CHITIN

I-6.1 Chitin as a Polymer

The term chitin currently refers to a polymer of N-Acetyl-D-Glucosamine, where a minority of the acetyl groups has been lost. Deacetylated chitin is called chitosan. The official name of chitin is (1 → 4)-2-acetamido-2-deoxy-β-D-glucan.

Chitin occurs in three polymorphic forms which differ in the arrangement of the molecular chains within the crystal cell. X-ray diffraction spectra have identified α-chitin as the tightly compacted most crystalline form, where the chains are arranged in an antiparallel fashion; β-chitin as the form where the chains are parallel and γ-chitin as the form where two chains are "up" to every one "down". By far the most abundant form is α-chitin. Intersheet and intrasheet hydrogen bonds confer peculiar macroscopic physicochemical properties to the polymer. The three forms of chitin may co-exist.[33]

Most of the research work carried out on chitin concerns the amino group, which is the most important function of the macromolecule.[33] The greater effectiveness of the alephatic amino group of chitin as compared to aromatic amino groups has been documented in literature.[34] The alphatic amino group acts as a Lewis base and complexes cations. Substituted anhydroglucosides, like aminoethylcellulose containing relatively few amino groups (9.5-1.5% nitrogen), have been documented as complexing agents for transition metals.[35]

Chitin, a completely substituted polysaccharide carrying one amine or amide group per glucose ring (9% nitrogen), exhibits higher metal uptake.[35,36] Metals like iron, zinc, lead, mercury, uranium, etc. have been documented as being taken up by chitin.[33,34,35] The formation of a coordination complex between the metal and the chitin nitrogen has been suggested. Metal uptake by chitin is dependent on solution pH and is optimum between pH = 3 and pH = 4.[33,35,36,37] Alkali metals, ammonium, magnesium, calcium, barium are not collected by chitin and

do not prevent collection of transition metals by chitin. Ion exchange has also been suggested as a process that may be active in certain metals uptake by chitin or chitosan.[33,37] When two or more transition metal ions are present in solution together, with a quantity of polymer insufficient for the complete collection of both, the cation that forms the most stable complex with the polymer will be preferentially collected leaving most of the other cation in solution.[33] In general, the preference of chitin for transition metals follows the Irving-Williams series[33,37].

I-6.2 Chitin in Fungi

In living systems chitin occurs in the form of microfibrils or microcrystallites. Chitin is a structural polymer of the fungal cell wall. In general, fungal cell walls can be regarded as a two-phase system; one phase consisting of chitin microfibrils embedded in an amorphous polysaccharidic matrix.[38] As much as 90% of the dry matter of fungal cell walls may be composed of homo- and heteropolysaccharides.

Fungal cell walls present multilaminate architecture consisting of chitin stratified crystallites and polysaccharidic filling material.[38,39,40] A cell wall model clearly showing the above stratification has been reported by Beran *et al.*[40] A more recent study on the cell wall chitin architecture of *Penicillium crysogenum* has suggested that the inner sections of the fungal cell wall contain an isotropic arrangement of chitin fibrils, while the external wall appears to contain axially oriented chitin fibrils.[41]

The presence of chitin in the fungal cell wall has been detected and measured by X-ray diffraction and microchemical techniques.[38,42,43] The chitin content of the fungal cell wall varies considerably from one species to another.[44,45-48] It can be as low as 2.6% of the cell wall dry weight (Neurospora crassa), to 53% of the cell wall dry weight (Rhizopus nigricans).[38,48] In certain cases, structural cell wall aminopolysaccharides may be present in the form of chitosan as in the case of Mucor rouxii.[38] It has been suggested that the chitin content of the fungal cell wall may change during the growth of the mycelia.[39,49]

Chitin is the only crystalline component of the fungal cell wall.[41] Chitin is, in general, widely distributed not only in fungi but also in animals and less evolved taxonomic groups such as Protozoa.[52]

CHAPTER II

EXPERIMENTAL

II-1 BIOMASS BIOSORPTION EQUILIBRIUM STUDIES

II-1.1 Biomass Samples Collection and Preparation

Samples of waste microbial biomass originating from industrial scale fermentations were requested from major fermentation industries in Canada and the U.S. Concurrently, return activated sludge was collected from two waste water treatment installations in the Montreal area; the municipal waste water treatment plant of Vaudreuil, Quebec, and the industrial waste water treatment plant at the Gulf Refinery in Montreal. Fermentation waste biomass was supplied in a dry form by the manufacturers.

All waste biomass samples that were supplied by the industry were indicated as sterile and were washed with distilled water as soon as they were received. Filtrasorb-400, a widely-used activated carbon (Calgon Co.), and IRA-400, an anionic ion exchange resin used by most uranium mills in the yellow cake production process, were also compared with the collected biological origin materials. Table II.1 presents the materials tested in the course of the present work.

II-1.2 Biosorption Isotherm Determination Technique

The standard method used for the determination of activated carbon adsorption isotherms was applied for the evaluation of uranium and thorium biosorption isotherms.[50]

TABLE II.1

Materials Examined in the Present Work for their U/Th Uptake Potential

1.	*Aspergillus niger*	Pfizer Inc., Groton, Con.
2.	*Aspergillus terreus*	Pfizer Inc., Groton, Con.
3.	*Streptomyces niveus*	UpJohn Co., Kalamazoo, Michigan
4.	*Penicillium chrysogenum*	Wyeth Laboratories Inc., West Chester, PA.
5.	*Pseudomonas fluorescens*	Pfizer Inc., Groton, Con.
6.	*Rhizopus arrhizus*	Canada Packers, Toronto, Ontario
7.	Municipal return activated sludge (VSS = 59.8%)	Vaudreuil Municipal W.W.T.P.
8.	Industrial (phenolic) return activated sludge (VSS = 99%)	Gulf refinery, Montreal, Quebec
9.	Filtrasorb 400 activated carbon	Calgon, Co.
10.	IRA-400, anionic exchange resin	B.D.H. Chemicals, Poole, U.K.

Uranium and thorium solutions of desired concentration were prepared by dissolving $UO_2(NO_3)_2 6H_2O$ and $Th(NO_3)_4 4H_2O$ in distilled deionized water.

Uranium and thorium solutions contacted the biomass samples in 500 ml ground glass-stoppered Erlenmeyer flasks. Suspension volume was always 100 ml unless otherwise specified.

Solutions were mixed at 230 RPM on a New Brunswick Scientific G10 Gyrotory Shaker capable of accommodating up to 40, 500 ml Erlenmeyer flasks.

The biomass was contacted with the U or Th solutions for 16 hrs at 23°C, except for the "extreme" tests carried out at 5°C and 40°C. Those "extreme" temperatures represented, respectively, the upper and lower limits expected in the actual solution process applications.

Contact time was determined by running preliminary kinetic experiments using the same shake flask mixing system as the one applied for the biosorption isotherm determinations. In all preliminary kinetic experiments the contact time necessary for equilibrium attainment was no longer than six hrs. The 16 hrs contact time applied was chosen with a substantial safety margin to ensure equilibrium.

Initial uranium solution concentrations ranged from 50 mg/l U^{+6} to 1000 mg/l U^{+6}; while thorium initial solution concentrations ranged from 30 mg/l to 100 mg/l, all below the solubility limits set by the solution pH values.[1]

Uranium and thorium biosorption isotherms were determined within the range of initial concentrations described above and at three different pH values; namely those of pH = 2, pH = 4 and pH = 5. The selection of the pH values was based on the chemistry of the hydrolysis of uranium and thorium aqueous solutions respectively. Values above pH = 5 were not tested because of the very low solubility of both U(VI) and Th(IV).

Microbial biomass increased the solution pH following initial contact (Appendix F). A similar observation has been reported in literature.[18,19] Solution pH affects significantly the composition of uranium and thorium solutions, consequently the examined biosorption systems were buffered at the desired pH values. Potassium bipthalate was used as a buffering agent for the pH = 4 and pH = 5 range; while HCl-NaCl buffer was employed for pH = 2. The significance of maintaining a constant solution pH, during biosorption, will become evident in Sections IV-A.10 and IV-B.10, which deal with the mechanism of U or Th biosorption by Rhizopus arrhizus.

Bipthalate and HCl/NaCl buffer solutions were tested for possible interference with the spectrophotometric uranium and thorium analytical determinations. Uranium or thorium solutions of a known U or Th concentration and different buffer content were analyzed. The absorbance values of buffer-containing solutions were equal to the absorbance values of the unbuffered solution indicating that the employed buffering agent did not interfere with the Arsenazo III analytical determination method.

The employed buffering systems were also tested for possible interference with the U or Th uptake capacity of R. arrhizus. The equilibrium U or Th uptake capacity was determined for buffered and unbuffered biosorption systems, under the same conditions of initial U or Th concentration and biomass dosage. The pH of the non-buffered system was maintained constant with the help of dilute HCl or NaOH solutions. There was no appreciable difference observed between the U or Th uptake capacities determined in the presence of or in the absence of the bipthalate buffering agent (Appendix A, Appendix B).

Following the 16 hours contact period, the biomass was separated from the solution. Separation was accomplished by vacuum filtration using 0.45 μm Sartorius membrane filters, which present the least washable T.O.C.[51] Each filter membrane, before being used, was washed with 250 ml of distilled deionized water. The first 10 ml of the filtrate were also discarded in order to minimize possible change of the U or Th equilibrium concentration of the filtrate due to possible retention of U or Th by the filter membrane. The equilibrium U or Th concentration of the filtrate (C_{eq}) was determined (I-A.3), and the respective uptake was calculated by a uranium mass balance as follows:

$$q = \frac{V.(C_o - C_{eq})}{M}$$

where V = sample volume, l.

C_o = initial U or Th concentration, mg/l.

C_{eq} = equilibrium U or Th concentration, mg/l.

M = biomass dosage, g.

q = U or Th uptake capacity, mg/g.

II-1.3 Uranium Analytical Determination

Uranium was determined spectrophotometrically with the Arsenazo III method.[23,28,29] Additional information on the method is given in Appendix F. The following procedure was followed:

A sample containing no more than 80 μg uranium was transferred in a test tube and mixed with approximately 10 ml of 4 N HCl.

Four pellets of zinc were added and allowed to react with the mixture for no less than 15 min.

The solution was transferred quantitatively to a 50 ml volumetric flask. The zinc was washed with 4 N HCl.

2.5 ml of freshly prepared 0.05% Arsenazo III solution were added.

The solution was diluted to volume (50 ml) with 4 N HCl, and the absorbance was measured at 665 nm in a 1 cm light path length cuvette.

For calibration purposes a 1000 mg/l standard U(VI) solution was prepared and standardized according to the procedure described by Marcenko.[28] Arsenazo III solution was also prepared following the procedure suggested by Marcenko.[28]

Absorbance values were recorded from a Bausch and Lomb Spectronic 70 single beam spectrophotometer employing a digital readout for better reading accuracy.

II-1.4 Thorium Analytical Determination

Thorium concentration was determined anlytically using the Arsenazo III spectrophotometric method.[25,28,29] The method is similar to the one used for the spectrophotometric determination of uranium. Appendix F contains additional information on the employed method.

The following procedure was followed:

- A sample containing no more than 30 μg Th(IV) was transferred to a 25 ml volumetric flask.
- 6 ml of concentrated HCl were added and mixed well.
- 2.5 ml of 0.05% Arsenazo III solution were added and the mixture was diluted with distilled water to the mark (25 ml).
- The absorbance was measured at 655 nm in a 1 cm path length cuvette.

The molar absorptivity of the complex is 1.15×10^5 in 3 M HCl.

A 500 mg/l Th(IV) standard solution was prepared for calibration purposes following the procedure suggested by Marcenko.[28] A Bausch and Lomb Spectronic 70 spectrophotometer was used to record absorbance values.

II-1.5 Analytical Determinations of Iron and Zinc

Iron was determined spectrophotometrically using the O-Phenanthroline standard method.[30]

Zinc was determined by atomic absorption spectroscopy using a Perkin Elmer 403 Atomic Absorption unit.

Fisher Scientific Co. atomic absorption standard solutions were employed for calibration of the Spectronic 70 spectrophotometer (Fe) and the atomic absorption unit (Zn).

II-2 PURE CELL WALL SAMPLE PREPARATION

The procedure described by Stagg and Feather was followed for the disruption of R. arrhizus mycelia.[44] 1400 mg of biomass were mixed with 50 g of 0.25-0.30 mm glass beads, previously cleaned with HCl, and 15 ml distilled water. The mixture was inserted in a Bronwill cell homogenizer for 21 min at 10°C. Following cell disruption the mixture was washed with 4% Sodium Dodecyl Sulfate (S.D.S.) solution. The glass beads were separated by gravity settling and the unbroken cells by centrifugation at 500 g in a J2-21 Beckman ultracentrifuge. The suspension was washed once more with S.D.S. solution and rinsed eight times with distilled water. Cell walls were collected at 14000 g, and immediately freeze-dried. Electron microscopic examination of the preparation revealed completely broken cell walls.

II-3 ELECTRON MICROSCOPY

Electron micrographs were made on a Phillips model 300 electron microscope at an accelerating voltage of 40 kv. Samples were fixed with a 2.5% solution of glutaraldehyde (E.M. grade), in 0.1 m cacodylate buffer (pH = 7.2) for two days at room temperature. Subsequently they

were dehydrated with a series of ethyl alcohols and embedded in Spurr epoxy resin. Sections (800 Å thick) were cut with an LKB Microtome III and mounted on copper grids.

II-4 X-RAYS ENERGY DISPERSION ANALYSIS

X-rays energy dispersion spectra were recorded, using the thin sections previously prepared for transmission electron microscopy. The system employed consisted of a JEOL JEM-100 CX electron microscope, an EDAX J-100 C-154-10 detection unit and a 707-A EDAX X-rays Energy Dispersive Analysis unit.

The microprobe was focussed at a magnification of 100,000 at 80 kV acceleration voltage.

II-5 MASS SPECTROSCOPY

Mass spectra were recorded from an LKB 9000 mass spectrometer, at an ion source energy of 70 eV, at 290°C and a current of 60 μA. Direct inlet temperature was 143°C.

II-6 INFRARED SPECTROSCOPY

Infrared spectra were recorded from a NICOLET 6000 FTIR unit equipped with a digital plotter. Some spectra were recorded on the Perkin Elmer 297 infrared spectrometer. All infrared spectra were obtained using KBr discs.

II-7 CHITIN U OR TH UPTAKE

Poly N-acetylglucosamine (chitin), purified powder from crab shells (Sigma Chemicals C-3641), was used to determine the chitin U and Th uptake capacity. Optimum biosorption pH was employed (pH = 4). Initial concentrations of 12, 20, 100 mg/l U(VI) and 12, 18, 100 mg/l Th(IV) were tested. Additional information on the chemical properties and the structure of chitin polymer is available in Section I.6.

II-8 N-ACETYL-D-GLUCOSAMINE INTERACTION WITH U OR TH

N-Acetyl-D-Glucosamine from BDH-Biochemicals (#38001) was used to study further the complexation of U or Th and chitin. N-Acetyl-D-Glucosamine is water soluble and was reacted with U or Th solutions at optimum biosorption pH (pH = 4). The infrared spectrum of the BDH product corresponded well to the IR spectrum of the compound published in literature.[31] Information on the N-Acetyl-D-Glucosamine metal complexation ability is available in Appendix F.

II-9 KINETIC STUDIES

II-9.1 Instrumentation and Apparatus

Preliminary kinetic information on biosorption of uranium and thorium by *Rhizopus arrhizus* has indicated that the process is very rapid. Similar information was also reported very recently for uranium biosorption by *Pseudomonas aeruginosa*.[32] Because of the rapidity of U or Th biosorption process, minimum time should be spent for the separation of biomass from the liquid, following a sample withdrawal. Immediate

separation would be ideal. Having the above objective in mind, the experimental reactor shown in Figure II.1 was designed and fabricated.

The fabricated reactor vessel was temperature controlled by a stream of water from a temperature control system consisting of a NESLAB U-Cool bath cooler and a TAMESON TX-3150 thermostatically controlled water bath.

The reactor mixture temperature was monitored by a CORE-PARMER 8502-20 digital thermometer.

Mixing was provided by a four-blade propeller driven by a ZERO-MAX electrical motor equipped with a ZERO-MAX POWER BLOCK capable of continuous adjustment of the RPM delivered to the propeller shaft. Propeller shaft RPM was monitored with a TAK-ETTE digital RPM meter capable of measuring RPM with an accuracy of ± 1 RPM. Propeller shaft RPM was also checked periodically with an adjustable frequency stroboscopic light source. Inside the reactor five baffles 145 mm long by 11 mm wide prevented vortex formation.

The reactor interior was either pressurized or evacuated through a three-way solenoid-valve connected to a WELCH DUO-SEAL vacuum pump and a N_2 cylinder. The solenoid was activated by a programmable timer switch governing the duration and frequency of the liquid sample withdrawal from the reactor.

The reactor bottom was slightly tapered and was threaded so that a separate bottom piece could be attached. The separate bottom piece housed a 0.45 μm Sartorius membrane filter of 4 cm diameter. The

FIGURE II.1 Schematic presentation of the experimental set up that was used for the execution of the kinetic experiments.

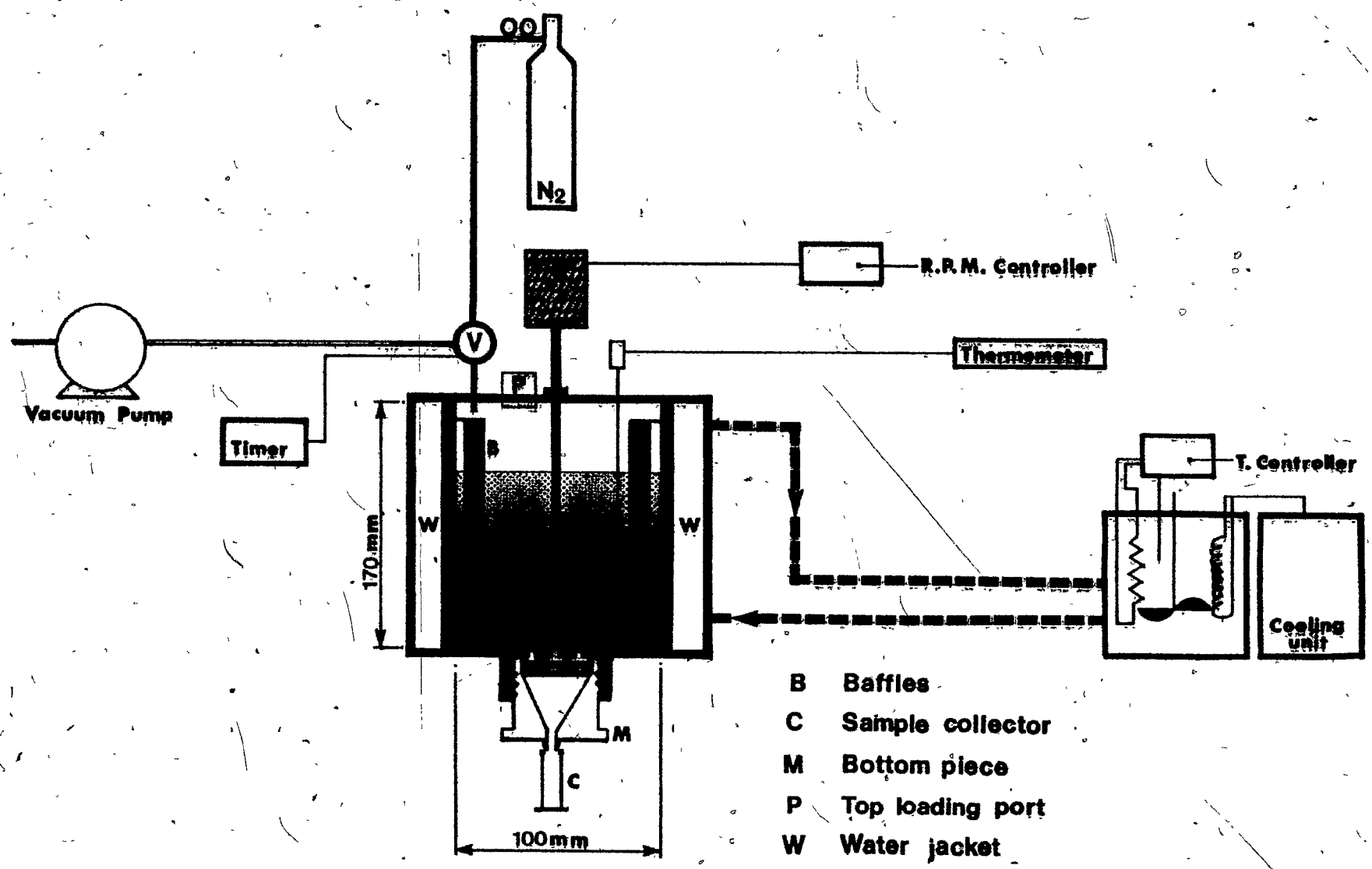
N2
R.P.M. Controller
Thermometer
Vacuum Pump
V
P
Timer
B
W
W
170 mm
T. Controller
Cooling unit
M
C
100 mm
B Baffles
C Sample collector
M Bottom piece
P Top loading port
W Water jacket

filter membrane was sandwiched between a perforated plexiglass and a Millipore 4 cm stainless steel filter support plate. A 1 mm thick Teflon flange was also inserted between the membrane filter and the steel filter support plate. The space below the filter support formed a funnel for the collection of the filtrate. The perforated (12 x ø 12 mm holes) plexiglass plate was flush with the reactor bottom once the bottom piece was fitted on the reactor. Figure II.2 presents a section of the separate bottom piece.

II-9.2 Experimental Procedure for Kinetic Experiments

Under normal operating conditions the reactor interior was maintained under mild vacuum. The vacuum was strong enough to prevent the reactor liquid from leaking out through the bottom filtration assembly. Whenever a liquid sample was to be withdrawn the solenoid valve was activated, switching the reactor interior to 20 psi pressure, thus forcing the liquid out through the filtration system into the receiving container. Approximately 5 ml of sample (filtrate) were collected within 5 to 10 seconds. An almost immediate separation of the biomass from the sample solution was achieved permitting withdrawal of the first sample within the first 60 seconds of initial contact of biomass with the U or Th solution. The sample was collected in two separate 10 ml volumetric cylinders. The first 2 to 3 ml of sample were collected in the first cylinder and tested for solution pH only. The second part of the sample was analyzed for U or Th concentration. A "flushing" of the sampling system was thus performed each time a sample was withdrawn; while solution pH was not tested in the same sample that would be analyzed

FIGURE II.2 Schematic presentation of separate bottom piece assembly.

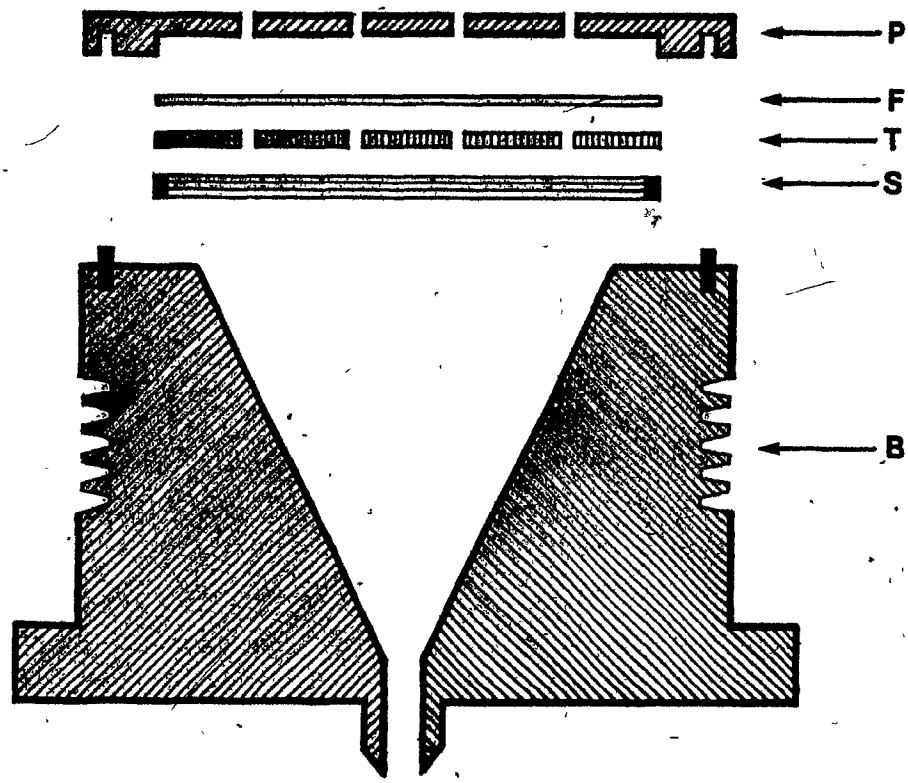

P : Plexiglass perforated plate
F : Filter membrane
T : Teflon flange
S : Steel filter support plate
B : Plexiglass bottom plate

for U or Th concentration, avoiding possible concentration changes.

Because of the already mentionned (II-1.2) ability of the Rhizopus arrhizus biomass to raise the solution pH and the decision not to use buffer during the kinetic experiments, the following pH control technique was adopted, which resulted in good pH stability throughout all kinetic experiments:

In a 2 l separatory funnel, 980 ml of the U or Th contact solution, with the appropriate pH, were prepared. In a second 250 ml separatory funnel the exactly weighed biomass dosage was mixed with 20 ml of distilled water, the pH of the suspension adjusted with HCl/KOH solution to the desired experimental pH value. The U or Th solution and the biomass suspension were brought to the temperature desired for the experiment. Meanwhile, the reactor temperature control system was also brought to the desired temperature equilibrium. The U or Th solution was first introduced in the reactor from the top port, while the reactor was maintained under mild vacuum.

The mixing system was started and the 20 ml of the biomass suspension were subsequently introduced in the reactor marking "time zero" or the beginning of the biosorption process. The loading port was immediately closed and the first sample was withdrawn within 60 seconds. A complete volume balance was possible at any point during the experiment as all volumes of solutions inserted or withdrawn from the reactor were carefully monitored. Because of the small sample size (3 to 5 ml), as compared to the 1000 ml initial volume of reaction mixture, no volume correction was used for the data. The maximum total

sample volume removed by the end of any experiment never exceeded 45 ml or 4.5% of the initial reaction mixture volume.

The response of the sampling system that was employed was examined as follows:

The reactor was filled with 1 l of Zn^{+2} solution of known concentration. The Zn^{+2} concentration in the reactor was increased by predetermined increments by injection of exact volumes of a concentrated standard Zn^{+2} solution. Following each injection, two consecutive samples were withdrawn from the reactor and analyzed for their Zn^{+2} concentration. The analytically determined Zn^{+2} concentration was compared to the calculated one.

CHAPTER III

RESULTS

III-A URANIUM

III-A.1 Uranium Biosorption Equilibrium Uptake Studies

The equilibrium uranium uptake capacities of all tested materials were determined and are summarized in Table III-A.1. The table presents equilibrium loadings in mg of U per g of biomass or other material at three selected equilibrium solution concentrations (C_{eq}) in mg/l.

The biomass of *Rhizopus arrhizus* not only exhibited the highest uranium loading, in excess of 180 mg/g, but also reduced the equilibrium uranium concentration to zero at approximately q = 60 mg/g, indicating a desirable steep biosorption isotherm (Figure III-A.1). *Rhizopus arrhizus* was, therefore, the biomass that was selected to be used for more in-depth investigation which is reported in the subsequent parts of the present work. Initial uranium concentration did not have an appreciable effect on observed biosorption isotherms. However, solution pH affected the uranium uptake considerably. In general, lower uptake was observed at pH = 2 (Figure III-A.2) than at pH = 4. No discernible difference was observed between the uranium uptake of any material at pH = 4 and pH = 5 (Figure III-A.2).

TABLE III-A.1

Uranium Biosorption Uptake Capacities, q (mg/g) . pH = 4,5

Residual Concentration mg/l	MATERIAL									
	A. terreus	*A. niger*	*P. fluorescens*	*S. niveus*	Municipal Act. Sludge	Phenolic Act. Sludge	*P. chrysogenum*	*R. arrhizus*	Ionex IRA-400	Act. Carbon F-400
5	1	7	-	11	5	9	28	50	26	15
30	1	12	6	17	11	24	60	118	45	34
700	1	35	6	40	45	79	164	> 180 (210)	90	160

FIGURE III-A.1 Qualitative comparison of uranium biosorption isotherms of some tested materials.

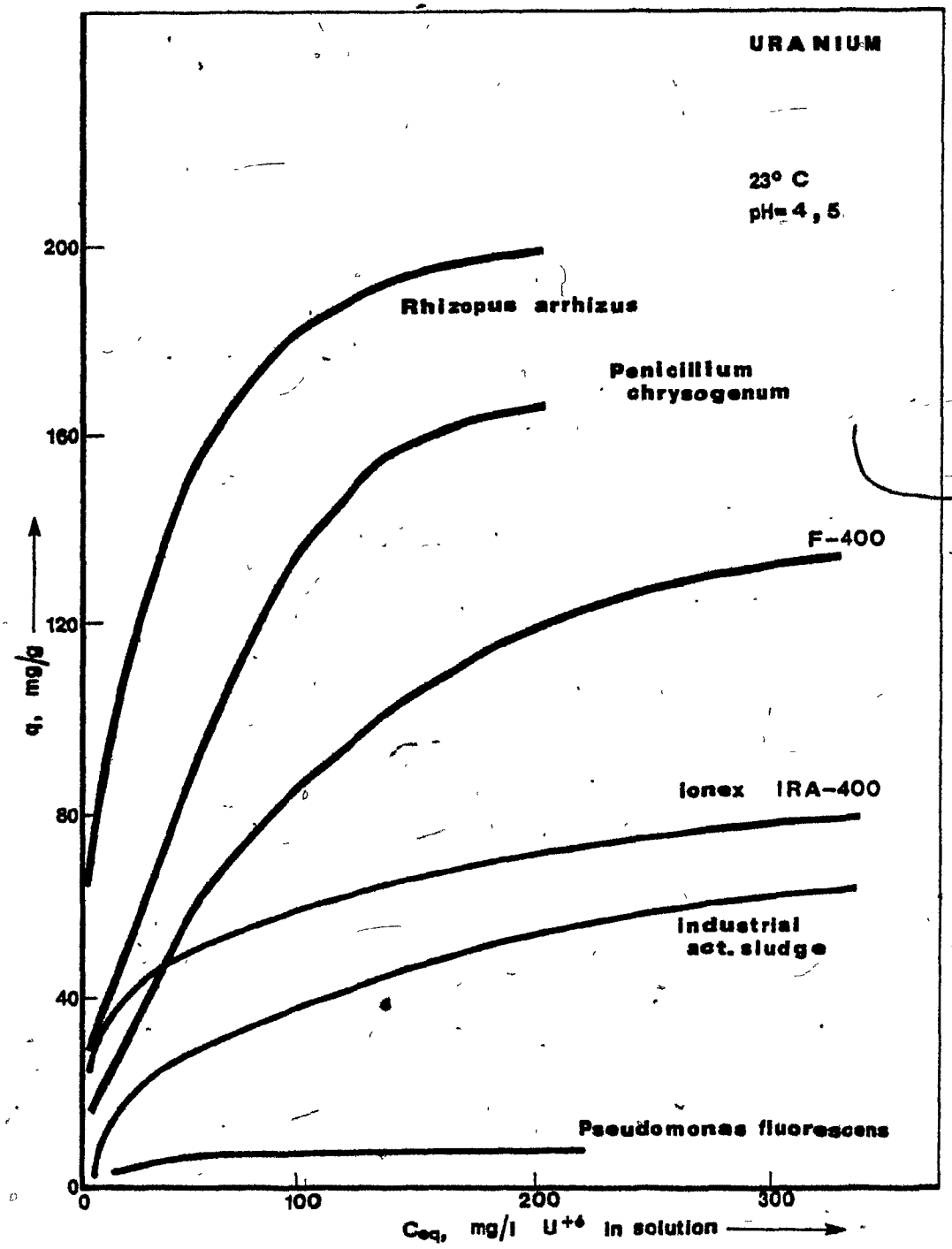
URANIUM
23° C
pH= 4 , 5
Rhizopus arrhizus
Penicillium chrysogenum
F-400
Ionex IRA-400
Industrial act. sludge
Pseudomonas fluorescens
q, mg/g
200
160
120
80
40
0
0
100
200
300
Ceq, mg/l U+6 in solution

III-A.2 Linearization of Biosorption Isotherms

Table III-A.2 summarizes the fitting of two widely accepted and easily linearized adsorption isotherm models, namely those of Langmuir and Freundlich, to the uranium biosorption isotherm data. The two models are briefly described in Table III-A.3.

Both models describe the available biosorption isotherm data well. In most cases, the Freundlich model appeared marginally better than the Langmuir model as the standard errors of estimate were lower. The Freundlich equation was linearized by taking the natural logarithm of both sides of the equation:

$$q = k\, C_{eq}^{1/n}$$

$$\ln q = \ln k + 1/n \ln C_{eq}$$

Appendix C presents a printout of the program employed for the estimation of the model parameters and the respective standard error of estimate (S.E.E.) for each set of biosorption isotherm data.

Linearized uranium biosorption isotherms for tested materials are presented in Figures III-A.2 to III-A.7. The effect of solution pH on uranium biosorptive uptake is shown clearly by the linearized biosorption isotherms. Reduced uptake was exhibited by R. arrhizus, S. niveus, "Phenolic" sludge, F-400, IRA-400 and A. niger at pH = 2, as compared to the uptake of the same material at pH = 5 (Figures III-A.2,

TABLE III-A.2

*S.E.E. Values for Uranium Biosorption Isotherms

Material	pH = 4.5		pH = 2	
	Langmuir	Freundlich (Q; n)	Langmuir	Freundlich (Q; n)
A. niger	6.388	6.330 (2.09; 1.75)	1.17	1.12 (6.92; 73.7)
A. terreus	-	-	-	-
P. fluorescens	1.311	1.307 (2.26; 5.26)	1.31	1.30 (3.00; 30.24)
S. niveus	2.587	2.233 (5.72; 2.88)	1.09	0.91 (5.62; 3.37)
Municipal sludge	3.300	1.733 (3.17; 2.50)	3.30	1.73 (10.75; 37.17)
"Phenolic" sludge	2.443	2.523 (5.33; 2.36)	1.61	1.79 (8.52; 53.28)
R. arrhizus	13.831	13.488 (14.25; 1.37)	13.83	13.49 (14.25; 1.37)
P. chrysogenum	13.521	14.067 (33.52; 5.36)	13.52	14.06 (33.52; 5.36)
IRA-400	5.525	6.102 (9.36; 2.14)	-	-
F-400	1.841	2.088 (8.15; 2.56)	-	-

*Overall S.E.E. values.

TABLE III-A.3

Adsorption Isotherm Models in a Liquid-Solid System

Model	Equation	Assumptions
Langmuir (1918)	$q = q_o \frac{bC_{eq}}{1 + bC_{eq}}$	1. Limiting adsorption loading q_o, refers to monolayer formation.
		2. Homogeneous surface of adsorbant.
	q_o, b = ct	3. No lateral interaction among adsorbed molecules.
Freundlich (1926)	$q = kC_{eq}^{1/n}$	1. Exponential distribution of surface sites energies.
	k,n = ct	2. b constant of the Langmuir model is a function of q.

ct = constant.

FIGURE III-A.2 Linearized uranium biosorption isotherm of <u>Rhizopus arrhizus</u>, whole cells and cell walls. Temperature effect. (1): $q = 25.16\ C^{1/2.25}$ (23°C); (2): $q = 121.25\ C^{1/11.60}$ (23°C); $q = 98.79\ C^{1/5.75}$ (40°C); $q = 65.61\ C^{1/4.35}$ (5°C). All at pH 4, 5.

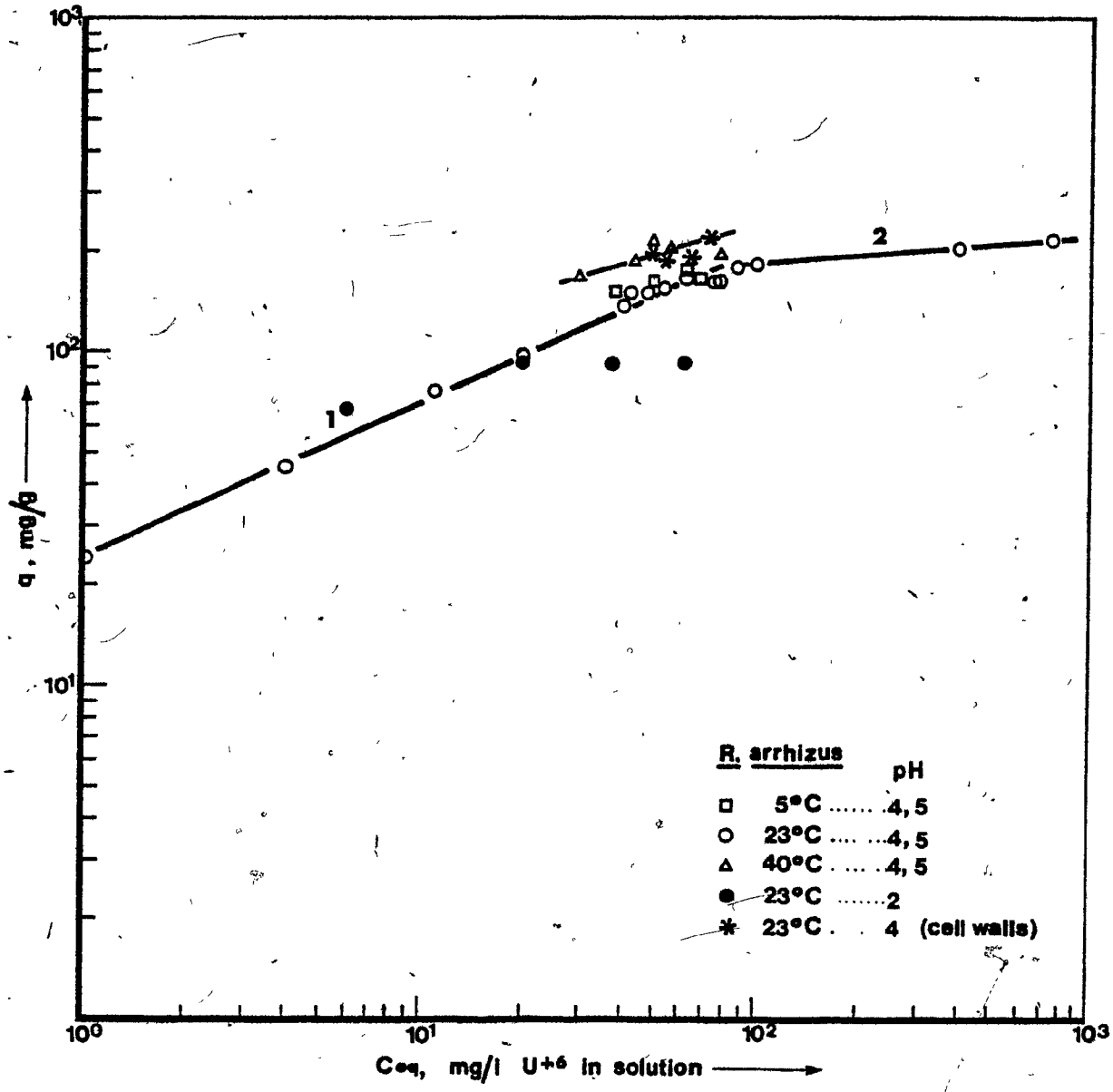
10^3
10^2
10^1
10^0
10^1
10^2
10^3
q, mg/g
Ceq, mg/l U+6 in solution
1
2
R. arrhizus
pH
5°C 4, 5
23°C 4, 5
40°C 4, 5
23°C 2
23°C . . 4 (cell walls)

III-A.3, III-A.5, III-A.6 and III-A.7). Similar uranium uptake was exhibited at all examined pH values by P. fluorescens, municipal sludge, P. chrysogenum (Figures III-A.3, III-A.4 and III-A.7).

The linearized biosorption isotherms of S. niveus (Figure III-A.3), P. fluorescens (Figure III-A.3), A. niger (Figure III-A.7) and P. chrysogenum (Figure III-A.7) do not accurately describe experimental data at equilibrium uranium concentrations above 600 mg/l. The above materials were saturated with uranium at these high solution concentrations and the observed uranium uptake, q, did not change when the solution uranium concentration was reduced. On a non-linearized isotherm the above points would represent a straight line parallel to the C_{eq} axis. The uranium biosorption isotherm of A. terreus has not been plotted because this biomass type exhibited negligible uranium uptake.

Detailed isotherm data for all materials tested are available in Appendix A.

III-A.3 Temperature Effect on q

R. arrhizus was the microorganism used for the examination of the effect of temperature on the biosorption loading (q) (Figure III-A.2).

A small increase in uranium biosorptive uptake was observed when the temperature increased from 5°C to 40°C. Table III-A.4 summarizes the differences in uranium biosorptive uptake within the examined

FIGURE III-A.3 Linearized uranium biosorption isotherms for *Pseudomonas fluorescens* ($q = 6.77\ C^{1/3.61}$) and *Streptomyces niveus* ($q = 6.77\ C^{1/3.61}$, pH = 4,5; $q = 4.76\ C^{1/3.45}$, pH = 2).

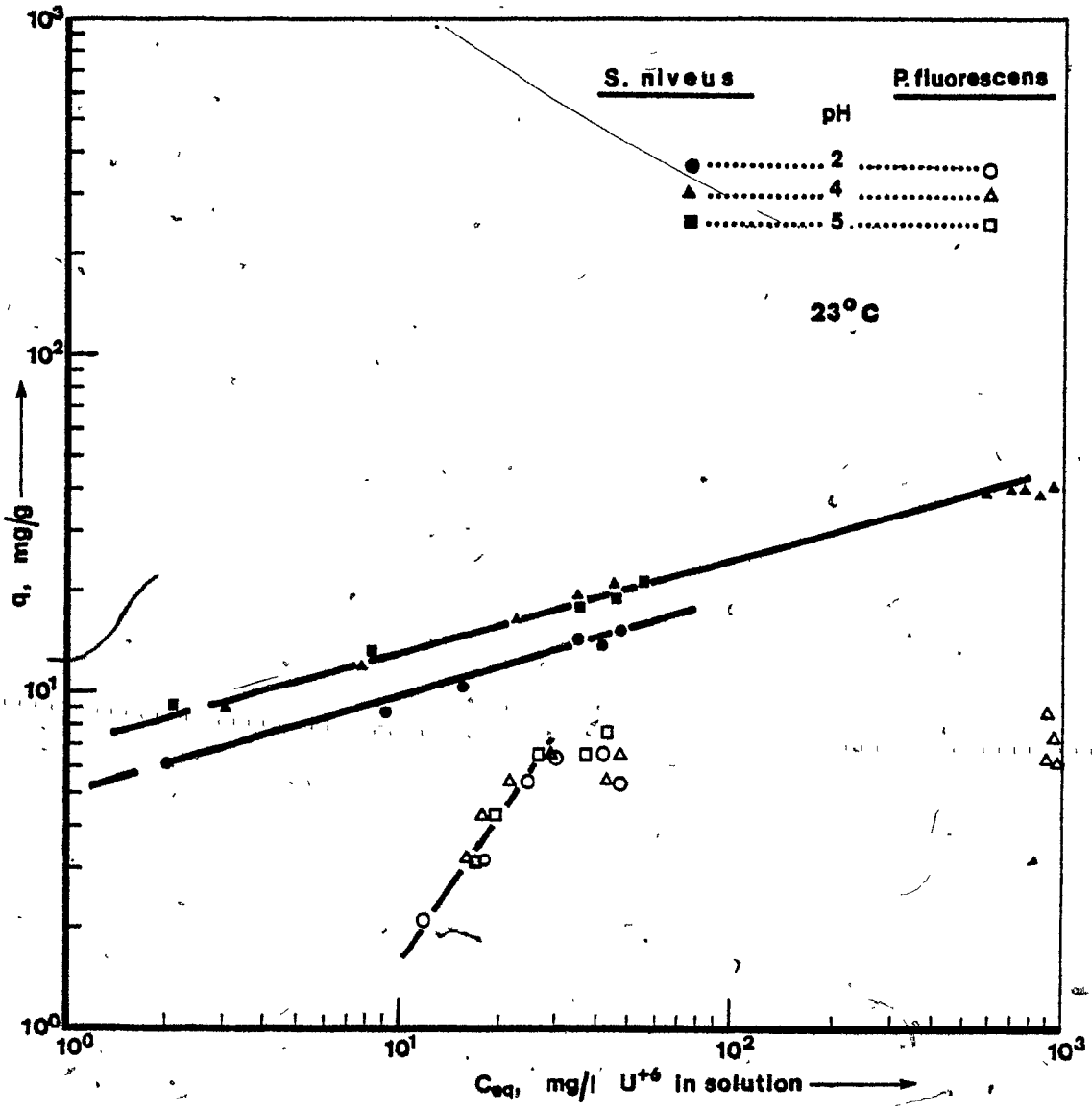
S. niveus
P. fluorescens
pH
2
4
5
23°C
q, mg/g
C_{eq}, mg/l U^{+6} in solution
10^0
10^1
10^2
10^3

FIGURE III-A.4 Linearized uranium biosorption isotherm for municipal activated sludge. ($q = 2.56C^{1/2.29}$, pH = 2, 4, 5)

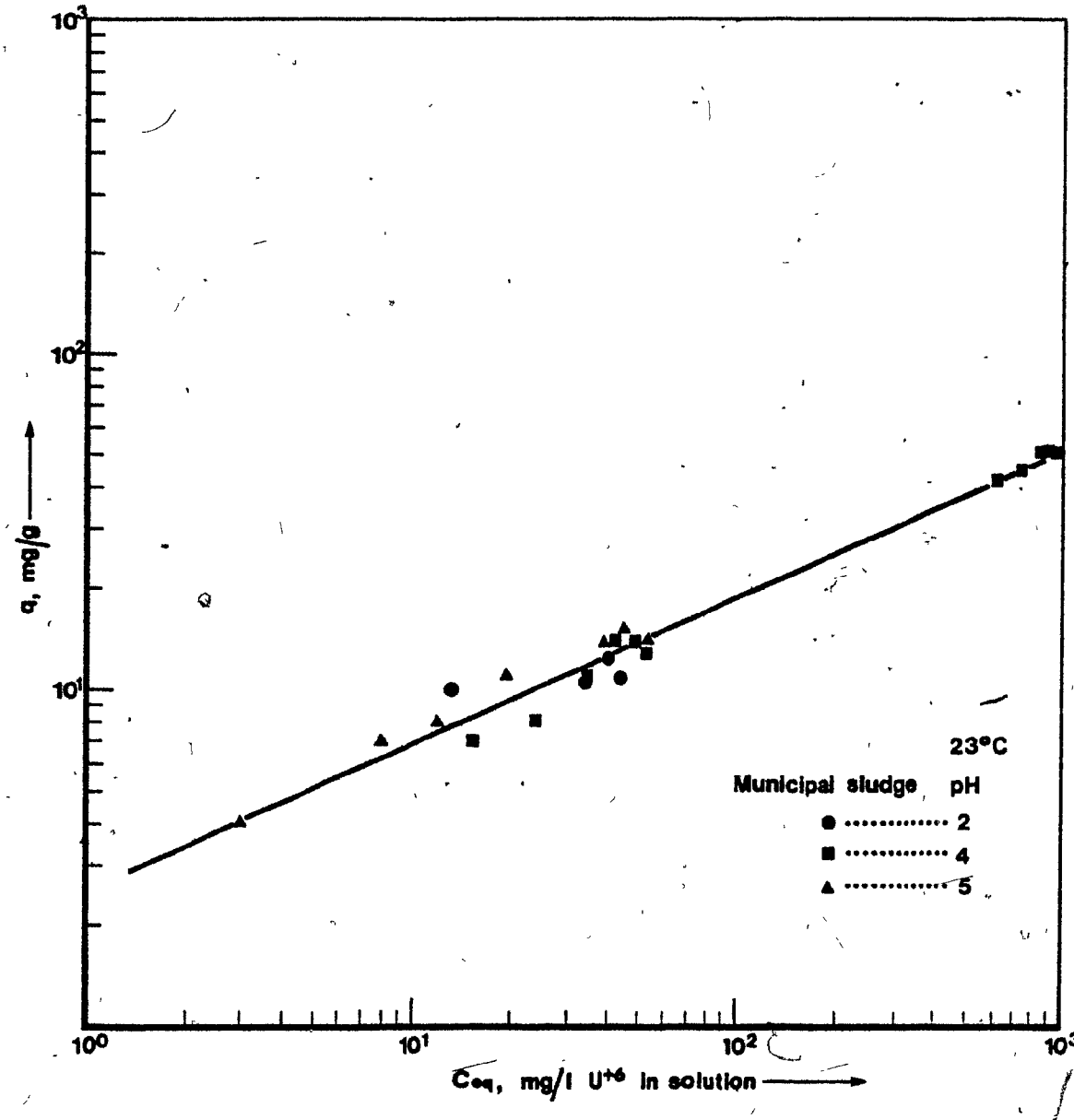
10^3
10^2
10^1
q, mg/g
10^0
10^1
10^2
10^3
C_{eq}, mg/l U^{+6} in solution
23°C
Municipal sludge pH
2
4
5

FIGURE III-A.5 Linearized uranium biosorption isotherm for "Phenolic" Activated sludge ($q = 6.04\ C^{1/6.04}$, pH = 2; (1) $q = 3.30\ C^{1/1.62}$; (2) $q = 6.15\ C^{1/2.55}$, pH = 4,5).

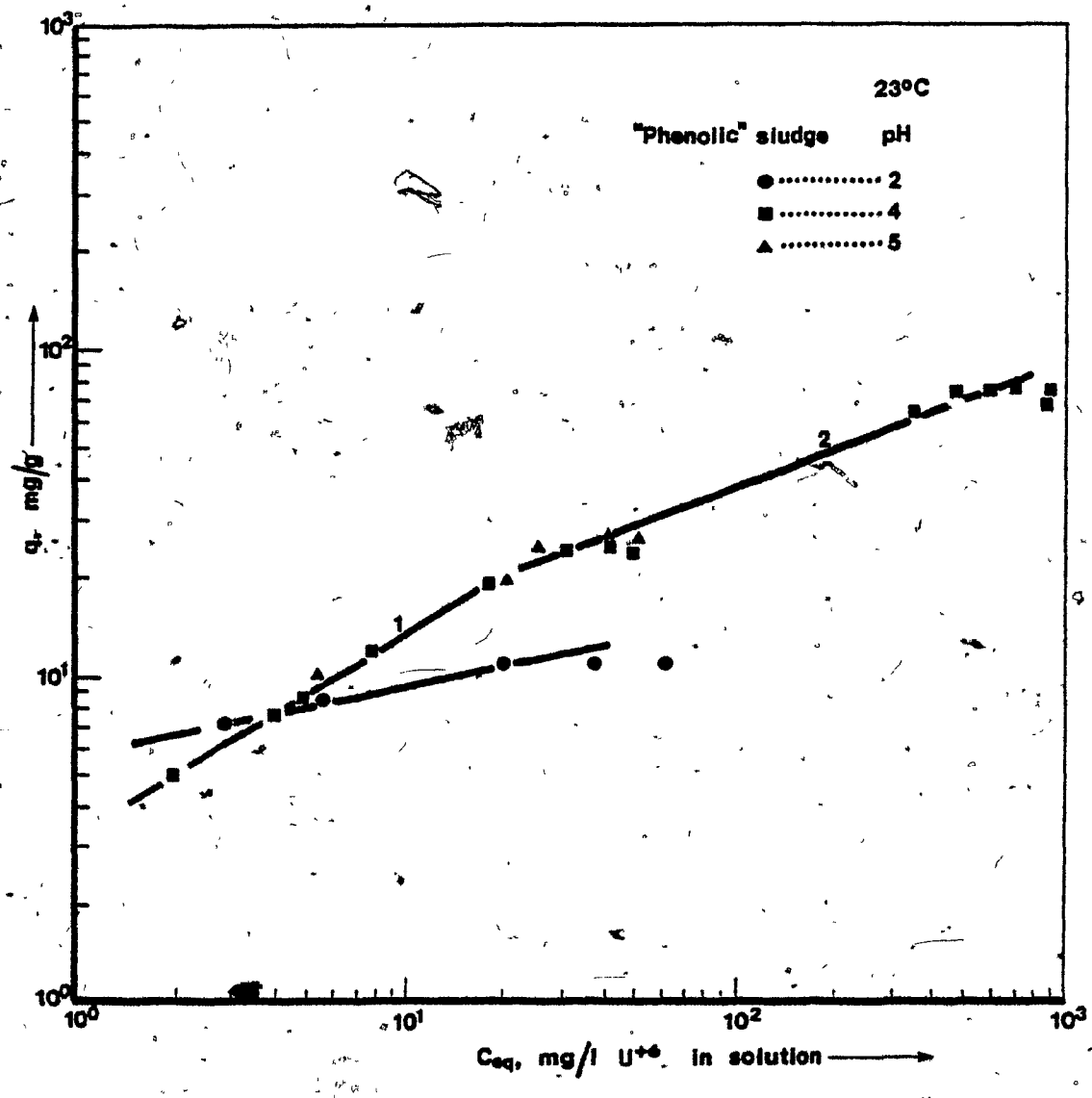
23°C
"Phenolic" sludge pH
2
4
5
1
2
10^3
10^2
10^1
10^0
q_e mg/g
10^0
10^1
10^2
10^3
C_{eq}, mg/l U^{+6} in solution

FIGURE III-A.6 Linearized uranium uptake isotherms for F-400 ($q = 6.76\ C^{1/2.09}$, pH = 4,5) and IRA-400. (1) $q = 6.50\ C^{1/0.99}$; (2) $q = 20.59\ C^{1/4.58}$.

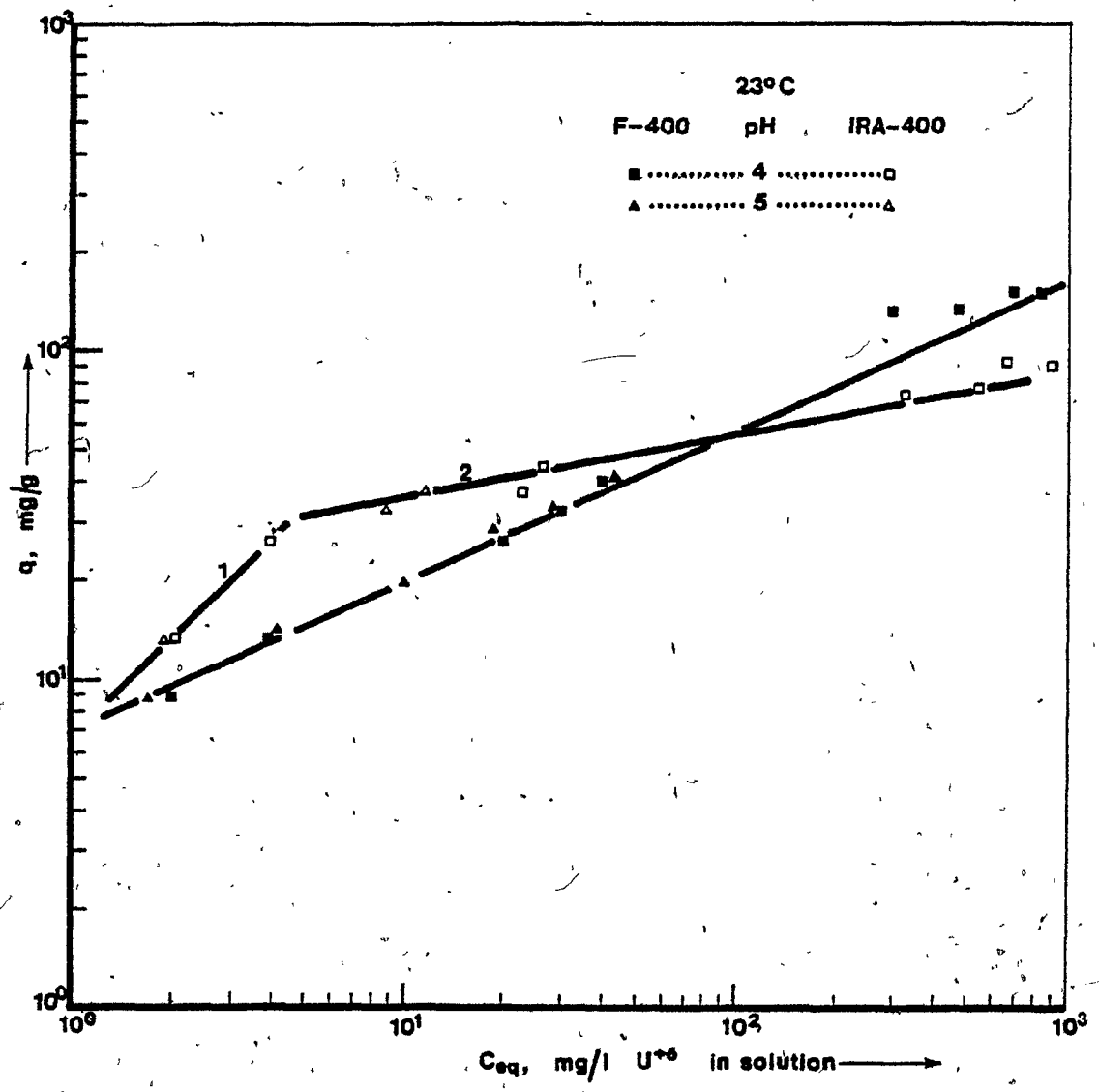
23°C
F-400 pH IRA-400
4
5
1
2
q, mg/g
C_{eq}, mg/l U^{+6} in solution
10^0
10^1
10^2
10^3

FIGURE III-A.7 Linearized uranium biosorption isotherms for *Aspergillus niger*, ($q = 2.57C^{1/2.10}$; $p = 4, 5$; $q = 2.10C^{1/2.88}$; pH = 2), and *Penicillium chrysogenum* ($q = 18.09C^{1/2.72}$; pH = 4.5)

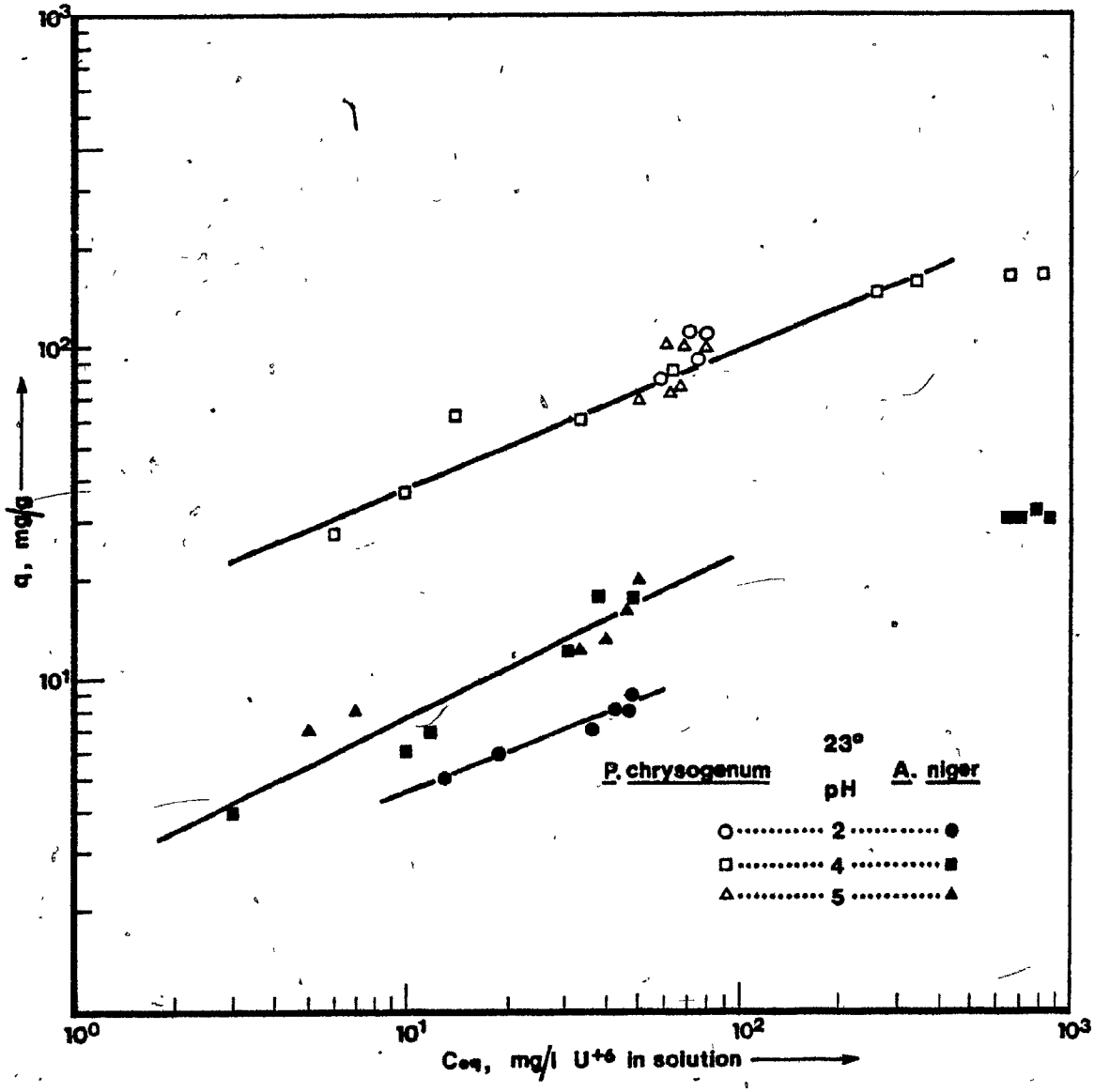
10^3
10^2
10^1
10^0
10^1
10^2
10^3
q, mg/g
Ceq, mg/l U^{+6} in solution
P. chrysogenum
23°
pH
A. niger
2
4
5

TABLE III-A.4

Temperature Effect on q . U(VI)

C_{eq} mg/l U^{+6}	Δq* Temperature Increase ($T_2 \rightarrow T_1$), °C		
	5 → 23	23 → 40	5 → 40
50	- 11	+ 36	+ 21
65	- 6	+ 27	+ 19
80	- 2	+ 20	+ 18

*q_{T_i} values calculated from regression equations,

$$\Delta q = \frac{q_{T_2} - q_{T_1}}{q_{T_1}} \times 100.$$

temperature range exhibited by R. arrhizus at different C_{eq} values. Observed differences can be considered significant for temperature changes from 23°C to 40°C and from 5°C to 40°C.

In general, the effect of temperature on uranium biosorptive uptake of R. arrhizus was not very pronounced.

III-A.4 Pure Cell Wall Preparation Uranium Uptake

Following the selection of Rhizopus arrhizus as the microbial biomass to be used for further detailed study, cell walls of this culture were isolated for examination (II.2). The uranium biosorptive uptake capacity of the cell wall sample was determined at pH = 4 and at 23°C.

The pure cell wall preparation presented marginally higher uranium uptake capacity than whole mycelia under the same conditions (Figure III-A.2).

Higher uptake capacity by the pure cell wall preparation might be interpreted as indicating that the cell wall is the biosorptively active part of the R. arrhizus mycelium, but confirmation was mandatory.

III-A.5 Electron Microscopy of Uranium Biosorption

Following the initial indication (III-A.4) that the cell wall might be the biosorptively active part of the fungal cell, further evidence was supplied by the examination of thin sections of uranium-

equilibrated R. arrhizus mycelia under a transmission electron microscope. Figure III-A.8 presents a typical electron micrograph of a R. arrhizus mycelium cell wall before exposure to a uranium-containing solution. Uranium uptake is obvious on the typical electron micrographs of uranium-exposed mycelium taken at three different magnifications (Figures III-A.9 to III-A.11). The uranium uptake of the specific sample presented on the electron micrographs was 186 mg/g at pH = 4.

Upon biosorption of uranium, the electron scattering ability of discrete inner layers of the cell wall increased (Figures III-A.9 to III-A.11). No other part of the mycelium appeared to take up uranium as was indicated by the absence of electron dense areas in other regions of the cell following exposure to the uranium solution (Figure III-A.9).

In order to confirm the identity of the electron dense material that concentrated in the fungal cell wall upon its exposure to uranium solution, X-ray Energy Dispersion Analysis was implemented. Spectra of the cell wall, the cell interior and the thin section background were recorded before and after uranium uptake. The instrument microprobe (II.4) was first focussed on the electron dense areas that appeared after biosorption of uranium. Figures III-A.12 to III-A.15 present typical examples of the recorded X-ray Energy Dispersion Analysis (E.D.A.) spectra.

Figure III-A.12 presents the X-ray E.D.A. spectrum of uranium-equilibrated R. arrhizus cell walls. The section of the spectrum containing the uranium M spectral line is shown. The exact position of the line is indicated by the white marker line. An energy level

FIGURE III-A.8 Virgin R. arrhizus cell wall electron micrograph. (80,000 X)

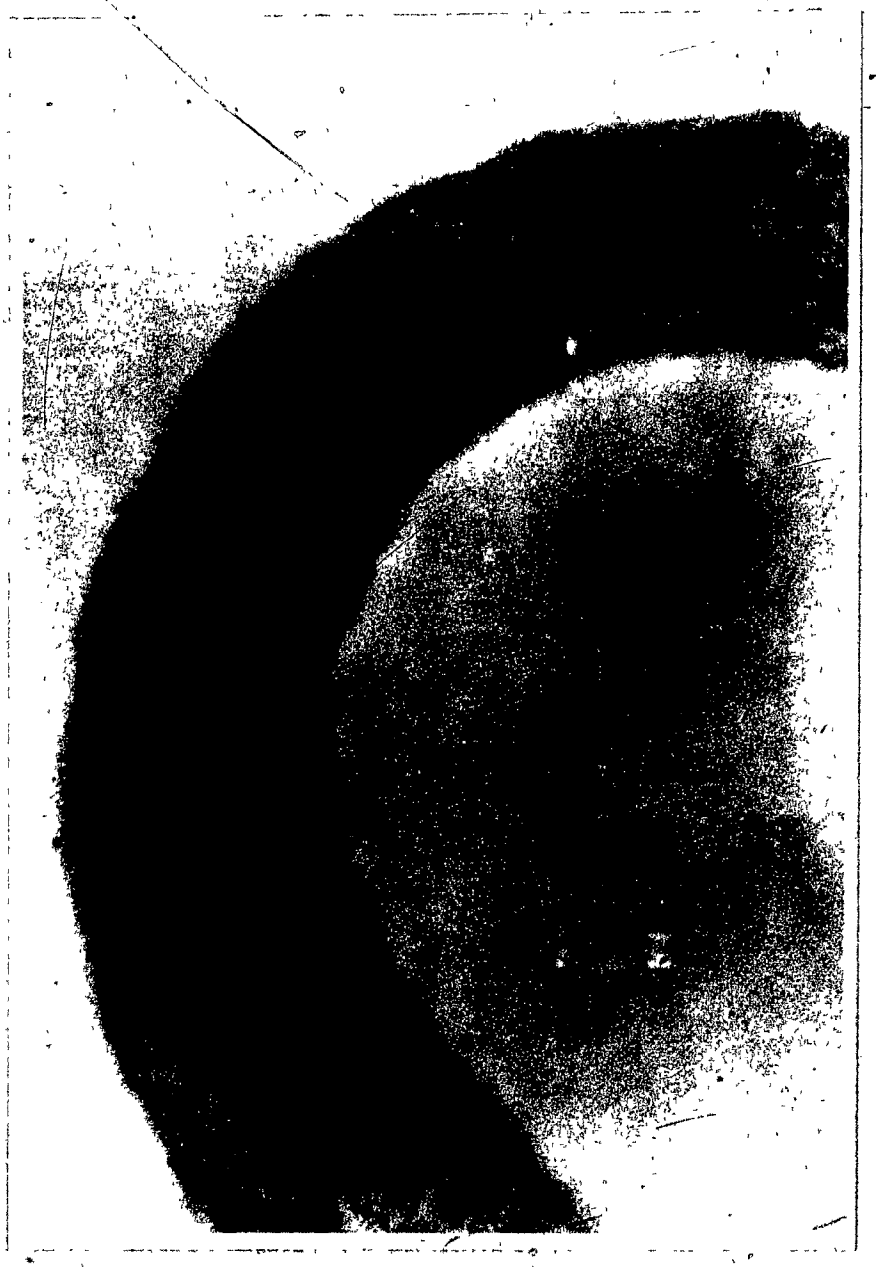

FIGURE III-A.9 R. arrhizus mycelium following uranium biosorption. Electron micrograph (19,750 X).

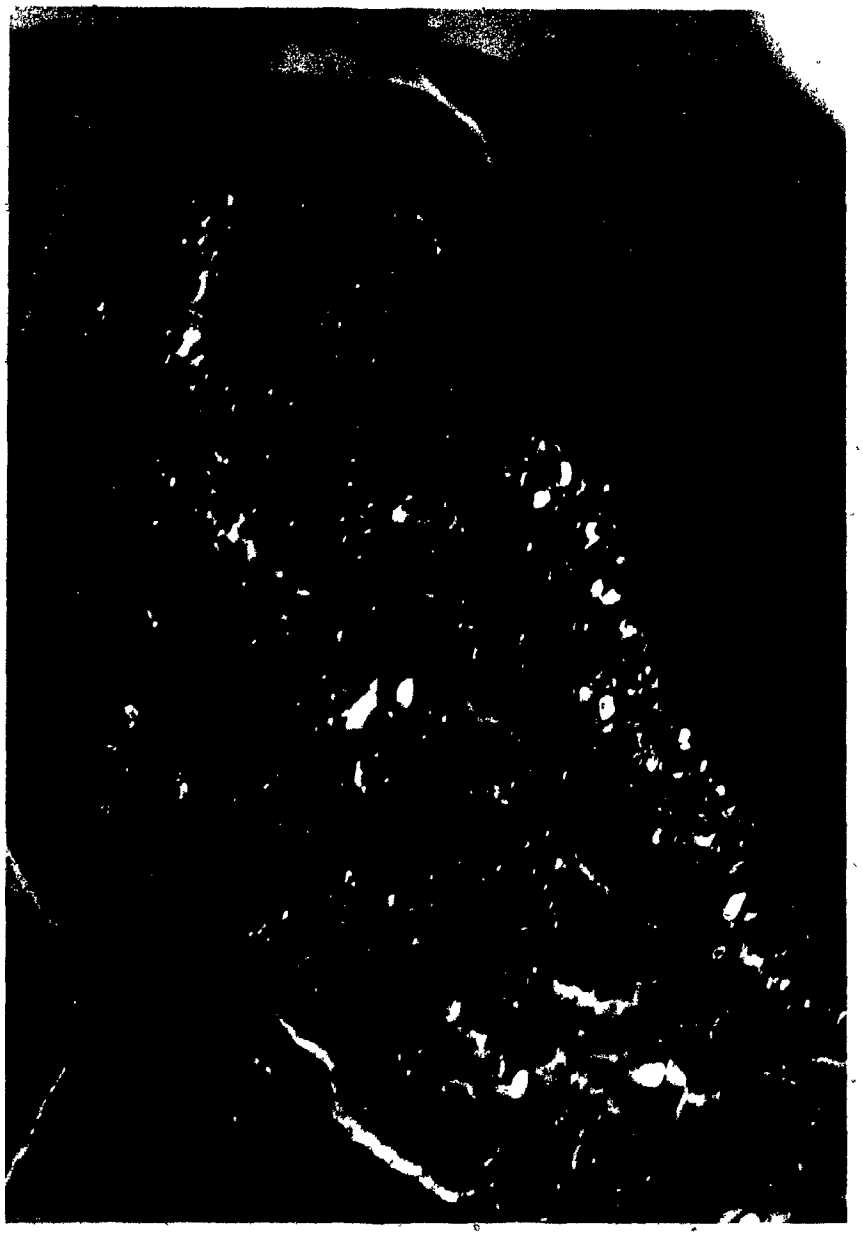

FIGURE III-A.10 R. arrhizus cell wall following uranium biosorption. Electron micrograph (41,000 X).

FIGURE III-A.11 R. arrhizus cell wall following uranium biosorption. Electron micrograph (100,000 X).

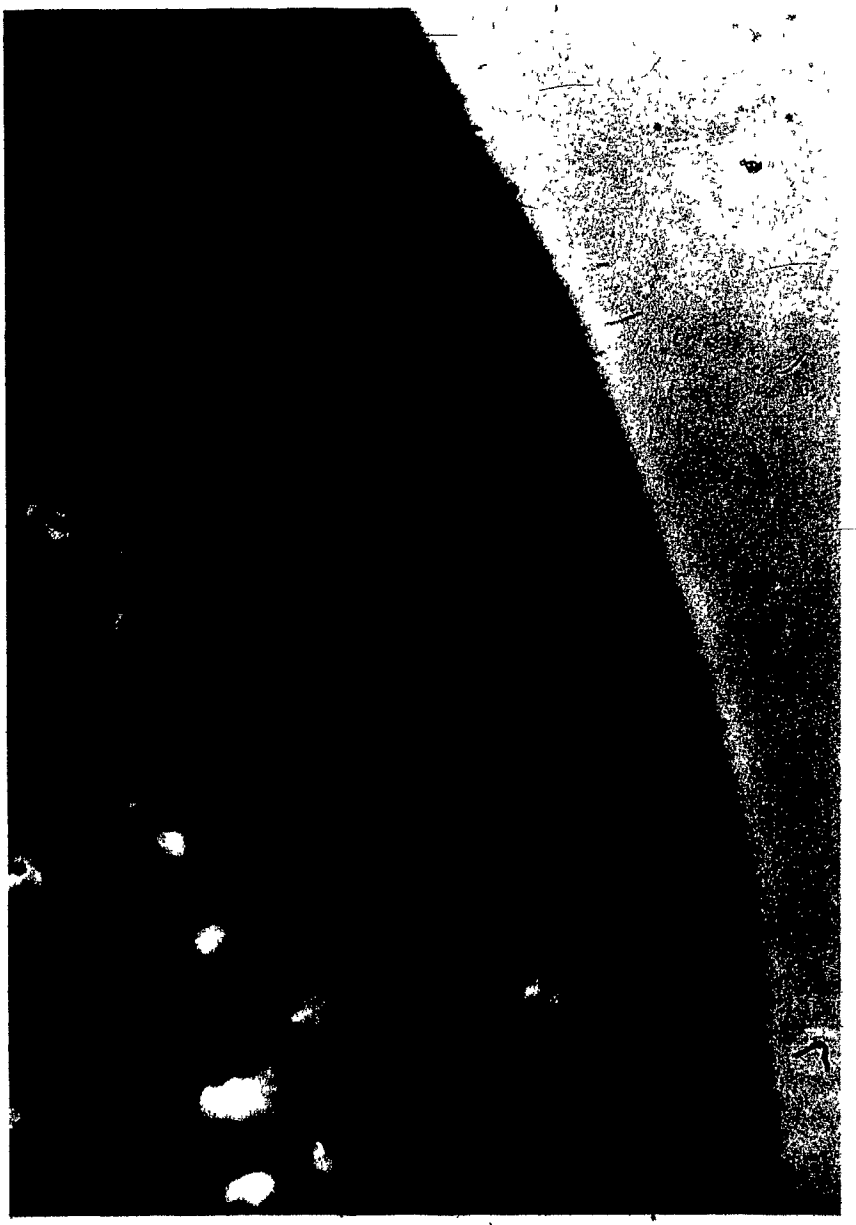

FIGURE III-A.12 Typical X-rays E.D.A. spectrum. Uranium M line of R. arrhizus cell wall electron dense areas following U(VI) biosorption.

FIGURE III-A.13 Typical X-rays E.D.A. spectrum. Uranium M line of R. arrhizus cell wall before biosorption and of cell wall interior before and after U(VI) biosorption.

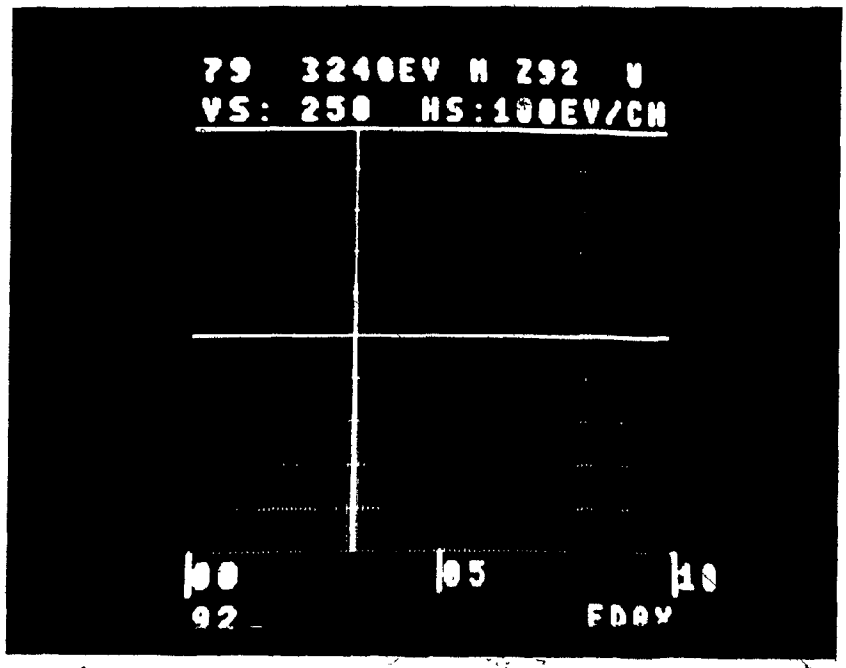
79 3240EV M Z92 U
VS: 250 HS:100EV/CH
00
05
10
92
FDAY

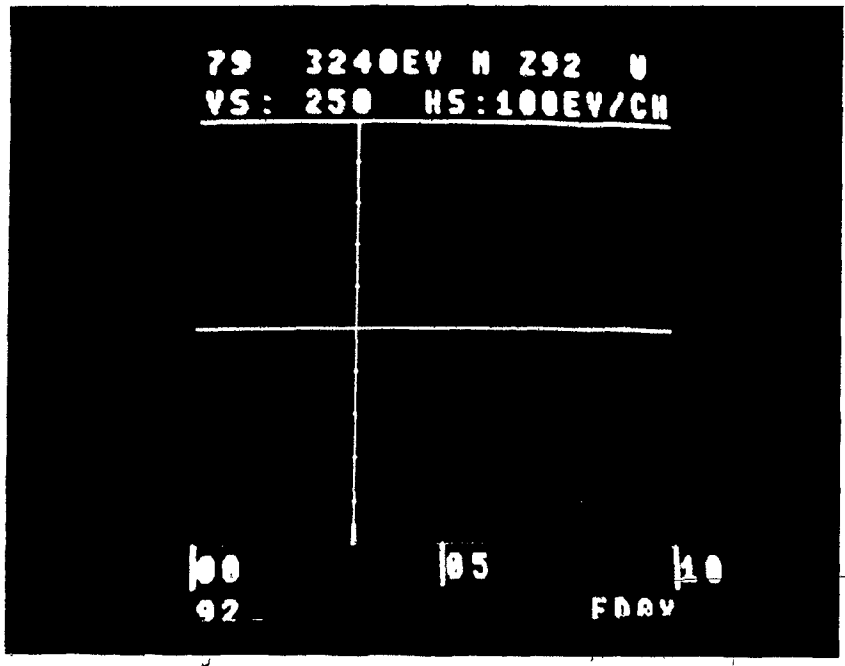
79 3240EV M Z92 U
VS: 250 HS:100EV/CH
00
05
10
92
FDAY

considerably higher than the background was observed, at the M uranium line. This revealed the presence of uranium in the analysed sample. Figure III-A.14 presents the section of the spectrum containing the uranium spectral line following uranium uptake. Again, an energy level significantly higher than the background was observed. The combined identification of energy levels significantly exceeding the background at the L and M uranium spectral lines confirmed that the electron dense areas of the uranium-equilibrated R. arrhizus cell walls contained uranium. A scan of the spectrum did not indicate the presence of another new element in the cell wall.

Figures III-A.13 and III-A.15 present typical X-ray E.D.A. spectra at the L and M uranium lines position that were recorded when the microprobe examined the background and the cell interior of R. arrhizus before and after uranium uptake. The cell wall of unreacted R. arrhizus cells was also examined. Both spectral lines were at background energy levels. The absence of uranium from the unreacted cell walls confirms the hypothesis that all uranium detected in the uranium-equilibrated R. arrhizus mycelia was the product of biosorption. The absence of detectable uranium from the cell interior and the background confirmed that biosorptive uptake of uranium by R. arrhizus is a phenomenon occurring mainly in the cell wall of the microorganism.

III-A.6 Pure Chitin Uranium Uptake

Chitin is an insoluble natural aminopolysaccharide. The equilibrium uranium uptake capacity of chitin was determined according

FIGURE III-A.14 Typical X-rays E.D.A. spectrum. Uranium L line of R. arrhizus cell wall electron dense areas following U(VI) biosorption.

FIGURE III-A.15 Typical X-rays E.D.A. spectrum. Uranium L line of R. arrhizus cell walls before uranium biosorption and of cell wall interior before and after U(VI) biosorption.

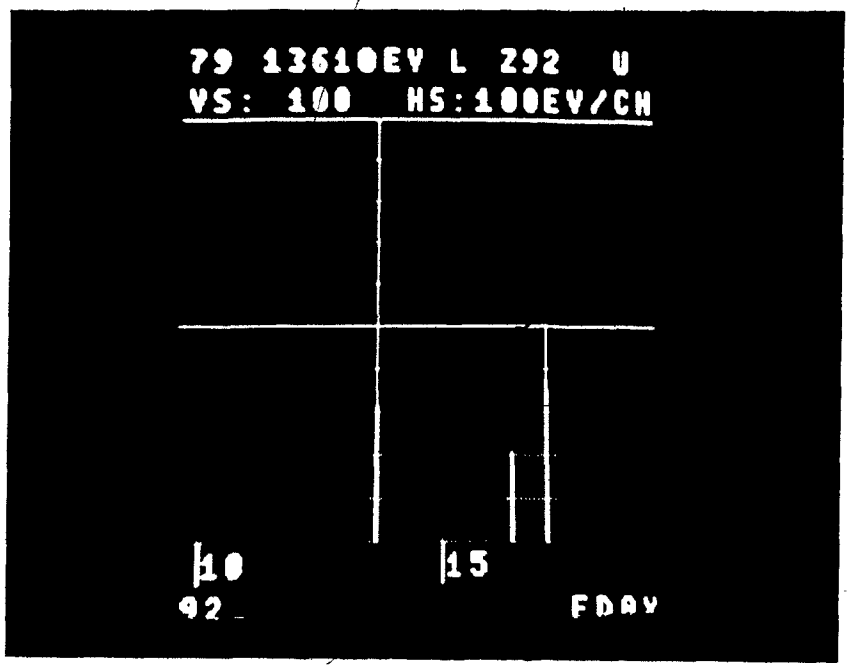
79 13610EV L 292 U
VS: 100 HS:100EV/CH
10
15
92
FDAY

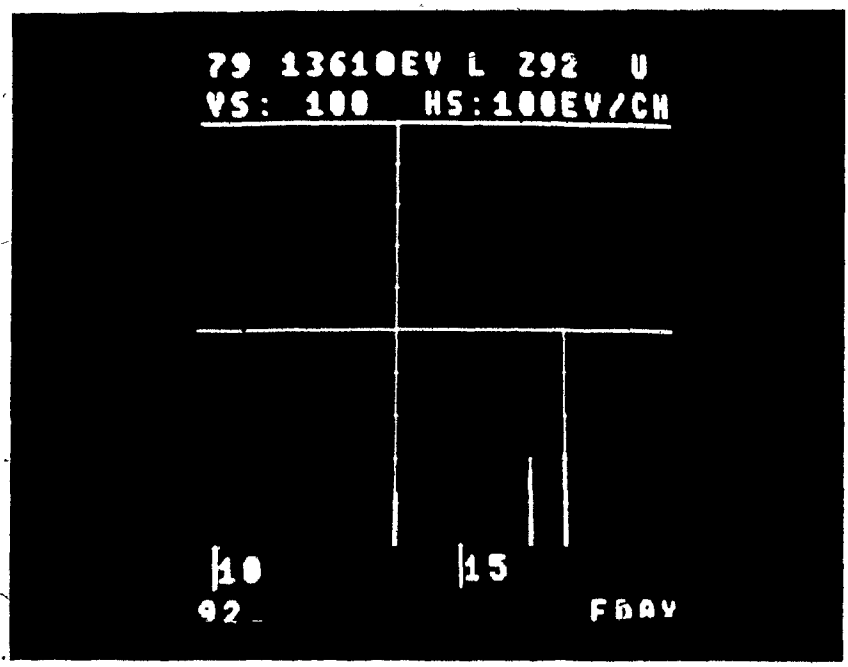
79 13610EV L 292 U
VS: 100 HS:100EV/CH
10
15
92
FDAY

to the method described in Section II.7. The uranium uptake capacity of chitin at pH = 4 and in absence of other cations was determined to be 6 mg/g (Appendix A). Following uranium uptake, a sample of the polymer was separated by filtration and washed with distilled water. The infrared (IR) and mass spectra of the reacted chitin were recorded. Figures III-A.16 and III-A.17 present the chitin infrared spectra before and after uranium uptake. The recorded infrared spectrum of pure chitin corresponds to that published in the literature. Discernible differences were not observed between the chitin spectra recorded before and after uranium uptake. The range where the characteristic uranyl ν_3 absorbance band (931 cm^{-1} to 908 cm^{-1}) was expected, is occupied by deep absorbance bands of the chitin spectrum (Figures III-A.16, III-A.17). The characteristic absorbance band of uranyl ion (ν_3) was not observed.

The mass spectra of chitin before and after uranium uptake were also recorded (II-5). The mass spectrum of the U-chitin complex did not show any species with $Z \geq 130$. In other words, it did not indicate the presence of uranium (Figure III-A.18).

III-A.7 N-Acetyl-D-Glucosamine Interaction with Uranium

As N-Acetyl-D-Glucosamine (NAGI) is the basic building block (monomer) of the chitin molecule, the interaction of NAGI with uranium was investigated (II-8). The effort was focussed towards isolating a uranium-NAGI complex.

FIGURE III-A.16 Infrared spectrum of virgin chitin.

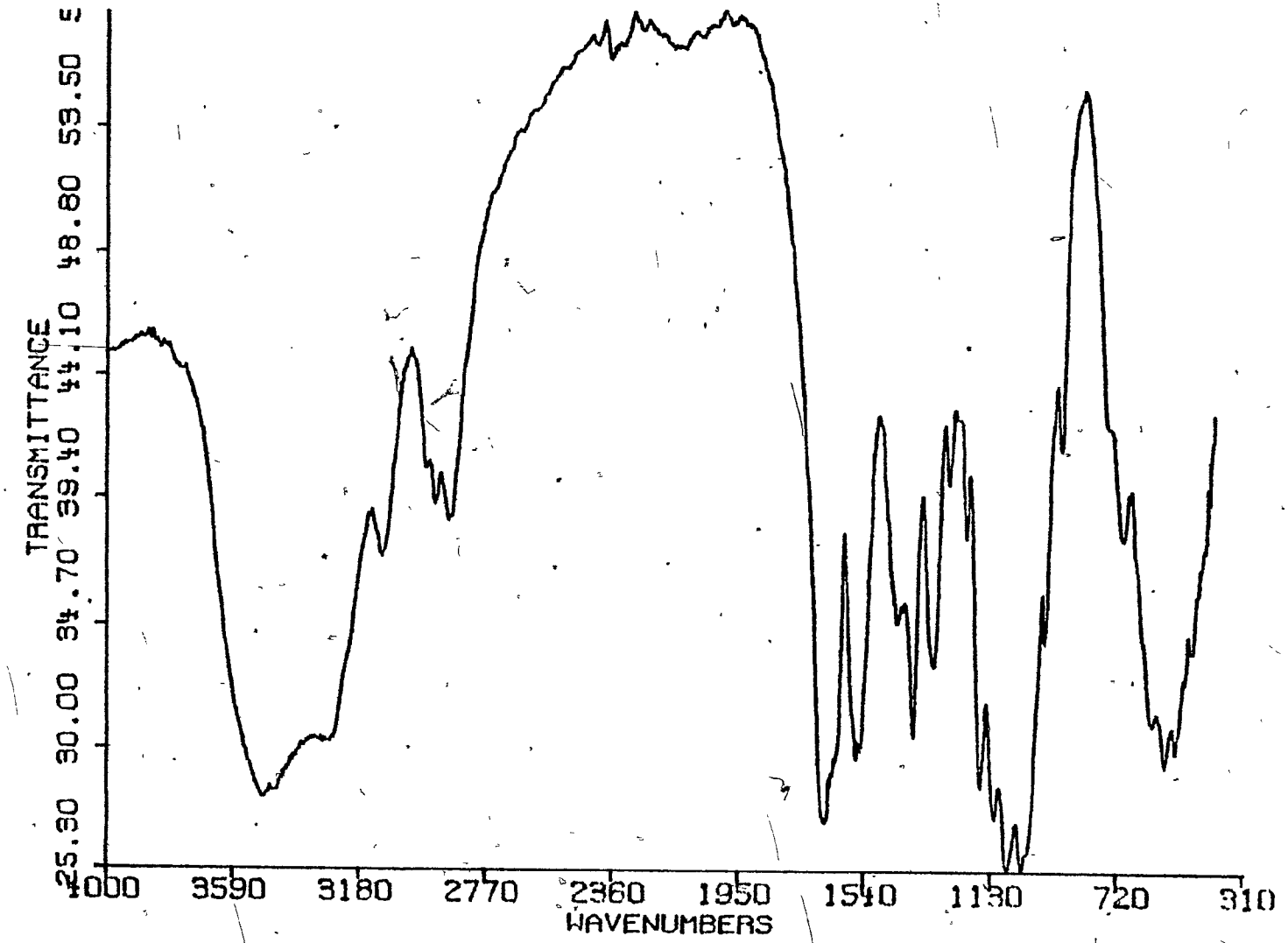
TRANSMITTANCE
25.30
30.00
34.70
39.40
44.10
48.80
53.50
4000
3590
3180
2770
2360
1950
1540
1130
720
310
WAVENUMBERS

FIGURE III-A.17 Infrared spectrum of U(VI) bearing chitin.

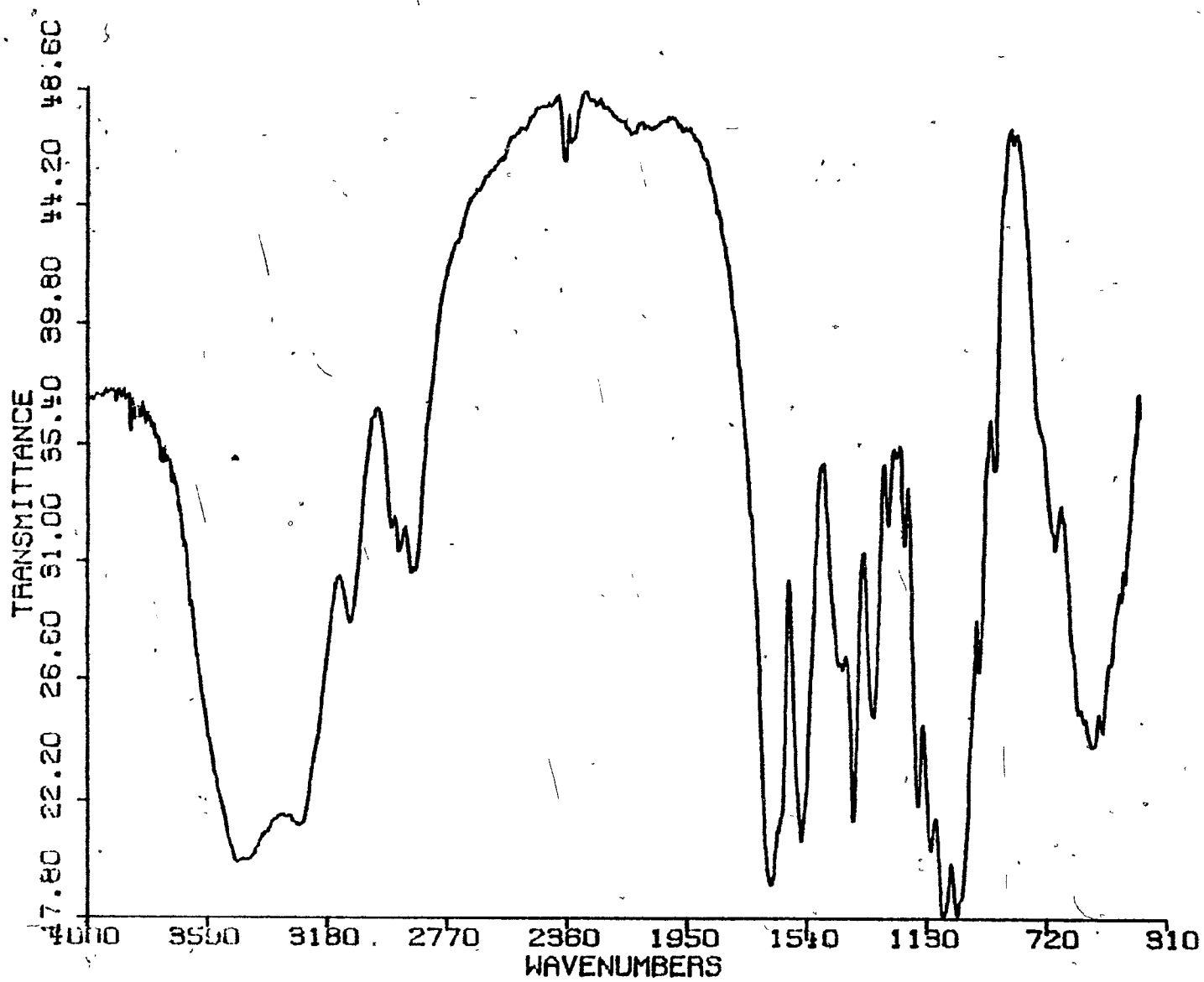
TRANSMITTANCE
17.80 22.20 26.60 31.00 35.40 39.80 44.20 48.60
4000 3590 3180 2770 2360 1950 1540 1130 720 310
WAVENUMBERS

FIGURE III-A.18 Mass spectrum of U(VI) bearing chitin.

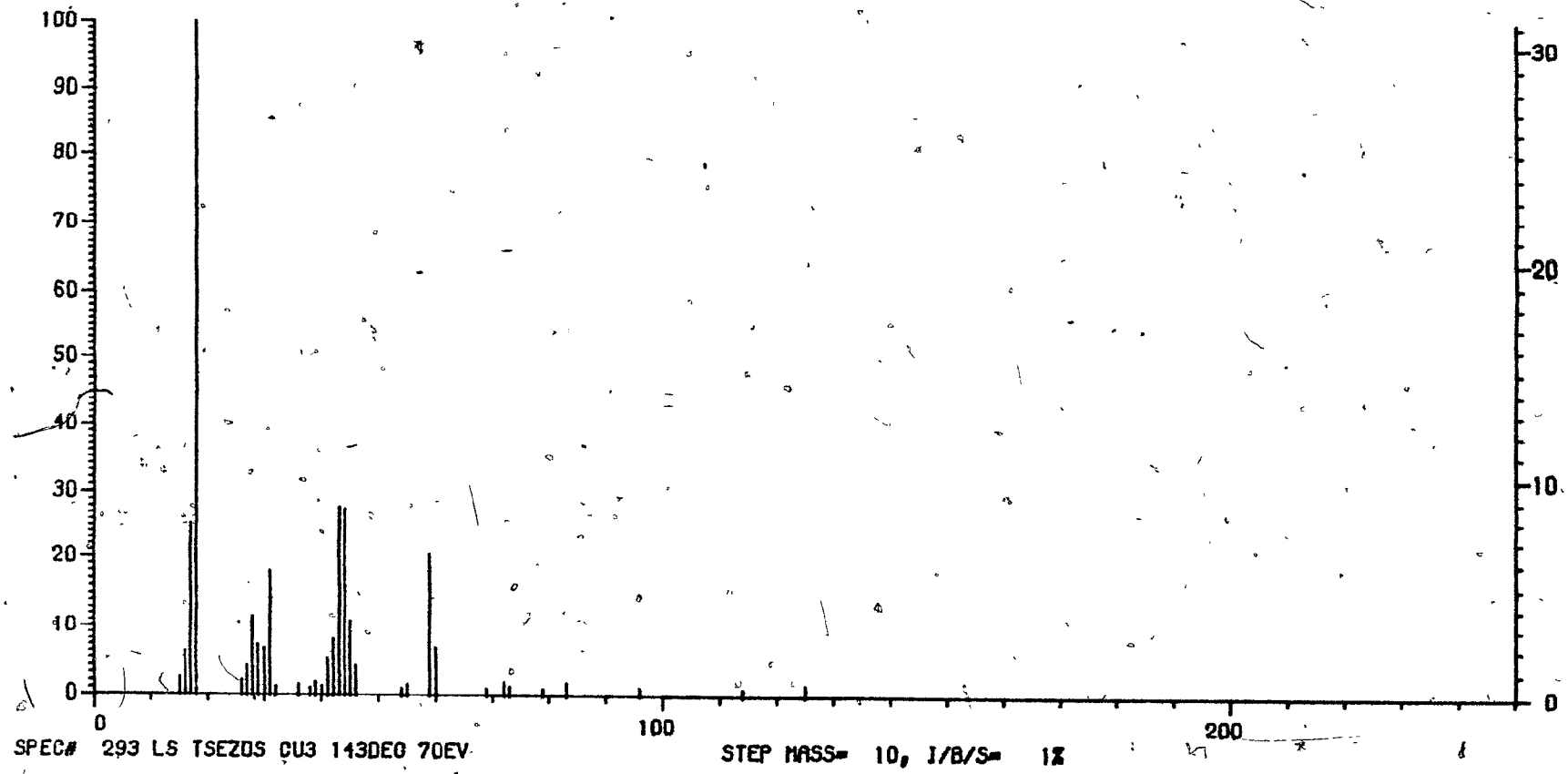
100
90
80
70
60
50
40
30
20
10
0
30
20
10
0
0
100
200
SPEC# 293 LS TSEZDS CU3 143DEG 70EV
STEP MASS= 10, I/B/S= 1%

Reaction between uranium and NAGI at 1:1 molar ratio was carried out at pH = 4 for a short period of approximately 20 min under conditions of mild stirring. It yielded a precipitate insoluble in water, absolute ethanol, or acetone. The precipitate (P1) was left to settle for 48 hours. The solution was filtered (through a 0.45 μm filter paper) and left standing. Two hours later new precipitate was observed (P2). The solution was filtered again and was left standing. Additional precipitate appeared much later (P3). The two control solutions containing only NAGI or uranyl nitrate under the same experimental conditions did not exhibit precipitate formation. Twelve days later 20 mg of NAGI were introduced into the uranyl nitrate control solution and the system was left standing. Approximately 48 hours later the precipitate appeared again, confirming that the observed precipitate was the result of the interaction between the uranyl ion and the NAGI molecules. The experiment was repeated with different concentrations of UO_2^{+2} and NAGI (0.1 M, 0.03 M, 0.003 M), always yielding similar results.

The infrared spectra of the precipitates were recorded in an effort to obtain information on their chemical composition.

All precipitates gave similar infrared spectra indicating similar chemical composition. Figure III-A.19 presents a typical IR spectrum of the precipitate P1 after drying under vacuum at an ambient temperature (23°C). Figure III-A.21 presents the infrared spectrum of the same precipitate following oven drying at 90°C for 12 hours. Comparing both spectra with the pure NAGI IR spectrum (Figure III-A.20), it can be seen that NAGI moieties were not present in the precipitate as, for

FIGURE III-A.19 P.1 precipitate infrared spectrum following vacuum drying at 23°C.

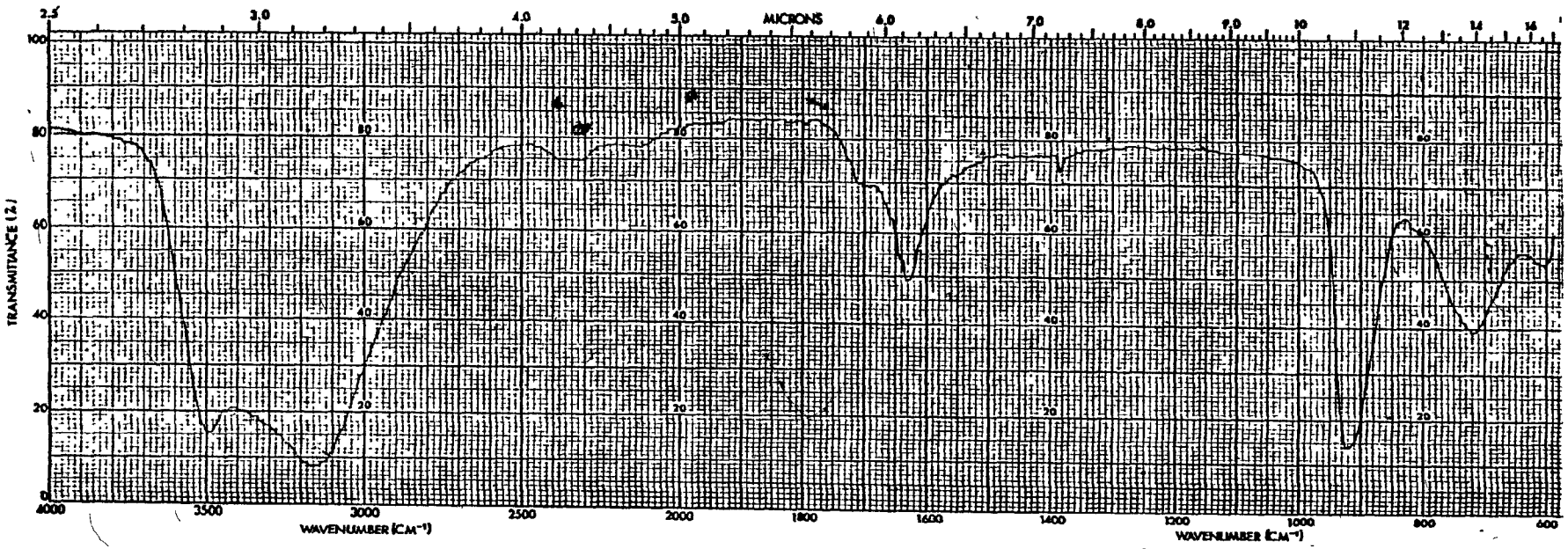
MICRONS
2.5
3.0
4.0
5.0
6.0
7.0
8.0
9.0
10
12
14
16
TRANSMITTANCE (%)
100
80
60
40
20
0
4000
3500
3000
2500
2000
1800
1600
1400
1200
1000
800
600
WAVENUMBER (CM⁻¹)
WAVENUMBER (CM⁻¹)

FIGURE III-A.20 Pure N-Acetyl -D-Glucosamine infrared spectrum.

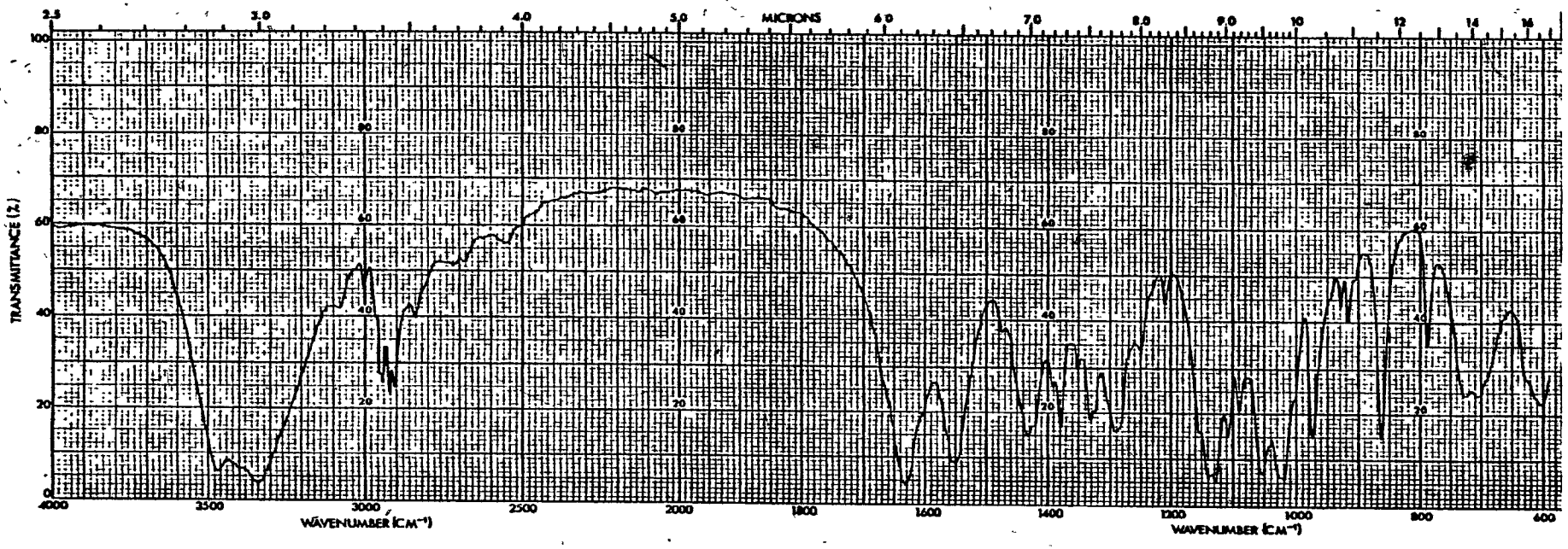
MICRONS
2.5
3.0
4.0
5.0
6.0
7.0
8.0
9.0
10
12
14
16
TRANSMITTANCE (%)
100
80
60
40
20
0
4000
3500
3000
2500
2000
1800
1600
1400
1200
1000
800
600
WAVENUMBER (CM⁻¹)
WAVENUMBER (CM⁻¹)

FIGURE III-A.21 P.1 precipitate infrared spectrum following drying at 90°C for 12 hrs.

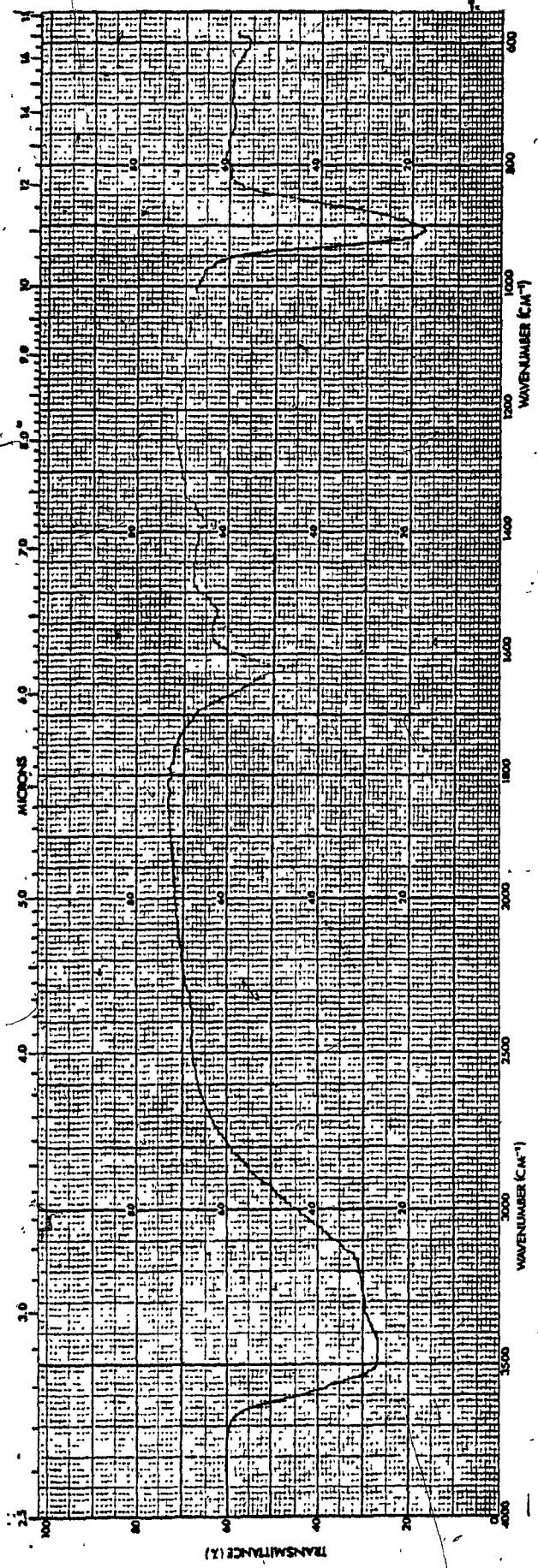
MICRONS
WAVENUMBER (CM⁻¹)
WAVENUMBER (CM⁻¹)
TRANSMITTANCE (%)

example, all amide bands are not present. A simple inorganic rather than organic, chemical composition is suggested, showing that the examined precipitate was not a uranium-NAGI complex. The presence of uranium in the precipitate was confirmed by the positive result of the Arsenazo III test on a solution containing precipitate (P1) dissolved in HCl.

III-A.8 Infrared Spectroscopy of Uranium Equilibrated *R. arrhizus* Cell Walls

In the preceeding sections the data were presented which led one to the conclusion that the cell wall of *R. arrhizus* is the part of the mycelium responsible for biosorption of uranium. The infrared spectra of *R. arrhizus* cell walls before (Figures III-A.22 and III-A.25) and after uranium uptake (Figures III-A.23 and III-A.26) were recorded with the intention of acquiring information on the nature of the chemical interaction between uranium and the cell wall.

A comparison of the 4000 cm^{-1} to 400 cm^{-1} range of the IR spectra (Figure III-A.24), while revealing no discernible shifts in the characteristic absorbance bands, exhibits one new peak at 908 cm^{-1}, on the uranium-exposed cell wall spectrum (Figure III-A.23). This new peak was assigned to the ν_3 uranyl ion characteristic frequency. A detailed discussion of the recorded 4000 to 400 cm^{-1} IR spectra is presented in Chapter IV.

The 400 to 340 cm^{-1} range of the cell wall IR spectrum before and after uranium uptake is presented in Figures III-A.25 and III-A.26, respectively. After uranium biosorption a new peak appeared at 374 cm^{-1}

FIGURE III-A.22 Infrared spectrum of virgin R. arrhizus cell walls.

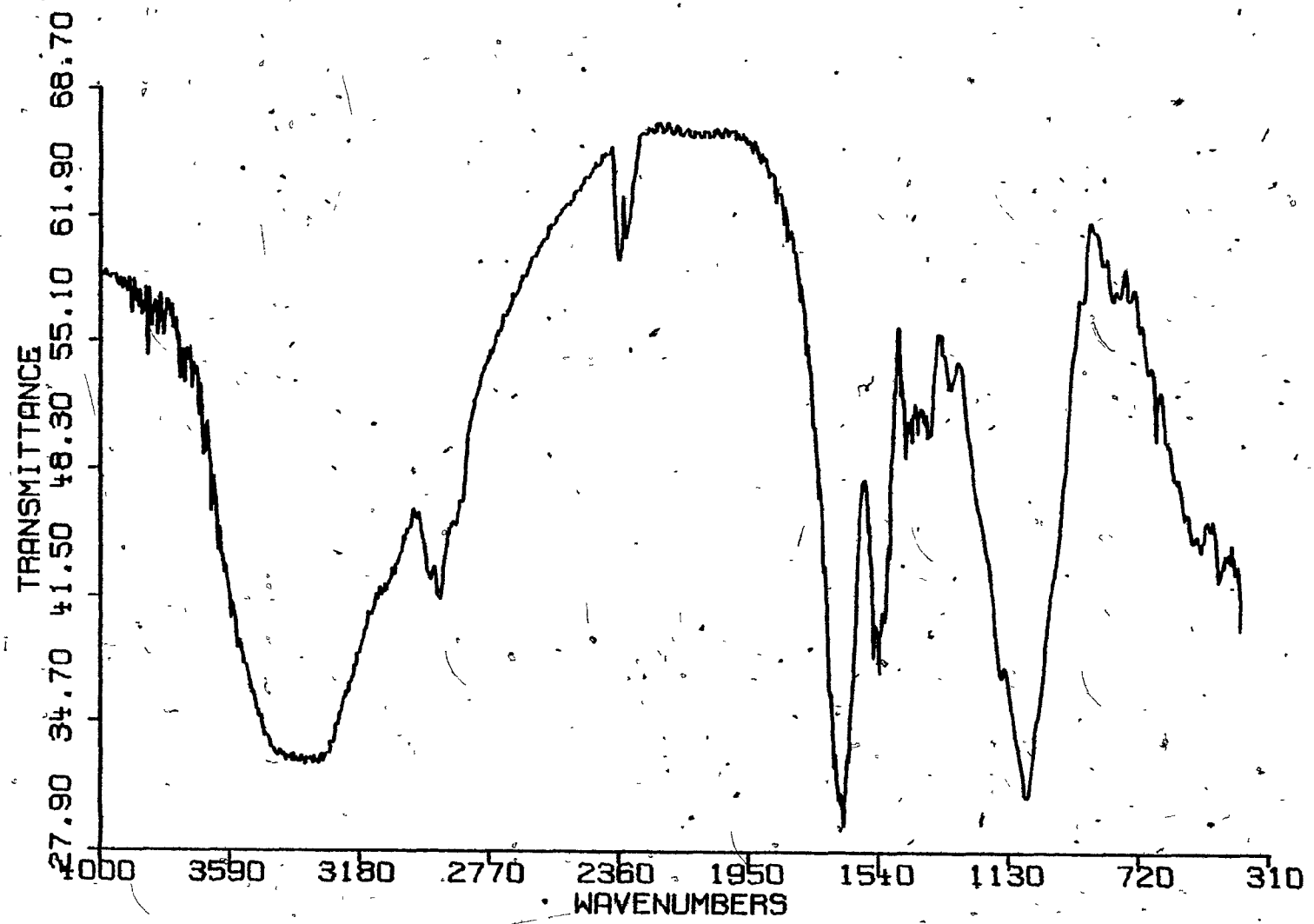
TRANSMITTANCE
68.70
61.90
55.10
48.30
41.50
34.70
27.90
4000
3590
3180
2770
2360
1950
1540
1130
720
310
WAVENUMBERS

FIGURE III-A.23 Infrared spectrum of R. arrhizus cell walls following uranium biosorption.

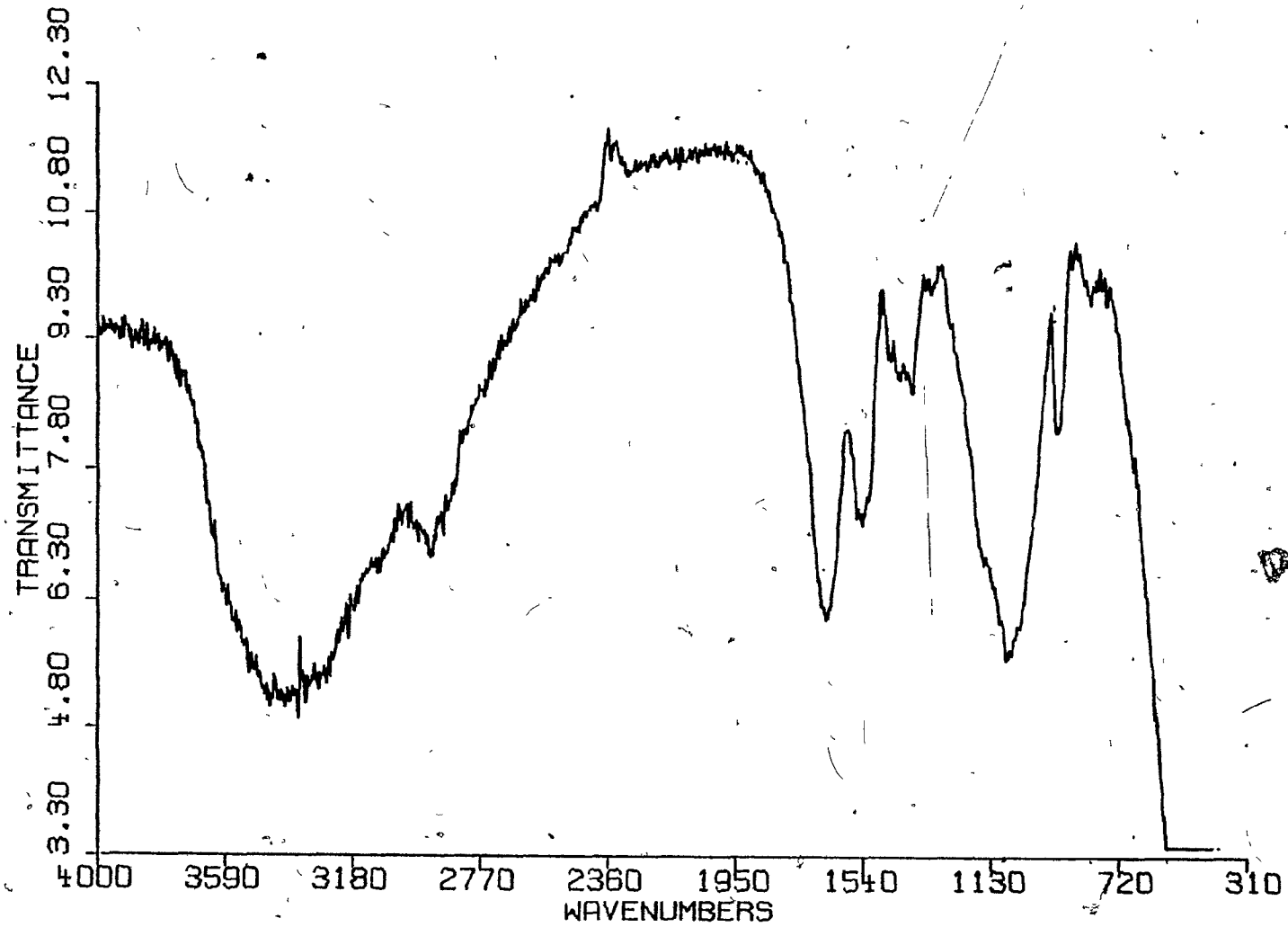
TRANSMITTANCE
3.30
4.80
6.30
7.80
9.30
10.80
12.30
4000
3590
3180
2770
2360
1950
1540
1130
720
310
WAVENUMBERS

FIGURE III-A.24 Comparison of the infrared spectrum of R. arrhizus cell walls before (1) and after (2) uranium biosorption.

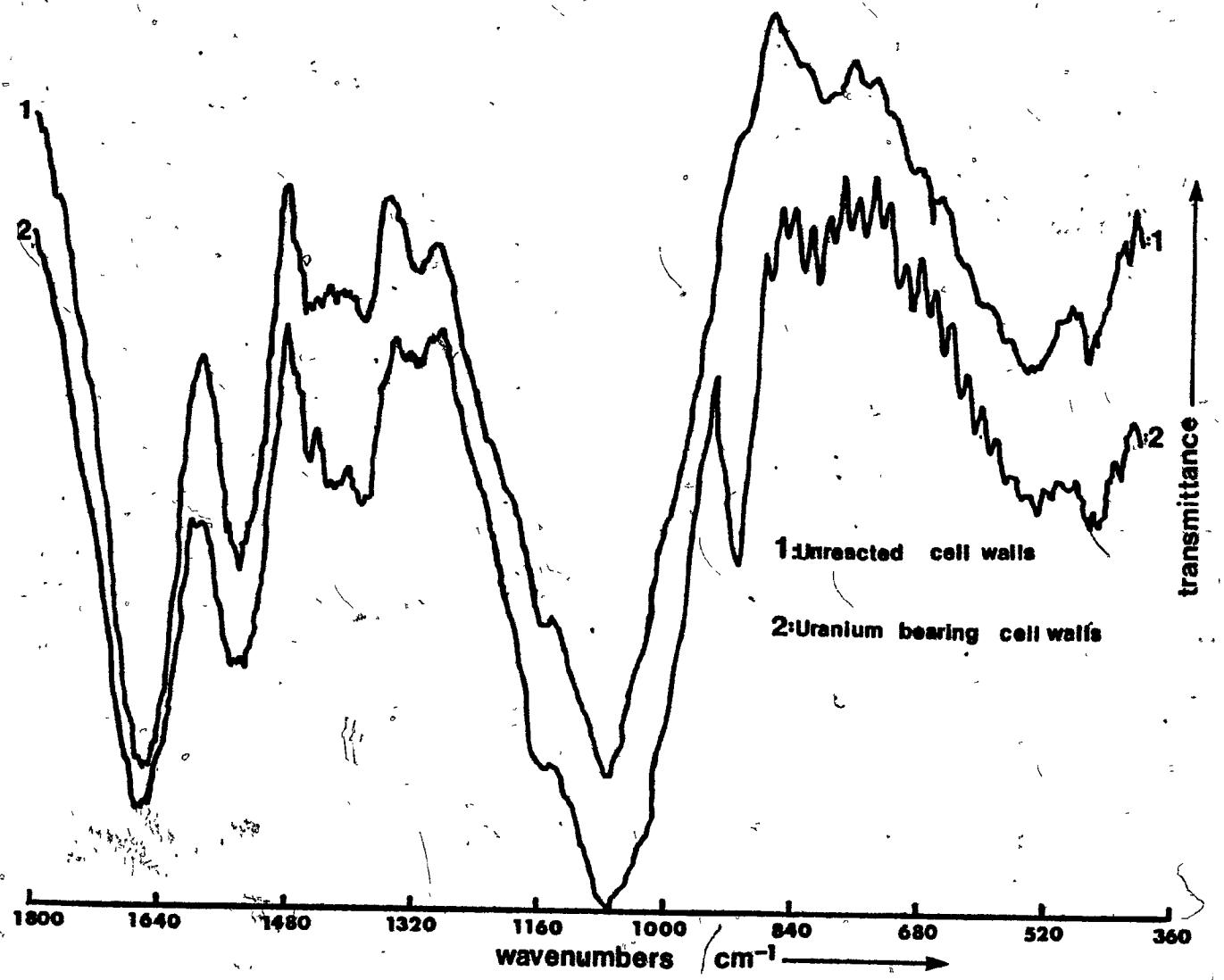
1
2
1
2
transmittance
1:Unreacted cell walls
2:Uranium bearing cell walls
1800
1640
1480
1320
1160
1000
840
680
520
360
wavenumbers cm⁻¹

FIGURE III-A.25 Far infrared spectrum of R. arrhizus cell walls before U(VI) biosorption.

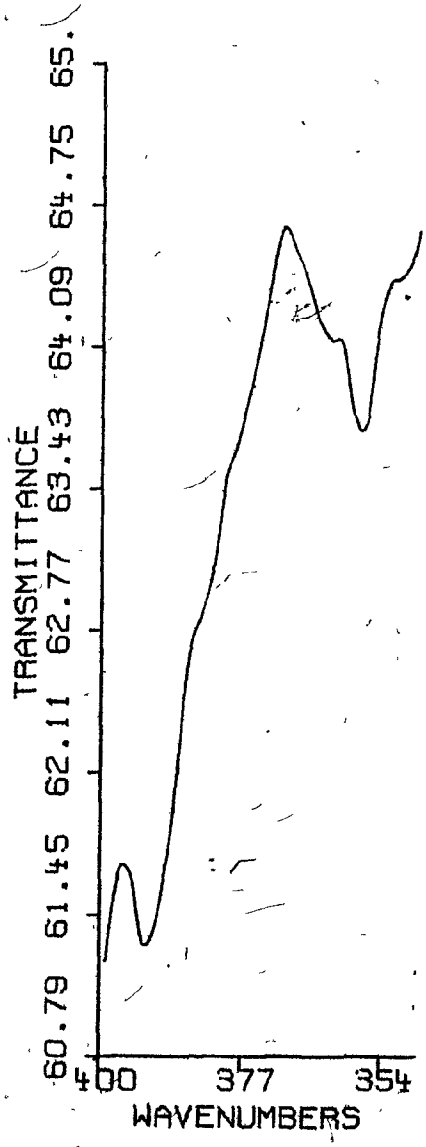
TRANSMITTANCE
60.79
61.45
62.11
62.77
63.43
64.09
64.75
65.
400
377
354
WAVENUMBERS

FIGURE III-A.26 Comparison of far (400-350 cm^{-1}) infrared spectra of R. arrhizus cell walls before (1) and after (2) U(VI) biosorption.

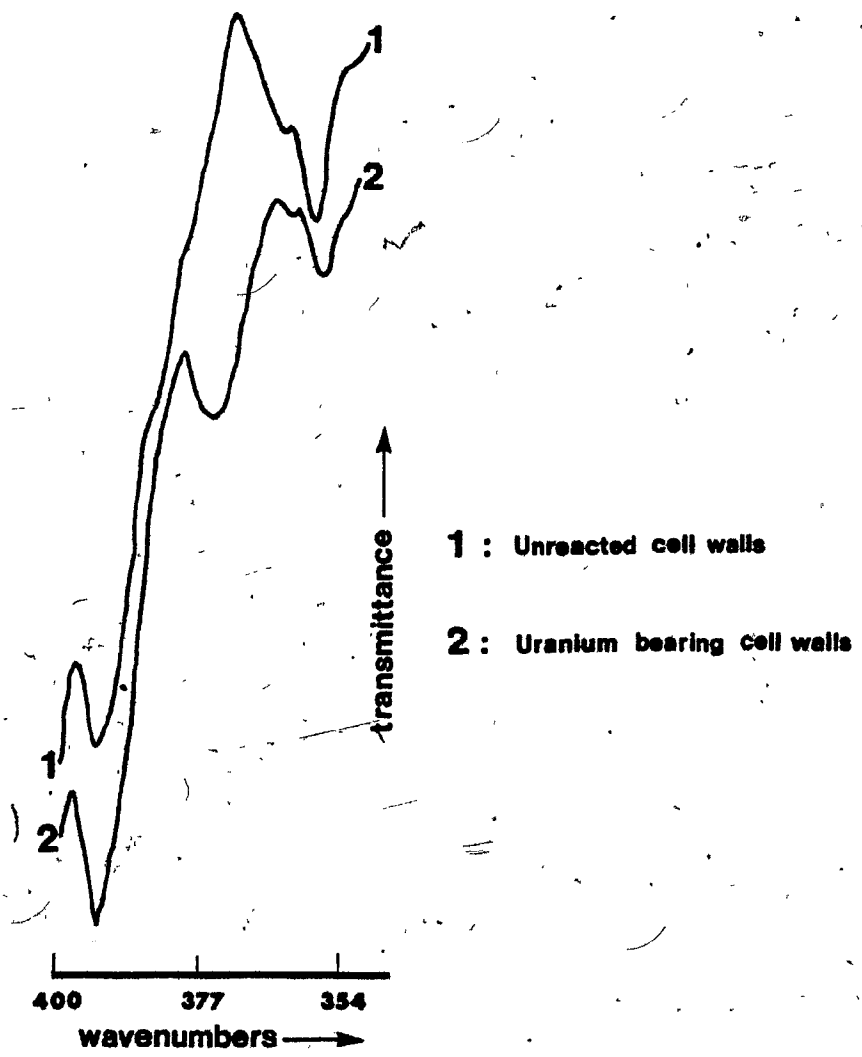
1
2
1
2
transmittance
400
377
354
wavenumbers
1 : Unreacted cell walls
2 : Uranium bearing cell walls

(Figure III-A.26). This new peak and the 908 cm^{-1} shifted ν_3 uranyl ion peak provide evidence of the coordination of uranium with the chitin nitrogen. Relevant discussion of the cell wall IR spectra in the range from 400 to 340 cm^{-1} is also presented in Chapter IV.

III-A.9 Co-ion Effect on Uranium Biosorption

The effect of the presence of the co-ions Fe^{+2} and Zn^{+2} in solution on the uranium biosorptive uptake capacity of R. arrhizus was examined. The percentage changes of uranium uptake are presented in Table III-A.5. At pH = 4 and constant initial uranium concentration (80 mg/l), bivalent iron suppressed the uranium biosorptive uptake capacity of R. arrhizus in direct proportion to the initial iron concentration in solution (Figure III-A.27).

Zinc caused similar suppression of uranium biosorptive uptake capacity for the two initial Zn^{+2} concentrations examined at pH = 4 and the same initial uranium concentration (Figure III-A.29).

The mechanism through which Zn^{+2} and Fe^{+2} suppress the uranium biosorptive uptake capacity of R. arrhizus will be discussed in Section IV-A.10.

At pH = 2, neither Zn^{+2} nor Fe^{+2} had an appreciable effect on R. arrhizus uranium uptake capacity, regardless of the initial co-ion concentration (Figures III-A.28 and III-A.30).

The co-ion uptake by R. arrhizus was determined, for either Fe^{+2} or Zn^{+2}, to be between 5 mg/g and 9 mg/g.

TABLE III-A.5

Co-Ion Effect on Uranium Biosorptive Uptake Capacity of R. arrhizus

Conditions	pH = 4, 80 mg/1 U^{+6}							pH = 2, 80 mg/1 U^{+6}					
Co-ion present	Fe^{+2}				Zn^{+2}			Fe^{+2}			Zn^{+2}		
Co-ion concentration mg/1	ø	30	100	1000	ø	20	50	ø	30	500	ø	20	50
U^{+6} uptake capacity mg/g*	170	133	73	45	170	118	118	88	92	88	88	90	90
% change of U^{+6} uptake	-	- 26%	- 59%	- 75%	-	- 34%	- 34%	-	- 4%	ø	-	+ 2%	+ 2%

* C_{eq} = 70 mg/1 U^{+6}

FIGURE III-A.27 Fe(II) effect on U(VI) biosorption plateau, pH = 4.

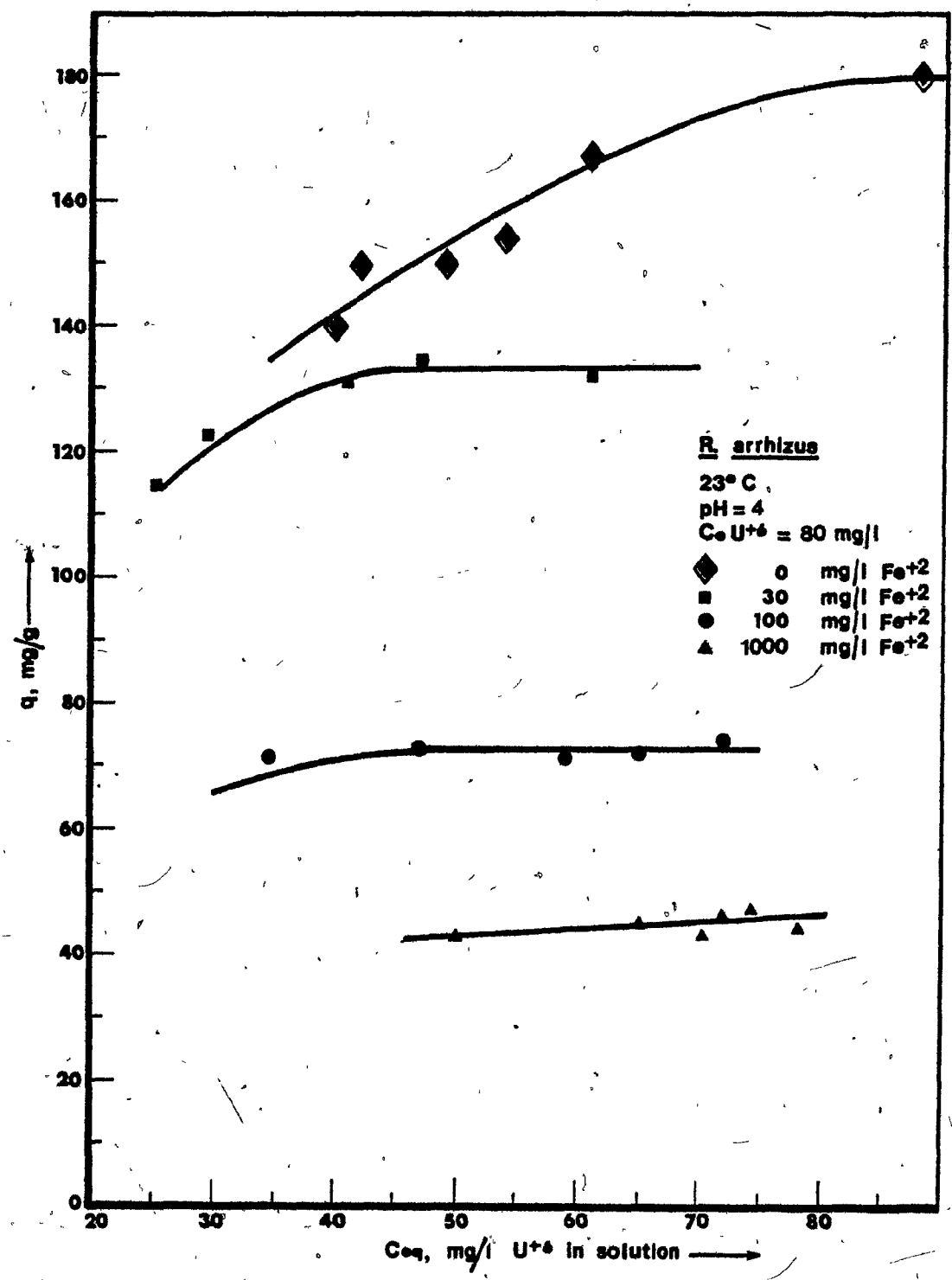
R. arrhizus
23° C
pH = 4
Co U+6 = 80 mg/l
0 mg/l Fe+2
30 mg/l Fe+2
100 mg/l Fe+2
1000 mg/l Fe+2
q, mg/g
Ceq, mg/l U+6 in solution
0
20
40
60
80
100
120
140
160
180
20
30
40
50
60
70
80

FIGURE III-A.28 Fe(II) effect on U(VI) biosorption plateau, pH = 2.

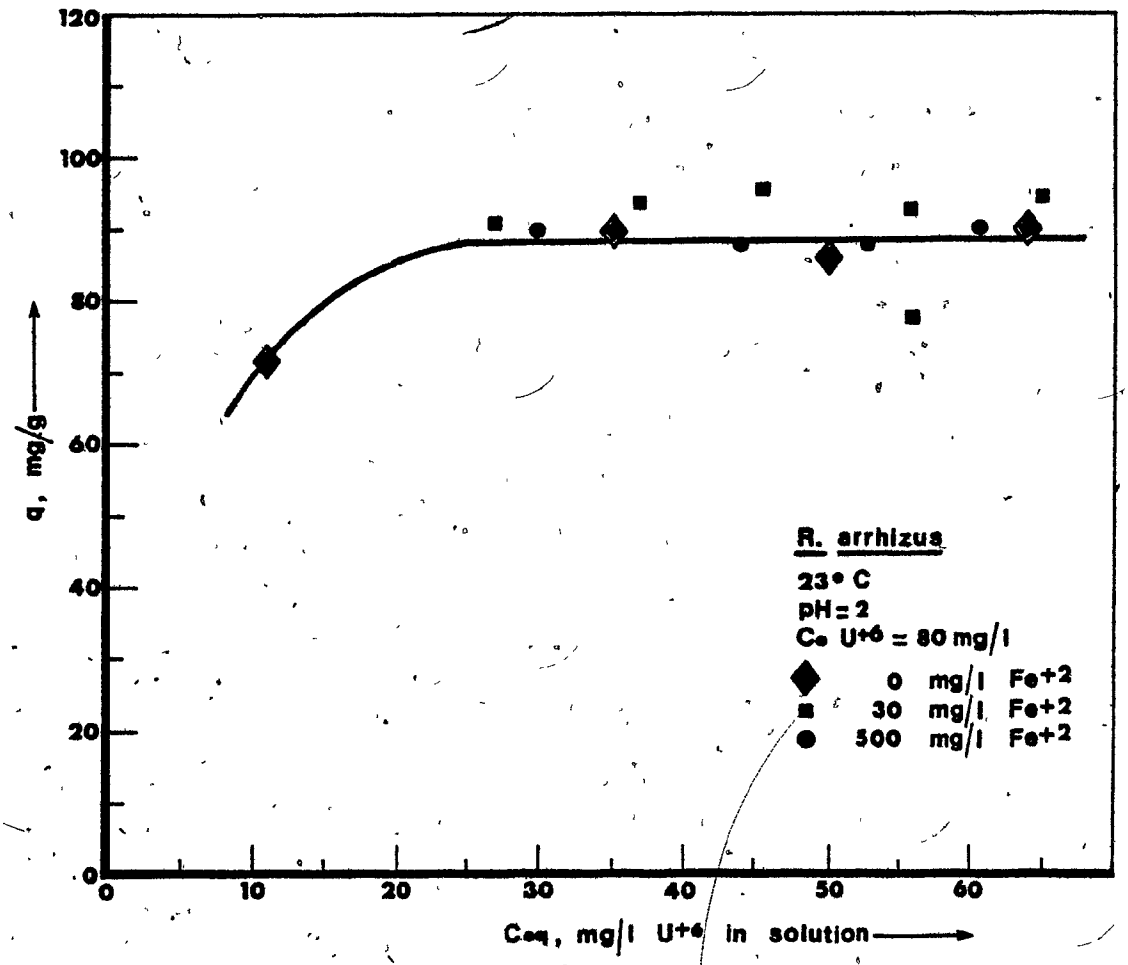
120
100
80
60
40
20
0
q, mg/g
0
10
20
30
40
50
60
Ceq, mg/l U+6 in solution
R. arrhizus
23° C
pH = 2
Co U+6 = 80 mg/l
0 mg/l Fe+2
30 mg/l Fe+2
500 mg/l Fe+2

FIGURE III-A.29 Zn(II) effect on U(VI) biosorption plateau, pH = 4.

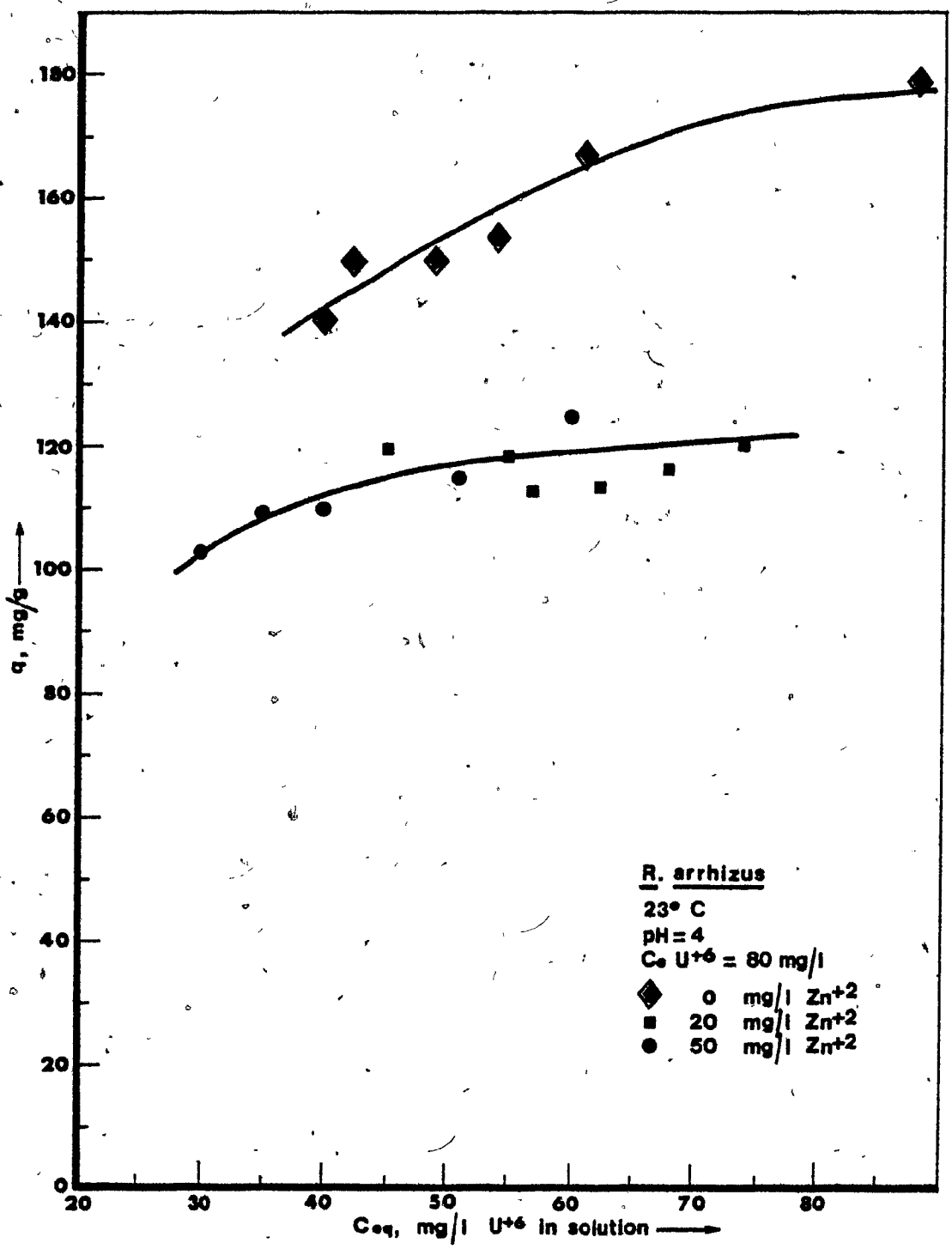
180
160
140
120
100
80
60
40
20
0
a, mg/g
20
30
40
50
60
70
80
Ceq, mg/l U+6 in solution
R. arrhizus
23° C
pH = 4
Ce U+6 = 80 mg/l
0 mg/l Zn+2
20 mg/l Zn+2
50 mg/l Zn+2

FIGURE III-A.30 Zn(II) effect on U(VI) biosorption plateau, pH = 2.

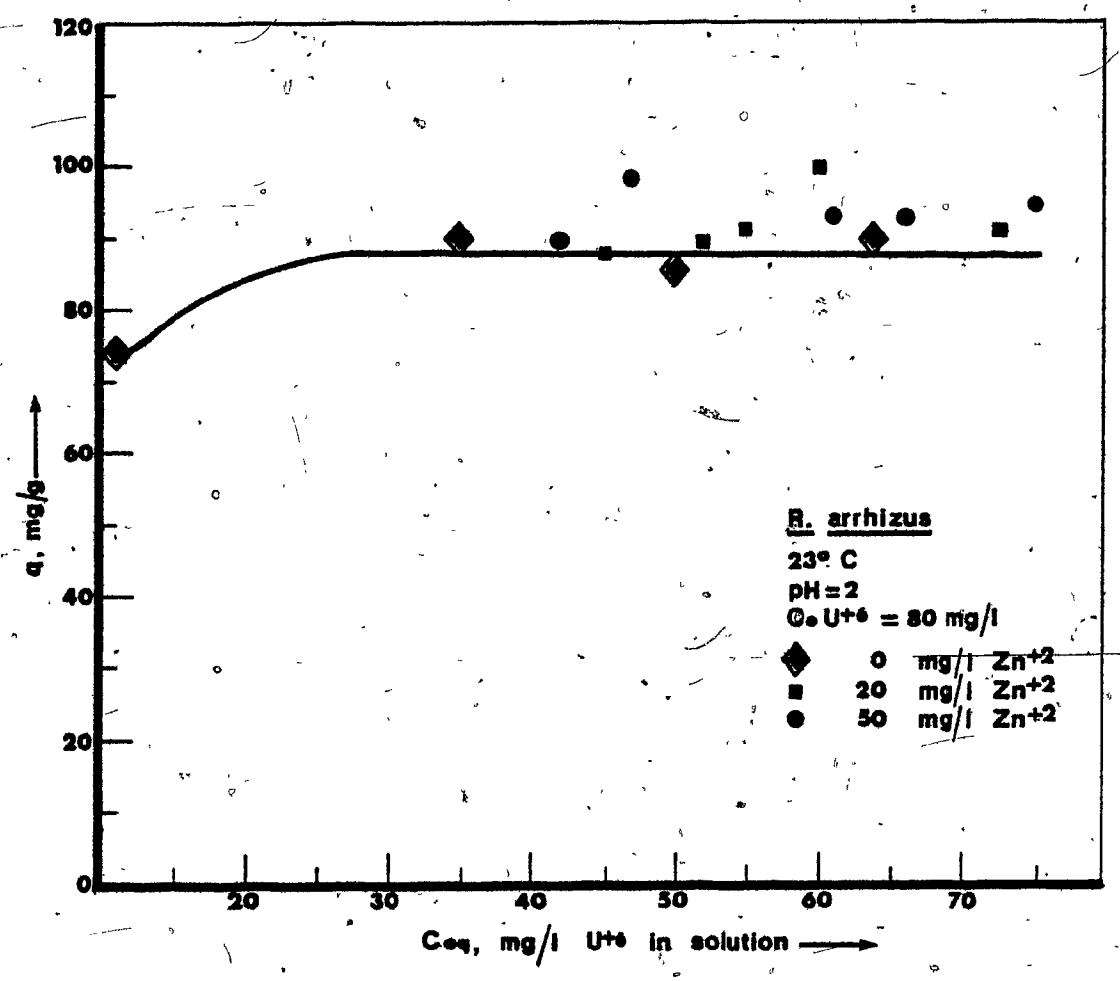
120
100
80
60
40
20
0
20
30
40
50
60
70
q, mg/g
Ceq, mg/l U+6 in solution
R. arrhizus
23° C
pH = 2
Co U+6 = 80 mg/l
0 mg/l Zn+2
20 mg/l Zn+2
50 mg/l Zn+2

III-A.10 Uranium Biosorption Kinetic Data

The instrumentation and the experimental techniques that were employed during the preliminary investigation of the kinetics of uranium biosorption by R. arrhizus have been described in Section II-8.

The response of the sampling system is summarized in Table III-A.6 where the analytically determined Zn^{+2} concentration of the sample is compared to the known Zn^{+2} concentration in the reactor solution. The data in the table clearly indicate that the sample concentration represented the reactor solution concentration accurately. Sample cross-contamination was not observed either as a step increase of the reactor solution Zn^{+2} concentration was accurately represented by respective samples withdrawn.

Table III-A.7 briefly presents the parameters under which typical kinetic experiments were executed. Kinetic experiments #3 and #4 were considered reference experiments. The effects of solution pH, temperature, initial uranium concentration and biomass dosage, may be seen in experiments #8, #7, #4 and #6, respectively.

All uranium biosorption kinetics curves determined at pH = 4 share common characteristics (Figures III-A.31 to III-A.33). Within the first 60 seconds of contact, the U(VI)-biomass system reached an initial equilibrium plateau that corresponded to approximately 66% of the total uranium uptake capacity of R. arrhizus. The biosorption

TABLE III-A.6

Sampling System Response Examination

Sample Number	Calculated Concentration C_c, mg/l	Measured Concentration C_m, mg/l	C_m/C_c %
1	10.0	10.0	100
2	12.0	12.0	100
3	13.9	14.1	102
4	17.9	17.8	99
5	21.9	21.5	98
6	23.9	24.0	100

TABLE III-A.7

Typical Experimental Conditions Employed in Uranium Kinetic Experiments

Experiment Set #	1	2	3	4	5	6	7	8
Agitation Rate RPM	800	1100	1300	1300	1300	1300	1300	1300
Initial U^{+6} Concentration mg/1	50	37	39	20	79	40	42	42
Biomass mg	150	120	148	148	143	77	149	135
Reaction Mixture Volume ml	995	989	990	997	1015	1000	1010	985
pH	4.0	4.0	4.0	4.0	4.0	4.0	4.0	2.0
T ^{o}C	23	23	23	23	23	23	6	23

FIGURE III-A.31 Uranium uptake rate curves.

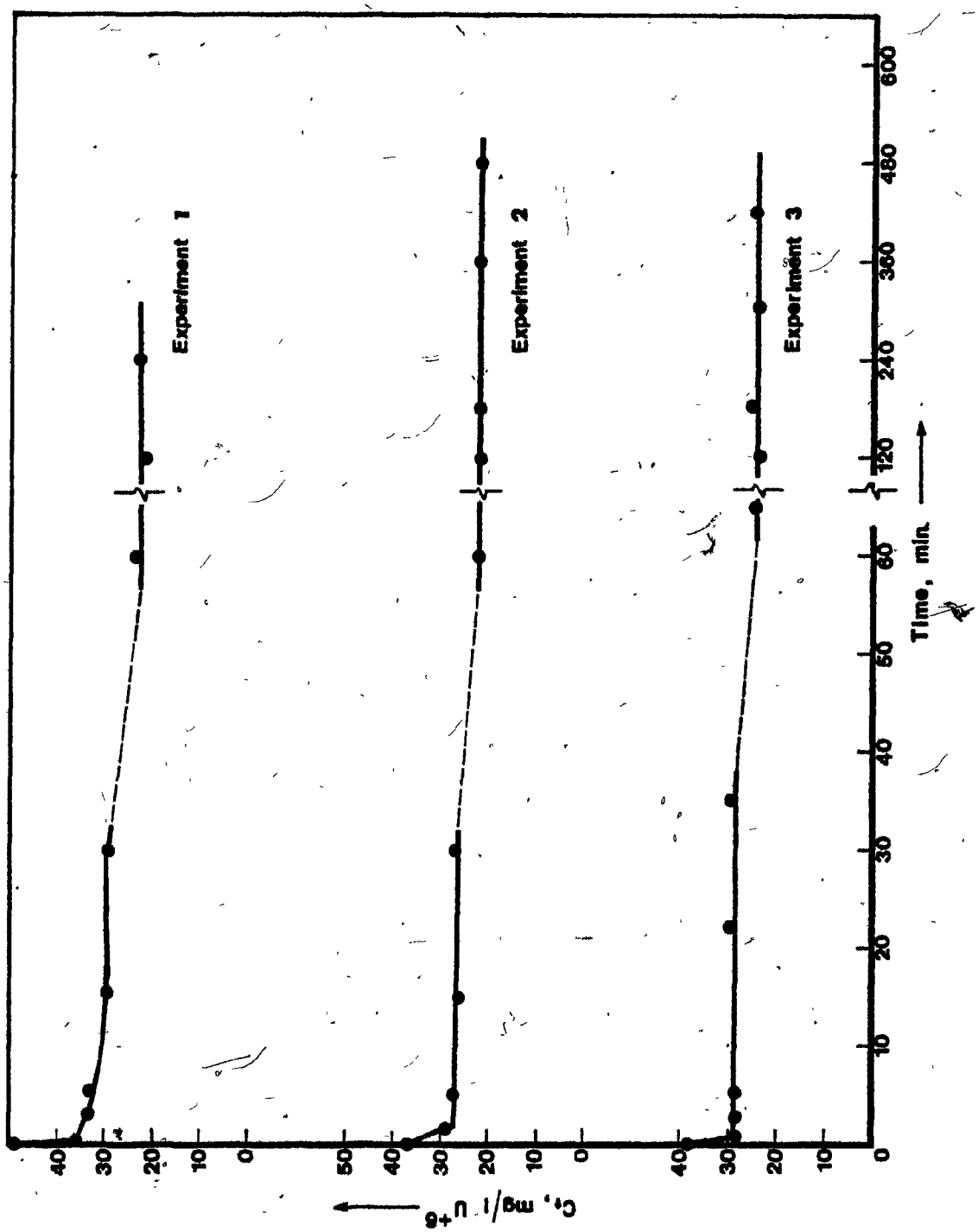
Experiment 1
Experiment 2
Experiment 3
Time, min.
C_t, mg/l U^{+6}
0
10
20
30
40
50
60
120
240
360
480
600

FIGURE III-A.32 Uranium uptake rate curves.

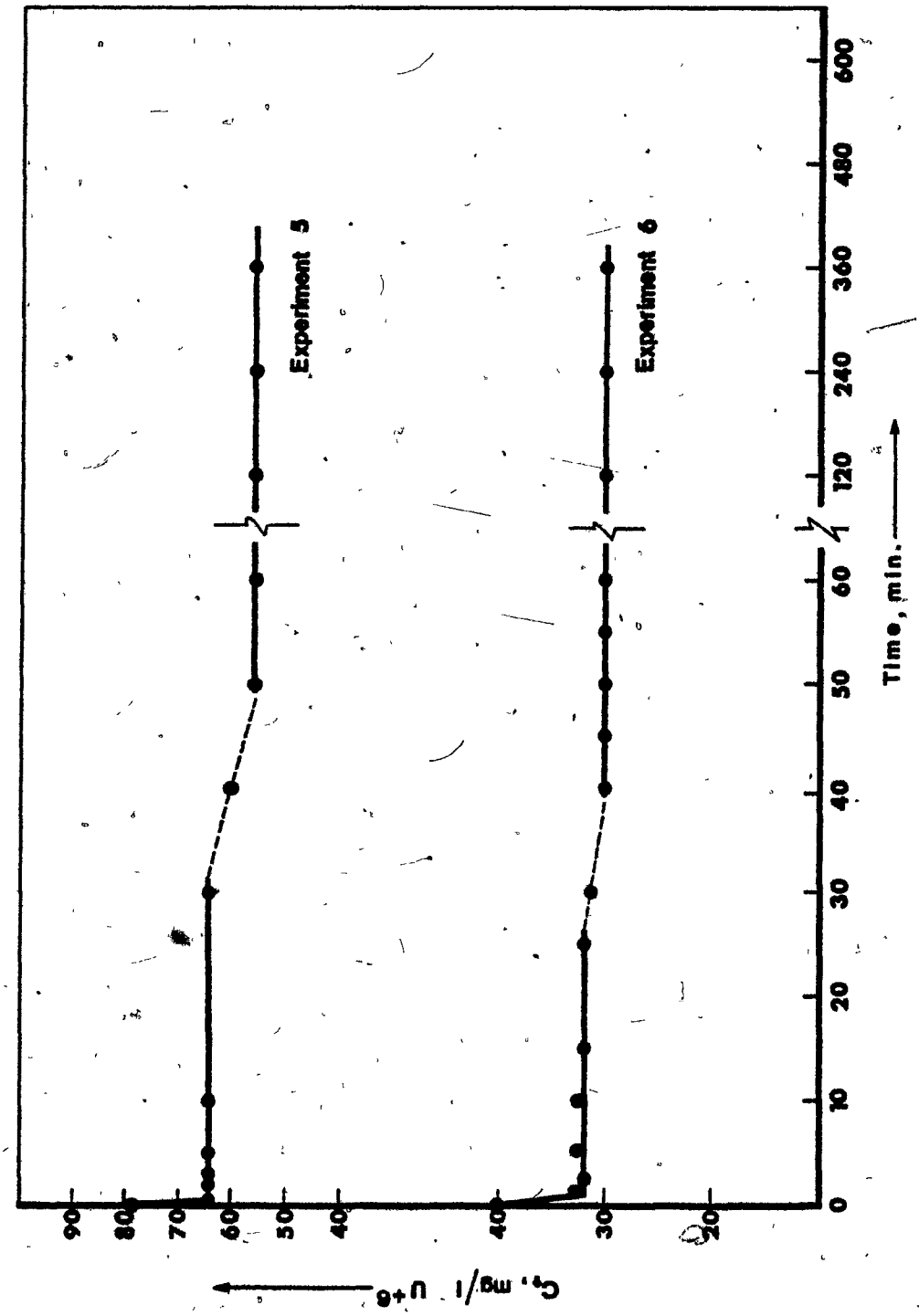
Experiment 5
Experiment 6
Time, min.
C_s, mg/l U^{+6}
0
10
20
30
40
50
60
120
240
360
480
600
90
80
70
60
50
40
40
30
20

FIGURE III-A.33 Uranium uptake rate curves.

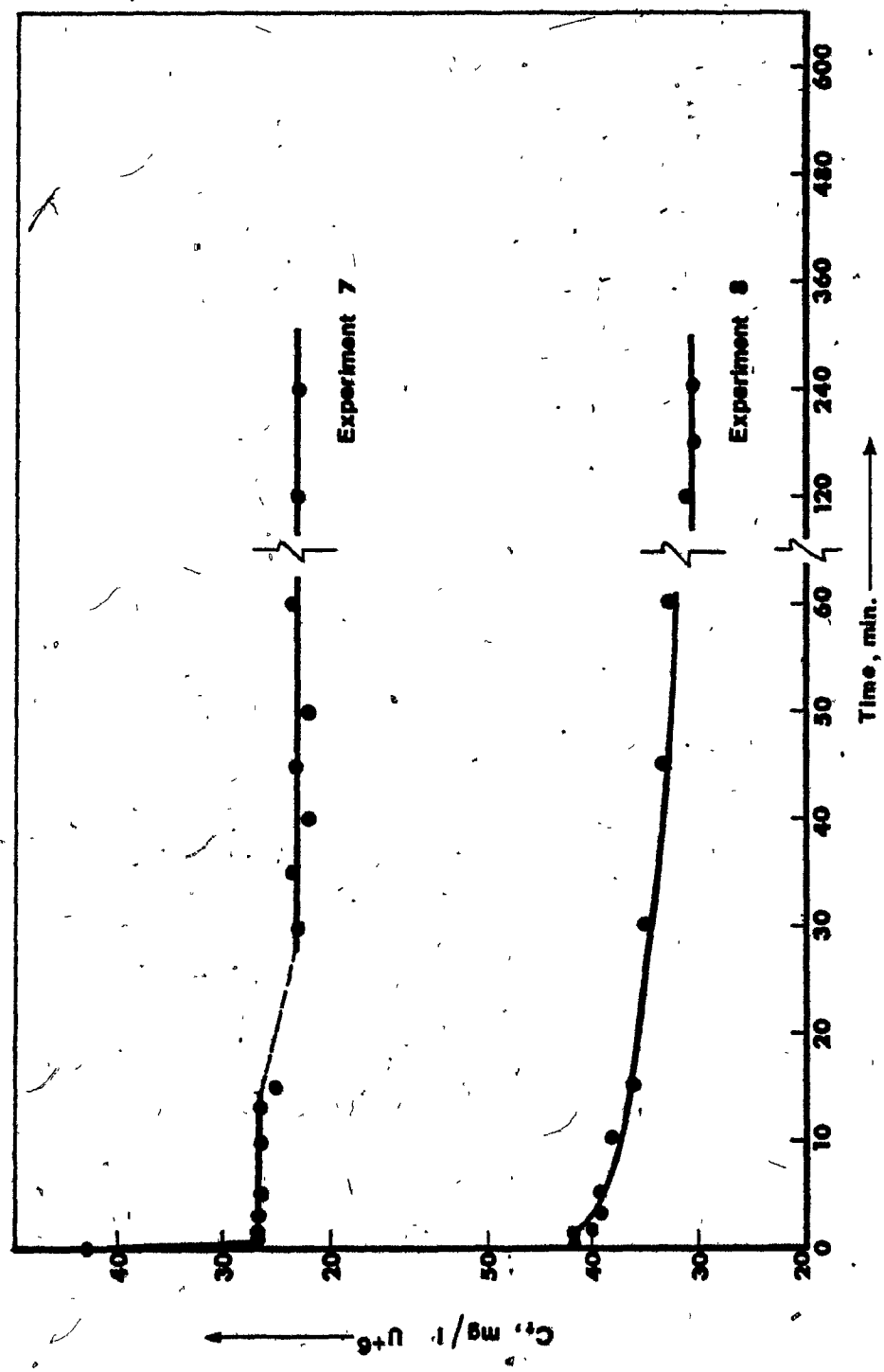
Experiment 7
Experiment 8
Time, min.
$C_{U^{+6}}$, mg/l
0
10
20
30
40
50
60
120
240
360
480
600
20
30
40
50
20
30
40

system remained stable at this initial plateau for approximately 0.5 hours. Within the next half-hour the biosorption system gradually reached the final equilibrium plateau corresponding to 100% of the uranium uptake capacity of the biomass. Solution pH strongly affected the rate of uranium uptake. At pH = 2 the uranium uptake rate was significantly lower (Figure III-A.33). Detailed experimental kinetic data for the experiments presented are available in Appendix E. A discussion of the kinetic results is available in Chapter IV.

III-B THORIUM

III-B.1 Thorium Equilibrium Uptake Studies

The experimentally determined thorium equilibrium uptake capacities of all tested materials are summarized in Table III-B.1. The thorium uptake capacities (mg/g) are presented at three selected thorium equilibrium solution concentrations.

Rhizopus arrhizus exhibited the highest thorium uptake capacity of approximately 170 mg/g, and a steep biosorption isotherm with high loadings at low equilibrium Th(IV) concentrations (Figure III-B.1). The biomass of *Rhizopus arrhizus* was, therefore, selected to be used for a more in-depth investigation of thorium biosorption.

Initial thorium concentration did not have a discernible effect on the observed thorium biosorption isotherms. Solution pH affected thorium biosorptive uptake. In general, lower thorium uptake was observed at pH = 2 than at pH = 4 or pH = 5 (Figures III-B.2, III-B.3). No difference in thorium biosorptive uptake was observed between pH = 4 and pH = 5 (Figure III-B.2). The effect of solution pH and initial

TABLE III-B.1

Thorium Biosorption Uptake Capacities, q (mg/g) . pH = 4,5

Residual Concentration mg/l	MATERIALS									
	A. terreus	*A. niger*	*P. fluorescens*	*S. niveus*	Municipal Act. Sludge	Phenolic Act. Sludge	*P. chrysogenum*	*R. arrhizus*	Ionex IRA-400	Act. Carbon F-400
5	3	10	8	10	36	27	118	132	3	29
30	6	17	13	17	48	46	145	163	8	(70)
100	8	25	19	25	(50)	(46)	(160)	(210)	(13)	(147)

FIGURE III-B.1 Qualitative comparison of thorium biosorption isotherms of some tested materials.

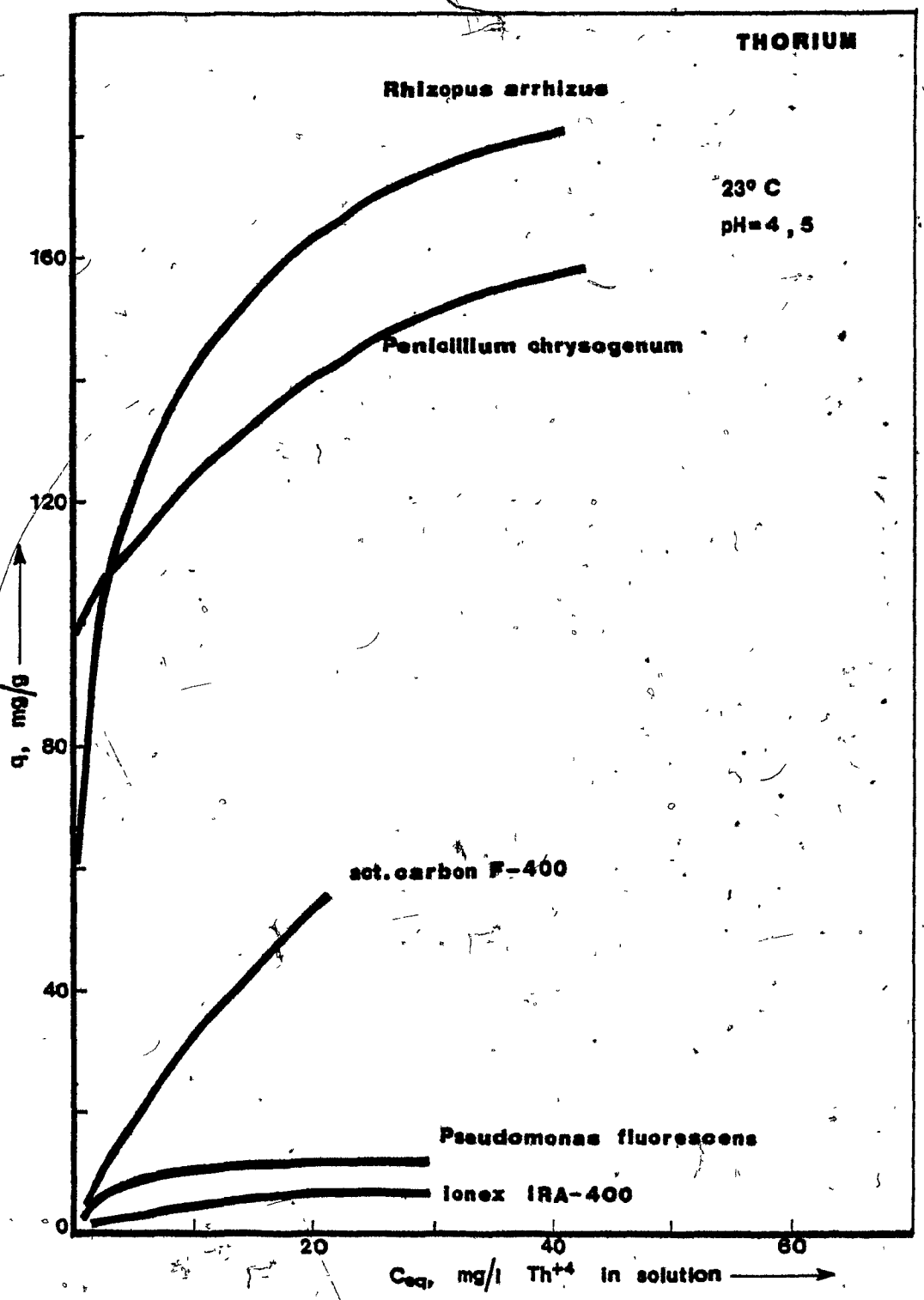
THORIUM
Rhizopus arrhizus
23° C
pH=4,5
Penicillium chrysogenum
act. carbon F-400
Pseudomonas fluorescens
Ionex IRA-400
160
120
80
40
0
20
40
60
q, mg/g
Ceq, mg/l Th+4 in solution

FIGURE III-B.2 Linearized thorium biosorption isotherms of *Rhizopus arrhizus* whole cells and cell walls. Temperature effect. (1) $q = 61.04\ C^{1/3.61}$ (5°C); (2) $q = 87.71\ C^{1/5.27}$ (23°C); (3) $q = 120.48\ C^{1/6.17}$ (40°C).

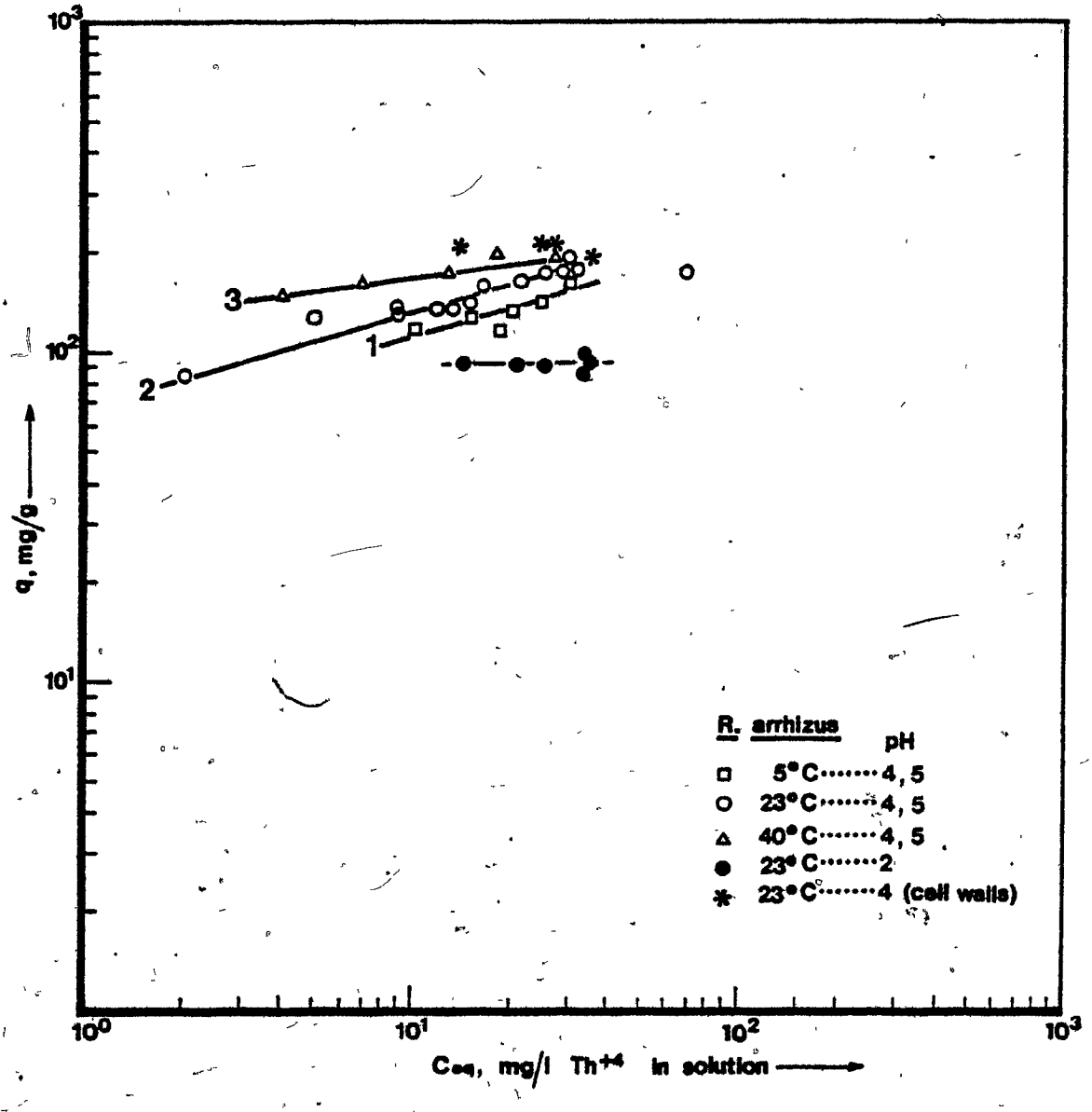
10^3
10^2
10^1
10^0
10^1
10^2
10^3
q, mg/g
C_{eq}, mg/l Th^{+4} in solution
1
2
3
R. arrhizus
pH
5°C·····4, 5
23°C·····4, 5
40°C·····4, 5
23°C·····2
23°C·····4 (cell walls)

FIGURE III-B.3 Linearized thorium biosorption isotherms for *Pseudomonas fluorescens* ($q = 2.54\ C^{1/2.82}$, pH = 2; $q = 4.83\ C^{1/3.37}$, pH = 4,5) and *Streptomyces niveus* ($q = 10.30\ C^{1/4.26}$, pH = 2; $q = 10.22\ C^{1/3.36}$, pH = 4,5).

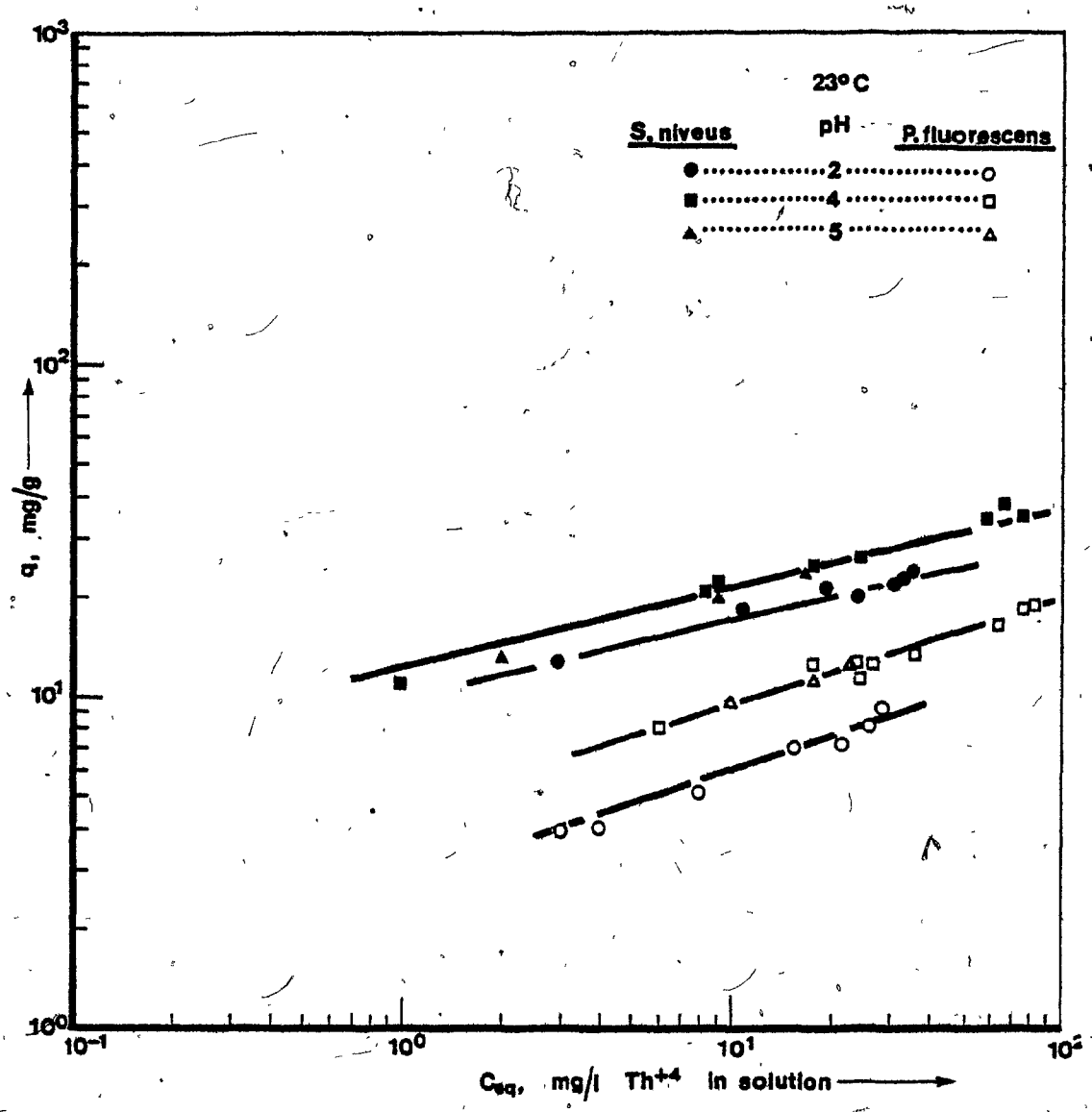
23° C
S. niveus
pH
P. fluorescens
2
4
5
q, mg/g
C_{eq}, mg/l Th^{+4} in solution
10^3
10^2
10^1
10^0
10^{-1}
10^0
10^1
10^2

Th(IV) concentration on q are discussed in Chapter IV.

III-B.2 Linearization of Thorium Biosorption Isotherms

The same methods as the ones described in Section III-A.2 were applied to linearize the thorium biosorption isotherm data and fit them to the adsorption isotherm models presented in Section III-A.2.

The S.E.E. values that resulted from the fitting of the Langmuir and Freundlich adsorption isotherm models to the experimentally determined thorium biosorption isotherm data are summarized in Table III-B.2. Both models successfully describe the biosorption isotherm data. Figures III-B.2 to III-B.8 present linearized thorium biosorption isotherms for the materials tested.

For some of the materials tested the Freundlich model was somewhat more successful in describing the experimental isotherm data; its S.E.E. values were slightly lower. All experimentally determined thorium biosorption isotherms were linearized according to the Freundlich model. Detailed data for all thorium biosorption isotherms are available in Appendix B.

III-B.3 Temperature Effect on q

The biomass of R. arrhizus was used to examine the effect of temperature on the thorium biosorptive uptake capacity, q (Figure III-B.2).

A small increase in thorium uptake was observed when the temperature increased from 5°C to 40°C. Table III-B.3 summarizes the

TABLE III-B.2

S.E.E.* Values for Thorium Biosorption Isotherms

Material	pH = 4,5		pH = 2	
	Langmuir	Freundlich (Q; n)	Langmuir	Freundlich (Q; n)
A. niger	0.84	1.29 (5.63; 3.14)	0.84	1.29 (5.63; 3.14)
A. terreus	3.46	4.06 (5.82; 76.04)	-	-
P. fluorescens	2.21	0.77 (6.68; 5.61)	0.14	1.30 (3.79; 77.78)
S. niveus	3.38	2.39 (10.37; 3.50)	3.38	2.39 (10.76; 3.76)
Municipal sludge	9.98	8.29 (16.34; 2.74)	9.98	8.30 (19.31; 3.27)
"Phenolic" sludge	2.52	5.79 (7.81; 2.74)	4.06	3.37 (21.44; 5.05)
R. arrhizus	47.44	22.09 (63.84; 3.05)	18.18	18.18 (52.42; 5.43)
P. chrysogenum	15.34	16.01 (107.27; 9.48)	8.93	10.65 (92.08; 28.68)
IRA-400	1.85	1.08 (1.31; 1.92)	-	-
F-400	12.56	12.82 (10.68; 1.87)	1.12	1.10 (0.30; 1.29)

* Overall S.E.E.

TABLE III-B.3

Temperature Effect on q . Th(IV)

C_{eq} mg/1 Th^{+4}	Δq* Temperature Increase ($T_1 \rightarrow T_2$ °C) 5 → 23	23 → 40	5 → 40
15	+ 14	+ 28	+ 45
20	+ 11	+ 26	+ 40
30	+ 6	+ 25	+ 33

*q_{T_i} values calculated from regression equations,

$$\Delta q = \frac{q_{T_2} - q_{T_1}}{q_{T_1}} \times 100.$$

FIGURE III-B.4 Linearized thorium biosorption isotherms for *Aspergillus niger* ($q = 6.08\ C^{1/3.23}$, pH = 2,4,5).

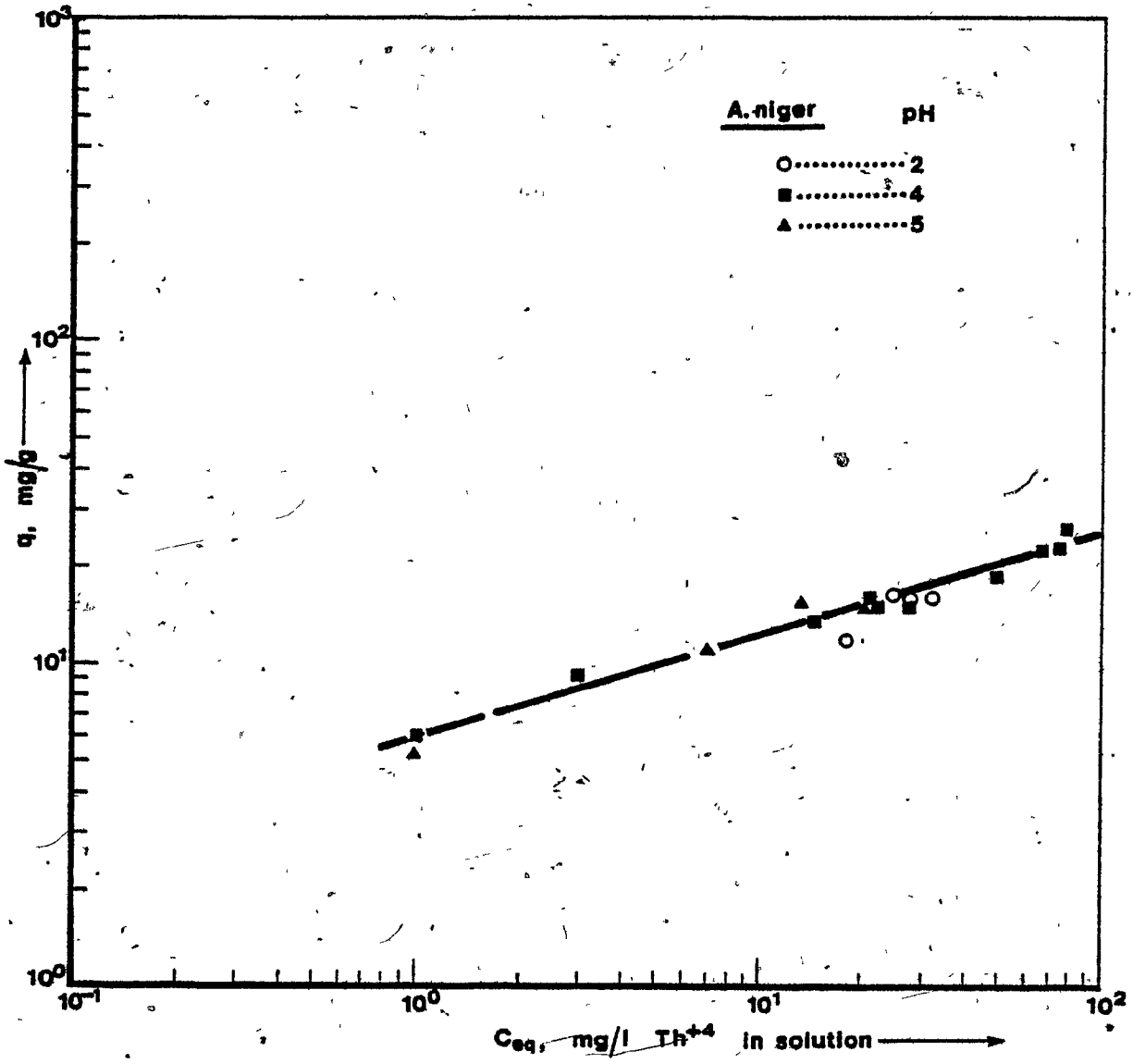
A. niger
pH
2
4
5
q, mg/g
10^3
10^2
10^1
10^0
10^{-1}
10^0
10^1
10^2
C_{eq}, mg/l Th^{+4} in solution

FIGURE III-B.5 Linearized thorium uptake isotherms for IRA-400 ($q = 1.54\ C^{1/2.16}$, pH = 4,5) and for F-400 ($q = 7.12\ C^{1/1.52}$, pH = 4,5).

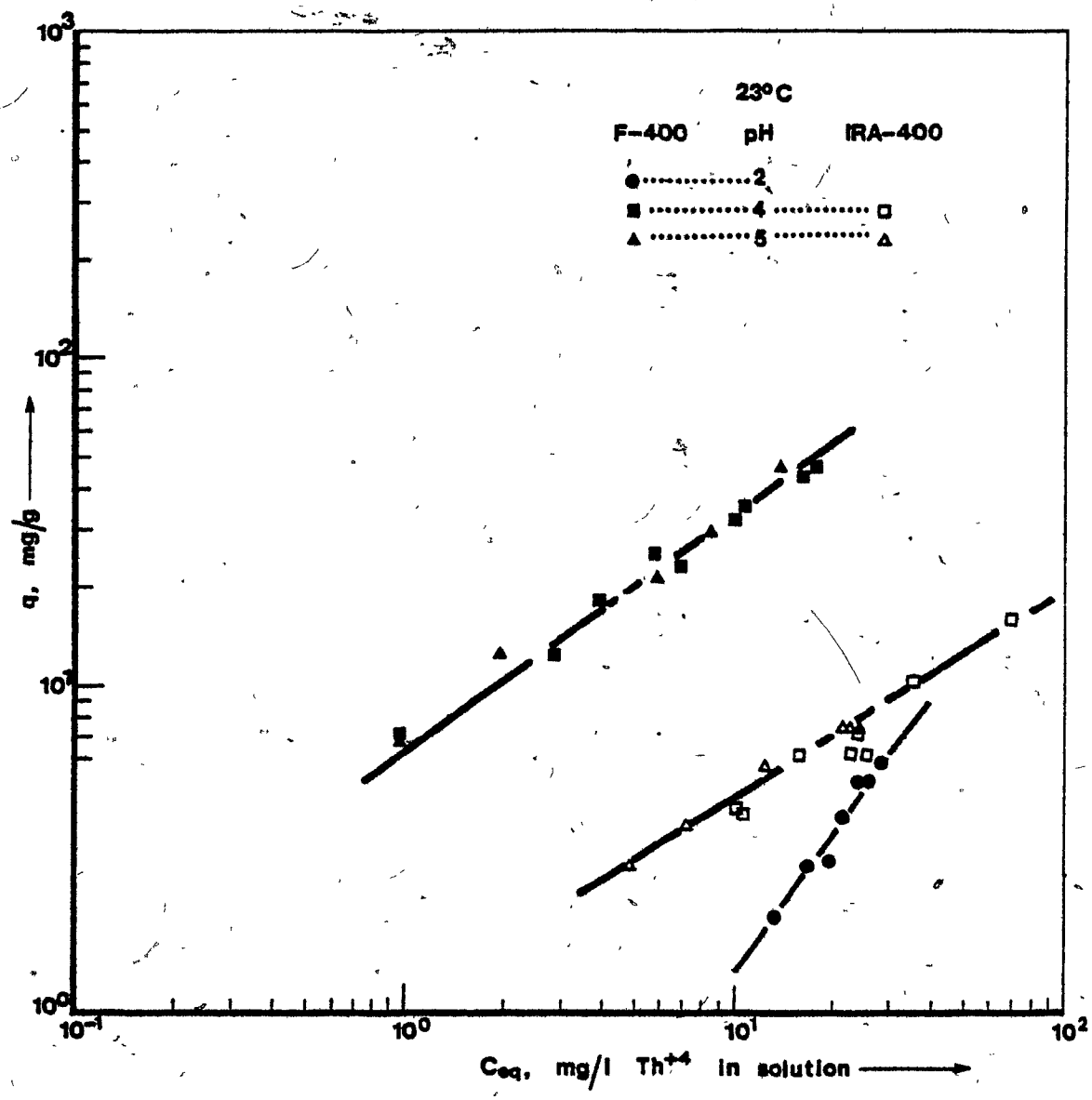
23°C
F-400
pH
IRA-400
2
4
5
10^3
10^2
10^1
10^0
10^{-1}
10^0
10^1
10^2
q, mg/g
C_{eq}, mg/l Th^{+4} in solution

FIGURE III-B.6 Linearized thorium biosorption isotherm for municipal activated sludge.
($q = 24.41C^{1/4.62}$, pH = 3, 4, 5)

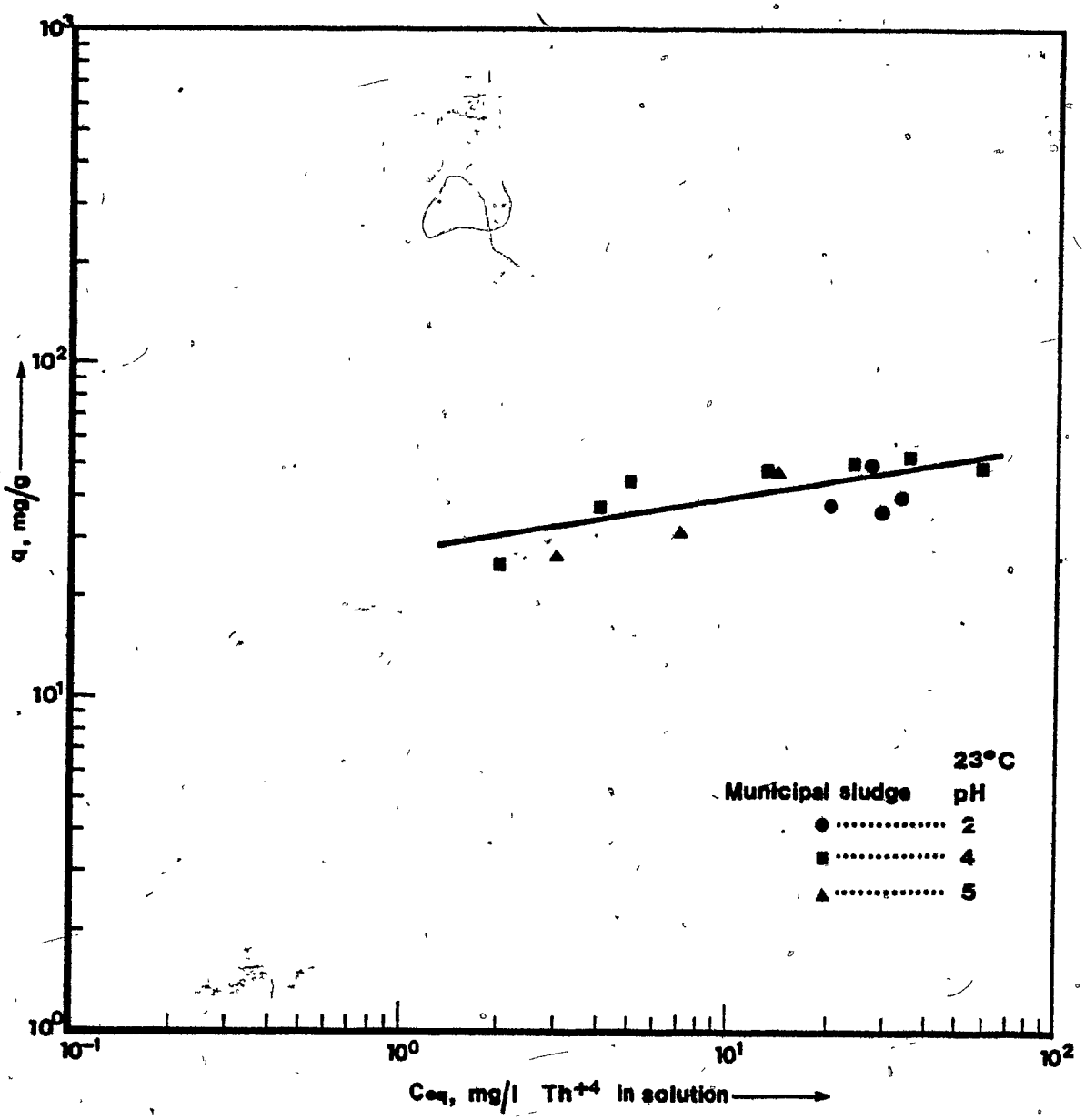
10^3
10^2
10^1
10^0
q, mg/g
10^{-1}
10^0
10^1
10^2
C_{eq}, mg/l Th^{+4} in solution
23°C
Municipal sludge
pH
2
4
5

FIGURE III-B.7 Linearized thorium biosorption isotherms for <u>Penicillium chrysogenum</u>.
($q = 96.13C^{1/8.42}$, pH = 4, 5)

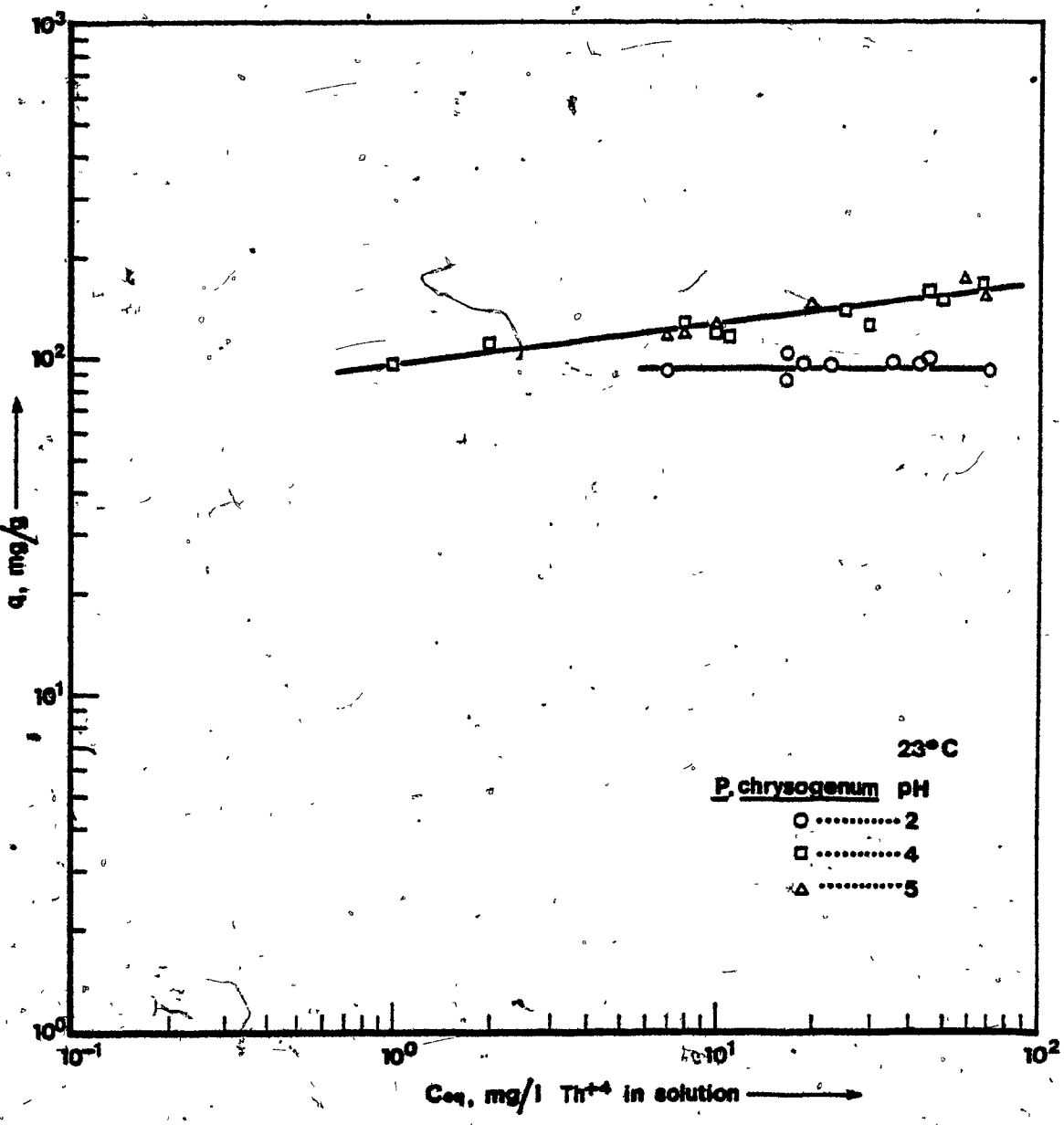
10^3
10^2
10^1
10^0
q, mg/g
10^{-1}
10^0
10^1
10^2
Ceq, mg/l Th^{+4} in solution
23°C
P. chrysogenum pH
2
4
5

FIGURE III-B.8 Linearized thorium biosorption isotherm for industrial activated sludge:
((1): $q = 13.28C^{1/2.34}$;
(2): $q = 43.54C^{1/0.01}$, pH = 4, 5)

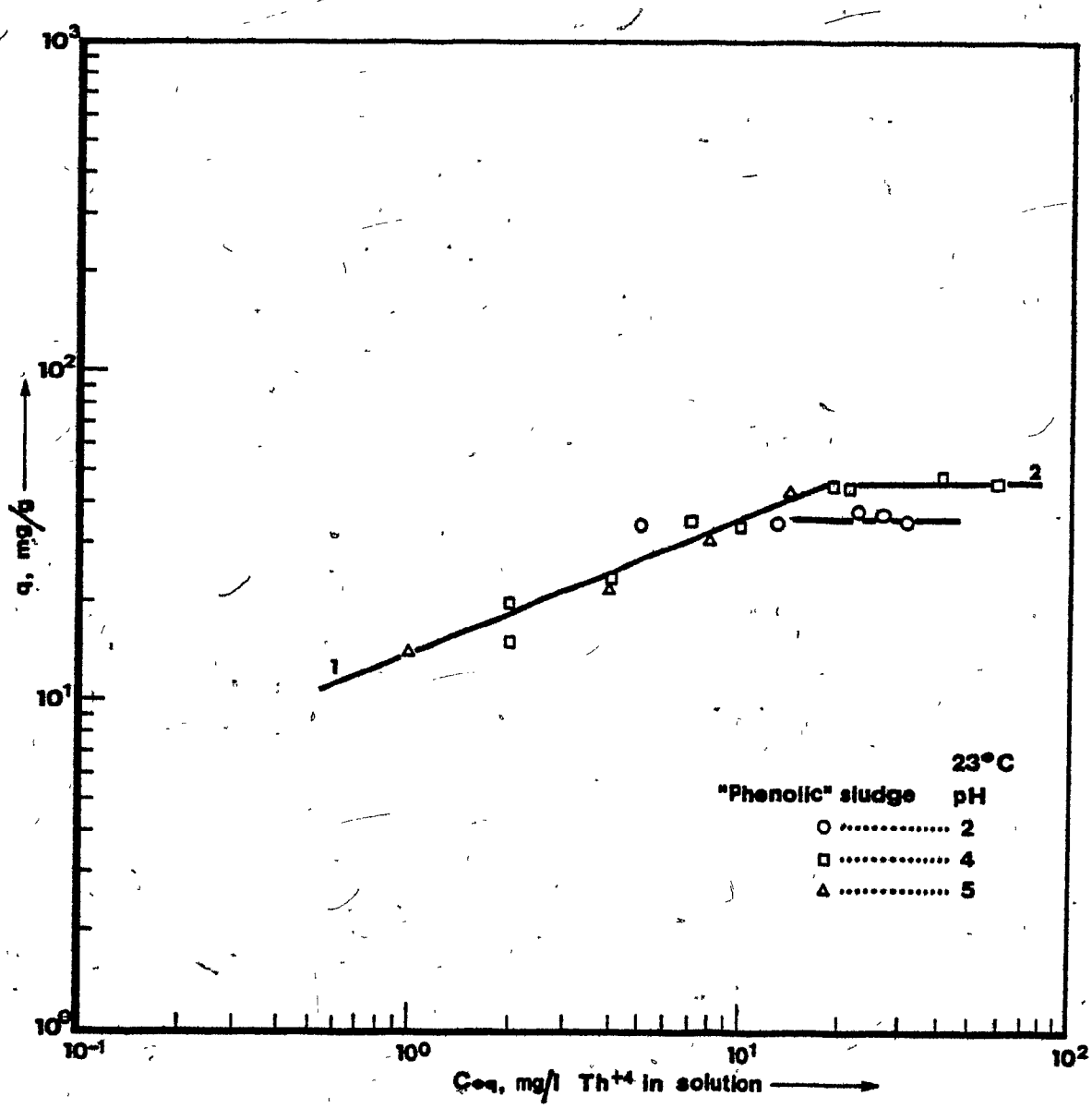
10^3
10^2
10^1
10^0
q, mg/g
1
2
23°C
"Phenolic" sludge pH
○ 2
□ 4
△ 5
10^{-1}
10^0
10^1
10^2
Ceq, mg/l Th^{+4} in solution

observed changes in thorium biosorptive uptake with temperature at three selected equilibrium thorium concentrations. Observed differences were significant for temperature changes from 23° to 40°C and from 5°C to 40°C.

The effect of temperature on the thorium biosorptive uptake capacity of R. arrhizus was not very pronounced.

III-B.4 Pure Cell Wall Preparation Thorium Uptake

The thorium uptake capacity of the R. arrhizus cell wall preparation was determined at pH = 4 and at 23°C. As in the case of uranium (III-A.4), the cell wall sample presented marginally higher thorium uptake than the whole mycelia under the same conditions (Figure III-B.2). This indicates that the cell wall of the R. arrhizus mycelium is mainly responsible for the biosorptive uptake of thorium. Confirmation of this indication was, however, necessary.

III-B.5 Electron Microscopy of Thorium Biosorption

In order to further investigate the indication that thorium is mainly taken up by the R. arrhizus cell wall, electron microscopic examination of R. arrhizus mycelia before and after thorium biosorption was undertaken. The same method as the one applied for uranium (II-3 and III-A.5) was employed. Figure III-B.9 presents a typical electron micrograph of a R. arrhizus mycelium cell wall before thorium biosorption. The absence of any electron-dense material is obvious. Thorium uptake is evident, as there are electron-dense regions, on the typical electron micrographs of thorium-exposed R. arrhizus mycelium cell walls

FIGURE III-B.9 Virgin *R. arrhizus* cell walls. Electron micrograph. (80,000 X).

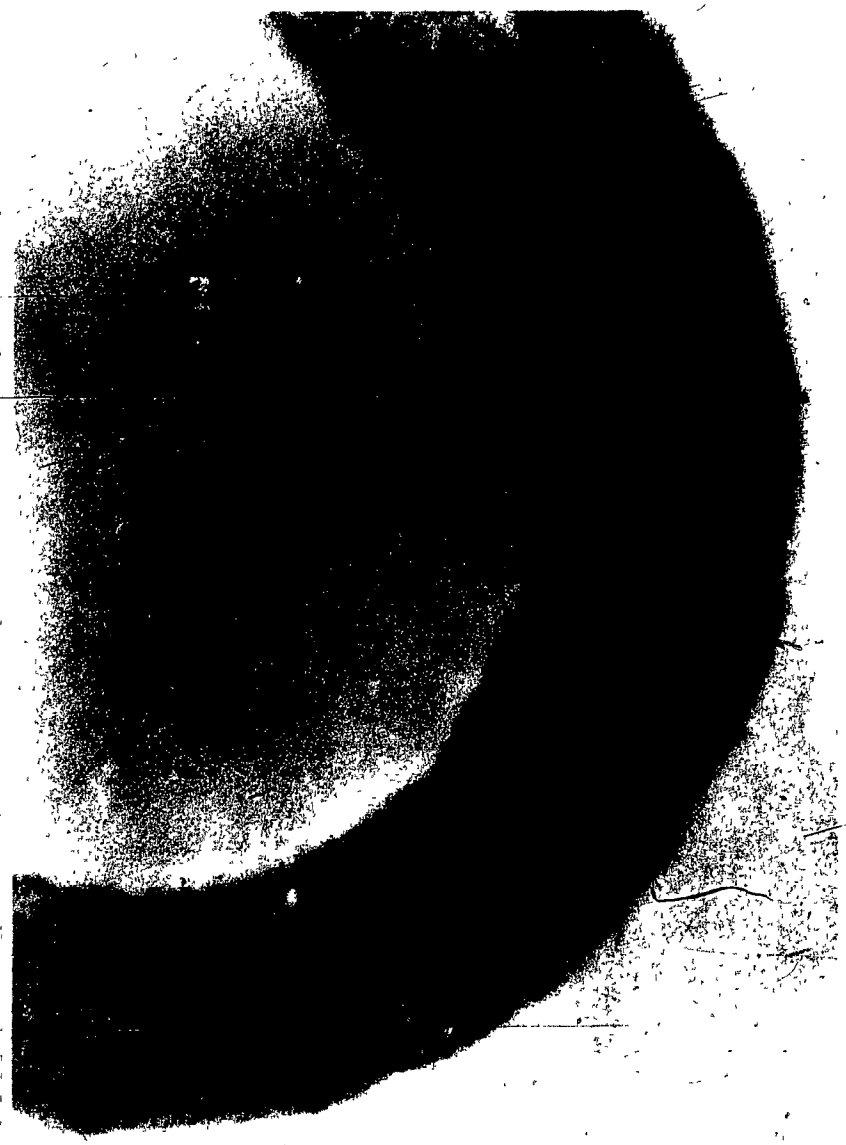

taken at two different magnifications (Figures III-B.10 to III-B.11). The thorium uptake of the specific sample presented on the micrographs was 168 mg/g at pH = 4. Figure III-B.12 presents an electron micrograph of R. arrhizus cell wall following thorium uptake at pH = 2.

Following thorium biosorption by R. arrhizus at pH = 4, a strongly electron dense area appeared on the outer section of the cell wall (Figure III-B.10). The appearance of this band indicated that the outer section of the mycelium cell wall had retained most of the biosorbed thorium.

The observed electron dense area can be considered to contain most of the biosorbed thorium as no other parts of the cell increased their electron scattering ability following thorium uptake.

Conclusive determination of the identity of the electron dense material as thorium was achieved through X-ray Energy Dispersion analysis of the thin sections that were examined under the electron microscope. Thorium was only detected in the outer, electron dense areas of the cell wall. Figures III-B.13 and III-B.14 present typical X-ray E.D.A. spectra of the outer region of the R. arrhizus cell wall before and after thorium uptake. The section of the spectrum containing the M thorium spectral line is shown. The white marker line indicates the exact position of the thorium spectral line. An energy level considerably above the background was observed following thorium uptake (Figure III-B.14). Figures III-B.15 and III-B.16 present typical x-ray E.D.A. spectra recorded when the probe was focussed on the inner cell wall region, the cytoplasmic region and the background. Before thorium uptake (Figure III-B.15) and after thorium biosorption (Figure III-B.16)

FIGURE III-B.10 R. arrhizus mycelium following thorium biosorption. Electron micrograph. (14,000 X). pH = 4

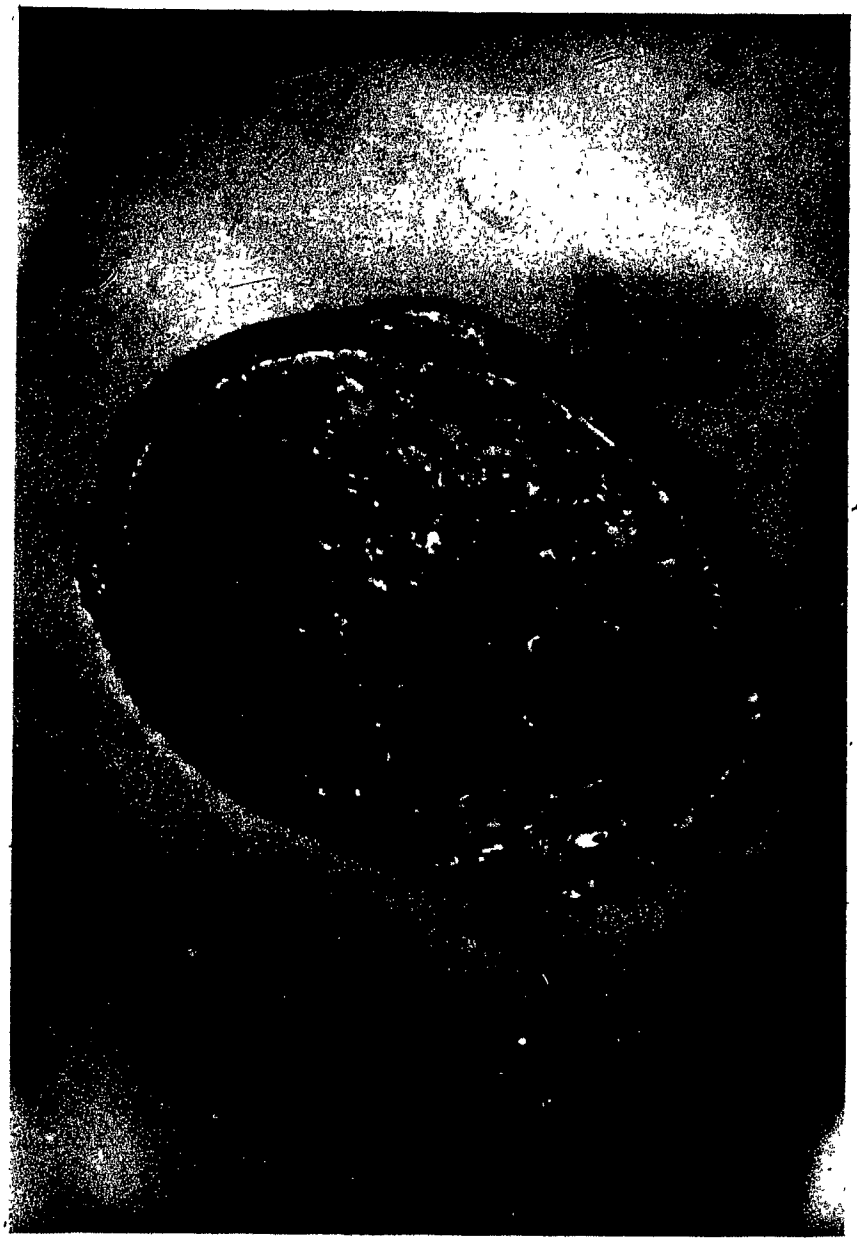

FIGURE III-B.11 R. arrhizus cell wall following thorium biosorption. Electron micrograph (80,000 X). pH = 4

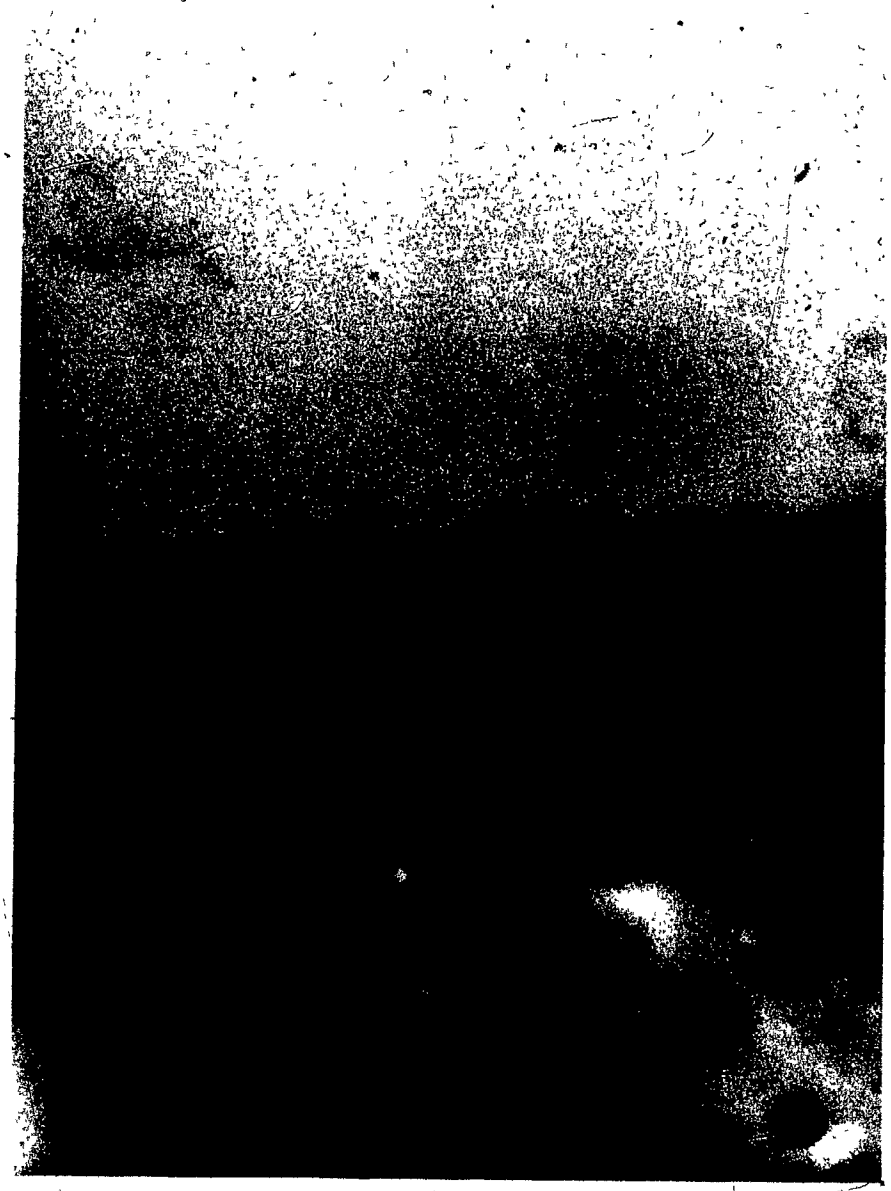

FIGURE III-B.12 R. arrhizus cell wall following thorium biosorption. Electron Micrograph (80,000 X). pH = 2

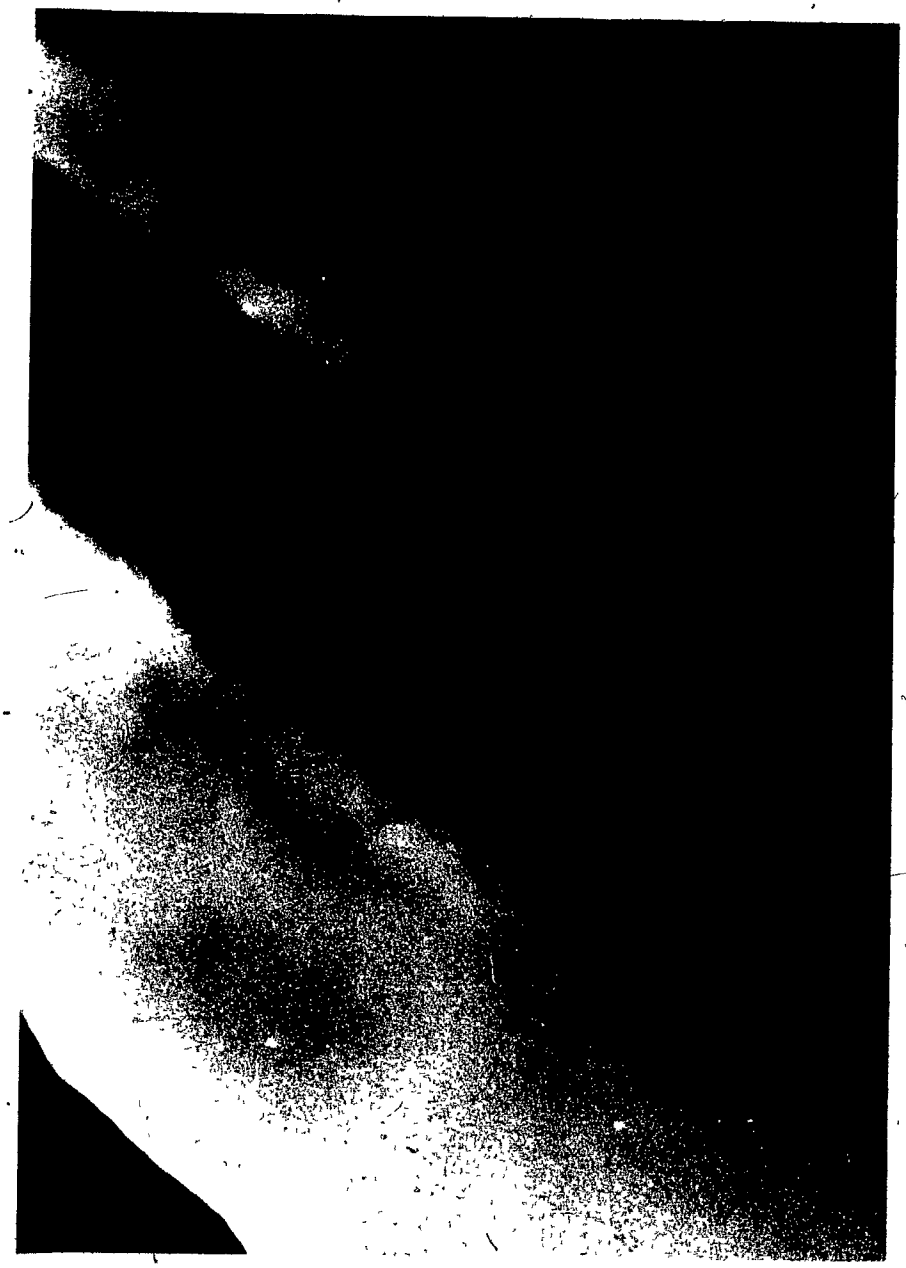

FIGURE III-B.13 Typical X-rays E.D.A. spectrum. Thorium M line of R. arrhizus cell wall electron dense areas before thorium biosorption.

FIGURE III-B.14 Typical X-rays E.D.A. spectrum. Thorium M line of R. arrhizus cell wall electron dense areas following thorium biosorption.

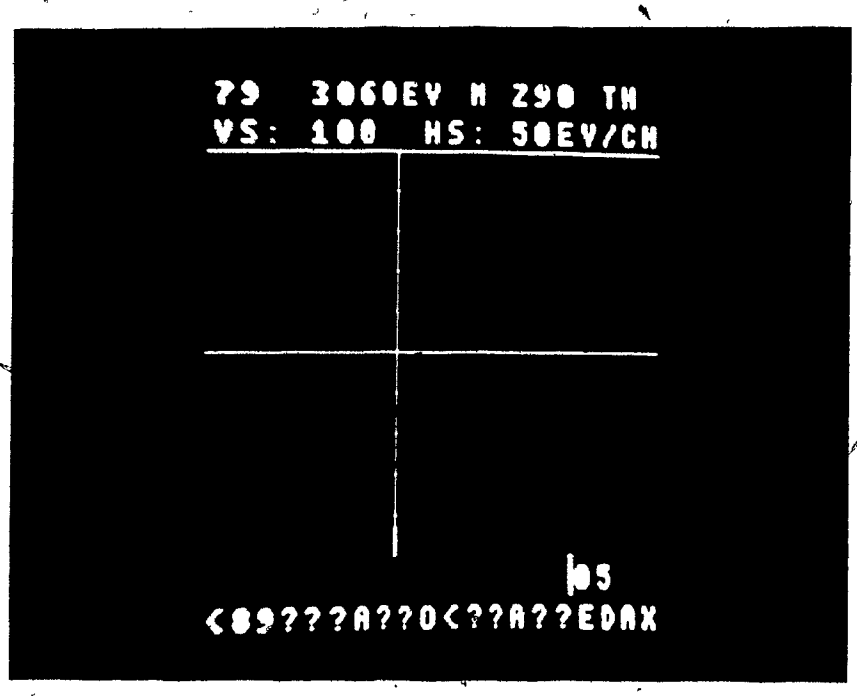
79 3060EV M Z90 TM
VS: 100 HS: 50EV/CH
05
<89???A??D<??A??EDAX

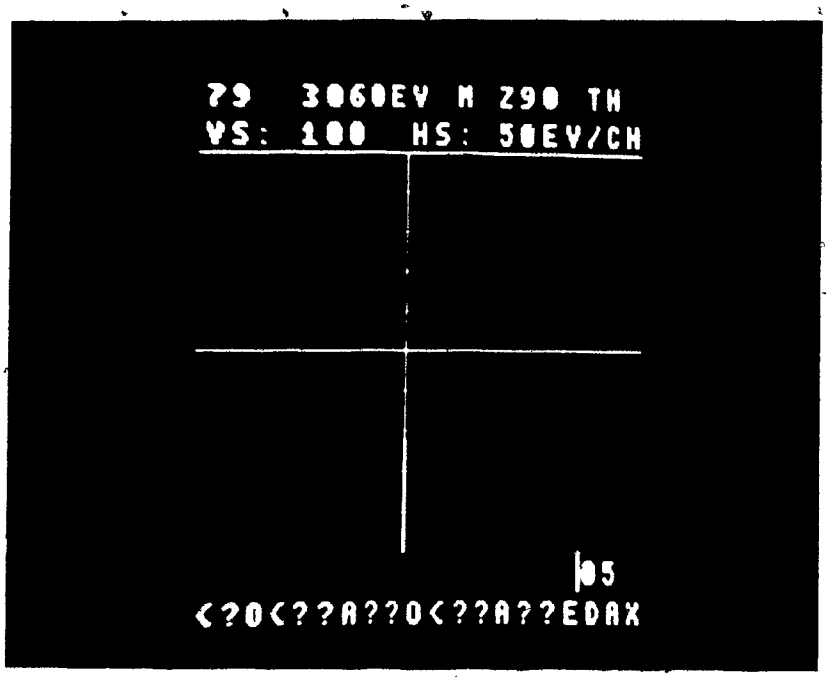
79 3060EV M Z90 TM
VS: 100 HS: 50EV/CH
05
<?D<??A??D<??A??EDAX

FIGURE III-B.15 Typical X-rays E.D.A. spectrum. Thorium M line of inner cell wall layers and cell interior before thorium biosorption.

FIGURE III-B.16 Typical X-rays E.D.A. spectrum. Thorium M line of inner cell wall layers and cell interior following thorium biosorption.

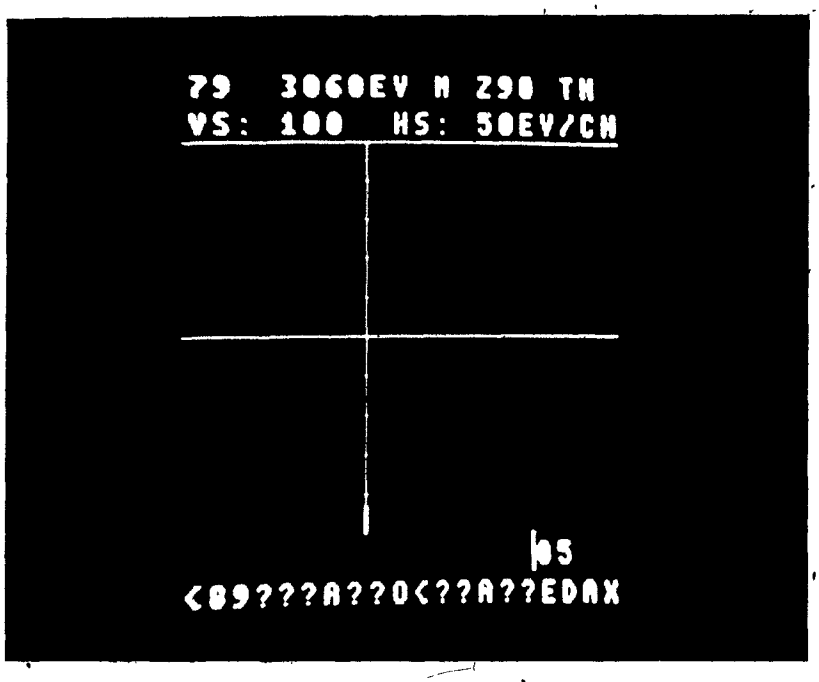
79 3060EV M 290 TM
VS: 100 HS: 50EV/CM
<89???A??D<??A??EDAX

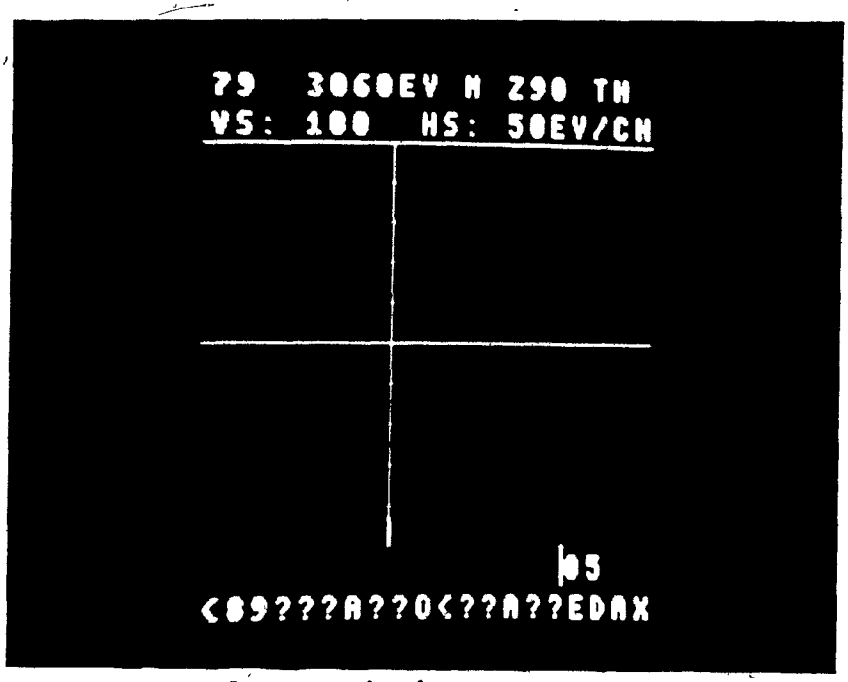
79 3060EV M 290 TM
VS: 100 HS: 50EV/CM
<89???A??D<??A??EDAX

the energy level at the thorium M spectral line remained at background levels, clearly demonstrating the absence of detectable thorium from these regions of the mycelium.

III-B.6 Pure Chitin Thorium Uptake

The thorium uptake capacity of pure chitin was determined at pH = 4 in the absence of other cations. The thorium chitin loading was 8 mg/g (Appendix B).

Following thorium uptake, a sample of the polymer was separated by filtration and rinsed with distilled water. The infrared and mass spectra of the reacted chitin were recorded. Figures III-B.17 and III-B.18 present the reacted and unreacted chitin IR spectra. No discernible shifts were observed on the chitin spectrum following thorium uptake.

The presence of thorium on the reacted chitin was not indicated by the recorded mass spectra (Figure III-B.19).

The recorded IR and mass spectra are discussed in Chapter IV.

III-B.7 N-Acetyl-D-Glucosamine Interaction with Thorium

The interaction between thorium and NAGI was investigated in the same way as for uranium and NAGI (II-8, III-A.6). Unlike uranium, thorium interaction with N-Acetyl-D-Glucosamine did not produce a precipitate that could be interpreted as an indication of either insoluble complex formation or of complex hydrolysis. It is possible that a NAGI-thorium complex would be water soluble and not easily hydrolysable.

FIGURE III-B.17 Infrared spectrum of virgin chitin.

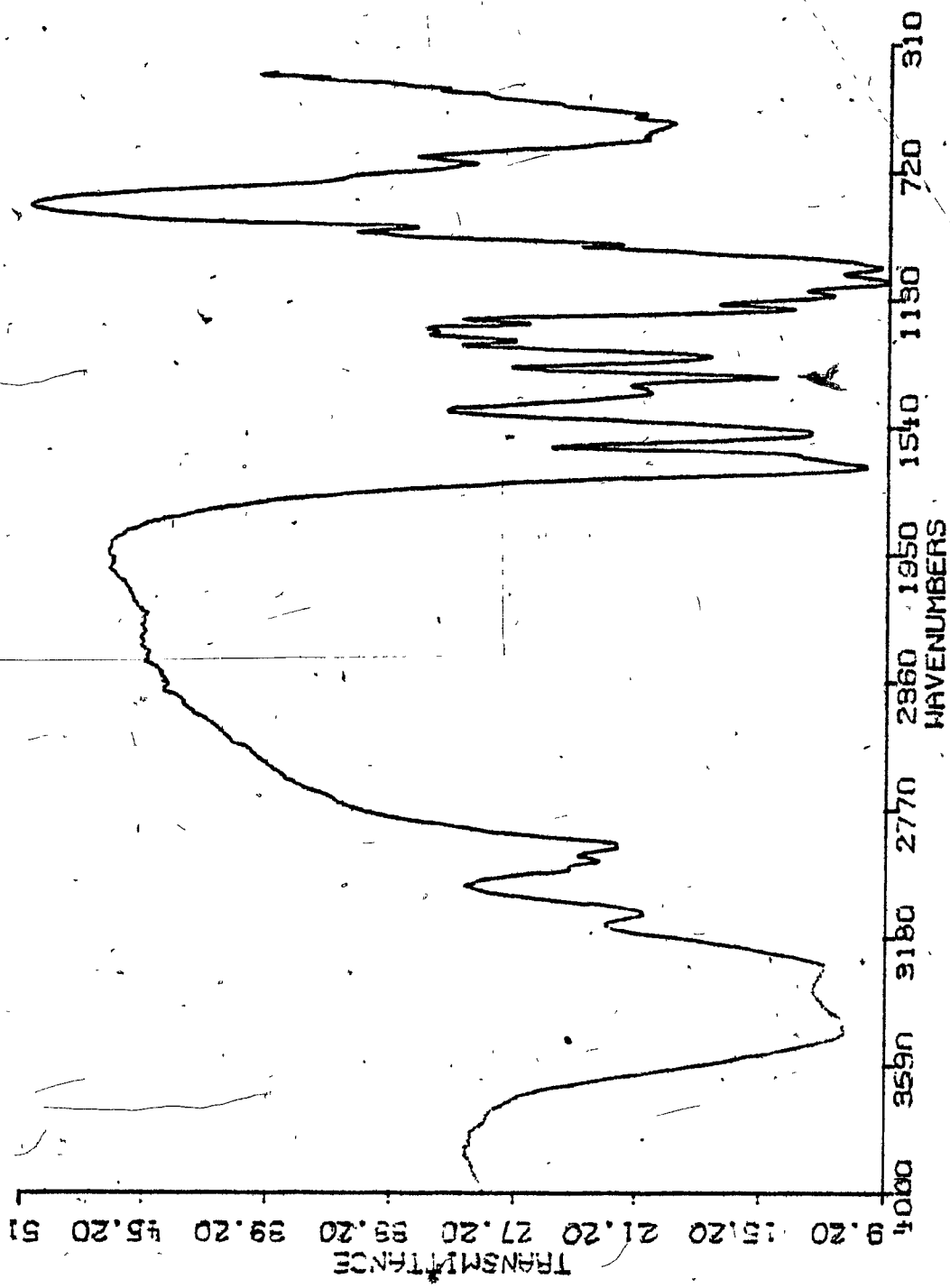
TRANSMITTANCE
9.20
15.20
21.20
27.20
33.20
39.20
45.20
51
4000
3590
3180
2770
2360
1950
1540
1130
720
310
WAVENUMBERS

FIGURE III-B.18 Infrared spectrum of Th(IV) bearing chitin.

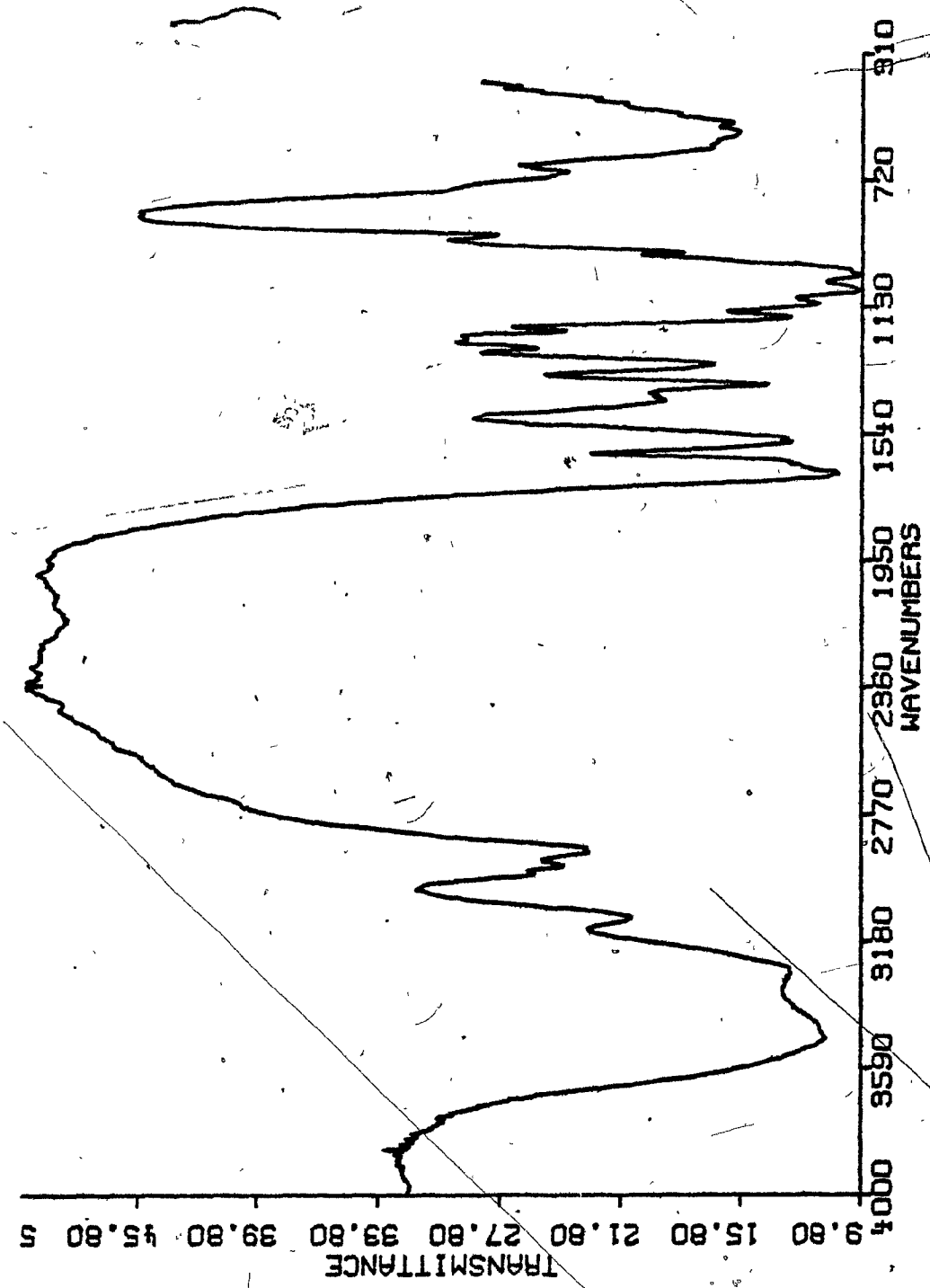
TRANSMITTANCE
9.80
15.80
21.80
27.80
33.80
39.80
45.80
5
4000
3590
3180
2770
2360
1950
1540
1150
720
310
WAVENUMBERS

FIGURE III-B.19 Mass spectrum of Th(IV) bearing chitin.

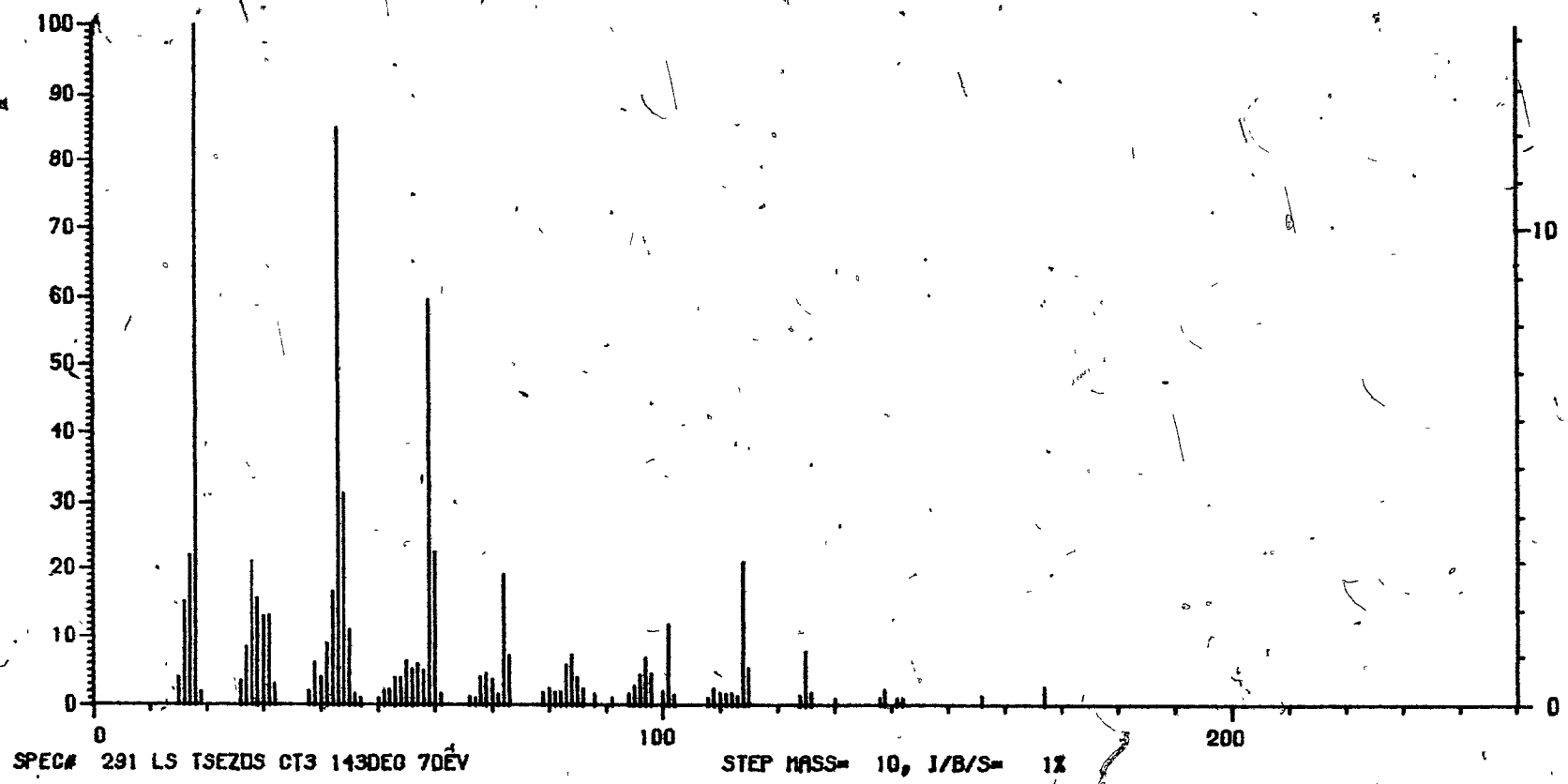
100
90
80
70
60
50
40
30
20
10
0
0
100
200
10
0
SPEC# 291 LS TSEZDS CT3 143DEG 70EV
STEP MASS= 10, I/B/S= 1%

III-B.8 Infrared Spectroscopy of Thorium Equilibrated *R. arrhizus* Cell Walls

The infrared spectra of virgin and thorium-equilibrated *R. arrhizus* cell walls were recorded in an effort to acquire some information on the nature of the interaction between thorium and the mycelium cell wall. Figures III-B.20 and III-B.21 present the 4000 to 400 cm^{-1} range of the IR spectra of the *R. arrhizus* cell wall before and after thorium uptake.

Following thorium biosorption some changes in the texture of some absorbance bands were obvious. However, discernible shifts were not observed (Figure III-B.22). The 4000 to 400 cm^{-1} range of the IR spectrum of the *R. arrhizus* cell walls did not provide information on the nature of the interaction between the *R. arrhizus* cell wall and thorium.

Figures III-B.23 and III-B.24 present the 400 to 340 cm^{-1} part of the infrared spectrum of virgin and thorium-equilibrated *R. arrhizus* cell walls. A new absorbance band that appeared following uptake by the cell wall at 362 cm^{-1} has been assigned to thorium-nitrogen bond strech vibrations. The new peak indicates the coordination of thorium with the chitin nitrogen (Figure III-B.24).

Discussion of the recorded infrared spectra is available in Chapter IV.

FIGURE III-B.20 Infrared spectrum of virgin R. arrhizus cell walls.

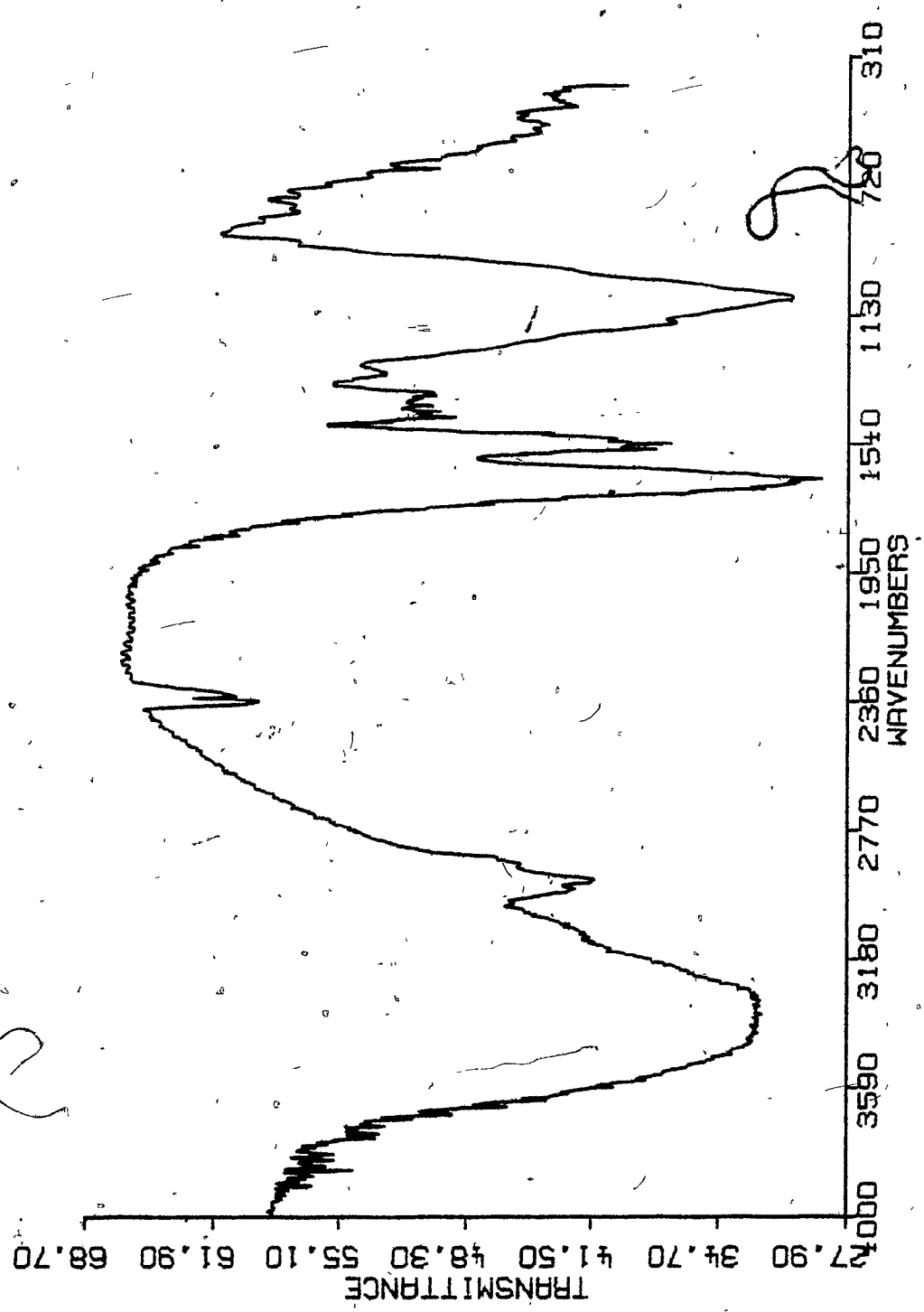
TRANSMITTANCE
27.90
34.70
41.50
48.30
55.10
61.90
68.70
4000
3590
3180
2770
2360
1950
1540
1130
720
310
WAVENUMBERS

FIGURE III-B.21 Infrared spectrum of R. arrhizus cell walls following thorium biosorption.

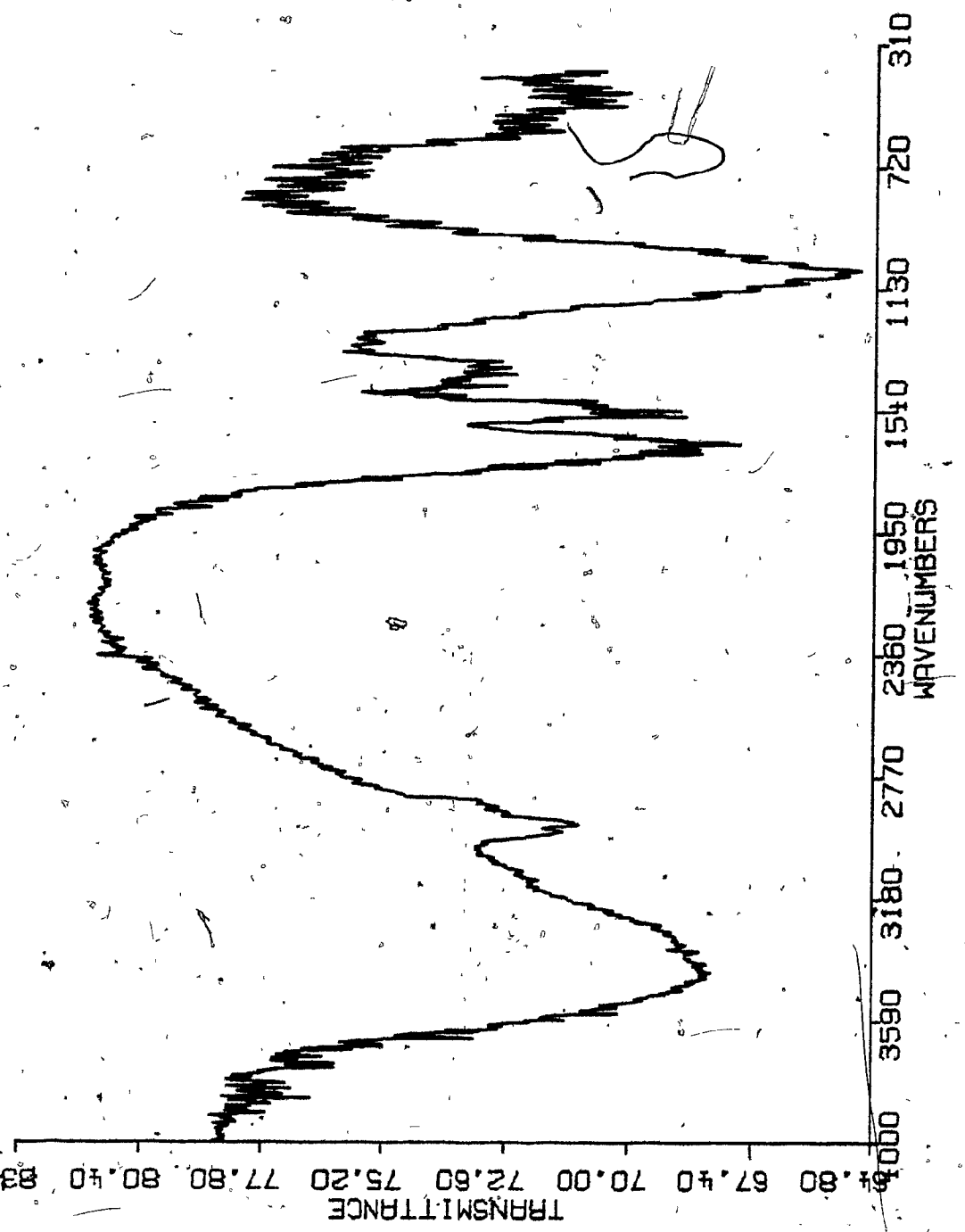
TRANSMITTANCE
64.80
67.40
70.00
72.60
75.20
77.80
80.40
83.0
4000
3590
3180
2770
2360
1950
1540
1130
720
310
WAVENUMBERS

FIGURE III-B.22 Comparison of R. arrhizus cell wall infrared spectra before (1) and after (2) Th(IV) biosorption.

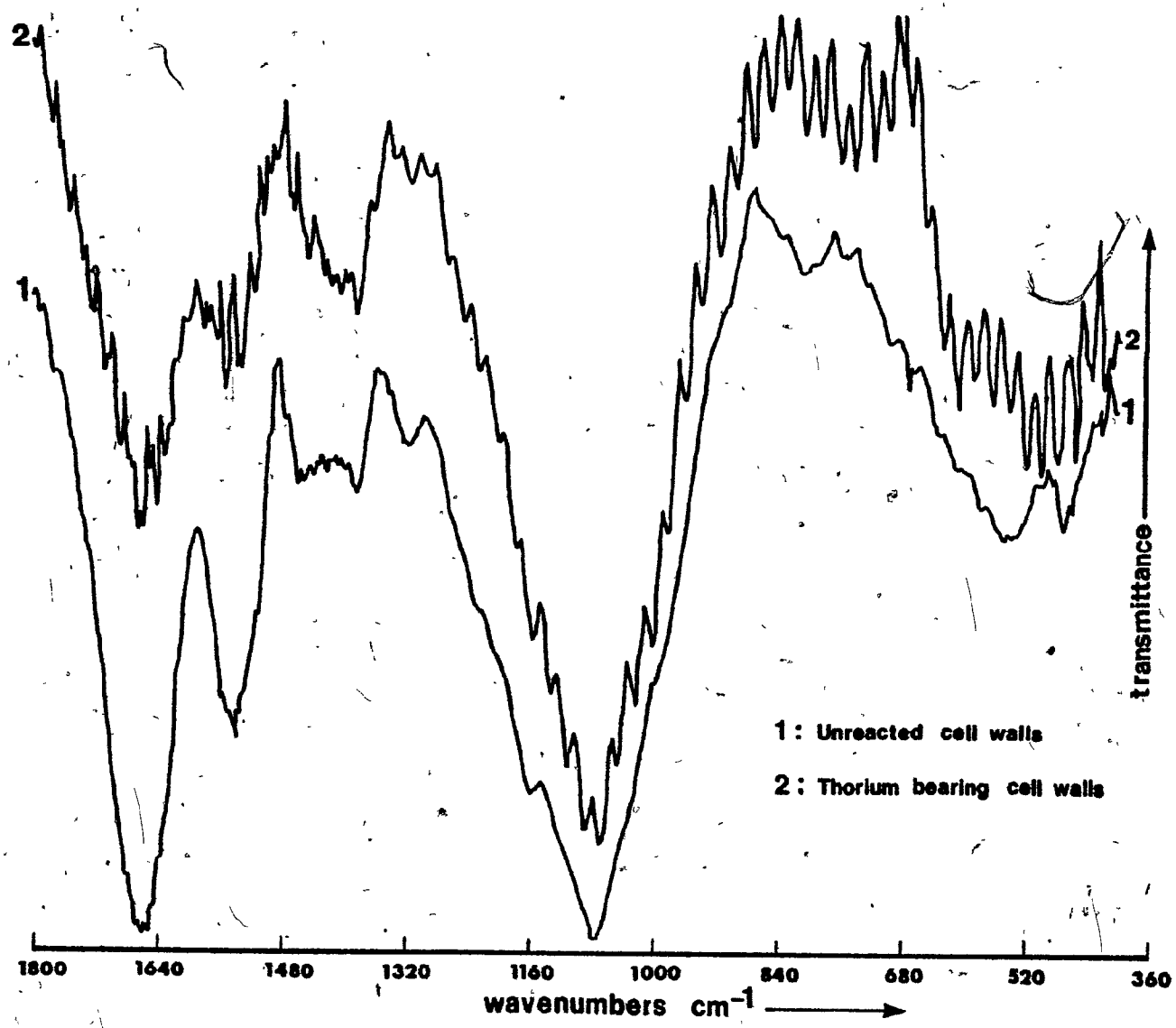
2
1
2
1
transmittance
1 : Unreacted cell walls
2 : Thorium bearing cell walls
1800
1640
1480
1320
1160
1000
840
680
520
360
wavenumbers cm^{-1}

FIGURE III-B.23 Far infrared spectrum of R. arrhizus cell walls before Th(IV) biosorption.

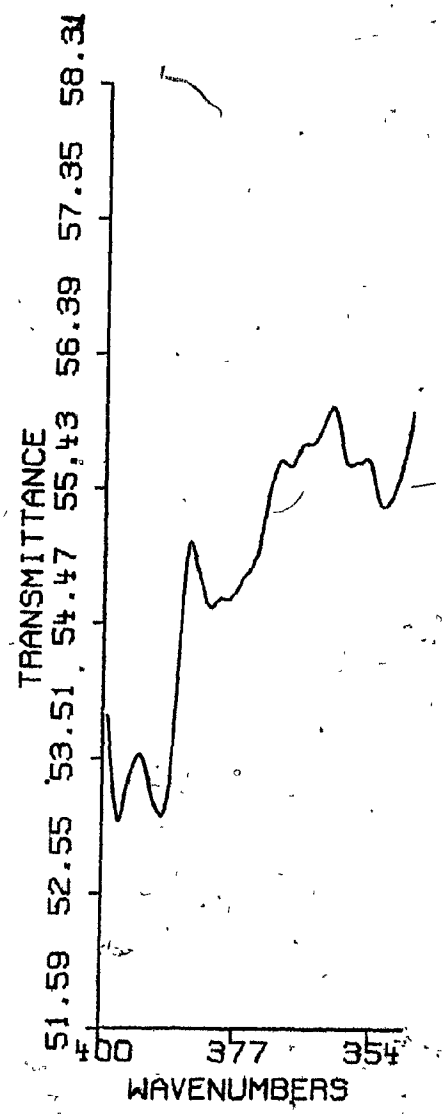
TRANSMITTANCE
51.59
52.55
53.51
54.47
55.43
56.39
57.35
58.31
400
377
354
WAVENUMBERS

FIGURE III-B.24 Comparison of far (400-350 cm^{-1}) infrared spectra of R. arrhizus cell walls before (1) and after (2) Th(IV) biosorption.

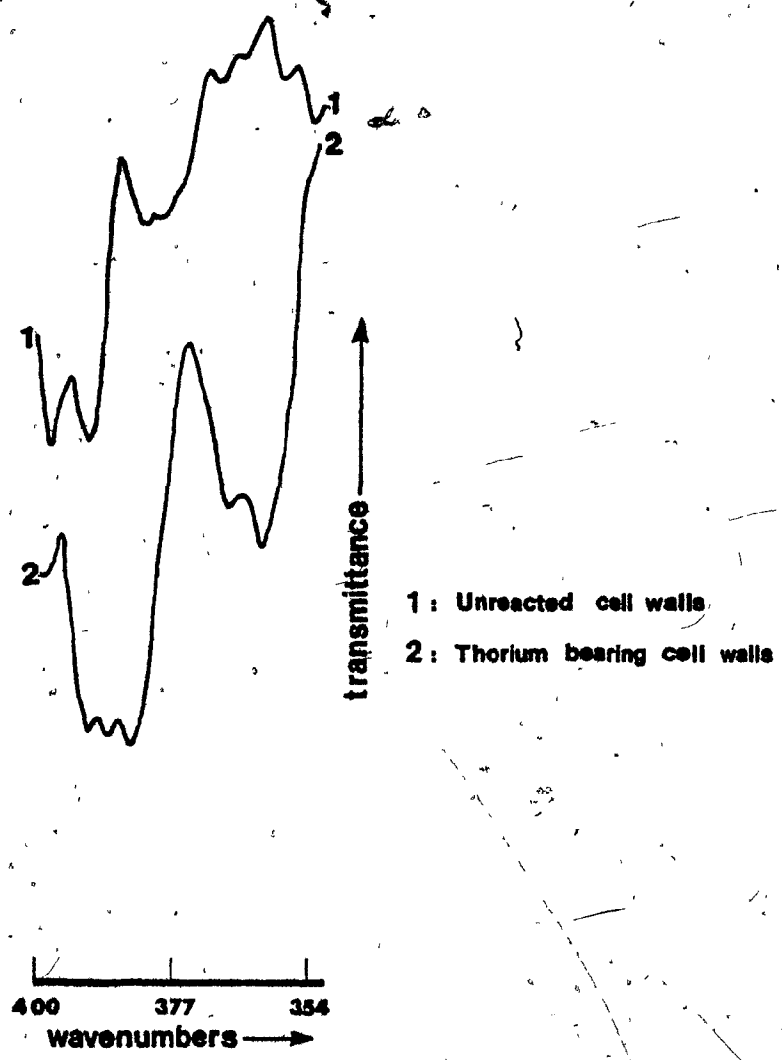
1
2
1
2
transmittance
1 : Unreacted cell walls
2 : Thorium bearing cell walls
400
377
354
wavenumbers

III-B.9 Co-ion Effect on Thorium Biosorption

The effect of the co-ions Fe^{+2} and Zn^{+2} on the thorium biosorptive uptake of R. arrhizus was examined. The percentage changes of thorium uptake at the examined co-ion initial concentrations are presented in Table III-B.4. The results clearly indicate that neither Zn^{+2} nor Fe^{+2} had any appreciable effect on the thorium uptake capacity of R. arrhizus under any of the conditions examined. Figures III-B.25 to III-B.28 present R. arrhizus thorium biosorption isotherms determined in the presence of different co-ion concentrations and solution pH values.

The co-ion uptake of R. arrhizus was determined to be approximately 5 to 9 mg/g for both Fe^{+2} and Zn^{+2} at pH = 4.

III-B.10 Thorium Biosorption Kinetic Data

The instrumentation and the experimental techniques employed in the preliminary examination of thorium biosorption kinetics by R. arrhizus have been described in Section II-9.

Table III-B.5 summarizes the average values of the main parameters of the kinetic experiments. All experimental thorium biosorption rate curves that were determined at pH = 4 exhibited common characteristics. The thorium-R. arrhizus biosorption system reached equilibrium within the first 60 seconds of contact and remained stable thereafter. Thorium uptake calculated for the biomass in the reactor at equilibrium was similar to that indicated by the biosorption isotherm at the same equilibrium Th(IV) concentration.

TABLE III-B.4

Co-Ion Effect on Thorium Biosorptive Uptake Capacity of *R. arrhizus*

Conditions	pH = 4, 30 mg/l Th^{+4}							pH = 2, 30 mg/l Th^{+4}					
Co-Ion Present	Fe^{+2}				Zn^{+2}			Fe^{+2}			Zn^{+2}		
Co-Ion Concentration mg/l	ø	30	100	1000	ø	20	50	ø	30	500	ø	20	50
Th^{+4} Uptake Capacity at 20 mg/l Th^{+4}	170	162	170	174	170	172	173	89	87	90	89	102	93
% Change of Th^{+4} Uptake Capacity	-	- 7%	0%	+ 2%	-	+ 1%	+ 2%	-	ø%	+ 1%	-	+ 14%	+ 4%

FIGURE III-B.25 Fe(II) effect on Th(IV) biosorption, pH = 4.

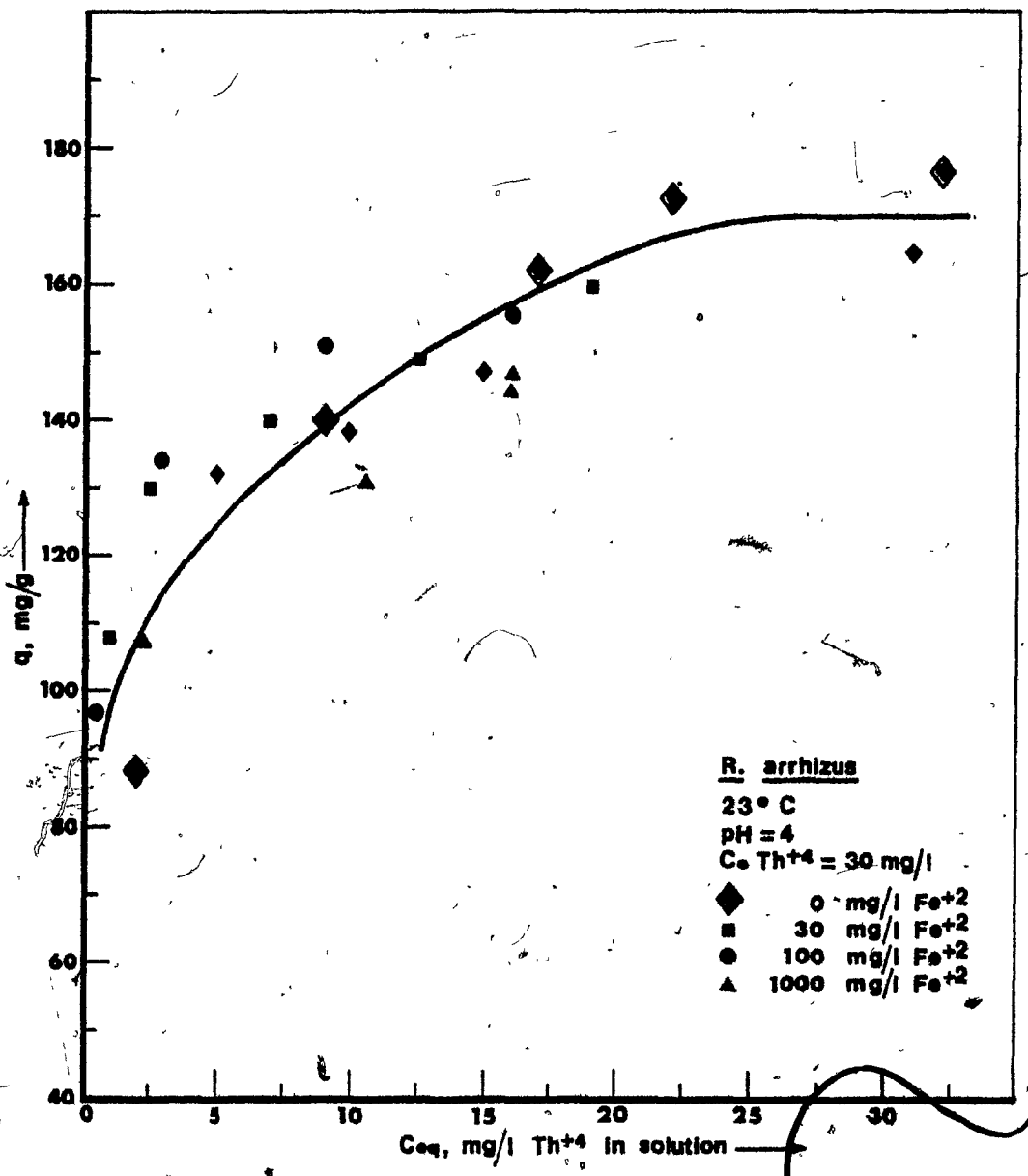
180
160
140
120
100
80
60
40
q, mg/g
0
5
10
15
20
25
30
Ceq, mg/l Th+4 in solution
R. arrhizus
23° C
pH = 4
Co Th+4 = 30 mg/l
0 mg/l Fe+2
30 mg/l Fe+2
100 mg/l Fe+2
1000 mg/l Fe+2

FIGURE III-B.26 · Fe(II) effect on Th(IV) biosorption plateau, pH = 2.

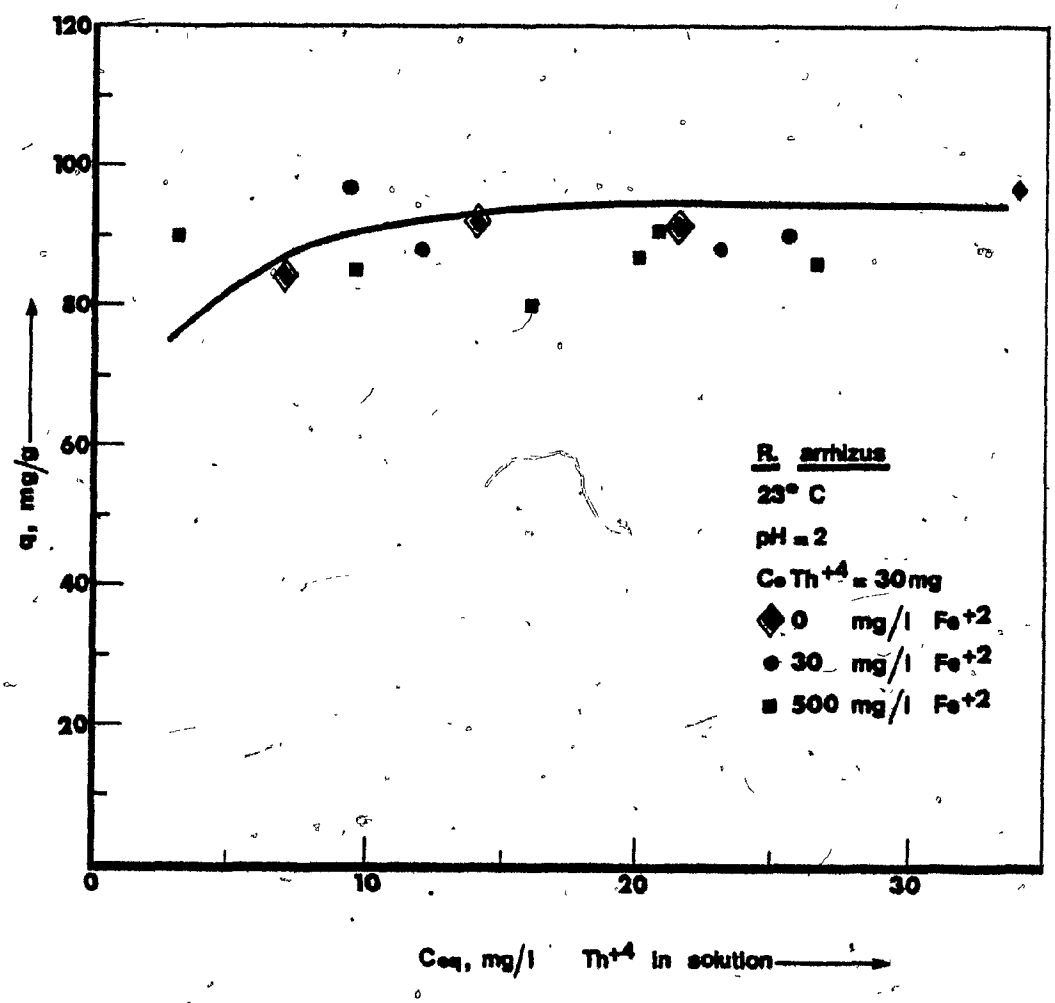
120
100
80
60
40
20
0
10
20
30
q, mg/g
Ceq, mg/l Th+4 in solution
R. arrhizus
23° C
pH = 2
Co Th+4 = 30 mg
0 mg/l Fe+2
30 mg/l Fe+2
500 mg/l Fe+2

FIGURE III-B.27 Zn(II) effect on Th(IV) biosorption, pH = 4.

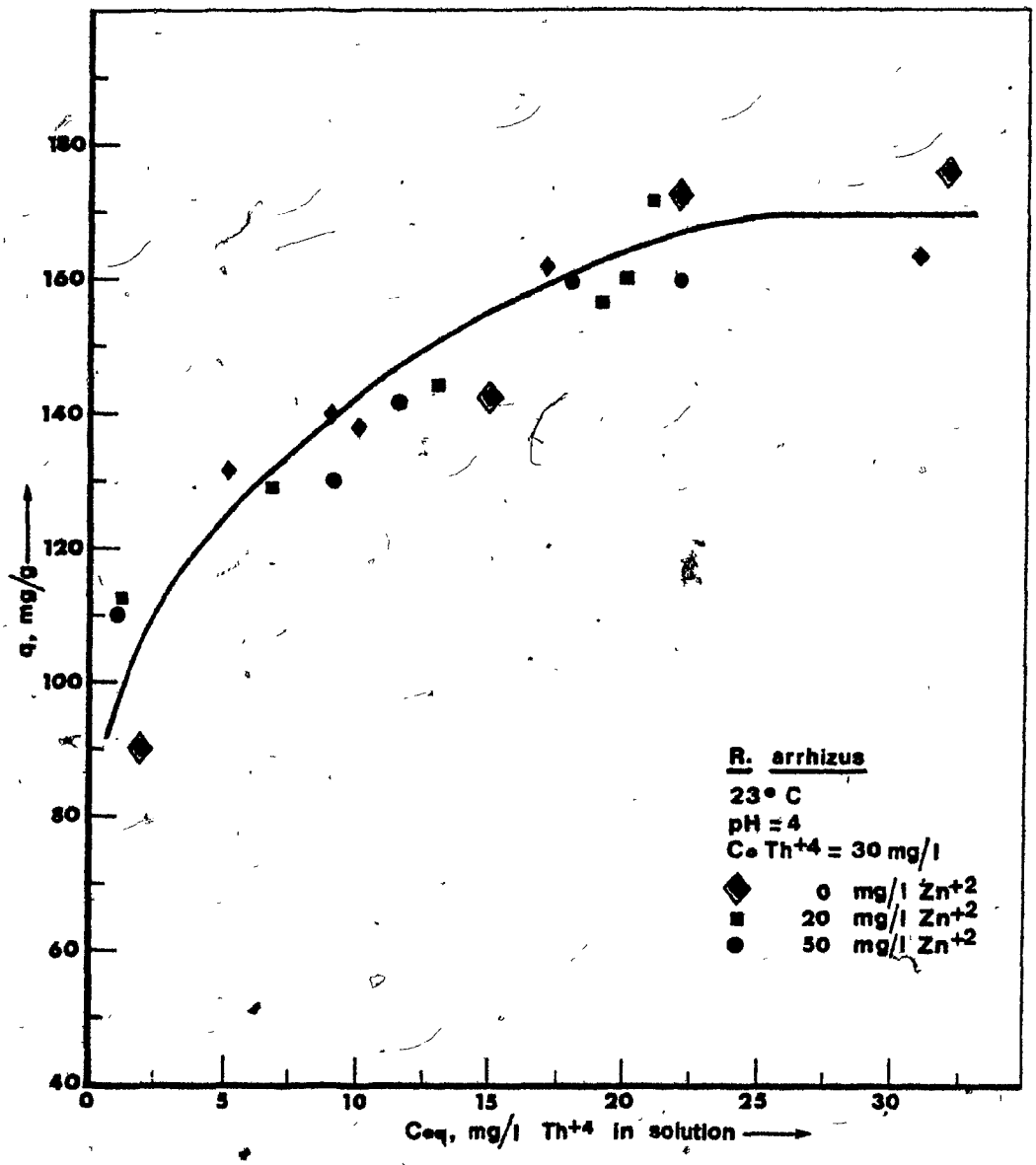
180
160
140
120
100
80
60
40
q, mg/g
0
5
10
15
20
25
30
Ceq, mg/l Th+4 in solution
R. arrhizus
23° C
pH = 4
Co Th+4 = 30 mg/l
0 mg/l Zn+2
20 mg/l Zn+2
50 mg/l Zn+2

FIGURE III-B.28 Zn(II) effect on Th(IV) biosorption plateau, pH = 2.

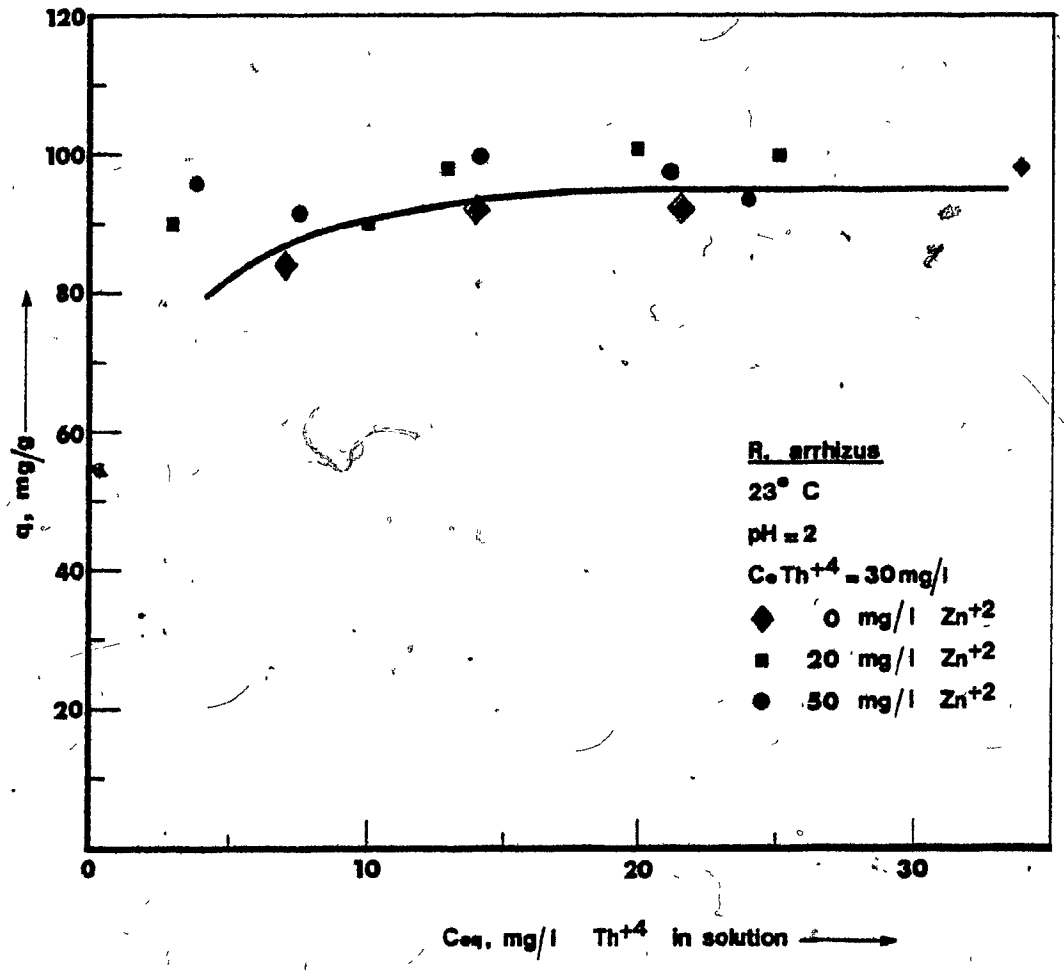
120
100
80
60
40
20
0
10
20
30
q, mg/g
Ceq, mg/l Th+4 in solution
R. arrhizus
23° C
pH = 2
CoTh+4 = 30 mg/l
0 mg/l Zn+2
20 mg/l Zn+2
50 mg/l Zn+2

TABLE III-B.5

Typical Experimental Conditions Employed in Thorium Kinetic Experiments

Experimental Set #	1	2	3	4	5	6	7
Agitation Rate RPM	1000	1300	1300	1300	1300	1300	1300
Initial Th^{+4} Concentration mg/l	21	17	15	16	30	17	14
Biomass mg	80	35	40	21	40	40	38
Reaction Mixture Volume ml	1100	1008	1000	1000	998	1005	1000
pH	4.0	3.9	3.9	4.0	4.0	2.0	4.0
T ^{o}C	23	23	23	23	23	23	8

Temperature change within the range of 8°C to 23°C did not affect the observed thorium uptake rate. Within the range examined neither initial thorium concentration nor biomass dosage change (Table III-B.5) had a discernible effect on the thorium uptake rate (Figures III-B.29, III-B.30, III-B.31). Solution pH, however, appeared to significantly affect the overall thorium uptake rate (Figure III-B.31). Detailed data for the presented kinetic experiments are available in Appendix E.

FIGURE III-B.29 Thorium uptake rate curves.

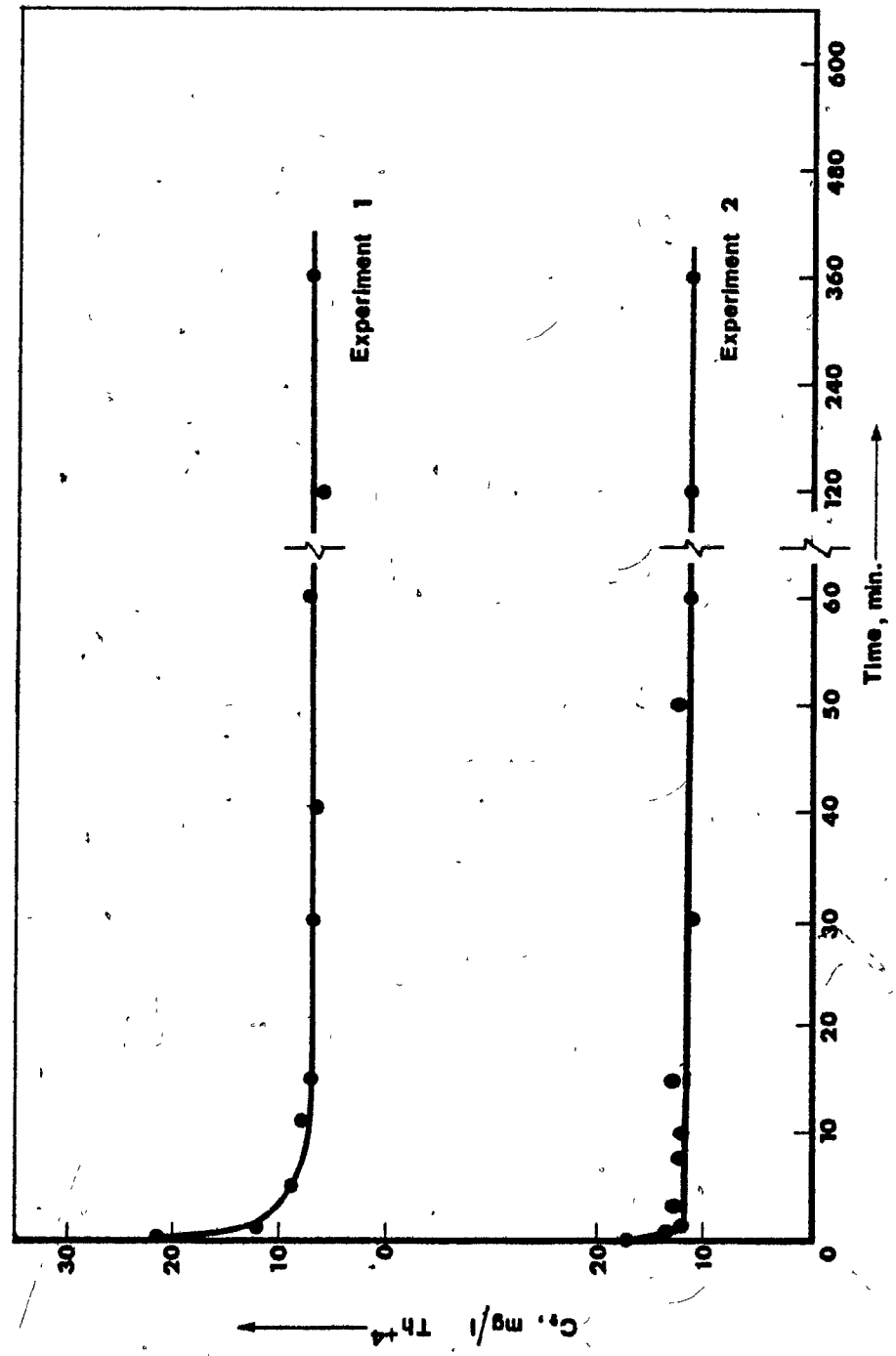
Experiment 1
Experiment 2
Time, min.
C_p, mg/l Th^{+4}
0
10
20
30
40
50
60
120
240
360
480
600

FIGURE III-B.30 Thorium uptake rate curves.

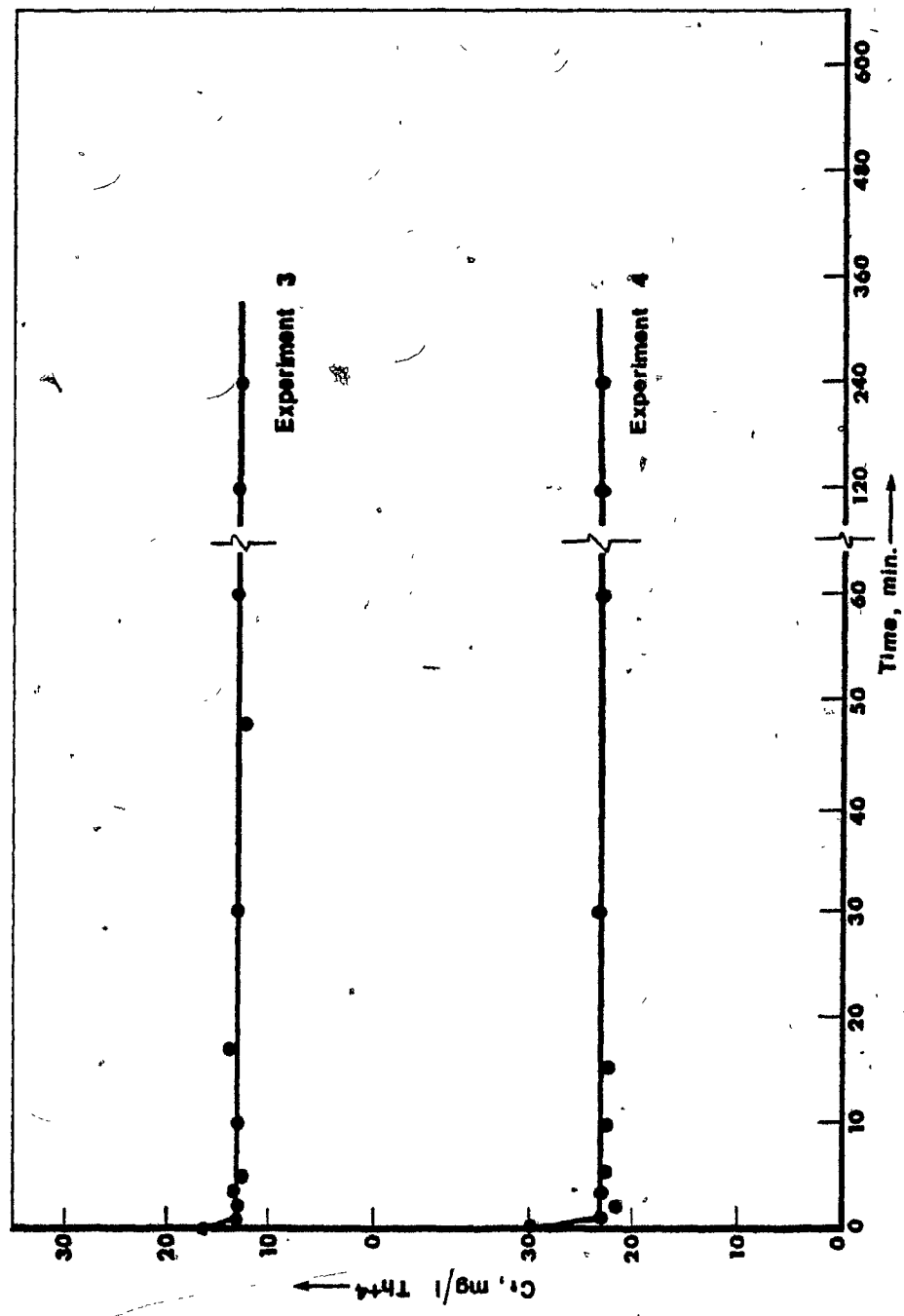
Experiment 3
Experiment 4
Time, min.
C, mg/l Th++
0
10
20
30
40
50
60
120
240
360
480
600

FIGURE III-B.31 Thorium uptake rate curves.

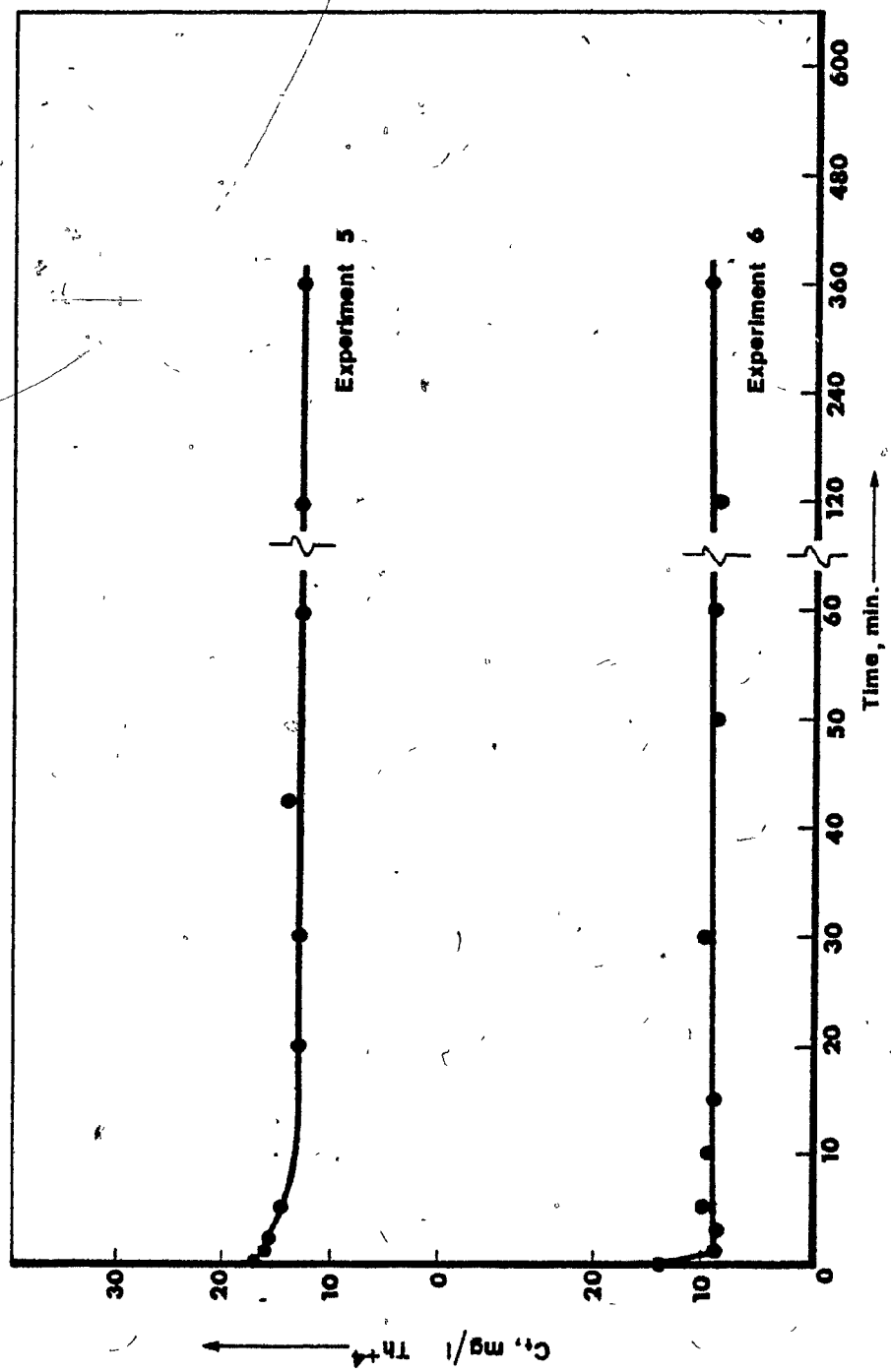
Experiment 5
Experiment 6
Time, min.
0
10
20
30
40
50
60
120
240
360
480
600
C_t, mg/l Th^{+4}
30
20
10
0
20
10

CHAPTER IV

DISCUSSION

IV-A URANIUM

IV-A.1 Uranium Biosorption Equilibrium Uptake Studies

Sections III-A.1 and III-A.2 presented the uranium biosorption isotherms of all the materials that were tested. The effects of solution pH, initial uranium concentration and solution temperature on q will be discussed in the following section.

IV-A.1.1 pH Effect on q

The examined biomass types can be separated into two groups. The first group was comprised of the biomass types that did not exhibit a significant difference in uranium uptake between pH = 2 and pH = 4. The biomass of *Pseudomonas fluorescens* (Figure III-A.3), *Aspergillus terreus*, and municipal waste activated sludge (Figure III-A.4) belong to this group, which, in general exhibited low uranium uptake capacities.

The second group exhibited significantly lower uranium uptake at pH = 2 than at pH = 4. Industrial waste activated sludge (Figure III-A.5), the ion exchange resin IRA 400 (Figure III-A.6), the activated carbon F-400 (Figure III-A.6) and *R. arrhizus* (Figure III-A.2) exhibited such behaviour.

No discernible difference in uranium uptake was observed between pH = 4 and pH = 5 for all materials tested (Figures III-A.2 to III-A.6).

Activated carbon and IRA-400 presented the highest difference in q between pH = 2 and pH = 4. More specifically, IRA-400 exhibited zero uptake at pH = 2 and a loading of about 80 mg/g at pH = 4. IRA-400 is an anionic resin and at pH = 2 uranium ions exist in the form of the simple uranyl cation UO_2^{+2}, which explains the observed zero uptake of uranium[22]. However, negatively charged hydrolysed complex uranium ions that exist between pH = 4 and pH = 5[20], can be retained by IRA-400. Hydrolysis products are in simultaneous dynamic equilibria and consequently the resin could reduce the solution uranium concentration down to zero (Figure III-A.1).

Filtrasorb 400 also exhibited zero loading at pH = 2 and a maximum uptake of approximately 150 mg/g at pH = 4. The activated carbon showed a preference for the adsorption of the hydrolysed uranium ions that exist above pH = 2.5, rather than the simpler uranyl-ion. The reduced solubility of uranium ions at pH = 4 or pH = 5 and the narrow overall pore volume distribution of this activated carbon may have resulted in the observed behaviour[50, 51, 52].

The UO_2^{+2} hydrolysis products distribution curves available in the literature[22] suggest that for low total U(VI) concentrations and for pH below 5, UO_2^{+2} continues to be one of the predominant uranium ionic species in solution. The following equations most probably describe

U(VI) hydrolysis in non-complexing media.[20,22]

$$UO_2^{+2} + H_2O \overset{K_1}{\rightleftharpoons} UO_2(OH)^{+1} + H^+ \quad (\log K_1 = -5.8)$$

$$2UO_2^{+2} + 2H_2O \overset{K_2}{\rightleftharpoons} (UO_2)_2(OH)_2^{+2} + 2H^+ \quad (\log K_2 = -5.62)$$

$$3UO_2^{+2} + 5H_2O \overset{K_3}{\rightleftharpoons} (UO_2)_3(OH)_5^{+1} + 5H^+ \quad (\log K_3 = -15.63)$$

One can assume that the above reactions approximate the hydrolysis equilibria in the dilute uranium aqueous solutions used in the present work. A uranium mass balance along with the three equilibrium expressions yield a system of four equations, the numerical solution of which allows estimation of the distribution of U(VI) among the principal hydrolysed uranium ionic species. For a total U(VI) concentration of 100 mg/l, about 80% of U(VI) exists in the form of UO_2^{+2} at pH=4, while at pH = 5 the UO_2^{+2} percentage drops to about 9%. At pH = 2, UO_2^{+2} is the dominant species present. It is evident from this analysis that the 20% reduction in UO_2^{+2} content of the solution, when solution pH changes from pH = 2 to pH = 4, does not account for the large difference in uranium uptake observed for some of the microorganisms, such as Rhizopus arrhizus (Figure III-A.2). In addition, the major decrease in UO_2^{+2} concentration between pH = 4 and pH = 5 was not accompanied by a discernible change in uranium uptake capacity. Therefore the concentration of the UO_2^{2+} ions in solution does not appear to be a main factor influencing the uranium biosorptive uptake capacity of the biomass.

Uranium solubility diminishes significantly with increasing pH [22]. The difference in solubility is much greater between pH = 2 and pH = 4 than between pH = 4 and pH = 5. Consequently, there appears to be a qualitative correlation between observed biosorptive uptake capacity and solubility. A further increase in solution pH, beyond pH = 6, has been reported to significantly reduce uranium biosorptive uptake [15]. This reduction in uptake coincides with an increase of uranium solubility in the form of uranates, and is in line with the indicated correlation of uranium solubility with uranium biosorptive uptake. Solution pH appears as a parameter that can affect considerably the uranium biosorptive uptake through the control of uranium solubility. The effect of uranium solubility on q will be discussed further in Section IV-A.10 which deals with the hypothesized mechanism of uranium biosorption.

IV-A.1.2 Effect of Initial Uranium Concentration on q

Initial uranium concentration had no discernible effect on the determined uranium biosorption isotherms (III-A.2). Starting with different conditions of initial uranium concentration and biomass dosage, the same isotherm curve was derived. This observation, coupled with the reproducibility of experimental results, indicate that the observed equilibrium uptake capacities can be considered to represent true equilibrium of the biosorption systems examined independent of the experimental conditions. In addition, it can be concluded that the equilibrium curves are independent of the samples used in each individual experiment and that

the biomass types examined behaved like uniform materials; the particle configuration (e.g. agglomerated mycelia) had no apparent effect on observed equilibrium uptakes.

IV-A.1.3 Temperature Effect on q

The effect of temperature on uranium biosorptive uptake of R. arrhizus was not very pronounced (II-1.2, III-A.3). In terms of process application this conclusion is significant as it indicates that the biosorptive uptake capacity of R. arrhizus does not change significantly within the $5^{o}C$-$40^{o}C$ temperature range that covers most actual waste water operations.

IV-A.1.4 Comparison of U Biosorption Equilibrium Data with Results Reported in the Literature

Some experimental data on biosorption of uranium by Penicillium chrysogenum were reported by Jilek et al.[15]. Their results indicated that, at pH = 3, "dried" P. chrysogenum mycelium was capable of maximum uranium uptake of approximately 145 mg/g, while "natural" mycelium took up approximately 175 mg/g, both results referring to a 24 hrs "culture time"[15]. Reinforced Penicillium chrysogenum biomass containing approximately 35% reinforcing inactive agents, has also been reported by the same research group as exhibiting uranium uptake capacity of approximately 100 mg uranium per gram of dry biosorbent (pH not reported).

The above results correspond well with the uranium biosorptive uptake capacity of about 165 mg/g (at pH = 4 and Ceq of about 700 mg/l)

determined for P. chrysogenum in the present work.

Chiu[14] also reported uranium uptakes by dry dead mycelia of unidentified species in the range of 160 mg/g. Results by Chiu cannot be compared directly with the results of the present work since his microorganisms were not identified. However vague his observations were, they can serve as an indication of the order of magnitude of uptake capacities that may be expected from some mycelia, and in that sense they correlate well with data obtained during the present work.

Shumate et al.[18, 19] have indicated uranium uptake capacity of 140 mg/g for a mixed living culture of denitrifying bacteria (pH = 3 to pH = 4). A temperature change from 25°C to 50°C had no discernible effect on the uranium distribution coefficient between the solution and the culture. Microorganisms grown independently over a period of 14 months yielded the same uranium biosorption isotherm, indicating the uniformity of their culture and the stability of the respective biosorption characteristics. All information reported by Shumate et al. corresponds well with data obtained in the course of the present work regarding the possible uranium biosorptive uptake capacities, temperature effect on q and the uniformity of the biomass in general (III-A.1.2).

IV-A.2 Linearization of Biosorption Isotherms

Section III-A.2 has shown that both Langmuir and Freundlich adsorption isotherm models describe uranium biosorption isotherm data

reasonably well (Table III-A.3). Higher S.E.E. values were determined for certain biosorption isotherms, as for example for R. arrhizus (Table III-A.3). In such cases the respective biosorption isotherm comprised a few points of different loadings at zero residual concentration. Points of that nature, (q_i, 0) obviously cannot be described by either of the two models, resulting in higher S.E.E. values.

For some of the examined materials, linearization of the data was best fitted by two intersecting lines, (e.g. Figure III-A.2 or Figure III-A.5), indicating a change in the response of the biosorption system below a certain equilibrium concentration. Similar behavior is sometimes noticed with activated carbon adsorption isotherms.

The good fit of both physicochemical adsorption isotherm models to all available biosorption isotherm data may be interpreted as an indication that adsorption is involved in the phenomenon of uranium biosorption. This subject is discussed further in section IV-A.10 that deals with the uranium biosorption mechanism hypothesis.

IV-A.3 Pure Cell Wall Preparation Uranium Uptake

In Section III-A.4 it was suggested that the higher uranium uptake exhibited by the pure cell wall preparation may be interpreted as indicating that the R. arrhizus cell wall is the biosorptively active part of the mycelium. Indeed, cell walls make up a considerable fraction of the total cell dry weight[41-44]. Assuming that the same average

quantity of uranium is taken up by each cell wall, regardless of whether the wall is part of a mycelium or has been separated in a cell wall preparation, then a somewhat higher q should be expected by the cell wall preparation since the same uranium quantity is taken up by a lesser weight of biosorbent.

IV-A.4 Electron Microscopy of Uranium Biosorption

The available electron micrographs (III-A.5) of virgin R. arrhizus cell walls (Figure III-A.8) indicate that the cell wall architecture exhibits a multilaminate or stratified architecture. This observation agrees well with the extensive information published in the literature on the composition and architecture of the fungal cell wall[31, 38, 39, 41-44, 47-49].

Biosorbed uranium appears to concentrate in discrete layers within the cell wall which is apparently the biosorptively active part of the R. arrhizus mycelium. Together the determination of the uranium uptake capacity of the pure cell wall preparation and the electron microscopy - Xrays E.D.A. study of R. arrhizus thin sections confirmed the above suggestion.

IV-A.5 Pure Chitin Uranium Uptake

As already mentioned (III-A.6), the infrared and mass spectra of uranium-equilibrated chitin did not reveal any information on the nature of the interaction between them. Virgin chitin IR spectrum masked the areas that could reveal such information. The very low

volatility of uranium precluded useful information from the mass spectra. Usually a volatile organometallic compound is formed whenever high atomic number elements are to be studied by mass spectroscopy. The mass spectrometer employed (II.5) uses a small sample size of approximately 50 μg. As a result, the total uranium mass present in the sample, given the low (6 mg/g) uranium uptake capacity of chitin, was approximately 0.3 μg. The very low quantity of uranium in the sample, the low uranium volatility and the fact that any ion contributing less than 1% to the total ionic current is not detected by the instrument, may have resulted in the inability of the method to detect the presence of uranium in the complex.

The ability of chitin to form a uranium complex is supported, however, by the direct experimental data as well as by similar results reported in the literature[33-37, 53, 54]. As for the uranium uptake capacity of chitin, Andreyev et al.[36] have reported the value of 4.5 mg/g (pH = 3), which corresponds well to the 6 mg/g uranium uptake capacity of chitin determined in the present work.

The observed 6 mg/g loading means that, on the average, 1 out of every 180 glucosamine rings has a coordinated uranium ion on it. The competition between uranium and H_3O^+ ions for coordinations with the chitin nitrogen (IV-A.10) is probably one of the factors responsible for the calculated 1:180 ratio of uranium bearing to uranium free rings. As a result of the competition only some of the glucosamine nitrogens become available to hydrolysed uranium ions for coordination. The equilibrium is influenced by solution pH.

IV-A.6 N-Acetyl-D-Glucosamine Interaction with Uranium

In Section III-A.7, an inorganic precipitate, the product of the interaction between uranium and NAGl, was described. The precipitate contained uranium and exhibited a simple IR spectrum (Figures III-A.19 to III-A.21).

The assignment of the observed absorbance bands has been based on published information.

The broad band at 1630 cm^{-1} has been assigned to H_2O bending vibrations in accordance with similar assignments in the literature[57,58,64]. This explains the significant weakening of the band upon drying the precipitate in an oven at 90°C for 12 hours (Figure III-A.21).

The deep band at 922 cm^{-1} has been assigned to the uranyl ion antisymmetric stretch (ν_3) vibrations, following similar assignments in the literature. More specifically, the ν_3 vibration of the uranyl nitrate hexahydrate is centered at 950 cm^{-1} [58, 59]. In a crystalline compound the U-O distance in the linear O-U-O [60] group depends on the structure of the crystal lattice in question, or, more specifically, on the symmetry of the site occupied by the U(VI) atom and the extent to which it is bound to the nearest neighbour atom[61, 62]. The length of the U-O band and the resulting ν_3 position on the spectrum have been correlated in the following formula developed by Veal *et al.*[61, 62].

$$R = 81.2\ V^{-2/3} + 0.895$$

where: R = U-O bond length in A°

V = ν_3 frequency in cm^{-1}

The examination of a series of organic and inorganic uranyl complexes by Bullock[59] showed a range from 900 cm^{-1} to 1000 cm^{-1} for the ν_3 vibration of the uranyl ion, while in certain uranate compounds ν_3 vibrations in the 784 cm^{-1} to 964 cm^{-1} range have been reported[61, 62]. It is felt, therefore, that the assignment of the 922 cm^{-1} absorbance band to the antisymmetric vibrations of the uranyl group in the precipitate P1 is justified.

The weak or very weak symmetric stretching frequency of the uranyl ion, ν_1, is usually centered around 850 cm^{-1}, but could not be definitely identified on the recorded IR spectra[57-59, 63]. Similar experience has, however, been reported for a large number of uranyl complexes by Bullock[59] as well as by Addison et al.[63]

The broad band at 720 cm^{-1} has been assigned to coordinated water molecules rocking, according to similar assignments reported in the literature[57, 64]. The assignment is also supported by the simultaneous presence of the 1630 cm^{-1} H_2O band vibrations, as well as the disappearance of the 720 cm^{-1} band and the weakening of the 1630 cm^{-1} band upon drying the precipitate at 90°C for 12 hrs (Figure III-A.21).

The wide double band at 3160 cm^{-1} and 3500 cm^{-1} can be assigned to H_2O molecules' stretch vibration, more specifically to hydroxyl antisymmetric and symmetric stretching vibration[57, 64]. Upon drying of the precipitate, the above bands became less intensive, while the ν_3 uranyl frequency shifted to 908 cm^{-1}.

The weakening of the water absorbance bands upon drying indicates a partial dehydration of the precipitate. The remaining water is held in the lattice of the crystal more firmly, as can be seen from the difficulty in evaporating it completely and the disappearance of the water rocking molecular vibrations. The IR spectrum of the precipitate suggests the chemical composition of a hydrated uranyl hydroxide. This suggested chemical composition is supported by the fact that $UO_2(OH)_2 \cdot H_2O$ has been suggested as the stable phase of the U(VI) hydroxide, at 25°C.[22]

The observed shift of the ν_3 uranyl frequency upon further drying of the precipitate suggests that the U-O bond length changed. Applying the Veal formula, an actual change can be calculated from 1.752A° to 1.761 A°. The change is not very large; nevertheless, it indicates some rearrangement within the precipitate with the uranyl ion appearing less free as indicated by the elongation of the U-O bond[61].

The results of the analysis of the precipitate indicate that the end-product of the reaction between uranyl nitrate and N-Acetyl-D-Glucosamine is uranyl hydroxide.

The initial objective of isolating the U-NAGl complex was not met. The complex under examination appeared to be water soluble along with the excess reagents.

The difficulty experienced during the present work in the attempt to isolate the uranium-NAGl complex is not uncommon. Some metal-glucosamine complexes investigated in the literature presented similar

problems[65, 66]. The ability of glucosamine, however, to form metal complexes by coordination to the amine nitrogen, has been confirmed[33, 65, 67]. The stability and equilibrium constants of seven metal complexes of glucosamine have been reported in the literature[66]. Usual composition of complexes are 1:1 and 2:1 of glucosamine to the metal ion. Certain complexes are susceptible to hydrolysis[66]. The end-product of the hydrolysis of glucosamine-metal complexes has been suggested as being the metal hydroxide[66].

In short, the above-cited literature information, the results of the IR analysis of the precipitates observed during the present work, and the fact that the observed precipitate is the product of the uranium-NAGl interaction, indicate that the isolated uranyl hydroxide is the hydrolysis product of the water-soluble and easily-hydrolysable U(VI)-NAGl complex.

IV-A.7 Infrared Spectroscopy of Uranium-Equilibrated *R. arrhizus* Cell Walls

Band assignments of the recorded spectra were based on published information.

The broad band centered at approximately 3480 cm^{-1} has been assigned to the hydroxyl group stretching vibrations[55, 56, 57, 68]. Polysaccharides constitute up to 90% of the dry cell wall weight so the observed strong -OH absorbance should be expected. At about 3260 cm^{-1}, N-H stretching vibrations absorb as well, but in that range the O-H and N-H bands overlap, and their separate identification is not possible.

The medium band at approximately 2930 cm^{-1} has been assigned to $-CH_3$ and $-CH_2$ stretching vibrations, while the double peak close to 2350 cm^{-1} has resulted from the atmospheric CO_2 that was not purged completely[60-63].

The strong band at 1650 cm^{-1} has been characterized as the amide I band of the spectrum. The band is also present in the pure chitin spectrum (III-A.5)[55]. The absorbance exhibited by the amide I band is considered[64] to be the combined effect of the carbonyl (-C = 0) stretch mode, the C-N stretch, and to some extent the N-H band[64]. The presence of the band on the cell wall spectrum was expected because chitin contains the $-N-C^{=0}-CH_3$ group. Primary amides exhibit a second band of weaker intensity, very close to the main carbonyl absorption band, in the 1650-1620 cm^{-1} range. The intensity of this second band (amide II) is usually approximately one half to one third that of the carbonyl absorption band, and is the product of N-H bond vibrations. The peak centered at approximately 1550 cm^{-1} on the recorded spectra fulfils the above characteristics.

In the light of similar assignments in the literature[55, 56, 69], it has been assigned as the amide II band of the spectrum.

The strong, wide band centered at around 980 cm^{-1} covers the range where C-O stretching vibrations, primarily of the alcohol groups, absorb (1000-1100 cm^{-1}) as well as the range where the oxygen bridge stretching modes absorb (1110, 1155 cm^{-1})[55]. The band is common in the

infrared spectra of the cell walls of fungi and is attributed to the polysaccharides of the cell wall[40, 69]. The band is also present in the IR spectra of polysaccharides[40].

The sharp peak at 640 cm^{-1} has been assigned to out-of-plane bending of the hydroxyl groups, following similar assignments in the literature[57, 58].

The new peak at 908 cm^{-1} that appears in the IR spectrum after biosorption of uranium has been assigned to the ν_3 stretch vibration of the uranyl ion following the reasoning presented in Section III-A.6.

The infrared spectra of the cell walls indicate a situation similar to the one encountered during the study of the uranium-chitin complex IR spectrum. No discernible shifts, for example in the amide bands, can be observed. However, the presence of the ν_3 uranyl absorbance band shifted to 908 cm^{-1} indicates that uranium is mostly retained by the cell wall in a form similar to the one in which it exists in the NAG1-U complex hydrolysis product, which also exhibited the ν_3 uranyl peak shifted to 908 cm^{-1} (III-A.6).

The 400 cm^{-1} to 340 cm^{-1} range of the cell wall IR spectrum before and after uranium uptake is presented in Figures III-A.21 and III-A.22. A new, moderate peak at 374 cm^{-1} appeared after uranium biosorption (Figure III-A.26). In the IR spectra of coordination compounds, the 300-500 cm^{-1} range has generally been assigned to the metal-nitrogen

stretch vibrations[57]. A large number of metal-amine complexes exhibit absorbance bands within that range as a result of the M-N bond stretching vibrations[57, 70]. Metal-nitrogen band stretching absorbance bands have also been reported at 358-367 cm^{-1} for complexes of thorium (a metal similar to uranium) with heterocyclic amines[71]. This justifies assigning the new 374 cm^{-1} peak to the uranium-nitrogen bond stretching vibrations. The new peak provides evidence for the proposed uranium coordination to the chitin nitrogen of the cell wall.

The infrared spectra of pure cell wall preparations of different fungi reported in the literature present remarkable similarities among themselves as well as to the spectra obtained during the present work[40, 69]. This similarity can be understood if one considers the fact that polysaccharides dominate the chemical composition of the cell wall of fungi[38, 39], and therefore impose the common characteristics of their infrared spectra on the fungal cell wall infrared spectra[40, 69].

IV-A.8 Co-ion Effect on Uranium Biosorption

The results in Table III-A.5 indicate that both Zn^{+2} and Fe^{+2} inhibit uranium biosorption even at low initial co-ion concentrations. Zinc appears to be more effective than iron. An initial zinc concentration of 20 mg/l resulted in a uranium uptake decrease of approximately 34%, while even higher iron concentration produced somewhat smaller U uptake inhibition (26%). It is also interesting to note that zinc is ahead of iron in the Irving-Williams series of complex stability.

The uncertainty in the determined co-ion uptake capacity resulted from the very small change observed in the co-ion concentration following biosorption. The measured co-ion concentration difference was very small and close to the accuracy of the analytical techniques employed.

IV-A.9 Uranium Biosorption Kinetic Data

The values of the main parameters that characterized the kinetic experiments have been presented in Table III-A.7.

The 40-80 mg/1 U^{+6} initial concentration range was selected because:

a) In that range sample processing and U^{+6} concentration determination were direct, without any intermediate dilution step that would introduce additional experimental error. The recorded absorbance values also fell within optimum range[28], thus improving the accuracy of U^{+6} concentration determination.

b) Similar uranium concentrations were also employed in the uranium biosorption equilibrium studies.

Following the selection of the initial and final uranium concentrations, the biomass dosage was calculated on the basis of a uranium uptake capacity of approximately 160 mg/g. A dosage of 135 mg biomass resulted in approximately 30% to 80% reduction of the initial U(VI) concentration.

It was decided to determine experimentally the agitation rate necessary to obtain kinetic data independent of the mixing rate in the reactor. The kinetic processes involved in biosorption reactions can be envisioned in a way similar to those of ion-exchange or activated carbon adsorption. The observed initial uranium biosorption uptake rate (III-A.10) depends upon the relative rates of the following steps:

1. Transport of uranium ions from the bulk solution to the external surface of the boundary film around the microbial cell.

2. Transport of uranium ions through the boundary film to the cell surface.

3. Transport of the uranium ions inwards, through the cell wall, to the active sites of biosorption.

4. Actual biosorption of the ion in the microbial cell.

It has been confirmed that uranium ions are biosorbed throughout the cell wall in distinctive layers. The slowest of the four steps would control the overall rate of uranium uptake observed in the reactor. In a well-mixed batch reactor such as the one used in the present work, step 1 is not expected to limit the removal rate. Concentration of the biosorbate is uniform in the bulk liquid phase. Actual biosorptive retention of the uranium ions (step 4) is also a rapid process as discussed in section III-A.10.

The kinetics of biosorption is therefore determined by either of steps 2 or 3. Film diffusion processes are generally dependent on stirring rate, while intraparticle diffusion processes are essentially

unaffected by agitation rates[75]. After the experimental runs 1, 2 and 3 were completed, the mixing rate of 1300 RPM was selected for the subsequent kinetic experiments. At 1300 RPM the observed biosorption rate was very rapid and there was no discernible increase of the uranium uptake rate when mixing increased from 1100 RPM to 1300 RPM. Biosorption rates observed in subsequent runs (4 to 8) are, for all practical purposes, not dependent on the diffusion through the particle boundary film.

The common characteristics of the determined uranium concentration rate curves have been presented in Section III-A.10. The shape of the concentration curves suggests that at least two different phenomena contribute to the observed overall uranium biosorptive uptake by R. arrhizus. The first phenomenon is very rapid, reaching equilibrium very rapidly, while the second appears slower and takes place at a later time. Final equilibrium was reached within approximately 1 hour. The relation of the suggested two phenomena to the uranium biosorption mechanism is discussed in Section IV-A.10.

Within the range examined, uranium and biomass concentrations had no apparent effect on U^{+6} uptake rate (Figure III-A.32). Initial equilibrium plateau was consistently reached within 60 seconds. Solution pH, however, strongly affected the initial uranium removal rate, (Figure III-A.33). At pH = 2, initial uranium uptake was very slow. In addition, the two distinct equilibrium plateaus as observed at pH = 4 were not apparent (Experiment #8). Acidic pH is unfavourable to uranium equilibrium uptake capacity of R. arrhizus as well as to the rate of uranium

removal. However, the total time necessary for attainment of final equilibrium at pH = 2 was approximately 60 minutes, similar to the total time necessary to attain final equilibrium at pH = 4.

Kinetic data on biosorption of uranium by R. arrhizus are not available in the literature. There is, however, some information on uranium uptake rates by different mycelia. Chiu[14] reported kinetic data on uranium uptake by uncharacterized living mycelia obtained from a shake-flask system. An approximate 15 minute equilibrium time was determined. Shumate et al.[19] also reported uranium uptake by living Saccharomyces cerevisiae and Pseudomonas aeruginosa, again using a shake-flask system. The respective equilibrium times were reported as 60 minutes and 10 minutes, and exhibited strong dependency on pH, temperature and initial uranium concentration. The pH of the contact system was not controlled and shifted during the contact period.

The data of Chiu[14] and Shumate et al.[19] cannot be directly correlated to the presently reported uranium biosorption rate data, for the following reasons:

(i) The microorganisms used in both studies were different, and were living.

(ii) Experimental conditions were not controlled. Mixing rate was most likely inadequate, and the pH, whose strong effect on biosorption has been documented, was not constant.

Hradkova *et al.*[72], however, have reported data on uranium uptake rate by reinforced dead *Penicillium chrysogenum*. They indicate a very rapid attainment of equilibrium within the first 90 seconds of contact. Their results correspond well to the results obtained in the course of the present work.

Rothstein and Larrabee[9] have reported a very high initial rate of uranium uptake by live yeast cells. Within the shortest time possible for sample withdrawal (120 seconds), their system approached equilibrium, removing 48% of the uranium in solution.

Similarly, Stramberg *et al.*[32] have reported uranium uptake rate data by resting *Pseudomonas aeruginosa* cells, indicating attainment of equilibrium within the shortest period possible for sample withdrawal (40 seconds).

Although the results of both Rothstein *et al.* and Stramberg *et al.* were derived from different biosorption systems, they support the validity of the kinetic rates determined in the present work as they indicate that uranium biosorptive uptake can be very rapid.

The general conclusion that can be drawn is that biosorption of uranium appears to be a very rapid process.

IV-A.10 Mechanism Hypothesis on Uranium Biosorption by Rhizopus arrhizus

The information discussed in the previous Sections IV-A.1 to IV-A.9 allows the formation of a hypothesis regarding the mechanism of

retention of uranium by the mecelium of R. arrhizus. The proposed uranium biosorption mechanism consists of three processes that are described below:

Process A

Process A involves a complex formation between dissolved uranium ionic species and the chitin chains of the R. arrhizus cell wall. Uranium coordinates to the amine nitrogen of the chitin crystallites, and is retained within the cell wall of the mycelium.

Supportive evidence for the proposed process A is:

1. It was concluded in Section IV-A.4 that biosorbed uranium is retained by the R. arrhizus cell wall.

2. Cell walls of fungi present a multilaminate architecture [38, 39, 40]. In general, the cell wall can be regarded as a two-phase system consisting of a chitin skeletal framework embedded in an amorphous polysaccharidic matrix[38,39, 40, 41] (Figure IV-A.1). Chemical analysis of the cell wall of Rhizopus nigricans has confirmed a high content of chitin (58%)[48]. Chitin has also been confirmed in Rhizopus by Frey[38] through the application of X-ray diffraction. The transmission electron micrographs of R. arrhizus mycelia before uranium uptake, presented in this work, confirmed the expected stratification of the chitin in the R. arrhizus cell wall.

3. The ability of chitin to form complexes with metal ions has been well documented in the literature[28, 29, 30, 31].

FIGURE IV-A.1 Chitin chain piles arrangement in fungal cell wall[40].

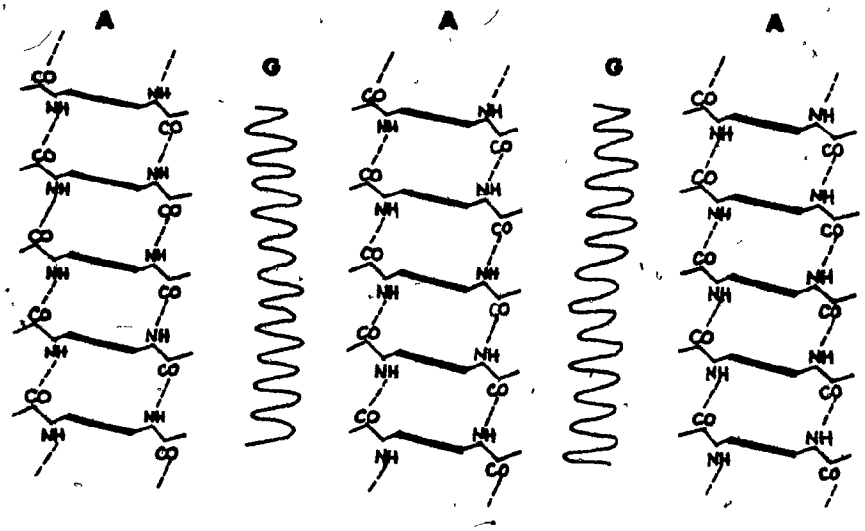

A Chitin chain piles
G Glucan

In Section I.6 the general metal uptake capacity of chitin was presented. Chitin is carrying one linear amino-group per glucose ring (Figure IV-A.2). The amino group has an electron pair available for coordination and behaves like a strong Lewis base[33, 36, 53]. Other Lewis bases present in the cell wall are the hydroxyl groups of the polysaccharides. Their complex formation ability, however, has been reported to be quite small or negligible[36, 65, 66, 67]. Chitin emerges as the main reactive site in the cell wall of R. arrhizus for the coordination of uranium. It is therefore reasonable to expect the formation of a coordination complex between uranium and the nitrogen of the cell wall chitin.

4. The uranium uptake capacity of pure chitin was experimentally confirmed during the present work (Section III-A.6). The formation of a chitin-uranium coordination complex has been reported in the literature[35,36].

5. The electron micrographs of uranium-equilibrated R. arrhizus thin sections have indicated a stratification of biosorbed uranium inside the cell wall (Figures III-A.10 to III-A.12). The observed stratification of biosorbed uranium is similar to the chitin stratification in the cell wall (Figure III-A.9), providing additional indirect evidence of an association between biosorbed uranium and chitin.

6. The infrared spectrum of uranium-equilibrated R. arrhizus pure cell walls presented a new absorbance band at approximately 372 cm^{-1}. As discussed in Section IV-A.7, this new band has been considered the result of the uranium-nitrogen bond vibrations. The presence of the band supports the proposed coordination of some of the biosorbed uranium to the chitin nitrogen.

FIGURE IV-A.2 Chitin unit cell.

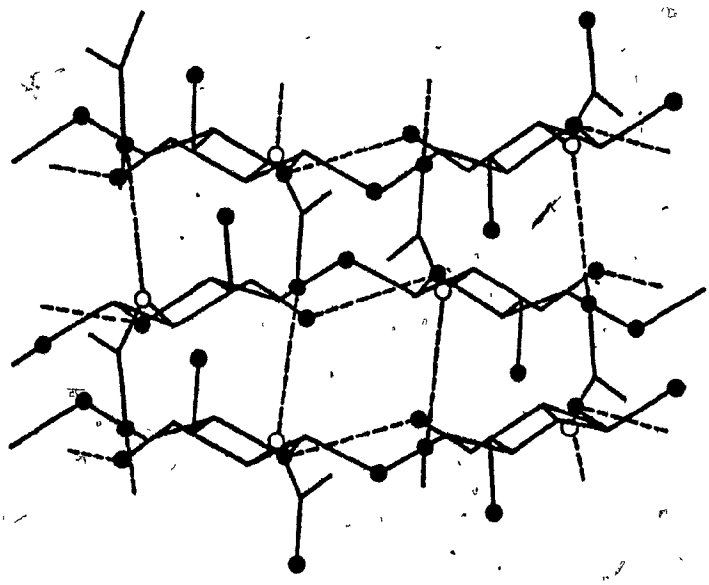

● Oxygen
○ Nitrogen
--- Hydrogen bonds

7. Some data on the complex formation between uranium and the chitin monomer N-Acetyl-D-Glucosamine have been presented in Sections III-A.7 and IV-A.6. Although the complex itself was not isolated, its hydrolysis product, uranyl hydroxide, was observed (IV-A.6), providing additional evidence of the proposed complexation of uranium by chitin.

8. The infrared spectrum of uranium-equilibrated R. arrhizus cell walls presented a new strong absorbance band at 908 cm^{-1}. This band has been assigned to the ν_3 characteristic frequency of the uranyl ion that has shifted from the original 950 cm^{-1} position in the $UO_2(NO_3)_2 \cdot 6H_2O$ spectrum (IV-A.7). The new position of the ν_3 uranyl ion frequency in the R. arrhizus cell wall is the same as the one observed in the IR spectrum of the NAGl-uranium complex hydrolysis product (IV-A.6). Consequently the complexation of uranium by the cell wall can be postulated, as part of the biosorbed uranium is present in the cell wall in the form of the complex hydrolysis product.

9. Iron and zinc complexation by chitin has been documented in the literature[33-37]. The stability of the chitin-metal complexes follows, as for most ligands, the Irving-Williams series[33,37]. Both iron and zinc compete with uranium for complexation by chitin. As a result of the competition reduced uranium uptake was observed (III-A.9, IV-A.8). The reduction of uranium uptake by R. arrhizus due to possible competition of the co-ions for the cell-wall chitin sites constitutes additional indirect evidence of the proposed uptake of uranium by complexation.

7. Some data on the complex formation between uranium and the chitin monomer N-Acetyl-D-Glucosamine have been presented in Sections III-A.7 and IV-A.6. Although the complex itself was not isolated, its hydrolysis product, uranyl hydroxide, was observed (IV-A.6), providing additional evidence of the proposed complexation of uranium by chitin.

8. The infrared spectrum of uranium-equilibrated R. arrhizus cell walls presented a new strong absorbance band at 908 cm^{-1}. This band has been assigned to the ν_3 characteristic frequency of the uranyl ion that has shifted from the original 950 cm^{-1} position in the $UO_2(NO_3)_2 \cdot 6H_2O$ spectrum (IV-A.7). The new position of the ν_3 uranyl ion frequency in the R. arrhizus cell wall is the same as the one observed in the IR spectrum of the NAGl-uranium complex hydrolysis product (IV-A.6). Consequently the complexation of uranium by the cell wall can be postulated, as part of the biosorbed uranium is present in the cell wall in the form of the complex hydrolysis product.

9. Iron and zinc complexation by chitin has been documented in the literature[33-37]. The stability of the chitin-metal complexes follows, as for most ligands, the Irwin-Williams series[33, 37]. Both iron and zinc compete with uranium for complexation by chitin. As a result of the competition reduced uranium uptake was observed (III-A.9, IV-A.8). The reduction of uranium uptake by R. arrhizus due to possible competition of the co-ions for the cell-wall chitin sites constitutes additional indirect evidence of the proposed uptake of uranium by complexation.

Process B

Process B of the hypothesized uranium biosorption mechanism involves the adsorption of additional uranium by the chitin network, close to the complexed by chitin nitrogen. The following experimental results provide evidence supporting the proposed adsorption process.

1. The experimentally determined uranium uptake capacity of chitin at pH = 4 is 6 mg/g. R. arrhizus uranium uptake capacity, under the same conditions, is 180 mg/g. Uranium taken up by R. arrhizus is concentrated in the cell wall of the mycelium which contains less than 100% w/w chitin. Uranium taken up by complexation alone can only account for a very small fraction (<6 mg/g) of the determined overall uranium biosorptive uptake capacity of R. arrhizus. Consequently, additional process(es) must contribute to the observed overall uranium uptake by biosorption.

2. All biosorbed uranium has been located within the cell wall of the mycelium (IV-A.4). Biosorbed uranium exhibits a stratification that coincides with the chitin stratification.

3. The available biosorption isotherm data fit the common adsorption isotherm models very well (III-A.2), indicating the adsorptive uptake of uranium by the R. arrhizus cell wall.

4. Adsorption is a very fast phenomenon when it is not limited by mass transfer[74, 75]. The fungal cell wall can be viewed as a porous structure because it allows the passage of intracellularly manufactured enzymes and other macromolecules[39, 41]. The kinetic data on

uranium biosorption by R. arrhizus presented in Section III-A.10 clearly indicate that the initial equilibrium plateau is established within 60 seconds. The processes involved in the first equilibrium plateau must, therefore, be very rapid. Chemical complexation and adsorption are both rapid processes and can therefore account for the observed rapid establishment of initial equilibrium.

5. Chiu[14] in his work on uranium uptake by unidentified penicillia, also indicated that adsorption is one of the processes involved in uranium biosorptive uptake by fungal mycelia.

6. Chitin nitrogen confers basic characteristics to this aminopolysaccharide. Representing the chitin monomer as GN, the dissociation equation of the amide would be:

$$GN^{+}{:}H + H_2O \rightleftarrows GN{:} + H_3O^{+}$$

The equilibrium is obviously a function of solution pH. Moieties $GN^{+}{:}H$ and $GN^{+}{:}$ are both available on the chitin chain indicating that during process A uranium has to compete with H_3O^{+} for the complexation sites on chitin (IV-A.5). When other co-ions are also present in solution, chemical equilibria become more complex. Blocking of chitin complexation sites by the co-ions reduces the quantity of chitin-complexed uranium (IV-A.8). The reduction of uranium uptake by Fe^{+2} or Zn^{+2} extends, however, beyond the 6 mg/g limit of total U(VI) uptake by complexation, as well as the additional 45 mg/g of Process C (IV-A.10). Table III-A.5 clearly shows a 125 mg/g decrease of q at 1000 mg/l Fe^{+2} initial solution concentration. This strong U uptake suppression can be accounted for

when we consider that a reduction of the quantity of complexed uranium is followed by a reduction of the adsorbed uranium as well. A relation is clearly indicated between complexed and adsorbed uranium. In a recent presentation on uptake of metals by the cell wall of B. subtilis, Beveridge[76] suggested that chemically retained metals may act as nucleation sites for further "deposition" of metal in the cell wall. The co-ions' effect on q suggests a similar role played by the chitin coordinated uranium in the biosorptive uptake of uranium by R. arrhizus.

7. In IV-B.10, where the mechanism of thorium biosorption is discussed, the experimental evidence available indicates that adsorption is involved in the thorium biosorption mechanism. Thorium adsorption by the outer layers of the R. arrhizus cell wall indicates the general ability of the cell wall to function as an adsorbant. It is the same adsorption potential of the cell wall that is considered responsible for the proposed process B of the uranium biosorption mechanism.

Process C

Process C of the uranium biosorption mechanism by R. arrhizus involves the hydrolysis of the uranium-chitin complex formed during Process A and the precipitation of the hydrolysis product (uranyl hydroxide) in the cell wall. Upon hydrolysis the freed chitin nitrogen may re-engage in uranium complexation until the accumulation of hydrolysis products inhibits the complexation-hydrolysis-precipitation cycle. At such a time the biosorption system arrives at final equilibrium.

Representing by GNU the chitin-uranium complex, Process C may be presented schematically as follows:

$$\text{GNU} \overset{H_2O}{\rightleftharpoons} \text{GN} + UO_2(OH)_2 \downarrow$$

$$\text{GN} \overset{U}{\rightleftharpoons} \text{GNU}$$

$$\text{GNU} \overset{H_2O}{\rightleftharpoons} \text{GN} + UO_2(OH)_2 \downarrow$$

Experimental evidence supporting the proposed Process C is discussed below:

1. The examined U-R. arrhizus biosorption system reached an initial equilibrium plateau within the first 60 seconds of contact (III-A.10). This plateau represented approximately 66% of the total biosorptive uranium uptake and is the cumulative result of the proposed Processes A and B. The secondary increase in U(VI) uptake observed approximately 0.5 hours later clearly indicates the presence of an additional process. The new process is distinct from the first two as it takes place at a considerably later time.

2. The U-NAG1 hydrolysis product appeared at a later time following the initial complex formation (III-A.7). NAG1 is the dominant monomer unit of chitin. Both uranium coordination to the amine nitrogen and the subsequent hydrolysis of the complex are independent of the glucosidic linkage of the NAG1 units in chitin. It is therefore reasonable to accept that the uranium-chitin complex hydrolysis is similar to that of the NAG1-U complex, resulting in the precipitation of $UO_2(OH)_2$ in the cell wall.

3. The infrared spectra of the uranium-equilibrated R. arrhizus cell walls and the NAG1-U hydrolysis product presented the same ν_3 characteristic frequency of the uranyl ion (908 cm^{-1}). The presence of U-chitin hydrolysis product in the cell wall (Process C) is therefore indicated by the IR spectra.

4. Hydrolysis of complexes is not usually associated with low solution pH values. Consequently, biosorption of uranium at pH = 2 should not exhibit the secondary uranium uptake increase that has been attributed to the hydrolysis of the U-chitin complex. The uranium uptake kinetic curve at pH = 2 (Figure III-A.29) confirmed the above prediction, thus supporting the proposed Process C.

5. The precipitation of metal hydroxide as a product of the hydrolysis of the glucosamine-metal complexes has been reported in the literature[66], and supports the proposed Process C of the uranium biosorption mechanism hypothesis.

Figures IV-A.3 to IV-A.5 present schematically the proposed mechanism of uranium biosorption by R. arrhizus.

Three processes have been proposed for the uranium biosorption mechanism hypothesis. Process A appears to contribute the least (<6 mg/g or <3%). The significance of Process A, however, if judged exclusively by the initial contribution to the total biosorptive uptake, would be miscalculated. Processes B and C are closely related to Process A. There appears to be a strong interaction among the three processes.

FIGURE IV-A.3 Process A of proposed uranium biosorption mechanism hypothesis.

Process A

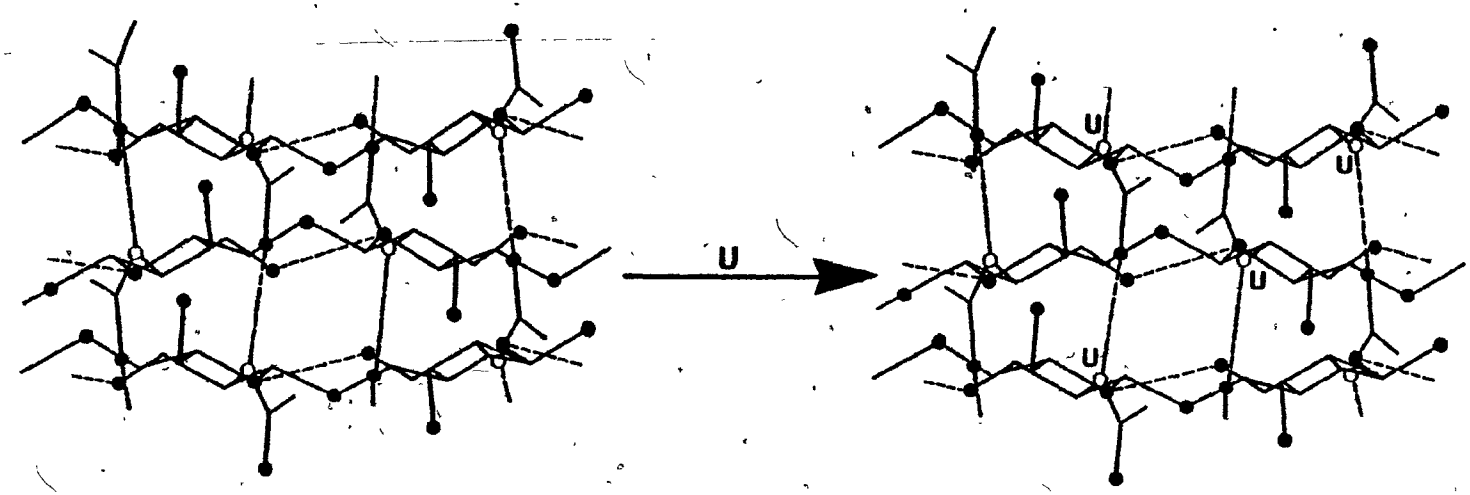

● : Oxygen

○ : Nitrogen

U: Complexed Uranium

222.

FIGURE IV-A.4 Process B of proposed uranium biosorption mechanism hypothesis.

Process B

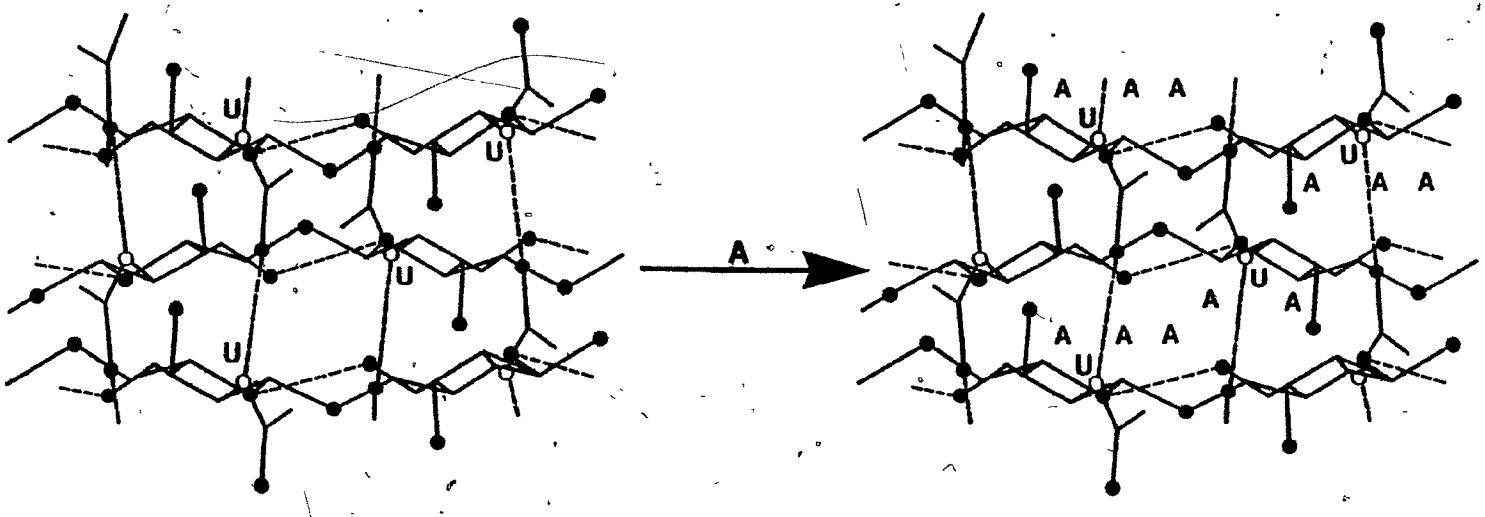

●: Oxygen
○: Nitrogen
U: Complexed Uranium
A: Adsorbed Uranium

FIGURE IV-A.5 Process C of proposed uranium biosorption mechanism hypothesis.

Process C

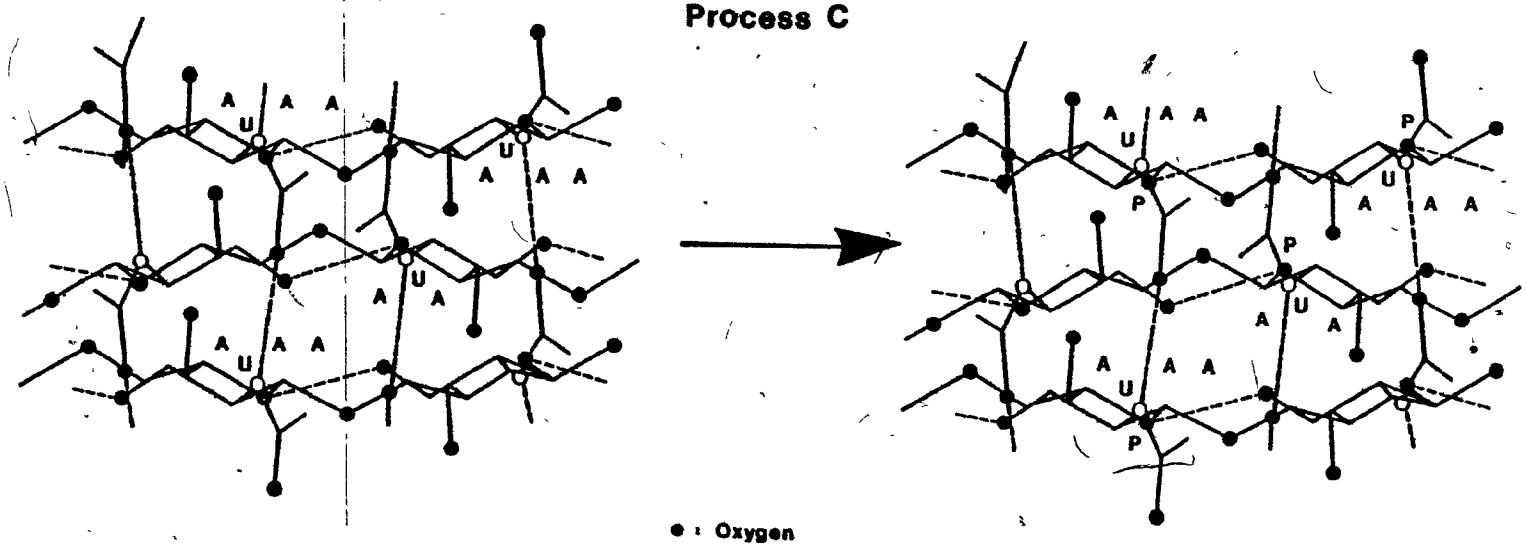

● : Oxygen

○ : Nitrogen

U : Complexed Uranium

A : Adsorbed Uranium

P : Uranyl Hydroxide

Complexation of uranium by chitin (Process A) triggers Process C and assists Process B. On the other hand, the accumulation of the adsorbed uranium by Process B affects the equilibrium of Process C. All three processes are important as they are interrelated and affect the overall equilibrium uptake capacity of the mycelium.

A decrease in solution pH has been confirmed to result in a reduction of the total U uptake capacity. Solution pH affects:

(i) Hydrolysis of the chitin amine. Low solution pH increases H_3O^+ concentration and intensifies the competition among H_3O^+ and uranium ions for the chitin complexation sites.

(ii) Uranium adsorption which is a process that depends significantly on the physical and chemical characteristics of the adsorbate[51]. At pH below 2.5 uranium exists in solution in the simple UO_2^{+2} form, while at pH $\geq$ 2.5 it hydrolyses extensively (I.4)[20,22,77,78]. Hydrolysis is accompanied by significant reduction in solubility. Lower solubility promotes adsorption. Higher solution pH, therefore, favours Process B by reducing uranium solubility and also by favouring uranium complexation by chitin (in the absence of other co-ions).

(iii) Hydrolysis of the uranium-chitin complex which is a strong function of pH (Process C).

In terms of technical application, it is important to note that, at pH = 4, the described uranium biosorption system approaches 66% of equilibrium within the first 60 seconds of contact. This partial

equilibrium is maintained for some time (III-A.10). High rate contact processes such as fluidized bed reactors could therefore be implemented efficiently. The utilization of even 66% of the equilibrium capacity provides an available equilibrium loading in excess of 120 mg/g which is still very attractive compared to other materials (Table III-A.1). It becomes even more attractive if we consider the rapid kinetics of the uptake. Solution pH should be close to 4 as at that pH value the uptake rate and the loading are optimum. At that pH, attention should be paid to the co-ions present in solution which can impare the overall process performance.

IV-A.11 Precision of Uranium Analytical Determination

An estimate of the precision of the uranium analytical method was obtained by analysing a uranium standard solution 16 times. The data are presented in Appendix A. Table IV-A.1 summarizes the statistical evaluation of the repeated tests.

TABLE IV-A.1

Statistics of Uranium Analytical Determination, Absorbance

Variable	Mean ($\bar{A}$)	Std. Deviation(s)	Range	Sample Size(n)
Absorbance	0.263	0.004	0.013	16

A frequency histogram of the determined absorbance values is also presented in Table IV-A.2 below:

TABLE IV-A.2

Absorbance Values Frequency Histogram

Frequency	5	2	2	7	$\eta = 16$
7				*	
6				*	
5	*			*	
4	*			*	
3	*			*	
2	*	*	*	*	
1	*	*	*	*	
	0.256	0.259	0.262	0.266	0.269

The 95% confidence limits computed from the data above give the following range:

$$\text{Lower limit} = \overline{A} - t_a \, S/\sqrt{\eta} = 0.261$$

$$\text{Upper limit} = \overline{A} + t_a \cdot S/\sqrt{\eta} = 0.265$$

The 95% confidence limits range extends to approximately 2% of the mean value, indicating good precision of the analytical technique. An estimate of the accuracy of the technique was obtained by comparing the mean concentration calculated from the absorbance precision data above (Appendix A) to the actual uranium concentration (30 mg/l) of the standard solution used. Table IV-A.3 presents a statistical evaluation of the U(VI) concentration determination.

TABLE IV-A.3

U(VI) Concentration Determination Statistics

Variable	Mean ($\bar{C}$)	Std. Deviation(s)	Range	Error
C, mg/1 U^{+6}	28.9	0.49	1.43	1.1

The difference (error) between the mean concentration value and the standard solution concentration was not smaller than 1 mg/1. The relative error is expected to increase at very low or high absorbance values; a characteristic inherent to all spectrophotometric techniques[28].

An estimate of the precision of the overall experimental technique used for the determination of the uranium biosorptive uptake capacity (q) was obtained by preparing and analysing 8 separate samples, all with identical initial U(VI) concentrations, pH, temperature, sample volume and, as close as possible, biomass dosage (Appendix A).

Table IV-A.4 presents a summary of the statistics concerning the experimental accuracy of q determination.

TABLE IV-A.4

Statistics of U(V1) Biosorptive Uptake Capacity Determination

Variable	Mean ($\bar{q}$)	Std. Deviation(s)	Range	Sample Size (n)
q (mg/g)	144	7.9	21	8

The 95% confidence limits calculated from the above information are[101]:

$$\bar{q} \pm t_a \cdot 7.9/\sqrt{8} = 144 \pm 7$$

The 95% confidence limits extend to approximately ±5% of the mean value: $\bar{q}$.

IV-B. THORIUM

IV-B.1 Thorium Biosorption Equilibrium Uptake Studies

Sections III-B.1 and III-B.2 presented all thorium biosorption isotherm data obtained in this work. The effects of solution pH, initial thorium concentration and solution temperature on q are discussed in the sections that follow.

IV-B.1.1 pH Effect on q

With the exception of *Aspergillus niger* and the municipal waste activated sludge, all materials examined exhibited lower thorium uptake at pH = 2 than at pH = 4 or 5.

One of the profound effects of solution pH on the *R. arrhizus*-thorium biosorption system is the rapid decrease of thorium solubility with increasing pH[22]. Thorium hydrolysis is more complicated than uranium hydrolysis[21, 22, 26, 27]. Thorium starts hydrolysing at pH = 2, and at pH $\geq$ 4 exists in solution mainly in the form of the hydroxide, $Th(OH)_4$, occurring as colloidal particles below 300A° in diameter[21]. Thorium solutions are supersaturated at pH = 3, at as low concentrations as 10^{-5} M Th^{+4} [22]. There appears to be a qualitative correlation between a reduction in thorium solubility and an increase in q. This correlation will be discussed further in Section IV-B.10. It is similar to the correlation suggested in Section IV-A.1.1 for uranium.

The ion exchange resin IRA-400 exhibited, as expected, poor thorium uptake. Activated carbon F-400, following the known correlation of adsorptive uptake with the solubility of the adsorbate, exhibited higher uptake (over 60 mg/g) at pH = 4 than at pH = 2 (5 mg/g).

IV-B.1.2 Effect of Initial Thorium Concentration on q

Initial thorium concentration had no effect on the thorium biosorption isotherms of all materials tested. The same equilibrium curve was approached from different combinations of initial thorium concentration and biosorbent dosage, thus indicating, as in the case of uranium (III-A.1.2), true equilibrium results independent of the specific sample used.

IV-B.1.3 Temperature Effect on q

As with uranium, thorium biosorptive uptake by R. arrhizus was not strongly influenced by temperature changes in the 5°C to 40°C range. In terms of process application, the significance of this conclusion is the same as that suggested in IV-A.1.3.

IV-B.1.4 Relation of Th Biosorption Equilibrium Data to Other Biosorption Equilibrium Data

Data on thorium biosorption are almost non-existent in the literature so as to compare with the results determined in the course of the present work. However, in the light of the chemical

similarities between uranium and thorium, the knowledge on uranium biosorption serves as an indirect indication of the potential of thorium biosorption.

Comparing the results reported in Table III-A.1 and III-B.1, uranium and thorium biosorptive uptake data correspond reasonably well for all materials tested.

IV-B.2 Linearization of Thorium Biosorption Isotherms

The higher S.E.E. values observed for some thorium biosorption isotherms may have been in part due to the presence of zero equilibrium concentration points (q_i, 0) on the isotherm that cannot be described successfully by either model. A similar observation has been made in Section IV-A.2 regarding the uranium biosorption isotherms.

The good fit of both physicochemical adsorption isotherm models to all available thorium biosorption isotherm data was interpreted as an indication that the process of adsorption is involved in the phenomenon of thorium biosorption. This is discussed further in Section IV-B.10.

IV-B.3 Pure Cell Wall Preparation Thorium Uptake

Following reasoning similar to that presented in Section IV-A.3, the higher thorium uptake exhibited by the *R. arrhizus* pure cell wall

preparation suggested that the mycelial cell wall of R. arrhizus was mainly responsible for thorium biosorption.

IV-B.4 Electron Microscopy of Thorium Biosorption

The data presented in Section III-B.5 confirmed that thorium biosorption is concentrated in the cell wall of R. arrhizus. The conclusion reached in Section IV-A.4 is not similar. Biosorbed uranium was distributed throughout the R. arrhizus cell wall in discrete strata similar to the chitin layers (Figure III-A.10). Thorium, on the contrary, was deposited on the outer surface of the R. arrhizus cell wall in a single layer (Figure III-B.10). This difference is significant as it indicates that there is some difference between the biosorptive uptake mechanisms of uranium and thorium by R. arrhizus. Figure III-B.12 presents a typical thin section electron micrograph of R. arrhizus following thorium uptake at pH = 2. The electron dense layer that appears on the outer surface of the cell wall when thorium is taken up at pH = 4 does not form when thorium is taken up at pH = 2. This difference is discussed in Section IV-B.10.

IV-B.5 Pure Chitin Thorium Uptake

Mass spectroscopy was unable to reveal the presence of thorium in reacted chitin probably for the same reasons it failed to indicate the presence of uranium in the uranium-chitin complex (III-A.6).

Information on the thorium uptake by chitin is unavailable in the literature. The experimental determination of the 8 mg/g uptake capacity of thorium by chitin is the only available direct evidence of thorium binding by chitin. Metal-chitin complex formation, however, has been studied extensively, and reports abound in the literature. There is strong evidence for the formation of coordination complexes between metal cations and the chitin nitrogen (Appendix F). The data presented in this work on uranium uptake by chitin (III-A.6), the general information in Appendix F.4 and the experimentally determined 8 mg/g thorium uptake by pure chitin suggests that thorium forms a coordination complex with chitin in a manner similar to that of uranium.

The observed uptake of thorium by chitin (8 mg/g) means that, on the average, 1 out of 130 glucosamine monomers has a coordinated thorium ion on it. The competition between thorium and H_3O^+ ions for coordination with the chitin nitrogen is probably one of the factors responsible for the calculated 1:130 ratio of thorium-bearing to thorium-free glucosamine monomers (IV-A.5). All nitrogen electron pairs do not appear to be available for thorium coordination, the equilibrium being influenced by solution pH (IV-A.10).

IV-B.6 N-Acetyl-D-Glucosamine Interaction with Thorium

The observed ability of chitin to take up thorium allows the suggestion that NAGl, the chitin monomer unit, also interacts with thorium. However, the NAGl-Th complex appeared water soluble and not

easily hydrolysable (III-B.6). Similar cases of water soluble and not easily hydrolysable glucosamine-metal complexes have been reported in the literature for some transition metals[65, 66, 67, 79]. These cases support the proposed existence of the chitin-Th complex.

IV-B.7 Infrared Spectroscopy of Thorium-Equilibrated *R. arrhizus* Cell Walls

Thus far, the cell wall of *R. arrhizus* has been confirmed as the part of the mycelium that is responsible for the observed biosorptive uptake of thorium. Chitin has also been confirmed as capable of retaining thorium, most likely by coordination of thorium with the chitin nitrogen (IV-B.5).

The band assignments of the recorded 4000-400 cm^{-1} IR spectra are the same as the ones presented in Section IV-A.7 and will not be repeated in the present Section.

In the 400 to 340 cm^{-1} section of the IR spectrum, absorbance bands centered at 397 cm^{-1}, 391 cm^{-1}, 368 cm^{-1}, 352 cm^{-1} and 341 cm^{-1} have been considered to be due to the presence of water vapour, and due to metal-water vibrations that occur in the 700-350 cm^{-1} range[57]. The 341 cm^{-1} and 368 cm^{-1} bands, for example, are also present in the gaseous H_2O IR spectrum[57, 64]. The new band that was identified at 362 cm^{-1} was assigned to the thorium nitrogen bond stretch vibrations. This assignment is supported by the following literature information:

i. Absorption in the range of 358 cm^{-1} to 367 cm^{-1} in the spectra of quinoline and isoquinoline-thorium complexes, absent in the IR spectra of the free bases, has been assigned to thorium-nitrogen bond stretch vibrations[71].

ii. The 362 cm^{-1} new absorption band lies within the range generally assigned to the metal-nitrogen bond stretch vibrations (III-A.7) 57, 70.

iii. A similar case was observed following uranium uptake by the cell wall. The new peak at 374 cm^{-1} has been assigned to the uranium-nitrogen coordination bond stretch vibrations (IV-A.7).

The proposed assignment of the 362 cm^{-1} absorbance band to the metal-nitrogen bond stretch vibrations supports the suggested coordination of thorium by the chitin nitrogen (IV-B.5).

IV-B.8 Co-ion Effect on Thorium Biosorption

Table III-B.4 suggests that, in contrast to the case of uranium biosorption, competition of other cations for the chitin complexation sites does not have an appreciable effect on the overall thorium biosorptive uptake. This, in turn, suggests that a mechanism different from the one presented in Section IV-A.10 for uranium is responsible for the biosorptive uptake of thorium. Section IV-B.10 will present the thorium uptake mechanism hypothesis, and will discuss further the observed co-ion effect on q.

In terms of process application, the results in Table III-B.4 are encouraging as they point out that, unlike uranium biosorption, in the case of thorium biosorption there was little effect of co-ions present in solution, namely Fe^{+2} and Zn^{+2}, on the overall thorium biosorptive uptake capacity of R. arrhizus.

IV-B.9 Thorium Biosorption Kinetic Data

Table III-B.5 presented the experimental conditions employed during the thorium uptake kinetic experiments.

The 15-30 mg/l Th^{+4} initial concentration range was selected for the following reasons:

a) Thorium hydrolyses in solution. Hydrolysed solutions of thorium are extensively supersaturated with respect to precipitation of the hydrous oxide or the oxide. Low thorium concentrations were therefore used to ensure the stability of the solutions, especially at pH = 4 (I.5).

b) Sample processing and the determination of Th^{+4} concentration are easier, as within this concentration range there is no need for sample dilution. The elimination of sample dilution increases the accuracy and the precision of the analytical procedure.

Following the selection of the initial thorium concentration, biomass dosage was calculated as explained in Section III-A.9.

The agitation rate was also selected following the same considerations as in Section IV-A.9, drawing also experience from the uranium experiments. The kinetic processes involved in thorium

biosorption can be regarded in a way similar to that described for uranium (IV-A.9). The overall rate of thorium uptake depends upon the limiting one of the following steps:

1. Transport of biosorbing thorium ions from the bulk solution to the external surface of the boundary film around the microbial cell.

2. Transport of thorium ions through the boundary film to the microbial cell surface.

3. Actual biosorption of thorium by the external section of the cell wall.

4. Transport of thorium ions through the cell wall to internal active sites (IV-B.10).

5. Biosorption of transported thorium ions by the internal active sites.

The slowest of the previous processes controls the overall rate of thorium uptake. In a well-mixed batch reactor, as the one used in the present work, step 1 does not represent any limitation. Thorium concentration is uniform in the bulk liquid phase. Biosorption of thorium by internal cell wall active sites is independent of the uptake by the external cell wall (IV-B.10), and contributes insignificantly to the overall biosorption uptake capacity of R. arrhizus. Steps 4 and 5 therefore are not expected to affect significantly the overall biosorption uptake rate. Actual biosorption by the external cell wall

(Step 3) is also considered to be a rapid process (IV-B.10), thus leaving step 2 as the process that most likely influences significantly thorium biosorption uptake rate. The mixing rate emerges as an important parameter that may considerably affect the observed overall biosorption uptake rate. Following the experience with uranium biosorption, agitation rates of 1000 RPM and 1300 RPM were tested (Figure III-B.25). At 1300 RPM the thorium uptake rate was not limited by film diffusion as equilibrium was attained within the first 30-60 seconds of contact (the shortest time possible for sampling). An agitation rate of 1300 RPM was therefore used for all subsequent kinetic experiments.

The common characteristics of the thorium biosorption rate curves have been presented in Section III-B.10. Unlike the case of uranium biosorption, the equilibrium plateau attained within the first 60 seconds of thorium biosorption remained stable thereafter. The plateau corresponded to the thorium equilibrium uptake capacity of R. arrhizus indicated by the biosorption isotherm for the respective thorium equilibrium concentration in the reactor.

Solution temperature, biomass dosage and initial thorium concentration did not have a discernible effect on the determined thorium uptake rate within the range examined. Solution pH, however, appeared to affect significantly the overall thorium uptake rate (Figure III-B.27). Acidic pH does not enhance either the equilibrium thorium uptake capacity of R. arrhizus (III-B.1) or the respective rate of thorium biosorption. The reasons for the effect of pH on thorium

biosorption uptake will be discussed in Section IV-B.10.

Kinetic data on biosorption of thorium by R. arrhizus are not available in the literature for comparison with the experimental data obtained in the course of the present work. However, uranium uptake rate data can be considered relevant information in support of the thorium biosorption kinetic data determined. Both uranium and thorium biosorption uptake rates appear equally rapid at the beginning of the process. Thorium, however, does not exhibit the slower secondary increase in uptake as was apparent with uranium. This will be discussed further in Section IV-B.10. Solution pH and agitation rate appear to be the parameters that, within the examined range, influence more effectively uranium and thorium uptake rates.

IV-B.10 Mechanism Hypothesis on Thorium Biosorption by Rhizopus arrhizus

The information accumulated on biosorptive uptake of thorium by R. arrhizus allows the formation of a mechanism hypothesis on the biosorptive sequestering of thorium by the mycelium. The proposed mechanism involves two separate processes that are described below.

Process A

Process A of the proposed mechanism hypothesis involves the formation of a coordination complex between thorium and the nitrogen of the cell wall chitin. This is similar to the formation of the uranium-chitin complex (IV-A.10).

Thorium coordinates with the cell wall chitin nitrogen and is retained by the cell wall of the mycelium. Evidence supporting the proposed Process A is supplied by the following experimental results.

1. In Section III-B.5 it was concluded that all biosorbed thorium is concentrated in the R. arrhizus cell wall which contains chitin.

2. The ability of chitin to retain thorium was experimentally confirmed in the present work. At pH = 4 pure chitin exhibited a thorium uptake capacity of 8 mg/g. Although not exclusively conclusive, this fact is a strong indication of the chitin role.

3. Both uranium and thorium have empty 6f orbitals and partially filled 5f orbitals[73] (Table IV-B.1). The 5f orbitals are more likely to engage in bonding, and there is some evidence of this behaviour[60].

TABLE IV-B.1

Outer Orbitals Electron Configuration of U and Th

Orbital / Element	5f	6d	7s
U	3	1	2
Th	0	2	2

The electron configuration suggests a considerable similarity in the chemical behaviour of U and Th[20, 24]. The similarity between the

chemical behaviour of U and Th suggests that, like uranium, thorium may coordinate with the chitin nitrogen (IV-A.10). As can be expected because of the similarities in the chemical behaviour of the two elements, the thorium uptake by chitin determined at 8 mg/g is close to the chitin-uranium uptake (6 mg/g).

4. Following thorium uptake, a new absorbance band appeared at 362 cm^{-1} on the IR spectrum of the R. arrhizus cell walls (Figure III-B.20). The 362 cm^{-1} absorbance peak has been assigned to the thorium-nitrogen bond vibrations (IV-B.7). The presence of the peak supports the proposed coordination of thorium with the cell wall chitin nitrogen.

Process B

Process B of the proposed thorium biosorption mechanism involves the adsorption of hydrolysed thorium ions by the outer layers of the R. arrhizus cell wall. The following experimental results support this hypothesis:

1. Thorium uptake by pure chitin has been determined to be only 8 mg/g. Chitin constitutes a fraction of the cell wall dry weight. Consequently, thorium uptake by mycelial cell walls by chitin complexation accounts for less than 8 mg/g. The experimentally determined overall biosorptive uptake of thorium by R. arrhizus is much greater (170 mg/g), suggesting the presence of a second process other than complexation by chitin. This second process contributes the major part ($\geq$95%) of the overall thorium biosorptive uptake observed.

2. Thorium biosorption isotherms were successfully described by the well accepted adsorption isotherm models of Langmuir and Freundlich (III-B.2). This indicates that adsorption is one of the processes involved in thorium biosorptive uptake by R. arrhizus.

3. Thorium starts hydrolysing at pH = 2 and above pH = 4 exists in solution mainly in the form of fine hydroxide particles of $Th(OH)_4$ [21]. Thorium hydrolysis follows complicated simultaneous equilibria. Thorium hydrolysis products exhibit a strong tendency to adsorb, as documented in the literature[21, 26, 27]. This tendency supports the proposed adsorption of thorium by the fungal cell wall.

4. The rate of biosorptive uptake of thorium by R. arrhizus was discussed in Sections III-B.10 and IV-B.9. The experimental results indicated that thorium biosorption is a very rapid process. Consequently, the processes proposed to participate in the thorium biosorption mechanism must be rapid. Adsorption in the absence of mass transfer limitations has been documented as a rapid process[74]. The proposed adsorption of hydrolysed thorium ions by the R. arrhizus cell wall is therefore compatible with the observed experimental kinetic results.

5. Adsorption of thorium hydrolysis products by the external cell wall appears to be unrelated to the thorium which is complexed by the stratified chitin microfibrils in the inner layers of the cell wall. The presence of co-ions like Fe^{+2} or Zn^{+2} (IV-B.8) results, as already discussed, in competition among the cations for the chitin complexation

sites. Any reduction in the quantity of thorium taken up by complexation because of co-ion competition would only constitute a small proportion of the overall biosorptive uptake. Consequently, the presence of co-ions in solution should have an insignificant effect on the observed overall thorium uptake by R. arrhizus. The experimental results confirmed this as a fact.

Unlike the case of uranium biosorption, where the proposed three processes appear to be interacting (IV-A.10), thorium biosorption processes (A and B) appear unrelated. Thorium biosorption by R. arrhizus at pH = 4 is dominated by the adsorption of thorium hydrolysis products. As a result, the observed effect of pH on thorium uptake can be better understood. A reduction in solution pH would affect:

i. The hydrolysis of the chitin amine, resulting in an increased competition by H_3O^+ for the complexation sites (III-A.10).

ii. The adsorptivity of thorium ions. The configuration as well as the solubility of thorium hydrolysis products is a strong function of solution pH. Reduction of solution pH results in increased solubility and consequently in reduced adsorptivity. Reduced adsorptivity diminishes the biosorptive uptake capacity of the biomass, as was observed at pH = 2.

No thorium uptake kinetic curve, at pH = 4, exhibited the secondary increase in uptake that was a common characteristic of all uranium kinetic curves at the same pH. As a result, it is reasonable to accept that process C of the uranium biosorption mechanism hypothesis is not applicable to the case of thorium biosorption. This

is supported by the information in Section III-B.6 which indicates that the chitin-thorium complex is water soluble and not easily hydrolysable.

Unlike uranium, thorium was adsorbed by the outer layers of the R. arrhizus cell wall, probably because of the size of the hydrolysed thorium ion at pH = 4. This hypothesis was supported by the thin section electron micrographs of R. arrhizus cell wall taken at pH = 2 following thorium uptake (Figure III-B.12). The distinct electron dense layer was not formed at pH = 2. At pH = 2 thorium exists in solution mainly in the form of Th^{+4}, which is considerably smaller than the $Th(OH)_4$ particles that predominate at pH = 4. The smaller Th^{+4} ions penetrate and absorb within the cell wall. The low contrast on the electron micrographs is probably due to the lower thorium uptake exhibited by R. arrhizus at pH = 2 (90 mg/g) than at pH = 4 (170 mg/g) and the increased dispersion of the electron dense thorium within the cell wall at pH = 2. Confirmation of thorium presence through Xray-E.D.A. was not possible because thorium concentration was below the detection limits of the technique.

It is significant for the process application of thorium biosorption that the examined thorium biosorption system reached final equilibrium very quickly. Consequently, the implementation of high rate contact processes (e.g. fluidized bed reactors) appears possible. The understanding of the processes involved in thorium biosorption by R. arrhizus should lead to the rational design of new technical applications for thorium biosorption.

IV-B.11 Precision of Thorium Analytical Determination

An estimate of the precision of the employed thorium analytical method was obtained by analysing a thorium standard solution 10 times. The data are available in Appendix B. Table IV-B.2 summarizes the statistical evaluation of the test of precision.

TABLE IV-B.2

Statistics of Thorium Analytical Determination Absorbance

Variable	Mean ($\bar{A}$)	Std. Deviation(s)	Range	Sample Size (n)
Absorbance	0.067	0.004	0.011	10

A frequency histogram of the determined absorbance values is presented in Table IV-B.3.

TABLE IV-B.3

Absorbance Values Frequency Histogram

Frequency:	3	Ø	5	2	n = 10
6					
5			*		
4			*		
3	*		*		
2	*		*	*	
1	*		*	*	
	0.060	0.063	0.066	0.069	0.072

The 95% confidence limits computed from the above data are

$$\overline{A} \pm t_a \cdot S \cdot / \sqrt{n} = 0.167 \pm 0.003$$

The range of the 95% confidence limits is equivalent to approximately 4% of the sample mean absorbance value.

An estimate of the accuracy of the thorium concentration determination technique can be obtained by comparing the mean concentration calculated from absorbance precision data above (Appendix A) to the actual thorium concentration, 20 mg/l Th^{+4}, of the standard solution used. Table IV-B.4 summarizes the statistical evaluation of the thorium concentration determination test.

TABLE IV-B.4

Thorium Concentration Determination Statistics

Variable	Mean ($\overline{C}$)	Std. Deviation(s)	Range	Error
C, mg/l Th^{+4}	18.7	0.464	1.23	1.3

The difference between the mean concentration and the known standard solution concentration, error, is not smaller than 1 mg/l, and is very close to the value estimated for the analytical determination of uranium concentration.

An estimate of the precision of the overall experimental procedure used for the determinations of the thorium biosorptive uptake capacity, q, was obtained by preparing and analysing 7 separate samples. All samples had identical initial thorium concentration, pH, temperature, sample volume, and, as close as possible, biomass dosage (Appendix B). Table IV-B.5 presents a summary of the statistical evaluation of the test.

TABLE IV-B.5

Statistics of Thorium Biosorptive Uptake Capacity Determination

Variable	Mean ($\bar{q}$)	Std. Deviation(s)	Range	Sample Size (n)
q (mg/g)	141	5.96	15	7

The 95% confidence limits calculated from the above information, (Table III-B.10), are:

$$q \pm t_a \cdot s/\sqrt{n} \simeq 141 \pm 6$$

The calculated 95% confidence limits range encompasses approximately ±4% of the mean, $\bar{q}$, value.

CHAPTER V

CONCLUSIONS

V-1 CONCLUSIONS

In the previous chapters the materials, methods and experimental results of the present work were presented. The information accumulated in the course of the present study leads to the following conclusions:

1. It is possible to remove uranium and thorium from aqueous solutions using the phenomenon of biosorption.

2. Microbial biomass of R. arrhizus is an effective biosorbent for both uranium and thorium, with uptake capacities from respective pure solutions of approximately 180 mg U^{+6}/g and 170 mg Th^{+4}/g.

3. Optimum biosorption pH lies in the range of pH = 4 to pH = 5. Reduced biosorptive uptake is exhibited by R. arrhizus, as well as by most of the tested biomass types, at lower solution pH (pH = 2).

4. Solution temperature changes in the range of $5^{o}C$ to $40^{o}C$ have little effect on R. arrhizus uranium and thorium biosorptive uptake capacity.

5. Changes in initial uranium or thorium concentration and biomass dosage had no discernible effect on R. arrhizus biosorptive uptake capacity of either of the two elements within the examined range.

6. The presence of other cations in solution may, at pH = 4 as indicated by the examined cases of Fe^{+2} and Zn^{+2}, reduce significantly the uranium biosorptive uptake capacity of R. arrhizus. Fe^{+2} and Zn^{+2} have no effect on the thorium biosorptive uptake capacity of R. arrhizus.

7. Biosorption of U and Th by R. arrhizus are rapid processes. Uranium uptake reaches approximately 66% equilibrium within 60 seconds, attaining final equilibrium within approximately 60 minutes. Thorium biosorption by R. arrhizus reaches final equilibrium within the first 60 seconds of contact. Reduction of solution pH to pH = 2 significantly reduces the rate of uptake of both uranium and thorium.

8. Biosorption of uranium is concentrated in the cell wall of R. arrhizus and involves three separate but interacting processes:

(A) Coordination of U(VI) by the primary amine nitrogen of the R. arrhizus cell wall chitin.

(B) Adsorption of uranium by the cell wall chitin network.

(C) Hydrolysis of the uranium-chitin complex and micro-precipitation of uranyl hydroxide in the cell wall chitin network.

9. Biosorption of thorium is a phenomenon concentrated in the cell wall of R. arrhizus and involves two separate processes:

(A) Coordination of thorium by the primary amine nitrogen of the cell wall chitin.

(B) Adsorption of thorium hydrolysis products by the (external) surface of the mycelium cell wall.

10. The proposed mechanism hypotheses for biosorption of uranium and thorium by R. arrhizus are not identical. It is therefore reasonable to accept that biosorption is not a phenomenon with one single mechanism. Each biosorption system investigated should be examined separately, perhaps in a way similar to the one followed in the present work. Some of the individual processes involved in biosorption (e.g. adsorption) appear to be common. Their interactions, however, in a specific biosorption system are not common, as they depend on the physical and chemical characteristics of both the biosorbent and the biosorbate.

V-2 ORIGINAL CONTRIBUTIONS

The present study constitutes the first systematic examination of the phenomenon of biosorption. As a result, several elements of the present study are considered to be original contributions to the advancement of knowledge:

1. Testing of the uranium and thorium biosorbent properties of the following biomass types:

Aspergillus niger

Aspergillus terreus

Streptomyces niveus

Pseudomonas fluorescens

Penicillium chrysogenum

Rhizopus arrhizus

Municipal waste activated sludge

Industrial waste activated sludge ("Phenolic")

2. The determination of the uranium biosorption isotherms for the above materials under controlled conditions and at pH values of 2, 4 and 5.

3. The determination of the thorium biosorption isotherms for the above materials under controlled conditions and at pH values of 2, 4 and 5.

4. Comparison of the uranium and thorium biosorption isotherms of the above materials to the uranium and thorium uptake isotherms of activated carbon Filtrasorb 400 and the ion exchange resin IRA-400.

5. The examination of the effect of the presence of Fe^{+2} and Zn^{+2} upon the uranium and thorium biosorption uptake capacity of the biomass of *R. arrhizus*.

6. The design and construction of a special reactor assembly for the study of the kinetics of uranium and thorium biosorption.

7. The determination of the rate of uptake of uranium and thorium by *R. arrhizus* biomass under controlled conditions.

8. The formulation of a mechanism hypothesis for uranium biosorption by *R. arrhizus*. The mechanism hypothesis is consistent with available experimental data.

9. The formulation of a mechanism hypothesis for biosorption of thorium by R. arrhizus. The hypothesis is consistent with available experimental data.

10. Examination of the R. arrhizus cell wall sequestering pattern of uranium and thorium deposition by transmission electron microscopy and X-rays Energy Dispersion Analysis.

11. Infrared spectroscopic analysis of uranium and thorium biosorption by the R. arrhizus cell wall.

In general, the work resulted in a better understanding of the phenomenon of biosorption and the constituent mechanisms.

CHAPTER VI

RECOMMENDATIONS

The present work has indicated the potential of developing novel sequestering agents, biosorbents, for the removal and recovery of high atomic number cations from solution. At least five industrial scale applications appear feasible:

1. Recovery of nuclear fuel elements from process solutions.

2. Decontamination of radioactive waste waters originating from uranium ore mining and processing operations.

3. Recovery of elements from sea water.

4. Decontamination of radioactive waste waters from nuclear power reactors.

5. Recovery of radionuclides from nuclear reactor waste waters.

Future research in the subject of biosorption may be directed towards providing information that will facilitate the proposed industrial applications of biosorption.

The general objectives of the proposed research should aim at the expansion of available biosorption data to include more elements and more types of biomass. More specifically, the following objectives may be pursued:

1. Testing of new biomass types for their biosorption uptake capacity.

2. Investigation of the potential of biosorption of selected elements other than uranium and thorium, identified in the nuclear fuel cycle solutions.

3. Testing of selected biomass types with actual process waste waters containing a mixture of elements.

4. Examination of different methods to impart desirable mechanical properties to the biosorbing biomass to be used in actual processes.

In parallel to the application-oriented research objectives described above, additional research is also recommended towards further examination of the kinetics of biosorption as well as the elucidation of the mechanism involved in the biosorptive uptake of elements by other types of biomass.

A more complete understanding of the phenomenon of biosorption is desirable for further efforts towards the manipulation of it for improved selectivity and efficiency.

REFERENCES

1. Moffett, D., "The Disposal of Solid Wastes and Liquid Effluents from the Milling of Uranium Ores", CANMET publication # M38-13176-19, 1976.

2. Hans, M.J., and Eadie, G.G., "Environmental Contamination from Uranium Mill Tailings Piles", E.P.A. Las Vegas facility report, Las Vegas, NV, 1975.

3. Goldsmith, W.A., "Radiological Aspects of Inactive Uranium Milling Sites: An Overview", Nuclear Safety, 17, 6, 1976.

4. E.P.S., "Mine and Mill Waste Water Treatment", Report EPS 3-WP-75-5, 1975.

5. Reed, A., Meeks, H.C., Pomeroy, S.E., and Hale, V., "Assessment of Environmental Aspects of Uranium Mining and Milling", N.T.I.S. PB 266413, Washington, D.C., 1976.

6. Richard, R.J., "Recovery of Uranium from Natural Mine Waters by Counter-current Ion Exchange", U.S. Department of Interior, Bureau of Mines, TN 23, U7, # 7471, 1971.

7. Eadie, G.G., Kaufmann, R.F., "Radiological Evaluation of the Effects of Uranium Mining and Milling Operations on Selected Ground Water Supplies in the Grants Mineral Belt, New Mexico", Health Physics, 32, pp.231-241, 1977.

8. Sears, M.B., "Radioactive Waste Treatment Costs and Environmental Impact for Milling of Uranium Ores", American Nuclear Society, Transactions, 24, 94-95, 1976.

9. Rothstein, A., Frenkel, A. and Larrabee, C., "The Relation of the Cell Surface to Metabolism", J. Cell. and Comp. Physiol, 32, 261.

10. Polikarpov, G.G., "Radioecology of Aquatic Organisms", North Holland Publishing Co., Reinhold Book Division, NY, 1966.

11. Tezuka, Y., "Cation Dependant Flocculation in a Flavobacterium Species Predominant in Activated Sludge", Appl. Microbiol., pp.222-226, Feb. 1969.

12. Tanaka, Y., Skoryna, S.C., "Organic Macromolecular Binders of Metal Ions", from "Intestinal Absorption of Metal Ions, Trace Elements and Radionuclides", Pergamon Press, NY, 1970.

13. Paskins-Hurlburt, A.J., Tanaka, Y., and Skoryna, S.C., "Carrageenan and the Binding of Lead", Botanica Marina, 19, pp.59-60, 1976.

14. Chiu, Y.S., "Recovery of Heavy Metals by Microbes", Ph.D. Thesis, University of Western Ontario, London, Ont., 1972.

15. Jilek, R., Fuska, J. and Nemec, P., "Biologicky Sorbent Pro Dekontaminac, Vod Od Uranu", Biologia (Bratislava), 33, 3, pp. 201-207, 1978.

16. Beveridge, T.J. and Murray, R.G.E., "Uptake and Retention of Metals by Cell Walls of Bacillus subtilis", Journal of Bacteriology, pp.1502-1518, Sept. 1976.

17. Beveridge, T.J., "The Response of the Cell Walls of Bacillus subtilis to Metals and to Electron Microscopic Stains", Can. J. Microbiol., 24, pp.89-104, 1978.

18. Shumate II, S.E., Strandberg, G.W. and Parrott, J.R. Jr., "Biological Removal of Metal Ions from Aqueous Process Streams", Biotechnology-Bioengineering Symposium No. 8, pp.13-20, 1978.

19. Shumate II, S.E., Strandberg, G.W., Parrott, J.R. Jr. and Locke, B.R., "Separation of Uranium from Process Waste Waters using Microbial Cells as Sorbents", Paper presented at the CIM Hydrometallurgy meeting held in Toronto, Canada, Nov. 11-13, 1979.

20. Palei, P.N., "Analytical Chemistry of Uranium", Ann Arbor-Humphrey Science Publishers, London, 1970.

21. Pershin, A.S., "Hydrolysis of Thorium Nitrate", Radiokhimiya, 14, 1, pp.88-94, 1972.

22. Baes, C.F. Jr., and Mesmer, R.E., "The Hydrolysis of Cations", Wiley-Interscience, J. Wiley and Sons, N.Y., 1976.

23. "Encyclopedia of Industrial Chemical Analysis", Uranium, Volume 17, J. Wiley and Sons, N.Y., 1974.

24. Ryabchikov, D.I. and Gol'braikh, E.K., "Analytical Chemistry of Thorium", Ann Arbor-Humphrey Science Publishers, Ann Arbor, London, 1969.

25. "Encyclopedia of Industrial Chemical Analysis", Thorium, Volume 17, J. Wiley and Sons, N.Y., 1974.

26. Abramson, M.B., Jaycock, M.J. and Ottewill, R.H., "The Adsorption of Cations at the Silver Iodide-Solution Interface, Part II, Thorium", J. Chem. Soc., pp.5041-5045, 1964.

27. Abramson, M.B., and Ottewil, R.H., "The Interaction of Myristic Acid Monolayers with Thorium and Lanthanum Solutions", Journal of Colloid Science, 17, pp. 883-894, 1962.

28. Marczenko, Z., "Spectrophotometric Determination of Elements", J. Wiley and Sons, N.Y., 1976.

29. Savvin, S.B., "Analytical Use of Arsenazo III, Determination of Thorium, Zirconium, Uranium and Rare Earth Elements", Talanta, 8, pp. 673-685, 1961.

30. "Standard Methods for the Examination of Water and Waste Water", APHA, AWWS, WPCF, Fourteenth Edition, 1975.

31. Pouchert, C.J., "The Aldrich Library of Infrared Spectra", Aldrich Chemicals Col, Wisconsin, 1975.

32. Strandberg, G.W., Shumate II, S.E., Parrott, J.R., Jr., and McWhirter, D.A., "Microbial Uptake of Uranium, Casium and Radium", Paper presented at the Second Chemical Congress of ACS, August 24-29, Las Vegas, 1980.

33. Muzzarelli, R.A.A., "Chitin", Pergamon Press, 1972.

34. Masri, M.S., Reuter, F.W., and Friedman, M., "Binding of Metal Cations by Natural Substances", J. of Applied Polymer Science, 18, pp. 675-681, 1974.

35. Muzzarelli, R.A.A., and Tubertini, O., "Chitin and Chitosan on Chromatographic Supports and Adsorbents for Collection of Metal Ions from Organic and Aqueous Solutions and Sea Water", Talanta, 16, pp. 1571-1577, 1969.

36. Andreyev, P.F., Plisko, E.A., and Rogozina, E.M., "Reaction of Dilute Solutions of Uranyl Salts with Chitin and Some Cellulose Esters", Geokhimiya, 6, pp. 536-639, 1962.

37. Subramanian, Y., Yoshinari, T., and d'Anglejan, B., "Studies on the Formation of Chitin-Metal Complexes", Marine Sciences Centre, McGill University, Report 27, November 1974.

38. Ainsworth, G.C., and Sussman, A.S., "The Fungi. An Advanced Treatise", Academic Press, N.Y., 1965.

39. Farkas, V., "Biosynthesis of Cell Walls of Fungi", Microbiol. Rev., pp. 117-141, 1980.

40. Beran, K., Rehacek, J., and Seichertova, O., "Infrared Spectral Analysis of the Cell Wall. The Application of the Method in the Study of Chitin in the Cell Wall of the Yeast Saccharomyces cerevisiae", Acta. Pac. Med. Proc. 2nd Intern. Symp. on Yeast Protoplast, 1968.

41. Troy, A.E., and Koffler, H., "The Chemistry and Molecular Architecture of the Cell Walls of Penicillium chrysogenum", The Journal of Biological Chemistry, 244, 20, 1969.

42. Ruiz-Herrera, J., "Chemical Components of the Cell Wall of Aspergillus Species", Arch. of Biochem. and Biophys., 122, pp. 118-125, 1957.

43. Hamilton, P.B., and Knight, S.G., "An Analysis of the Cell Walls of Penicillium chrysogenum", Arch. of Biochem. and Biophys., 99, pp. 282-287, 1962.

44. Stagg, C.M., and Feather, M.S., "The Characterization of a Chitin-Associated D-Glucan from the Cell Walls of Aspergillus niger", Biochimica et Biophysica Acta, 320, pp. 64-72, 1973.

45. O'Brien, R.W., and Ralph, B.J., "The Cell Wall Composition and Taxonomy of Some Basidiomycetes and Ascomycetes", Annals of Botany, N.S., 30, 120, 1966.

46. Crook, E.M., and Johnston, I.R., "The Qualitative Analysis of the Cell Walls of Selective Species of Fungi", Biochem. J., 83, pp. 325-331, 1962.

47. Horikoshi, K., and Arima, K., "X-ray Diffraction Patterns of the Cell Wall of Aspergillus oryzae", Biochm. Biophys. Acta, 57, pp. 392-394, 1962.

48. Miyazaki, T., and Irino, T., "Studies on Fungal Polysaccharides. IX. The Acidic Polysaccharide from the Cell Wall of Rhizopus nigricans", Chem. Pharm. Bull., 19, 12, pp. 2545-2550, 1971.

49. Blumenthal, H.J., and Roseman, S., "Quantitative Estimation of Chitin in Fungi", J. Bacteriol., 74, pp. 222-224, 1957.

50. Benedek, A., "Carbon Evaluation and Process Design", Proceedings of the P.C.T. Activated Carbon Adsorption in Pollution Control, sponsored by Environment Canada, Ottawa, Ontario, 1974.

51. Tsezos, M., "Adsorption of Bioresidual Organics in a Fluidized Bed Biological Reactor", M.Eng. Thesis, McMaster University, Hamilton, Ont., 1978.

52. Chen, W., "The Effect of Surface Curvature on the Adsorption Capability of Porous Adsorbants", Ph.D. Thesis, University of South Carolina, 1969.

53. Muzzarelli, R.A.A., and Sipos, L., "Chitosan for the Collection from Sea Water of Naturally Occurring Zinc, Cadmium, Lead and Copper", Talanta, 18, pp. 853-858, 1971.

54. Glowacka, D., and Popowicz, J., "Zastosowanie Chityny do Chromatograficznego Rozdzialu UO_2^{2+}od Fe^{+3}, Ca^{2+}, Mg^{+2}", Rocz-i. Akad. Med. Bialyst., 11, pp. 47-51, 1965.

55. Pearson, F.G., Marchessault, R.H., and Liang, C.Y., "Infrared Spectra of Crystalline Polysaccharides. V. Chitin", J. of Polymer Science, 43, pp. 101-116, 1960.

56. Marchessault, R.H., and Liang, C.Y., "Infrared Spectra of Crystalline Polysaccharides. III. Mercerized Cellulose", J. of Polymer Science, 43, pp. 71-84, 1960.

57. Nakamoto, K., "Infrared Spectra of Inorganic and Coordination Compounds", Wiley Interscience, N.Y., 1969.

58. Ferraro, J.R., and Walker, A., "Comparison of the Infrared Spectra of the Hydrates and Anhydrous Salts in the Systems $UO_2(NO_3)_2$ and $Th(NO_3)_4$", J. of Chemical Physics, 45, 2, 1966.

59. Bullock, J.I., "Infrared Spectra of Some Uranyl Nitrate Complexes", J. Inorg. Nucl. Chem., 29, pp. 2257-2264, 1967.

60. Parish, R.V., "The Metallic Elements", Longman Ltd., London, 1977.

61. Allen, G.C., and Griffiths, A.J., "Vibrational Spectroscopy of Strondium Uranate (Ul) Compounds", J. of Chemical Society, Dalton, pp. 1144-1148, 1977.

62. Allen, G.C., and Griffiths, A.J., "Vibrational Spectroscopy of Alkaline-earth Metal Uranate Compounds", J. of Chemical Society, Dalton, pp. 315-319, 1979.

63. Addison, C.C., Champ, H.A.J., Hodge, N., and Norbury, A.H., "Anhydrous Uranyl Nitrate and Its Complexes with Some Oxygen and Nitrogen Donors", J. of Chemical Society, pp. 2354-2360, 1964.

64. Bellamy, L.J., "The Infrared Spectra of Complex Molecules", Chapman and Hall, London, 1975.

65. Sahu, C.R., and Mitra, A.K., "Fundamental Studies on the Interaction of Transition Metals with Carbohydrate Derivatives as Ligands. I. Reaction of 2-Deoxy-2-Amino-D-Glucopyranoside with Salts of Iron, Cobalt and Nickel", J. Indian Chem. Soc., 48, 9, 1971.

66. Tamura, Z., and Miyazaki, M., "Metal Complexes of D-Glucosamine and its Derivatives. IV. Determination of Stability and Equilibrium Constants of Metal Complexes of D-Glucosamine by pH Titration Method", Chem. Pharm. Bull., 13, 3, 1965.

67. Tamura, Z., Miyazaki, M., and Suzuki, T., "Metal Complexes of D-Glucosamine and its Derivatives. III. Determination of Acid Dissociation Constants of D-Glucosamine and its Three O-Methyl Derivatives", Chem. Parm. Bull., 13, 3, 1965.

68. Zhbankov, R.G., "Infrared Spectra of Cellulose and its Derivatives", Consultants Bureau, N.Y., 1966.

69. Michell, A.J., and Scurfield, G., "Composition of Extracted Fungal Cell Walls as Indicated by Infrared Spectroscopy", Archives of Biochemistry and Biophysics, 120, pp. 628-637, 1967.

70. Nagakawa, I., and Shimanouchi, T., "Far Infrared Spectra and Metal Ligand Force Constants of Metal Ammine Complexes", Spectrochimica Acta, 22, pp. 759-775, 1966.

71. Srivastava, T.N., Tandon, S.K., and Bhakru, N., "Complexes of Zirconium and Thorium Perchlorates with Some Heterocyclic Bases", J. Inorg. Nucl. Chem., 40, pp. 1180-1181, 1977.

72. Hradkova, B., Jilek, R., Stamberg, K., and Slovak, Z., "Sorpce Uranu Biosorbents", Symposium Pracorniku Banskeho Prumyslu, 215, 1975.

73. Bell, C.F., and Lott, K.A., "Modern Approach to Inorganic Chemistry", Butterworths, London, 1972.

74. Furusawa, T., and Smith, J.M., "Fluid Particle and Intraparticle Mass Transport Rates in Slurries", Ind. Eng. Chem. Fund., 12, 2, 1973.

75. Weber, W.J., Jr., "Physicochemical Processes", Wiley-Interscience, N.Y., 1972.

76. Beveridge, T.J., "Metal Uptake by Bacterial Walls", Paper presented at the Second Chemical Congress of ACS, August 24-29, Las Vegas, 1980.

77. Hearne, J.A., and White, A.G., "The Heat of Solution of Uranium Tetrachloride and the Hydrolysis of the Uranium (IV) Ion", J. of Chemical Society, pp. 2081-2085, 1957.

78. Hearne, J.A., and White, A.G., "Hydrolysis of the Uranyl Ion", J. of Chemical Society, pp. 2168-2174, 1957.

79. Tamura, Z., and Miyazaki, M., "Metal Complexes of D-Glucosamine and its Derivatives. V. Spectrophotometric Investigation on Copper (II), Nickel (II), and Cobalt (II). Complexes of D-Glucosamine and the Preparation of Glucosamine-Copper Complex", Chem. Pharm. Bull., 13, 3, 1965.

80. Ferraro, J.R., and Walker, A., "Far Infrared Spectra of Anhydrous Metallic Nitrates", J. of Chemical Physics, 42, 4, 1965.

81. Walker, A., and Ferraro, J.R., "Infrared Spectra of Anhydrous Rare-Earth Nitrates from 4000-100 cm^{-1}", J. of Chemical Physics, 43, 8, 1965.

82. Terrassé, J.M., Poulet, H., and Mathieu, J.P., "Spectres de Vibration et Fréquences Fundamentales de Composés de Coordination Hexamminés", Spectrochimica Acta, 20, pp. 305-315, 1964.

83. Hill, R.J., and Rickard, C.E.F., "Complexes of Thorium (IV) and Uranium (IV) with Some Schiff Bases", J. Inorg. Nucl. Chem., 40, pp. 793-797, 1978.

84. Elsabee, M.Z., Mattar, M., and Habashy, B.M., "Bonding Between Cu(II) Complexes with Celluloses and Related Carbohydrates", J. of Polymer Science, 14, pp. 1773-1781, 1976.

85. Gatehouse, B.M., Livingstone, S.E., and Nyholm, R.S., "Infrared Spectra of Some Nitrato-coordination Complexes", J. of Chemical Society, pp. 4222-5226, 1957.

86. Johnstone, R.A.W., "Mass Spectrometry for Organic Chemists", Cambridge Chemistry Texts, U.K., 1972.

87. Davies, O.L. and Goldsmith, P.L., "Statistical Methods in Research and Production", Oliver and Boyd, Edinburgh, 1972.

88. Geissman, T.A., "Principles of Organic Chemistry", W.H. Freeman and Co., San Francisco, 1976.

89. Parker, F.S., "Infrared Spectroscopy in Biochemistry Biology and Medicine", Plenum Press, N.Y., 1971.

90. Moller, K.D. and Rothschild, W.G., "Far Infrared Spectroscopy", Wiley-Interscience, N.Y., 1971.

91. Kay, D.H., "Techniques for Electron Microscopy", Blackwell Scientific Publications, Oxford, 1965.

92. Muzzarelli, R.A.A., Ferrero, A. and Pizzoli, M., "Light-scattering, X-ray Diffraction, Elemental Analysis and Infrared Spectrophotometry Characterization of Chitosan, a Chelating Polymer", Talanta, 19, pp.1222-1226, 1972.

93. Bond, W.D., Clairborne, H.C. and Leuze, R.E., "Methods for Removal of Actinides from High Level Wastes", Nuclear Technology, 24, pp.362-370, 1974.

94. Clark, D.A., "State of the Art: Uranium Mining, Milling, and Refining Industry", N.T.I.S. PB-235 557, 1974.

95. Anonymous, "Evaluation of the Impact of the Mines Development, Incorporated Mill on Water Quality Conditions in the Cheyenne River", N.T.I.S. PB-255 270, 1971.

96. Anonymous, "Stream Surreys in Vicinity of Uranium Mills. II. Area of Moab, Utah, August 1960", N.T.I.S. PB-260 277, 1961.

97. Anonymous, "Stream Surveys in Vicinity of Uranium Mills, I. Area of Grand Junction, Colorado, August 1960", N.T.I.S. PB-260 276, 1961.

98. Baker, M. Jr., "Inactive and Abandoned Underground Mines. Water Pollution Prevention and Control", N.T.I.S. PB-258 263, 1975.

99. Updegraff, D.M. and Douros, J.D., "The Relationship of Micro-organisms for Uranium Deposits", Develop. Industr. Microbiol., 13, pp.76-90, 1972.

100. Vydra, F. and Galba, J., "Sorption von Metallokomplexen an Silicagel III. Sorption von Hydrolysen produkten des Th^{+4}, Fe^{+3}, Al^{+3} und Cr^{+3}", Collection Czechoslov. Chem. Commun., 32, pp.3530-3536, 1967.

APPENDICES

APPENDIX A

URANIUM UPTAKE DATA

A.1 Uranium Biosorption Isotherms

1. *Rhizopus arrhizus*

Biomass g	C_{eq}, U^{+6} mg/l	$\Delta C, U^{+6}$ mg/l	q, U^{+6} mg/g	T °C	pH
0.1015	780	220	216	23	4
0.3009	391	609	202	23	4
0.5009	101	899	179	23	4
0.6143	54	946	154	23	4
1.0017	20	980	98	23	4
0.0039	88	7	180	23	4
0.0104	78	17	164	23	4
0.0109	77	18	165	23	4
0.0198	62	33	167	23	4
0.0399	40	55	138	23	4
0.0514	11	39	76	23	5
0.1015	4	46	45	23	5
0.2044	1	49	24	23	5
0.4049	1	49	13	23	5
0.5903	1	49	8	23	5
0.7194	1	49	7	23	5
1.0313	1	49	5	23	5
0.0106	76	17	160	23	5
0.0501	11	36	72	23	2
0.1031	3	44	43	23	2
0.1987	2	46	23	23	2
0.4002	1	46	11	23	2
0.0611	35	55	90	23	2
0.0465	50	40	86	23	2
0.0292	64	26	89	23	2
0.0300	49	45	150	23	4
0.0327	42	49	150	23	4
0.0297	46	48	162	23	4
0.0303	60	34	112	23	4

.....(cont'd.)

1 (cont'd.)

Biomass g	C_{eq}, U^{+6} mg/l	$\Delta C, U^{+6}$ mg/l	q, U^{+6} mg/g	T °C	pH
0.0103	81	19	184	5	4
0.0207	64	36	174	5	4
0.0305	50	49	161	5	4
0.0402	38	61	152	5	4
0.0194	68	32	165	5	4
0.0107	78	21	196	40	4
0.0204	57	42	206	40	4
0.0301	43	56	186	40	4
0.0407	30	69	170	40	4
0.0202	50	44	218	40	4
Cell Wall Preparation Plateau (Sample Volume 50 ml)					
0.0054	73	23	213	23	4
0.0085	65	31	182	23	4
0.0116	50	46	198	23	4
0.0110	55	41	186	23	4
2. *Penicillium chrysogenum* (23°C)					
0.0201	34	12	60		4
0.0505	14	32	63		4
0.0996	10	36	36		4
0.1497	6	40	27		4
0.2063	1	45	22		4
0.0196	78	20	102		5
0.0398	68	30	75		5
0.0460	65	33	72		5
0.0694	51	47	68		5
0.0265	70	27	102		5
0.0994	840	160	161		4
0.1980	676	324	164		4
0.4167	339	661	159		4
0.4597	260	662	144		4
0.0205	77	23	112		2
0.0252	72	28	111		2
0.0276	74	26	94		2
0.0424	64	36	85		2
0.0489	60	40	82		2

.....(cont'd.)

Biomass g	C_{eq}, U^{+6} mg/l	$\Delta C, U^{+6}$ mg/l	q, U^{+6} mg/g	pH
3. Aspergilus niger (23°C)				
0.3037	863	93	31	4
0.5086	795	161	32	4
0.7128	707	249	35	4
0.9324	663	293	31	4
0.0484	47	8	17	4
0.1003	38	18	18	4
0.2068	31	25	12	4
0.5997	12	44	7	4
0.7976	10	46	6	4
1.2199	3	53	4	4
0.0270	51	5	19	5
0.0610	46	10	16	5
0.1240	40	16	13	5
0.5795	7	49	8	5
0.7191	5	51	7	5
0.1765	34	22	12	5
0.0059	50	1	17	5
0.0494	47	4	8	2
0.1126	42	9	8	2
0.4965	19	32	6	2
0.6958	13	38	5	2
0.0339	48	3	9	2
0.2027	36	15	7	2
4. Aspergilus terreus (23°C)				
0.0562	935	0	0	4
0.1031	932	3	3	4
0.3101	923	12	4	4
0.5029	935	0	0	4
0.6548	890	45	7	4
1.0237	930	5	0	4
0.0306	46	1	3	4
0.0510	46	1	2	4
0.1095	45	2	2	4
0.2977	42	5	2	4
0.4990	38	9	2	4
0.7118	47	0	0	4
0.9189	47	0	0	4
1.0972	45	2	0	4
0.0568	46	0	0	5
0.1029	46	0	0	5
0.2051	43	3	1	5
0.3944	41	5	1	5

.....(cont'd.)

4. (cont'd.)

Biomass g	C_{eq}, U^{+6} mg/l	$\Delta C, U^{+6}$ mg/l	q, U^{+6} mg/g	pH
0.6095	40	6	1	5
0.7952	38	8	1	5
1.0400	35	11	1	5
0.0299	47	0	0	2
0.0504	47	0	0	2
0.0918	46	1	1	2
0.3228	45	2	1	2
0.5353	44	3	1	2
0.7389	43	4	1	2
0.9171	41	6	1	2
1.0836	41	6	1	2

5. Strephomyces niveus (23°C)

0.0485	936	20	41	4
0.1092	913	43	39	4
0.2996	848	108	36	4
0.4999	758	198	40	4
0.7029	683	273	39	4
0.9590	586	370	39	4
0.0537	45	11	21	4
0.1125	34	22	19	4
0.1996	23	33	17	4
0.4027	8	48	12	4
0.6000	3	53	9	4
0.8090	2	54	7	4
0.0069	54	2	22	5
0.0541	46	10	18	5
0.1204	35	20	17	5
0.3526	8	48	13	5
0.5700	2	56	9	5
0.6900	2	56	8	5
0.0131	47	2	15	2
0.0580	41	8	14	2
0.0972	35	14	14	2
0.3247	15	34	10	2
0.4540	9	40	9	2
0.7804	2	47	6	2

.....(cont'd.)

Biomass g	C_{eq}, U^{+6} mg/l	$\Delta C, U^{+6}$ mg/l	q, U^{+6} mg/g	pH
6. Pseudomonas fluorescens (23°C)				
0.0156	46	1	6	4
0.0474	45	2	4	4
0.1103	42	5	5	4
0.3130	28	19	6	4
0.4985	21	26	5	4
0.7325	18	29	4	4
0.9716	16	31	3	4
1.1979	15	31	3	4
0.0503	967	3	6	4
0.1001	964	6	6	4
0.2009	955	15	7	4
0.4149	937	33	8	4
0.7191	915	55	7	4
1.0261	873	97	9	4
0.0209	46	1	5	2
0.0410	45	2	5	2
0.0999	41	6	6	2
0.3075	29	18	6	2
0.5006	24	23	5	2
0.6690	20	27	4	2
0.9487	18	29	3	2
1.7489	12	35	2	2
0.1023	42	7	7	5
0.2158	36	13	6	5
0.4119	26	23	6	5
0.5896	22	27	5	5
0.8426	19	30	4	5
1.0460	17	32	3	5
7. Municipal Waste Activated Sludge (23°C)				
0.0308	52	4	13	4
0.0507	49	7	14	4
0.1004	42	14	14	4
0.2004	34	22	11	4
0.3967	24	32	8	4
0.5953	15	41	7	4
0.0471	956	24	51	4
0.0996	928	52	52	4
0.2017	877	103	51	4
0.3072	832	148	48	4
0.5020	748	232	46	4
0.8375	624	356	43	4
0.0731	45	11	15	5
0.0208	53	3	14	5
0.1220	39	17	14	5

.....(cont'd.)

7. (cont'd.)

Biomass g	C_{eq}, U^{+6} mg/l	$\Delta C, U^{+6}$ mg/l	q, U^{+6} mg/g	pH
0.3423	19	37	11	5
0.5792	12	44	8	5
0.6907	8	48	7	5
1.3260	3	53	4	5
0.0188	44	2	11	2
0.0445	40	6	13	2
0.0988	34	11	11	2
0.3037	13	32	10	2

8. Industrial Waste Activated Sludge (Phenolic) (23°C)

0.0285	49	7	25	4
0.0541	42	14	26	4
0.1019	31	25	24	4
0.1971	18	38	19	4
0.3970	8	48	12	4
0.5976	5	51	9	4
0.7650	4	52	7	4
1.0781	2	54	5	4
0.0510	928	40	78	4
0.0999	894	75	75	4
0.2988	733	236	79	4
0.5069	594	375	74	4
0.6976	476	493	71	4
0.9319	351	618	66	4
0.0192	51	5	26	5
0.0507	42	14	28	5
0.1203	26	30	25	5
0.5102	5	51	10	5
0.5680	1	55	10	5
0.6876	1	55	8	5
1.0947	1	55	5	5
0.0945	61	10	11	2
0.3037	37	33	11	2
0.4531	20	51	11	2
0.7756	6	65	8	2
0.9899	3	68	7	2

.....(cont'd.)

Dosage g	C_{eq}, U^{+6} mg/l	$\Delta C, U^{+6}$ mg/l	q, U^{+6} mg/g	pH
9. Activated Carbon: Filtrasorb 400 (23°C)				
0.0159	41	6	38	4
0.0530	30	17	32	4
0.1022	20	27	26	4
0.3081	4	43	14	4
0.5038	2	45	9	4
0.1010	815	154	152	4
0.1931	662	307	159	4
0.3685	474	495	134	4
0.5034	350	619	123	4
0.0117	42	5	43	5
0.0548	29	18	33	5
0.0992	19	28	28	5
0.2978	4	43	15	5
0.5040	10	31	19	5
0.4533	48	0	0	2
0.0991	48	0	0	2
0.3003	46	2	1	2
0.5012	45	3	1	2
0.6935	42	6	1	2
0.9031	39	9	1	2
10. Ion Exchange Resin: IRA-400 (23°C)				
0.0439	27	20	45	4
0.0642	23	24	37	4
0.1618	4	43	26	4
0.3430	2	45	13	4
0.5327	0	47	9	4
0.7448	0	47	6	4
0.0619	900	56	90	4
0.3224	666	290	90	4
0.5205	548	408	78	4
0.8643	325	631	73	4
0.0913	12	34	37	5
0.1100	9	37	33	5
0.3254	2	44	13	5
0.5087	0	46	9	5
0.0360	47	0	0	2
0.0820	47	0	0	2
0.1330	47	0	0	2
0.3194	47	0	0	2
0.5247	47	0	0	2
0.6862	47	0	0	2
1.0957	47	0	0	2

A.2 Chitin Uranium Uptake

The table that follows summarizes the four experiments executed in order to determine the uranium uptake capacity of pure chitin.

Experiment #	Chitin mg	U^{+6} uptaken mg	g mg/g	pH	T °C
1	5.0	0.018	5	4	23
2	18.0	0.108	6	4	23
3	30.0	0.190	6	4	23
4	30.6	0.180	6	4	23

A.3 Precision-accuracy of U(VI) Analytical Determination

Microorganum: Rhizopus arrhizus (pH = 4)

Analysis #	Absorbance	Concentration (mg/l)
1	0.258	28.301
2	0.256	28.082
3	0.257	28.192
4	0.260	28.521
5	0.259	28.411
6	0.259	28.411
7	0.267	29.289
8	0.267	29.289
9	0.267	29.289
10	0.267	29.289
11	0.261	28.630
12	0.265	29.069
13	0.265	29.069
14	0.269	29.508
15	0.267	29.289
16	0.267	29.289

The correlation coefficient of the calibration curve was $r = 1.000$, the standard error of the regression coefficient 0.967 and the standard error of estimate was 0.483. The following data were used for the determination of the calibration curve:

Concentration (mg/l U(VI))	Absorbance
0	0
10	0.085
20	0.183
30	0.269
40	0.369

A.4 Precision of Uranium Biosorptive Uptake Capacity (q) Determination

Microorganism: *Rhizopus arrhizus* (pH = 4)

Biomass g	C_{eq}, U^{+6} mg/l	$\Delta C, U^{+6}$ mg/l	q mg/g
0.0309	59	41	133
0.0313	55	45	144
0.0300	55	45	150
0.0309	54	46	149
0.0300	54	46	153
0.0293	60	40	135
0.0300	59	41	137
0.0305	53	47	154

A.5 Bipthalate Effect on q, Uranium

Microorganism Rhizopus arrhizus (pH = 4, 23°C)

Biomass g	C_{eq}, U^{+6} mg/l	C, U^{+6} mg/l	q mg/g	$\bar{q}$ mg/g	q from Biosorption Isotherm
0.0295	48	46	156		
0.0300	49	45	150	153	148
0.0303	48	46	152		

APPENDIX B

THORIUM UPTAKE DATA

B.1 Thorium Biosorption Isotherms

1. *Rhizopus arrhizus* (23°C)

Biomass mg	C_{eq}, Th^{+4} mg/l	ΔC, Th^{+4} mg/l	q mg/g	pH
0.0112	14	16	143	4
0.0507	0	30	59	4
0.0981	0	30	31	4
0.0048	22	8	166	5
0.0152	9	21	138	5
0.0317	2	28	88	5
0.0353	0	30	85	5
0.0154	69	28	182	4
0.0402	31	66	164	4
0.0696	5	92	132	4
0.0096	33	17	177	4
0.0201	17	23	164	4
0.0291	9	41	141	4
0.0050	30	8	160	4
0.0049	30	8	163	4
0.0076	25	13	171	4
0.0180	14	16	89	2
0.0274	7	23	56	2
0.0174	14	16	92	2
0.0051	34	5	98	2
0.0098	21	9	92	2
0.0043	35	4	93	2
0.0084	33	7	83	2
0.0166	25	15	90	2
0.0299	15	43	144	4
0.0303	14	44	145	4
0.0298	15	43	144	4
0.0297	16	42	141	4
0.0309	15	43	139	4
0.0301	13	45	146	4

.....(cont'd.)

1. (cont'd.) (5°C)

Biomass mg	C_{eq}, Th^{+4} mg/l	ΔC, Th^{+4} mg/l	q mg/g	pH
0.0246	16	32	130	4
0.0117	30	19	162	4
0.0163	25	24	147	4
0.0218	19	30	137	4
0.0260	18	31	119	4
0.0305	10	38	125	4
0.0101	31	17	168	4
0.0201	20	28	139	4

1. (40°C)

0.0101	28	21	208	4
0.0153	18	31	203	4
0.0205	13	36	176	4
0.0301	4	45	150	4
0.0103	28	21	204	4
0.0203	13	36	177	4
0.0247	7	42	170	4

Cell Wall Preparation Plateau (Sample Volume 50 ml) (23°C)

0.0079	18	32	202	4
0.0037	26	14	189	4
0.0038	25	16	210	4
0.0065	13	27	207	4

2. *Penicillium chrysogenum* (23°C)

Biomass mg	C_{eq} mg/l	ΔC mg/l	q mg/g	pH
0.0081	46	13	160	4
0.0248	25	34	137	4
0.0399	8	51	128	4
0.0609	1	59	97	4
0.0200	50	30	150	4
0.0581	10	70	120	4
0.0691	2	78	112	4

....(cont'd.)

2. (cont'd.)

Biomass mg	C_{eq} mg/l	ΔC mg/l	q mg/g	pH
0.0196	70	30	153	5
0.0158	10	20	126	5
0.0452	0	30	66	5
0.0194	58	34	175	5
0.0494	20	72	146	5
0.0722	7	85	118	5
0.1312	0	92	70	5
0.0215	68	36	167	4
0.0510	30	64	125	4
0.0714	11	83	116	4
0.0941	0	94	100	4
0.0214	71	20	93	2
0.0499	43	48	96	2
0.0694	23	67	96	2
0.0902	7	82	91	2
0.0412	19	41	99	2
0.0150	46	15	100	2
0.0257	36	25	97	2
0.0413	17	44	106	2
0.0496	17	44	89	2

3. Aspergillus niger (23°C)

0.0215	27	3	14	4
0.0524	22	8	15	4
0.1046	15	15	14	4
0.3021	3	27	9	4
0.5014	1	29	6	4
0.0545	80	14	26	4
0.0710	77	17	24	4
0.1106	68	26	23	4
0.2358	50	44	19	4
0.4440	21	73	16	4
0.0509	21	8	16	5
0.1012	14	15	15	5
0.1981	7	22	11	5

.....(cont'd.)

3. (cont'd.)

Biomass g	C_{eq}, Th^{+4} mg/l	$\Delta C, Th^{+4}$ mg/l	q mg/g	pH
0.5566	1	28	5	5
0.6817	1	28	4	5
0.0509	32	8	16	2
0.0687	28	12	17	2
0.0900	25	15	17	2
0.1041	18	12	12	2
0.6160	0	30	5	2

4. Aspergillus terreus (23°C)

0.0499	27	3	6	4
0.1031	25	5	5	4
0.3000	15	15	5	4
0.5014	11	19	4	4
0.0529	89	5	9	4
0.0722	92	2	3	4
0.1195	85	9	7	4
0.2019	78	15	7	4
0.4943	64	30	6	4
0.0506	26	3	6	5
0.0997	21	8	8	5
0.2013	18	11	5	5
0.4073	12	17	4	5
0.5900	9	20	3	5
0.6977	6	23	3	5
0.0220	30	0	0	2
0.0484	30	0	0	2
0.1000	29	1	1	2
0.2010	29	1	1	2
0.3778	27	2	1	2
0.5811	26	3	1	2
0.7365	25	5	1	2

5. Streptomyces niveus (23°C)

0.0213	24	6	28	4
0.0508	17	13	25	4
0.1011	8	22	21	4
0.3023	1	30	10	4
0.5032	0	30	6	4
0.0528	76	18	34	4
0.0702	67	27	38	4

.....(cont'd.)

5. (cont'd.)

Biomass g	$C_{eq}, Th^{\pm 4}$ mg/l	$\Delta C, Th^{\pm 4}$ mg/l	q mg/g	pH
0.1007	59	35	35	4
0.2082	35	59	28	4
0.4144	9	85	16	4
0.0500	17	12	24	5
0.1015	9	20	20	5
0.1973	2	27	13	5
0.4102	1	28	7	5
0.5064	0	29	6	5
0.0304	24	6	20	2
0.0494	19	11	22	2
0.1005	11	19	19	2
0.2028	3	27	13	2
0.3831	0	30	8	2
0.5532	0	30	5	2
0.0199	35	5	25	2
0.0297	33	7	23	2
0.0401	31	9	22	2

6. Pseudomonas fluorescens (23°C)

0.0228	27	3	13	4
0.0469	24	6	13	4
0.1008	17	13	13	4
0.3008	6	24	8	4
0.5028	1	29	6	4
0.0721	83	13	18	4
0.1001	77	18	17	4
0.1989	63	33	16	4
0.4385	34	62	14	4
0.6001	24	72	12	4
0.0508	23	6	12	5
0.0998	18	11	11	5
0.2020	10	19	9	5
0.3939	1	28	7	5
0.7054	0	29	4	5
0.0218	28	2	9	2
0.0507	26	4	8	2
0.1103	22	8	7	2
0.1982	16	14	7	2
0.3971	8	22	5	2
0.5912	4	26	4	2
0.7467	3	27	4	2

7. Municipal Waste Activated Sludge (23°C)

Biomass mg	C_{eq}, Th^{+4} mg/l	ΔC, Th^{+4} mg/l	q mg/g	pH
0.0100	24	5	50	4
0.0546	5	24	44	4
0.1093	2	27	25	4
0.2040	1	28	14	4
0.3937	1	28	7	4
0.0410	58	20	49	4
0.1314	13	65	49	4
0.0806	35	43	53	4
0.2014	4	74	37	4
0.4046	1	77	19	4
0.0305	14	15	49	5
0.0692	7	22	31	5
0.1019	3	26	26	5
0.1953	0	28	14	5
0.3956	0	29	7	5
0.0263	20	10	38	2
0.0984	0	30	30	2
0.0100	33	4	40	2
0.0200	27	10	50	2
0.0239	29	8	33	2

8. Industrial Waste Activated Sludge (Phenolic) (23°C)

0.0201	19	9	45	4
0.0532	10	18	34	4
0.1012	4	24	24	4
0.1730	2	26	15	4
0.3547	0	28	8	4
0.0398	60	18	45	4
0.0788	41	37	47	4
0.1236	22	56	45	4
0.1986	7	71	36	4
0.3703	2	76	20	4
0.0326	14	14	43	5
0.0642	8	20	31	5
0.1091	4	24	22	5
0.1973	1	27	14	5
0.3872	0	28	7	5
0.0199	22	7	35	2
0.0490	13	17	35	2
0.0695	5	25	36	2
0.1478	0	30	20	2
0.2970	0	30	10	2
0.0198	31	7	35	2
0.0301	27	11	37	2
0.0397	23	15	38	2

9. Activated Carbon Filtrasorb 400 (F-400) (23°C)

Dosage mg	C_{eq}, Th^{+4} mg/l	$\Delta C, Th^{+4}$ mg/l	q mg/g	pH
0.0209	18	10	48	4
0.0509	11	18	35	4
0.0942	7	22	23	4
0.2009	3	26	13	4
0.4090	1	28	7	4
0.1435	17	63	44	4
0.2156	10	70	32	4
0.2921	6	74	25	4
0.4005	4	76	19	4
0.0298	15	14	47	5
0.0695	8	20	29	5
0.1053	6	22	21	5
0.2022	2	26	13	5
0.4083	1	27	7	5
0.5276	0	28	5	5
0.0328	28	2	6	2
0.0587	27	3	5	2
0.1086	25	5	5	2
0.2132	22	8	4	2
0.3565	19	11	3	2
0.4604	17	13	3	2
0.6219	14	16	2	2

10. Ion Exchange Resin IRA-400 (23°C)

0.0465	27	3	6	4
0.0959	24	6	6	4
0.2500	17	14	6	4
0.4733	11	19	4	4
0.7576	25	53	7	4
0.3886	54	24	6	4
0.0278	26.	2	7	5
0.0439	25	3	7	5
0.0934	21	7	7	5
0.2777	12	16	6	5
0.5532	7	21	4	5
0.8139	5	23	3	5
0.0622	29	1	2	2
0.1045	29	1	1	2
0.1789	29	1	0	2

.....(cont'd.)

10 (cont'd.)

Dosage mg	C_{eq}, Th^{+4} mg/l	$\Delta C, Th^{+4}$ mg/ l	q mg/g	pH
0.3185	30	0	0	2
0.3892	30	0	0	2
0.6162	29	1	0	2
0.5400	36	54	10	4
0.1866	72	28	15	4

B.2 Chitin Thorium Uptake

The table that follows summarizes the experimental determination of pure chitin thorium uptake capacity.

Experiment #	Chitin Dosage g	Th(IV) Uptaken mg	q mg/g	pH	T °C
1	0.0050	0.04	8	4	23
2	0.0193	0.15	8	4	23
3	0.0300	0.24	8	4	23
4	0.0300	0.24	8	4	23

B.3 Precision-Accuracy of Thorium Analytical Determination

Microorganism: Rhizopus arrhizus, pH = 4, 23°C

Analysis #	Absorbance	Calculated Th(IV) Concentration mg/l
1	0.167	18.72
2	0.162	18.16
3	0.167	18.72
4	0.172	19.28
5	0.169	18.94
6	0.161	18.05

.....(cont'd.)

B.3 (cont'd.)

Analysis #	Absorbance	Calculated Th^{+4} Concentration mg/l
7	0.167	18.72
8	0.169	18.94
9	0.161	18.05
10	0.172	19.28

Concentration values were computed from the following calibration curve:

Concentration (mg/l Th^{+4})	Absorbance
0	0
10	0.080
20	0.178
30	0.273
40	0.354

The correlation coefficient of the calibration curve was $r = 0.999$. The standard error of the regression coefficient was 1.267 and the standard error of estimate 0.618.

B.4 Precision of Thorium Biosorptive Uptake Capacity (q) Determination

Microorganism: *Rhizopus arrhizus*, pH = 4, 23°C

.....(cont'd.)

B.4 (cont'd.)

Biomass g	C_{eq}, Th^{+4} mg/l	ΔC, Th^{+4} mg/l	q mg/g
0.0299	15	43	144
0.0300	14	44	147
0.0298	15	43	143
0.0297	16	42	140
0.0304	18	40	133
0.0302	14	44	146
0.0304	15	40	132

B.5 Bipthalate Effect on q. Thorium

Microorganism: *Rhizopus arrhizus*, pH = 4, 23°C

Data with no biphalate buffer present:

Biomass g	C_{eq}, Th^{+4} mg/l	ΔC, Th^{+4} mg/l	q mg/g	$\bar{q}$ mg/g	q from Biosorption Isotherm
0.0303	4	36	119		
0.0293	4	36	123	123	120
0.0282	4	36	128		
0.0294	4	36	122		

APPENDIX C

IMPLEMENTED COMPUTER PROGRAMS

C.1 Biosorptive Uptake Capacity (q) Calculation

The following program was used to calculate the biosorptive uptake capacity (q) at different equilibrium concentrations. The regression coefficients A_o, A_1, ... A_n were supplied, as constants, following a separate regression through the calibration points. A calibration curve was not accepted unless the correlation coefficient was better than 0.995.

```
$WATFIV ,TIME=10,PAGES=50,NOEXT,NOWARN
      DIMENSION BIOW1(20),BIOW2(20),BIONT(20),VO(20)
      DIMENSION CEQ(20),DCEQ(20),UBIOS(20),ULOAD(20)
      AO=0.0
      A1=509.62231
      A2=0.0
      A3=0.0
      VOBL=0.197
      NOD=4
      SAMVOL=.1
      DO  100  I=1,NOD
      READ (5,40)  BIOW1(I), BIOW2(I)
   40 FORMAT(F10.5,F10.5)
      BIONT(I)=BIOW2(I)-BIOW1(I)
  100 CONTINUE
      BLNK=A3*(VOBL**3)+A2*(VOBL**2)+A1*VOBL+AO
      DO 150 I=1,NOD
      READ(5,120) VO(I)
  120 FORMAT(F10.5)
      CEQ(I)=A3*(VO(I)**3)+A2*(VO(I)**2)+A1*VO(I)+AO
      DCEQ(I)=BLNK-CEQ(I)
      UBIOS(I)=DCEQ(I)*SAMVOL
      ULOAD(I)=UBIOS(I)/BIONT(I)
  150 CONTINUE
      WRITE(6,520)
  520 FORMAT(15X,1HI,3X,5HBIONT,8X,3HCEQ,8X4HDCEQ,8X5HUBIOS,7X,5HULOAD)
      DO 550 I=1,NOD
      WRITE(6,600) I,BIONT(I),CEQ(I),DCEQ(I),UBIOS(I),ULOAD(I)
  600 FORMAT(15X,I2,5X,F7.4,5(5X,F7.2))
  550 CONTINUE
      STOP
      END
```

C.2 Biosorption Isotherm Model Fitting

The following program, developed at the University of Toronto and kindly supplied by Dr. Lou's office, was used to estimate the model parameters and the respective standard error of estimate for a given set of biosorption isotherm data.

```
C       OPTIMIZATION BY DIRECT SEARCH AND REGION CONTRACTION
        IMPLICIT REAL*8(A-H,O-Z)
        DIMENSION Y(101,20), XP(8), X(8), REG(8), XS(8)
        DIMENSION  Q(30),CEQ(30)
        NOB=18
        N=2
        KI  = 5
        KO  = 6
        NIT=200
        NO  = 0
        KK  = -1
        DO 50  L=1,NOB
        READ(KI,11)  Q(L),CEQ(L)
   50   CONTINUE
   11   FORMAT(2F10.2)
        DO 93  J=1,101
        READ(KI,41)  (Y(J,I),I=1,20)
        DO 89 K=1,20
   89   Y(J,K)  =  Y(J,K) - 0.5
   93   CONTINUE
   41   FORMAT(20F4.3)
C       SPECIFICATION OF INITIAL CONDITIONS AND SIZE OF SEARCH REGION
        XP(1)=40.
        XP(2)=.07
        XP(1)=66.
        XP(2)=.12
        XP(1)=50.
        XP(2)=100.
        XP(2)=1.
        XP(1)=1.
        XP(2)=3.
        ABC =  .95
        REG(1)=10.
        REG(2)=2.
        REG(1)=100.
        REG(2)=100.
        TEST=10.E10
        WRITE(KO,27)
   27   FORMAT(1H1)
        WRITE(KO,28)
   28   FORMAT(1X,'ITERATION NO',2X,'NO OF FNCS',3X,'FUNCTION',6X,'VALUES
       1OF VARIABLES ...'/)
        DO 100 J=1,NIT
        KK = KK + 1
        KN = KK + N
        IF(KN.GT.20) KK=0
        DO 94 K=1,101
        DO 42 I=1,N
   42   X(I) = XP(I) + Y(K,I+KK)*REG(I)
        IF(X(2).LT..2)  GOTO  30
        F=0.
        DO  99  L=1,NOB
        F=F+(Q(L)-X (1)*CEQ(L)**(1./X (2)))**2
   99   CONTINUE
        NO = NO + 1
        IF(F.GT.TEST)  GOTO  30
        TEST = F
C
C       THE BEST VALUE OF THE FUNCTION AND THE CORRESPONDING VALUES OF X ARE KEPT
        FM = F
        DO 43 I=1,N
   43   XS(I) = X(I)
   30   CONTINUE
   94   CONTINUE
        WRITE(KO,96)  J, NO, FM, (XS(I),I=1,N)
   96   FORMAT(1X,I7,I14,F14.5,8F11.5)
C
C       THE REGION IS REDUCED BY THE QUANTITY ABC DEFINED IN STATEMENT 6
        DO 95 I=1,N
        REG(I)  = REG(I)*ABC
        XP(I) = XS(I)
   95   CONTINUE
  100   CONTINUE
C
C        CALCULATE  THE  STANDARD  ERROR  OF  ESTIMATE
        SDV=(FM/NOB)**.5
        WRITE(KO,200) SDV
  200   FORMAT(////,5X,'STANDARD  ERROR  OF  ESTIMATE  =',F10.6)
        STOP
        END
```

APPENDIX D

CO-ION EFFECT ON q

D.1 Effect of Fe^{+2} on Uranium Uptake of R. arrhizus

Biomass mg	C_{eq}, U^{+6} mg/l	$\Delta C, U^{+6}$ mg/l	q, U^{+6} mg/g	Initial, Fe^{+2} mg/l	pH
0.0152	72	7	46	1000	4
0.0103	74	5	48	1000	4
0.0046	77	2	43	1000	4
0.0208	70	9	43	1000	4
0.0317	65	14	44	1000	4
0.0674	50	29	43	1000	4
0.0121	71	9	74	100	4
0.0212	65	15	71	100	4
0.0309	58	22	71	100	4
0.0463	46	34	73	100	4
0.0[illegible]2	35	45	71	100	4
0.0310	58	22	71	100	4
0.0118	65	16	135	30	4
0.0159	60	21	132	30	4
0.0254	47	34	135	30	4
0.0306	41	40	131	30	4
0.0408	31	50	123	30	4
0.0497	25	57	115	30	4
0.0300	40	41	137	30	4
0.0156	65	15	96	30	2
0.0259	56	24	93	30	2
0.0356	45	35	98	30	2
0.0454	37	43	95	30	2
0.0577	27	53	92	30	2
0.0208	61	19	91	500	2
0.0308	56	24	78	500	2
0.0400	45	35	88	500	2
0.0301	53	27	90	500	2
0.0549	30	50	91	500	2

D.2 Effect of Zn^{+2} on Uranium Uptake by R. arrhizus

Biomass mg	C_{eq}, U^{+6} mg/l	$\Delta C, U^{+6}$ mg/l	q, U^{+6} mg/g	Initial Zn^{+2} mg/l	pH
0.0160	60	20	125	50	4
0.0253	51	29	114	50	4
0.0364	40	40	110	50	4
0.0414	35	45	109	50	4
0.0489	30	50	102	50	4
0.0042	74	5	119	20	4
0.0095	68	11	116	20	4
0.0141	63	16	113	20	4
0.0200	57	22	110	20	4
0.0303	43	36	119	20	4
0.0052	75	5	96	50	2
0.0150	66	14	93	50	2
0.0209	61	19	93	50	2
0.0332	47	33	99	50	2
0.0422	42	38	90	50	2
0.0076	72	7	92	20	2
0.0386	45	34	88	20	2
0.0190	60	19	100	20	2
0.0260	55	24	92	20	2
0.0301	52	27	90	20	2

D.3 Effect of Fe^{+2} on Thorium Uptake by R. arrhizus

Biomass mg	C_{eq}, Th^{+4} mg/l	$\Delta C, Th^{+4}$ mg/l	q, Th^{+4} mg/g	Initial Fe^{+2} mg/l	pH
0.0046	22	8	174	1000	4
0.0095	16	14	147	1000	4
0.0097	16	14	144	1000	4
0.0149	10	19	127	1000	4
0.0268	1	29	108	1000	4
0.0330	1	29	88	1000	4
0.0097	16	15	155	100	4
0.0139	9	21	151	100	4
0.0202	3	27	134	100	4

.....(cont'd.)

D.3 (cont'd.)

Biomass mg	C_{eq},Th^{+4} mg/l	ΔC,Th^{+4} mg/l	q,Th^{+4} mg/g	Initial Fe^{+2} mg/l	pH
0.0299	1	29	97	100	4
0.0136	9	21	154	100	4
0.0112	13	16	143	30	4
0.0157	7	22	140	30	4
0.0203	3	26	128	30	4
0.0258	1	28	108	30	4
0.0068	19	11	162	30	4
0.0215	9	21	98	500	2
0.0204	12	18	88	500	2
0.0044	26	4	90	500	2
0.0100	21	9	90	500	2
0.0079	23	7	88	500	2
0.0212	9	21	99	500	2
0.0115	20	10	87	30	2
0.0178	16	14	79	30	2
0.0240	10	20	83	30	2
0.0306	2	28	92	30	2
0.0046	26	4	86	30	2

D.4 Effect of Zn^{+2} on Thorium Uptake by *R. arrhizus*

Biomass mg	C_{eq},Th^{+4} mg/l	ΔC,Th^{+4} mg/l	q,Th^{+4} mg/g	Initial Zn^{+2} mg/l	pH
0.0050	22	8	160	50	4
0.0080	18	12	150	50	4
0.0163	9	21	129	50	4
0.0257	1	29	113	50	4
0.0360	0	30	83	50	4
0.0400	0	30	75	50	4
0.0127	12	18	142	50	4
0.0053	21	9	170	20	4
0.0070	19	11	157	20	4
0.0118	13	17	144	20	4
0.0180	7	23	128	20	4
0.0259	1	29	112	20	4
0.0069	19	11	159	20	4
0.0054	24	5	93	50	2

.....(cont'd.)

D.4 (cont'd.)

Biomass mg	C_{eq},Th^{+4} mg/l	ΔC,Th^{+4} mg/l	q,Th^{+4} mg/g	Initial Zn^{+2} mg/l	pH
0.0082	21	8	98	50	2
0.0146	14	15	103	50	2
0.0228	8	21	92	50	2
0.0260	4	25	96	50	2
0.0050	24	5	100	20	2
0.0088	20	9	102	20	2
0.0163	13	16	98	20	2
0.0211	7	22	104	20	2
0.0288	3	26	90	20	2

APPENDIX E

KINETIC DATA

Appendix E presents the numerical values of the data points reported on the typical kinetic curves of Chapter III.

E.1 Uranium Uptake Kinetic Data

Time min.	C_o, U^{+6} mg/l	C_t, U^{+6} mg/l	q_t, U^{+6} mg/g
Experiment #1, pH = 4			
0	50	-	-
0.5	50	36	93
3	50	33	113
5.5	50	34	107
16.5	50	29	140
30	50	28	147
60	50	24	173
120	50	23	180
240	50	24	173
Experiment #2, pH = 4			
0	37	-	-
1	37	29	67
5	37	27	84
15	37	26	92
30	37	27	83
60	37	23	117
120	37	22	125
180	37	22	125
360	37	23	117
640	37	22	125

.....(cont'd.)

E.1 (cont'd.)

Time min.	C_o, U^{+6} mg/l	C_t, U^{+6} mg/l	q_t, U^{+6} mg/g
Experiment #3, pH = 4			
0	39	-	-
0.5	39	29	67
2	39	28	74
5	39	29	67
7	39	29	67
22	39	29	67
35	39	30	61
65	39	25	95
120	39	24	101
180	39	25	95
300	39	24	101
420	39	24	101
Experiment #5, pH = 4			
0	79	-	-
0.5	79	64	105
2	79	64	105
3	79	64	105
5	79	64	105
10	79	64	105
30	79	64	105
40	79	60	133
50	79	57	154
60	79	56	161
120	79	57	154
240	79	57	154
360	79	56	161
Experiment #6, pH = 4			
0	40	-	-
1.5	40	33	91
3	40	38	26
5	40	33	91
10	40	33	91
15	40	32	104
25	40	32	104

.....(cont'd.)

E.1 (cont'd.)

Time min.	C_o, U^{+6} mg/l	C_t, U^{+6} mg/l	q_t, U^{+6} mg/g
Experiment #6 (cont'd.)			
40	40	30	130
45	40	30	130
50	40	30	130
55	40	30	130
60	40	29	143
120	40	29	143
240	40	30	130
360	40	29	143
Experiment #7, pH = 4			
0	42	-	-
0.5	42	27	101
1.5	42	27	101
3	42	27	101
5	42	26	107
10	42	26	107
15	42	25	114
30	42	23	128
35	42	24	121
40	42	23	128
45	42	24	121
50	42	23	128
60	42	24	121
90	42	23	128
120	42	23	128
240	42	23	128
Experiment #8, pH = 2			
0	42	-	-
0.5	42	42	0
1	42	40	15
3	42	39	22
5	42	39	22
10	42	38	30
15	42	36	53
30	42	35	52
45	42	33	67
60	42	33	67
90	42	32	74
120	42	31	81
180	42	31	81

E.2 Thorium Uptake Kinetic Data

Time min.	C_o, Th^{+4} mg/l	C_t, Th^{+4} mg/l	q, Th^{+4} mg/g
Experiment #1, pH = 4			
0	21	-	-
1	21	12	112
5	21	9	150
11	21	8	162
16	21	7	175
31	21	7	175
40	21	7	175
60	21	7	175
120	21	6	187
360	21	7	175
Experiment #2, pH = 4			
0	17	-	-
0.5	17	13	114
1	17	12	143
3	17	13	114
7	17	12	143
10	17	12	143
15	17	13	114
30	17	11	171
50	17	12	143
60	17	12	143
90	17	12	143
120	17	12	143
360	17	11	171
Experiment #4, pH = 4			
0	16	-	-
0.5	16	13	143
1.5	16	13	96
3	16	14	143
5	16	13	143
10	16	13	143
17	16	14	96
30	16	13	143
47	16	13	143
60	16	13	143
120	16	13	143

.....(cont'd.)

E.2 (cont'd.)

Time min.	C_o, Th^{+4} mg/l	C_t, Th^{+4} mg/l	q, Th^{+4} mg/g
Experiment #5, pH = 4			
0	30	-	-
0.8	30	23	175
1.5	30	22	200
3	30	23	175
5	30	23	175
10	30	23	175
15	30	23	175
30	30	24	200
60	30	23	175
120	30	23	175
Experiment #6, pH = 2			
0	17	-	-
1	17	16	25
2	17	15	50
5	17	14	75
10	17	15	50
15	17	13	100
30	17	13	100
45	17	14	75
60	17	13	100
120	17	13	100
360	17	13	100
Experiment #7, pH = 4			
0	14	-	-
1	14	9	132
3	14	9	132
5	14	10	105
11	14	9	132
30	14	9	132
50	14	10	105
60	14	9	132
120	14	9	132
360	14	9	132

APPENDIX F

Additional Information on Biosorption of Uranium and Thorium

F.1 Co-ion Effect on U and Th Biosorption

Actual waste waters contain a variety of anions and cations. Table I.1 in Chapter I has summarized the most important chemical and radioactive parameters for the uranium mining-milling process waste waters. Iron, zinc, lead, copper and manganese appear as common cations in most waste waters. Iron is present in the highest concentrations.[1] Waste water pH ranges from pH = 2 to almost neutral, depending on whether the tailings area is active or inactive and on whether the waste water is a surface runoff or seepage flow.[1]

It was decided to select the two co-ions most abundant in usual waste waters and examine their effect on R. arrhizus U and Th biosorptive uptake capacity. Initial co-ion concentrations were selected according to their respective expected concentrations in waste waters. As a result initial iron concentrations of up to 1000 mg/l were tested, while zinc initial concentrations were limited to a maximum of 50 mg/l.

Two different solution pH values were tested, pH = 2 and pH = .4. Idle tailings areas, because of the acid generation process, generate acidic waste water with pH values from pH = 2 to pH = 6.5.[1,4] The proposed U and Th biosorptive mechanism hypotheses have indicated that solution pH affects strongly the overall U and Th biosorptive uptake capacity

of R. arrhizus (III-A.10, III-B.10). The significance of solution pH and the wide range of actual waste water pH values dictated the need to test the co-ion effect on the U and Th biosorptive uptake capacity at the values of pH = 2 and pH = 4. The same buffering systems as the ones described in Section II.1.2 were applied. The buffering systems did not interfere with the applied analytical methods, as it was indicated after following the procedure described in Section II.1.2.

F.2 Uranium Analytical Determination

As already described in Section II.1.3, the Arsenazo III spectrophotometric method developed by Savvin was employed.[29] Arsenazo III, a reagent developed in 1959, reacts with uranium (IV) in a strongly acidic medium and gives a violet complex.[28] This method is the most sensitive of all spectrophotometric methods capable of determining uranium. The method gives the best results with a two to five molar excess of the reagent. The color appears instantaneously and remains stable for at least two hours. Absorbance depends on the acidity of the medium and is constant over the acidity range of 4 N to 8 N HCl.[20] The fairly narrow peak of the complex absorbance curves and the high stability of the complex raise the sensitivity of the reaction. The influence of anions and cations, with the exception of Zr and Th, is very small. Zirconium can be masked when oxalic acid is introduced in the sample. Thorium, however, presents a serious problem and needs to be separated from uranium before the U(IV) determination.[20]

Uranium (VI) can, also, be determined with the help of Arsenazo III. The sensitivity and the selectivity of the method, however, are reduced. Iron zirconium, thorium and other elements interfere strongly. Uranium (VI) can be effectively determined by reducing U(VI) to U(IV) with the help of granular zinc in 4 N HCl.

The molar absorptivity of the Arsenazo III-U(IV) complex in 4-8 N HCl, with at least three-fold molar excess of Arsenazo III; is approximately 1.27×10^5 at $\lambda = 665$ nm.[28]

F.3 Thorium Analytical Determination

The Arsenazo III spectrophotometric method for the analytical determination of thorium was used, as outlined in Section II.1.4. Arsenazo III reacts with thorium in strongly acidic solution to form a grey-green water soluble complex.[28] With excess of Arsenazo III, a 2:1 complex with thorium is formed. The method is very sensitive and the absorbance varies only slightly with change in HCl concentration between 1 and 10 N.

The Arsenazo III method has a high selectivity for thorium. With oxalic acid as a masking agent, thorium can be determined in 2.5 to 3.5 N HCl in the presence of zirconium, hafnium and niobium.[28] Aluminum and rare earths do not interfere. Uranium, however, presents a problem.

The molar absorptivity of the complex at 3 N HCl is 1.15×10^5 at $\lambda = 655$ nm.[28]

F.4 N-acetyl-D-glucosamine-metal Complexes

N-acetyl-D-glucosamine ($C_8H_{14}O_6N$) is the chitin monomer unit. The complex formation ability of D-glucosamine has been confirmed in literature for a large number of metal ions.[66,67,79] In general, the compound behaves like a Lewis base. The complex formation ability may be the result of either the oxygen (hydroxyl groups) or the nitrogen atoms. The complex formation ability of the -OH groups has, however, been suggested as quite small or negligible [66], thus leaving the amine nitrogen on the active complexation site. The stability constants of nine metal complexes have been reported in literature.[66,67] The susceibility of the D-glucosamine-metal complexes to hydrolysis is not uniform. Easily hydrolysable complexes have been suggested on yielding metal hydroxide as the final hydrolysis product.[66] The complexes have been suggested as being susceptible to dimerization. Certain D-glucosamine-metal complexes have been isolated as precipitates (Cu); others, however, have not (Co,Fe).[65,66] Complex formation preference follows, in general, the Irving-Williams series.

F.5 Effect of Biomass on Solution pH

In earlier sections (II-1,2, II-9.2), it was noted that upon contact biomass raised solution pH and necessitated the use of a buffering system during the equilibrium and the kinetic studies. In view of the information reported in the present work, this behavior may be considered as the result of uptake of H_3O^+ ions by certain cell wall active sites like the chitin nitrogen, as described qualitatively below:

$$\overset{+}{GN}: \overset{H_3O^+}{\rightleftharpoons} \overset{+}{GN}:H + H_2O$$

Once equilibrium is established no further change of solution pH should be observed as a result of the biomass presence. Such a behavior was experienced during the kinetic experiments and was implemented as the necessary pH control method (II.9.2).